



**UNIVERSITÀ DEGLI STUDI DI PAVIA**  
**DOTTORATO IN SCIENZE CHIMICHE**  
**E FARMACEUTICHE**  
**XXIX CICLO**

**Coordinatore: Chiar.mo Prof. Mauro Freccero**

***NEW INTERMEDIATES FROM***  
***PHOTOGENERATED PHENYL CATIONS***

**Tutore**  
**Chiar.mo Prof. Maurizio Fagnoni**

**Tesi di Dottorato di**  
**STEFANO CRESPI**

**a.a. 2015- 2016**



*“And we’re on our own  
and we find there’s no-one that’s  
waiting for the light to call.”  
Solar Winds, Devin Townsend*

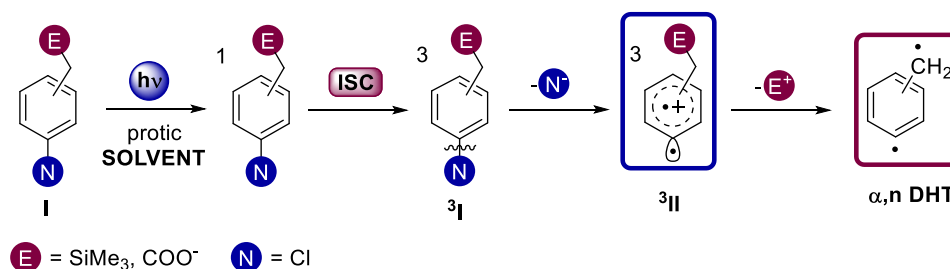
## ABSTRACT

**Riassunto della Tesi di Dottorato di ricerca in Scienze Chimiche (XXIX Ciclo)  
di STEFANO CRESPI**

*" New intermediates from photogenerated phenyl cations "*

**Curriculum B Sintesi, Struttura e Reattività di Molecole Organiche e Inorganiche  
Dipartimento di Chimica  
(Tutor: Chiar.mo Prof. Maurizio Fagnoni)**

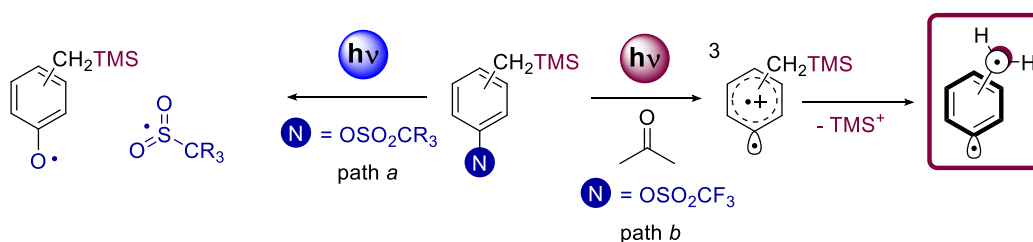
This thesis is focused on the chemistry of the triplet phenyl cation and on the generation of novel useful intermediates such as didehydrotoluenes, DHTs.<sup>[1]</sup> These diradicals can be considered as models of intermediates having antineoplastic and cytotoxic activity, therefore their study was deemed particularly appealing. Our group have developed in the recent years a one-photon-double-elimination procedure to generate photochemically all of the three isomeric  $\alpha,n$ -DHTs, from electron-rich aromatics **I** bearing a nucleofugal group positioned on the ring ( $N = -Cl$ ) and an electrofugal group ( $E = -SiMe_3$  and  $-COO^-$ ), as depicted in Scheme 1. The procedure has its key point in the population of the triplet state  $^3\mathbf{I}$  and its cleavage to afford the triplet phenyl cation  $^3\mathbf{II}$  that could lose the electrofugal group affording the aforementioned diradical.



**Scheme 1**

In particular, the photochemical properties of the mesylates, triflates and diethyl phosphates esters of benzyl trimethylsilane are described. Those compounds are herein investigated as potential nucleofugal groups, thus their properties are screened both through a peculiar photochemical and photophysical study and also by means of computational chemistry (CPCM-(U)B3LYP/6-31G(d) level of theory). The phosphates appear to be less reactive than the sulfonate esters in all of the tested conditions due to fluorescence deactivation of their excited states, while the sulfonates underwent cleavage of the O-S bond upon direct irradiation (Scheme 2, path a). Sensitization with acetone

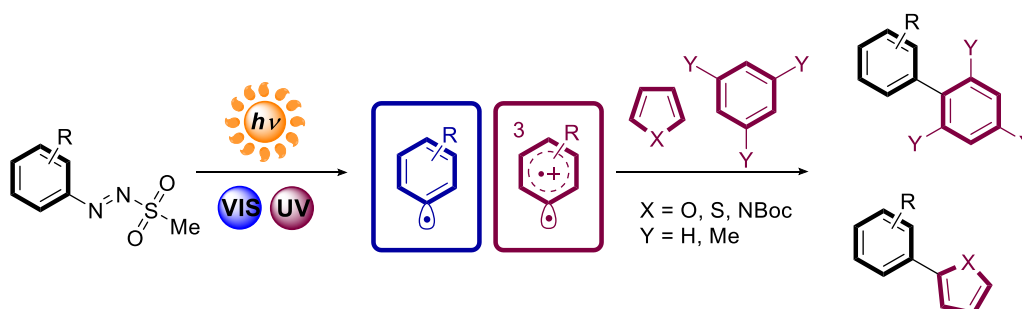
allowed the efficient population of the triplet state only in triflates, and all of the three isomeric DHTs by heterolytic cleavage of the Ar–O bond (Scheme 2, path b).<sup>[2]</sup>



**Scheme 2**

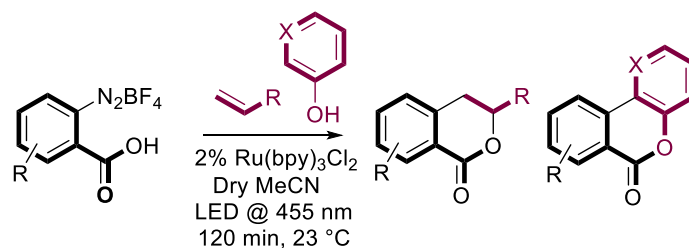
The phosphonic acid moiety is subsequently studied as novel electrofugal group. This functionality is particularly interesting from different point of views, in particular it allows the solubility in aqueous media of the DHT precursor and could impart a pH dependent reactivity that in some instances could be tuned to obtain selectively the dihydrotoluene. The mechanism of elimination of this electrofugal group is studied also using CASSCF/6-31G(d), in order to clarify the similarities with other structures that are able to generate the DHT, *viz.* the chlorophenylacetic acids.<sup>[3]</sup> Moreover it was deemed worthwhile to elucidate the process of phosphate loss from benzylic position upon irradiation, that is scarcely described in literature.

Due to the great limitations on the applicability of the triplet aryl cation chemistry owing to the highly energetic wavelengths needed for its generation, a part of the thesis will be devoted on the study of novel precursors for the solar–light promoted generation of this species. Therefore, the study of the photochemistry of the arylazo mesylates (Scheme 3) is reported. These compounds are easily synthesized and purified from the corresponding diazonium salts and are thermally stable. The study of the photochemistry of these colored molecules allowed to unravel a wavelength selective generation of aryl radicals and triplet aryl cations. Consequently, a solar light metal free approach to the synthesis of (hetero)biaryls was developed and optimized, allowing the synthesis of a small library of products.<sup>[4]</sup>



**Scheme 3**

The mechanistical issues underlying the photogeneration of the triplet aryl cation remain, however, partially undisclosed, therefore an in–deep computational approach to the photochemistry of the chloroanilines will be considered to shed more light on the photoreactivity of the chloroaromatics. The last part of the thesis will be focused on the period of the PhD spent at the University of Regensburg under the supervision of Professor Dr. B. König, with the aim of studying novel approaches to different intermediates such as benzyne and aryl radicals by means of photocatalysis (Scheme 4). In particular, a photocatalytic Meerwein approach to the synthesis of isochromanones and isochromenones is described. The method was mechanistically studied and optimized, allowing the synthesis of differently substituted polycyclic molecules.

**Scheme 4**

## ACKNOWLEDGEMENTS

In primo luogo desidero ringraziare il mio supervisore e tutor, Prof. Maurizio Fagnoni, per aver creduto in me ed avermi guidato lungo questo percorso durato tre anni. I would also express my sincere gratitude towards Prof. Dr. Burkhard König, that accepted me in his lab for my research stay at the University of Regensburg. Un ringraziamento di cuore va a tutti i membri del PhotoGreen Lab, partendo dal Prof. A. Albin e dai professori Stefano e Davide, che non hanno mai fatto mancare il loro sostegno, consigli e tirate d'orecchi. Ovviamente tre anni non sarebbero passati così velocemente senza dei compagni di laboratorio come Otta, Edo, Luca e Silvia, che hanno reso piacevole (e direi talvolta indimenticabile) quest'avventura. Grazie all'eminetissimo Prof. Bonesi per la simpatia e i consigli<sup>1</sup> e al Prof. DD per la sua pazza amicizia. Ovviamente non posso dimenticare i miei due dottorandi preferiti, Tia ed Eli, compagni di (dis)avventure nel XXIX ciclo.

Un grazie enorme va alla mia famiglia, ad Angelo e Paola, che mi sono sempre stati vicini con una pazienza infinita e a Giulia<sup>2</sup> che mi ha accompagnato da ben prima di questi tre anni e che non ha mai smesso di camminare al mio fianco.

Grazie agli amici di una vita, Gigi, Lorenzo, Alfredo, e Greg and thanks to the new ones, Karin, Nadi and Tonj,<sup>3</sup> that let me have the time of my life.

---

<sup>1</sup> E per avermi mostrato gli infiniti significati contenuti nelle parole “idrossido di sodio”.

<sup>2</sup> Che qualche volta la pazienza la perde anche e se ne esce con un “Suvvia!”. (tre su tre!)

<sup>3</sup> To whom I taught what “being a member of the group” truly means.

# CONTENTS

<b>1 INTRODUCTION</b> .....	<b>1</b>
1.1 PHOTOCHEMICAL GENERATION OF CHEMICAL INTERMEDIATES. THE PHENYL CATION. .....	1
1.2 CONDITIONS FOR TRIPLET PHENYL CATION PHOTOGENERATION .....	5
1.3 TRIPLET PHENYL CATION: SYNTHETIC APPLICATIONS. ....	7
1.4 GENERATION OF NOVEL INTERMEDIATES FROM THE TRIPLET ARYL CATION.....	8
1.4.1 <i>From triplet aryl cations to benzyne</i> .....	9
1.4.2 <i>From triplet aryl cations to didehydrotoluenes</i> .....	10
1.5 AIM OF THE THESIS .....	15
<b>2 COMPETING PATHWAYS IN THE PHOTO GENERATION OF DIDEHYDROTOLUENES FROM (TRIMETHYLSILYLMETHYL) ARYL SULFONATES AND PHOSPHATES</b> .....	<b>17</b>
2.1 INTRODUCTION .....	17
2.2 RESULTS .....	18
2.2.1 <i>Experimental studies</i> .....	18
2.2.2 <i>Computational study</i> .....	22
2.3 DISCUSSION .....	23
2.4 CONCLUSIONS.....	27
<b>3 PH DEPENDENT PHOTO GENERATION OF DIDEHYDROTOLUENES FROM CHLORO BENZYLPHOSPHONIC ACIDS</b> .....	<b>29</b>
3.1 INTRODUCTION .....	29
3.2 RESULTS .....	31
3.2.1 <i>Experimental studies</i> .....	31
3.2.2 <i>Computational Studies</i> .....	37
3.3 DISCUSSION .....	41
3.4 CONCLUSIONS.....	43
<b>4 WAVELENGTH SELECTIVE GENERATION OF ARYL RADICALS AND ARYL CATIONS FOR METAL-FREE PHOTOARYLATIONS</b> .....	<b>45</b>
4.1 INTRODUCTION .....	45
4.2 RESULTS .....	47
4.2.1 <i>Photochemical Arylation of (hetero)Aromatics via Arylazo Mesylates</i> .....	47
4.2.2 <i>Mechanistic Investigations on the Photoreactivity of Azosulfones 1</i> .....	51
4.3 DISCUSSION .....	52



4.3.1 Importance of the Method .....	53
<b>5 COMPUTATIONAL STUDY ON THE EXCITED STATE DEACTIVATION MECHANISM OF THE CHLOROANILINES .....</b>	<b>56</b>
5.1 INTRODUCTION .....	56
5.2 RESULTS AND DISCUSSION .....	59
5.3 CONCLUSIONS.....	69
<b>6 PHOTOCATALYTIC APPROACH TO INTERMEDIATE GENERATION ...</b>	<b>70</b>
6.1 PHOTO-MEERWEIN APPROACH TO THE SYNTHESIS OF ISOCHROMANONES AND ISOCHROMENONES.....	70
6.1.1 Introduction.....	70
6.1.2 Results and Discussion.....	72
6.1.3 Conclusion.....	77
6.2 STUDY ON THE PHOTOCATALYTIC GENERATION OF BENZYNE .....	78
6.2.1 Introduction.....	78
6.2.2 Results and Discussion.....	80
6.2.3 Conclusion and future perspectives.....	84
<b>7 EXPERIMENTAL SECTION .....</b>	<b>85</b>
7.1 EXPERIMENTAL DETAILS RELATIVE TO CHAPTER 2.....	85
7.1.1 Synthetic procedures .....	85
7.1.2 Photophysical parameters for compounds 1–3. ....	91
7.1.3 Computational Details.....	97
7.2 EXPERIMENTAL DETAILS RELATIVE TO CHAPTER 3.....	113
7.2.1 Synthesis of compounds 1a–c, 5 and 13.....	114
7.2.2 Potentiometric Titration of 1a–c.....	118
7.2.3 Absorption and emission spectra of compound 1–c.....	119
7.2.4 Computational Details.....	124
7.3 EXPERIMENTAL DETAILS RELATIVE TO CHAPTER 4.....	130
7.3.1 General procedure for the synthesis of arylazo sulfones 1a–h. ....	130
7.3.2 Photophysical data of arylazo sulfones 1a–h.....	132
7.3.3 UV absorption spectra of compounds 1a–h in MeCN ( $5 \times 10^{-5}$ M).....	133
7.3.4 Optimization of the reaction conditions for the synthesis of 2a. ....	137
7.3.5 General Procedure for Solar Light Metal-free Arylations via Aryl Azosulfones. .....	139
7.4 EXPERIMENTAL DETAILS RELATIVE TO CHAPTER 5.....	144

7.4.1 Cartesian coordinates of stationary points and conical intersections of compounds 1-10.....	146
7.4.2 Cartesian coordinates of the optimized geometries for the isodesmic reaction (A-F).....	150
7.5 EXPERIMENTAL DETAILS RELATIVE TO CHAPTER 6.....	153
7.5.1 Preparation of aryldiazonium tetrafluoroborates 1a-1d.....	154
7.5.2 Reaction time optimization.....	154
7.5.3 Photocatalytic synthesis of isochromanones and isochromenones.....	154
7.5.4 Experimental procedure for capturing intermediate radicals with TEMPO.....	159
7.5.5 Synthesis of 1,4-dihydro-1,4-epoxynaphthalene (21) <sup>[353]</sup> .....	160
<b>BIBLIOGRAPHY.....</b>	<b>163</b>

# 1 INTRODUCTION

## 1.1 Photochemical generation of chemical intermediates. The phenyl cation.

Organic chemistry is the branch of chemistry that more than the others is deeply connected with the study of the mechanisms, dynamics and structural features of the molecules in order to both predict and explain the outcome of a chemical reaction.<sup>[5-9]</sup> Whether the goal of the organic chemist is to understand the nature of a transformation or to build novel structures, the starting point remains thus the study of the mechanism of a particular reaction. Consequently, the role of the intermediate and the impetus to rationalize their chemical behaviour has emerged as a central topic in the field of organic chemistry.<sup>[10,11]</sup> The elucidation of a particular reaction mechanism requires therefore the study of the intermediates that are intervening (**In**, Figure 1.1).

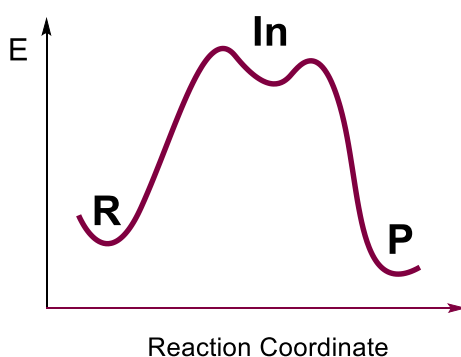


**Figure 1.1** Pictorial representation of the energy landscape of a thermal reaction.

The pathway that the reaction has to follow to connect the reactant (**R**, Figure 1.1), to the intermediate **In** usually proceeds energetically uphill, thus it is compulsory either to heat

or to treat **R** with a suitable reagent to surmount the activation barrier. Albeit the energy of the system increases, under these conditions the molecule remains in the lower (ground) state.

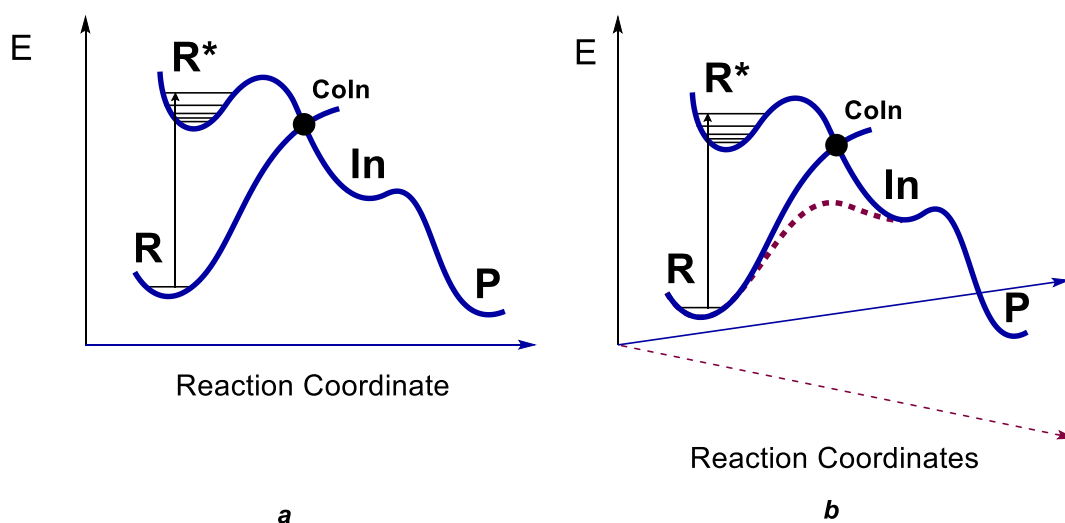


**Figure 1.2** *a.* Pictorial representation of the pathway followed by a prototypical photochemical reaction. *b.* Comparison between the energy barriers of a photochemical (in blue) and a thermal (in dashed red) reaction.

Photochemistry and in particular organic photochemistry occupies a special role in the generation of organic reactive intermediates.<sup>[11,12]</sup> Indeed, the photochemical approach allows the system to populate a higher excited state (**R\***, Figure 1.2a) through the absorption of a photon of suitable wavelength, that can be considered the perfect chemical reagent which leaves no residual byproducts behind.<sup>[13]</sup> The molecule can consequently evolve on a different *Potential Energy Surface* (PES) than the ground state one, overcoming usually smaller barriers and finally funnelling into the lowest state through a Conical Intersection (CoIn, Figure 1.2a) and populating the intermediate **In**, basically following a different reaction coordinate than the one allowed for the corresponding thermal transformation. Therefore, photochemistry not only “enhances the power of chemical synthesis by removing current thermodynamic restrictions”,<sup>[14]</sup> but permits in certain conditions to efficiently generate selectively different intermediates otherwise not easily thermally accessible.<sup>[3]</sup> Hence, both the study and the synthetic employment of those reactive species can be efficiently achieved by means of photochemistry.

The possibility offered by photochemistry allowed our group to gain deep insights on the reactivity of the phenyl cation.<sup>[15]</sup> This peculiar intermediate exists in two different spin states, *viz.* the singlet <sup>1</sup>**I** and the triplet <sup>3</sup>**I**, that show distinctive morphologies and, obviously, electronic structures.<sup>[16–18]</sup> Theoretical calculations show that the singlet cation

possesses a localized charge ( $\pi^6\sigma^0$  electronic structure, Chart 1.1a) that imparts a structural deformation to the aromatic backbone, assuming a puckered, cumulene-like structure at the  $C_6-C_1-C_2$  moiety  ${}^1I'$ . These deformations are dependent on the position and nature of the substituents.<sup>[18]</sup> On the contrary, the triplet cation is characterized by a carbene character, consequence of its ability to delocalize the charge on the aromatic ring ( $\pi^5\sigma^1$  electronic structure, Chart 1.1b).<sup>[19]</sup>

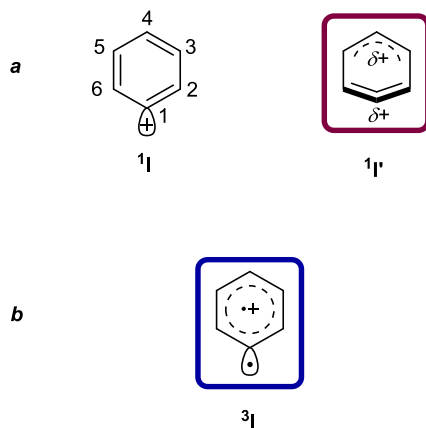
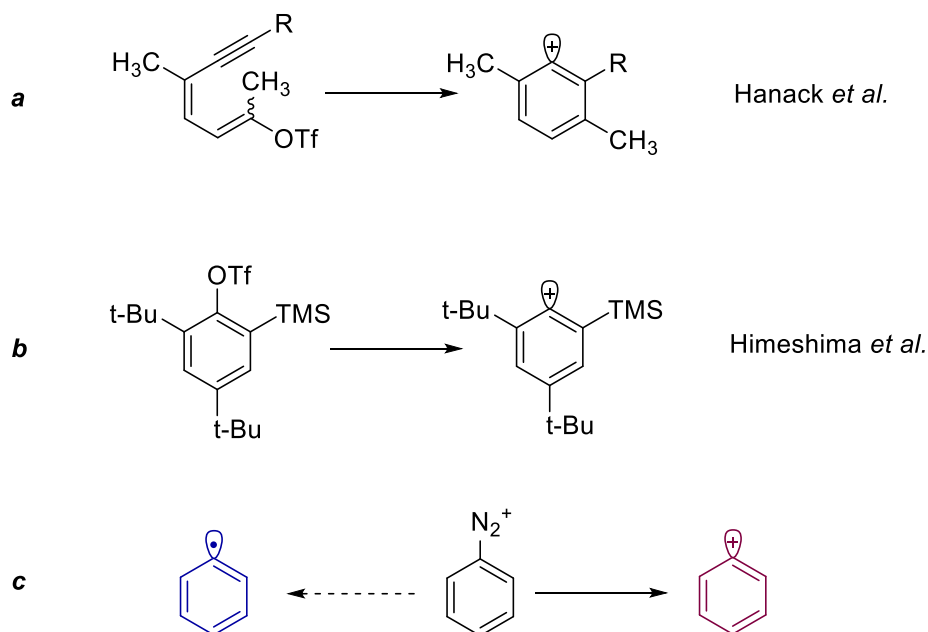


Chart 1.1

The differences in the electronic structure are mirrored by a markedly different reactivity. While the singlet is an unselective electrophile, the triplet state is trapped efficiently by using  $\pi$ -nucleophiles, but not with  $n$ -type ones (*i.e.* alcohols, water...) if not charged, *i.e.* iodides.<sup>[20–22]</sup>

Even though the phenyl cation is synthetically appealing, its thermal generation is not an easy task. The available strategies involve either the solvolysis of dienynyil triflates (Scheme 1.1a),<sup>[23–25]</sup> or of perfluoroalkylaryl sulfonyl esters ortho-substituted with a stabilizing TMS group (Scheme 1.1b)<sup>[26–28]</sup> or from the dediazonization diazonium salts. The last method is not completely selective since a competitive formation of aryl radicals took likewise place under thermal conditions (Scheme 1.1c).<sup>[29,30]</sup>

### New Intermediates from Photogenerated Phenyl Cations



**Scheme 1.1**

The thermal pathway is anyhow bounded to the exclusive formation of the singlet phenyl cation, the less synthetically appealing spin state, due to the impossibility to undergo an Inter System Crossing to the more valuable triplet. Notably in some cases the forbidden triplet state is lower in energy than its parent singlet, and their relative stability is influenced by nature and position of the substituents on the aryl ring.<sup>[18]</sup> Hence substituting the ring with Electron Withdrawing Groups (EWG, Figure 1.3), alkyls or directly considering the parent phenyl cation (R = H, Figure 1.3) stabilizes the singlet state (S) with respect to the triplet (T, if R = H S/T gap is *ca.* 21.3 kcal mol<sup>-1</sup>). On the other hand, strong electron donating substituents (EDG) in ortho and para position stabilize the triplet state with respect to the singlet. As an example, the triplet is the ground state in the case of the 4-amino-, 4-thiomethoxy-, and 4-methoxyphenyl cation (with the S1-T1 gap at 15, 7, and 6 kcal mol<sup>-1</sup>, respectively). Noteworthy, in meta derivatives carrying the same EDG the singlet is isoenergetic or slightly more stable (R = OMe) than the triplet.<sup>[18]</sup>

The generation of the aryl cation *via* photochemical means, however, enlarges the possibilities offered by thermal chemistry, allowing to populate the synthetically more promising triplet state.

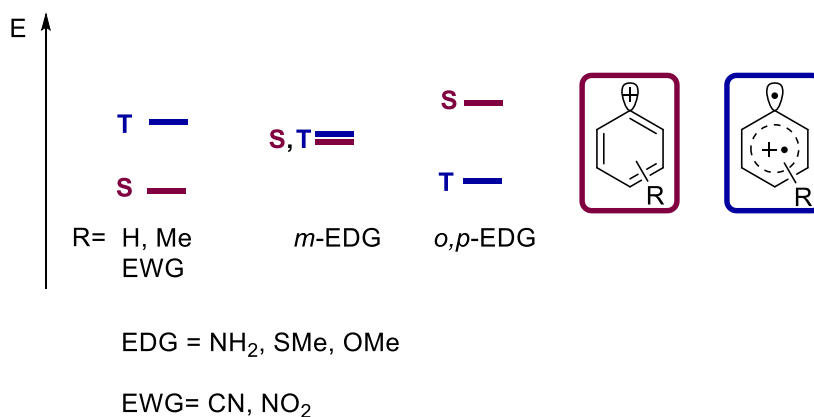


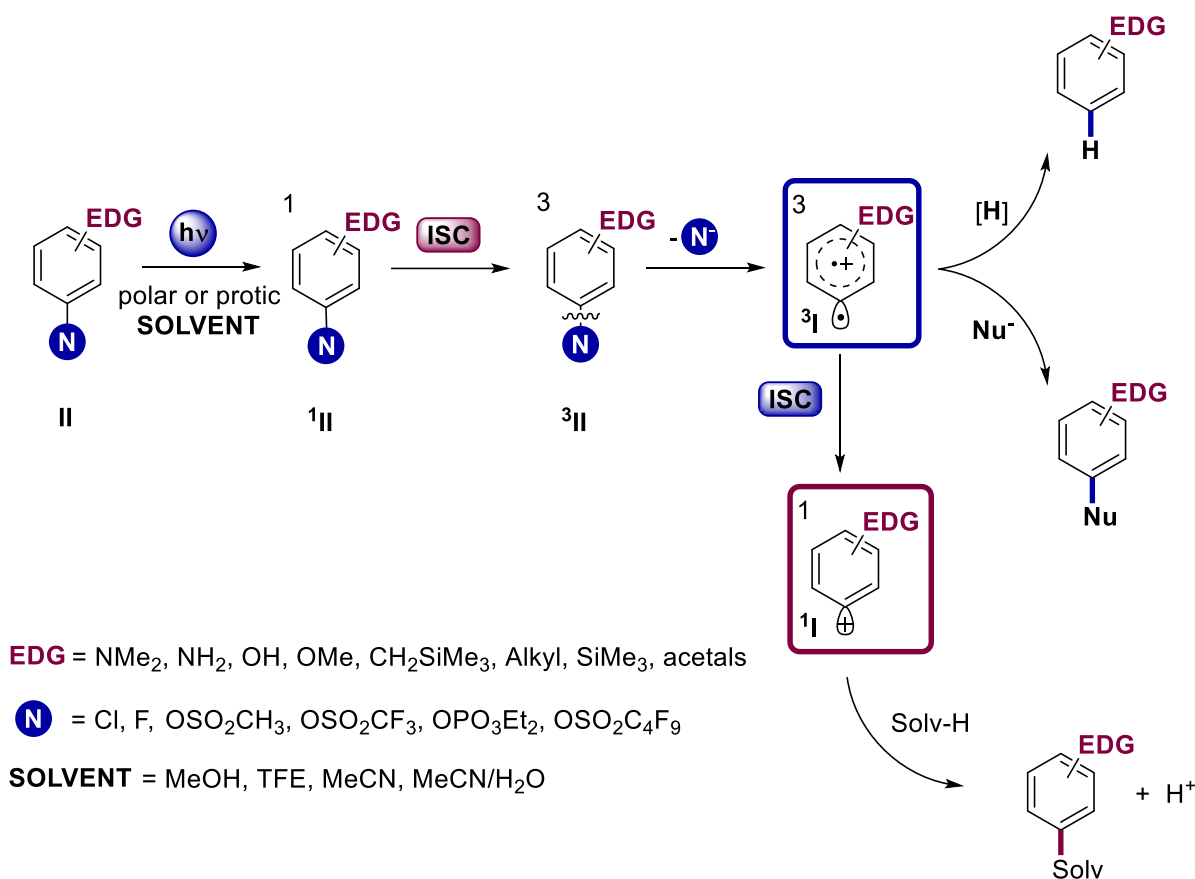
**Figure 1.3** Effect of Electron-Withdrawing (EWG) and Electron-Donating (EDG) Substituents on the energy order of the aryl cation spin-states.

## 1.2 Conditions for triplet phenyl cation photogeneration

Since 2003, a photochemical procedure that easily gives access to the triplet phenyl cation has been developed by my group,<sup>[17]</sup> allowing to enunciate a paradigm for aryl cation generators by photochemical means.<sup>[15,31–34]</sup> The molecule to be irradiated should be an electron-rich aromatic molecule, bearing an EDG group (R, Scheme 1.2) in ortho or para position to a suitable leaving group (X, Scheme 1.2). The molecule should be able to efficiently populate the triplet state through an Inter-System Crossing (*vide infra*) and the reaction must be carried out in either polar or protic solvents. Furthermore, the efficiency of the process largely depends on the nature of the leaving anion X<sup>-</sup>, on the other substituents present on the aromatic ring and on their relative positions.

The classical reaction pathway is described in Scheme 1.2. Irradiation of **II** in polar/protic media leads to a singlet excited <sup>1</sup>**II** state that efficiently populates the triplet state <sup>3</sup>**II** through ISC. At this stage the nucleofugal group X is lost in a heterolytic fashion affording the corresponding triplet aryl cation <sup>3</sup>**I**, that could be either reduced (commonly by the solvent) or trapped by a suitable π-bond nucleophile. <sup>3</sup>**I** could also undergo a further Intersystem Crossing, leading to its singlet homologue <sup>1</sup>**I**, that can be easily and unselectively trapped by the solvent.

## New Intermediates from Photogenerated Phenyl Cations



**Scheme 1.2**

Para-chloroaniline represents the perfect example of this reactivity.<sup>[17]</sup> Under irradiation with UV light this molecule exhibits an extremely high quantum yield of detachment of the chloride anion ( $\Phi_{\text{-Cl}^-} = 0.77$  in MeCN and 0.68 in MeOH). Use of laser flash photolysis showed that aryl-halogen bond cleavage happens from a triplet state. Moreover, the nature and the structure of its excited triplet state triplet was undisclosed by means of computational chemistry. UB3LYP/6-31G(d) calculations shows that para-chloroaniline in its lower triplet state possesses a puckered structure with the chlorine atom out sticking out of the benzene ring plane (Figure 1.4). Furthermore, the chloride loss is calculated to be exothermic in polar media (MeCN bulk,  $\Delta E = -31.4 \text{ kcal mol}^{-1}$ ), with a quite accessible transition state ( $\Delta E = +8.9 \text{ kcal mol}^{-1}$ ).



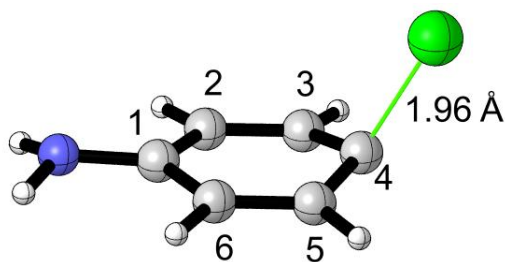
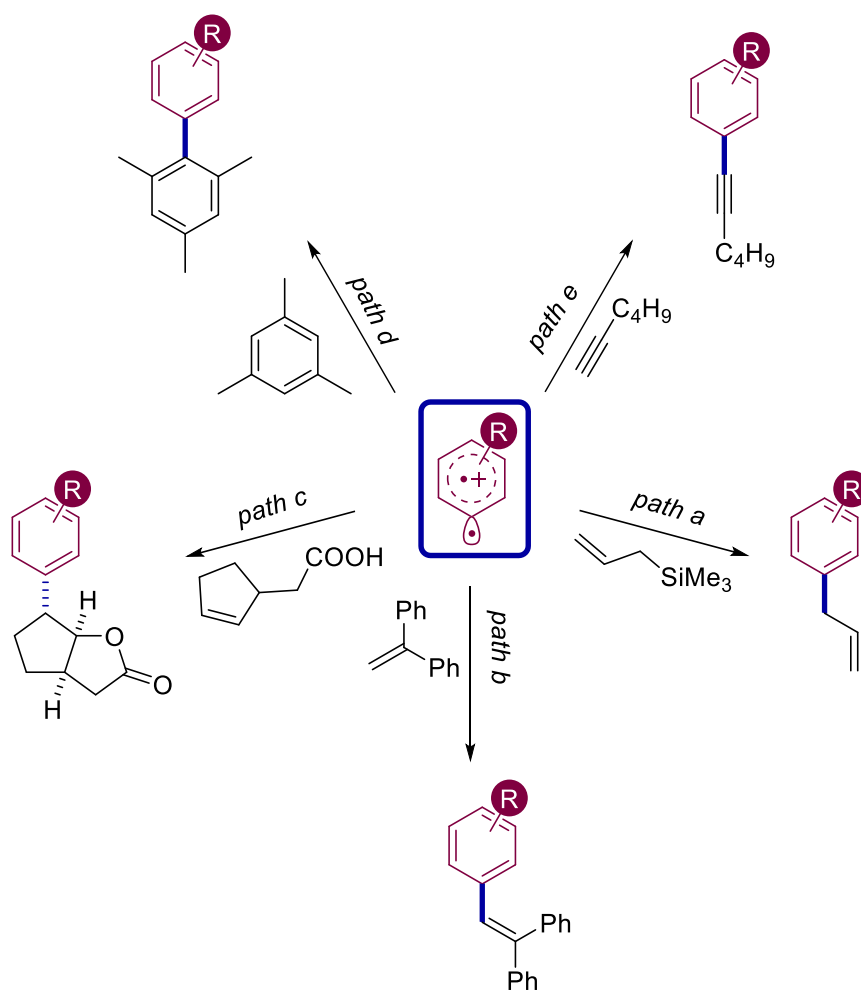


**Figure 1.4** Triplet state of para-chloroaniline. C<sub>4</sub>-Cl length (Å) at UB3LYP/6-31G(d) level is reported.<sup>[17]</sup>

The photochemical method of phenyl cation generation grants a series of improvement on the thermal procedure. Not only opens the pathway to the population of the not thermally accessible triplet state, but it does so starting from easily synthesizable and modifiable aromatic reagents. However, one great drawback that should be pointed out is the wavelength used for this photochemical reaction to occur. Usually only highly energetic UV light sources (*viz.* 254 nm or 310 nm mercury-vapour lamps) are able to promote the population of the first singlet state of the reagent (**<sup>1</sup>II**, Scheme 1.2),<sup>[35]</sup> Hence the discovery of new precursors for the photogeneration of the triplet phenyl cation that could be excited with longer wavelength is deemed to be substantial for the future development of the method.

### 1.3 Triplet phenyl cation: synthetic applications.

The chemistry of the triplet cations has revealed interesting facets. In particular, they behave as selective electrophiles, typically adding to alkenes<sup>[36–38]</sup> alkynes,<sup>[39,40]</sup> and (hetero)aromatics<sup>[41–43]</sup> thus leading to convenient, metal-free, phenylation procedures.<sup>[12,15,21,35]</sup> As an example of applicability of the intermediate, different allyl substituted molecules (including natural products such as methyleugenol and saphrole) were synthesized using allyltrimethylsilane (ATMS) as trapping reagent for the triplet aryl cation (*path a*, Scheme 1.3).<sup>[44]</sup> Use of vinyl nucleophiles led to the synthesis of compounds following a metal-free Heck approach (*path b*, Scheme 1.3), as exemplified by the reaction of the cation with diphenylethylene to form triaryl alkenes.<sup>[38,45]</sup> Furthermore, trapping unsaturated carboxylic acids (*i.e.* ω-alkenoic acids, *path c*, Scheme 1.3) results in a tandem aryl-carbon carbon-oxygen bond formation, producing a variety of cyclic products belonging to the benzyl 5-γ-lactones family.<sup>[40]</sup> Sterically crowded biphenyls could be synthesized following this approach (*path d*, Scheme 1.3), while a Sonogashira-like reaction is achieved using different alkynes as traps (*path e*, Scheme 1.3).<sup>[39]</sup>

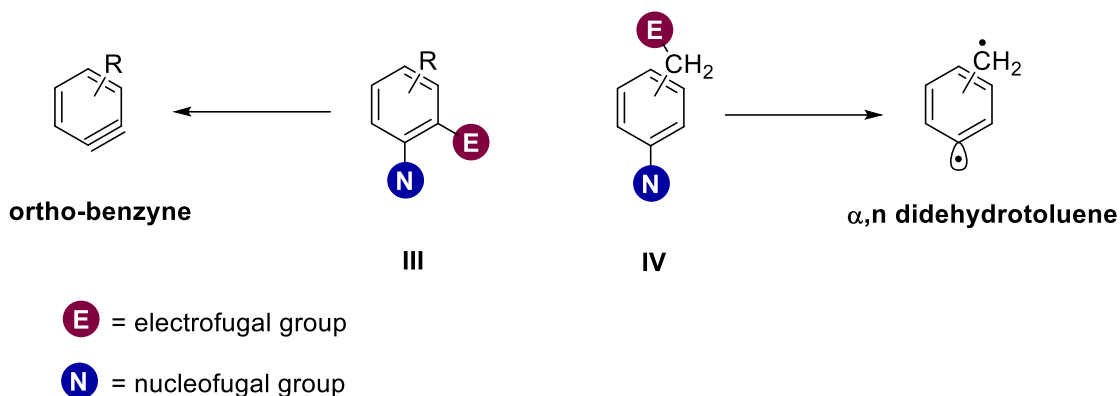


Scheme 1.3

However, the triplet aryl cation extreme reactivity and short lifetime (*ca.*  $0.3 \mu\text{s}$  in  $2 \times 10^{-4}$  M cyclohexane solution for dimethylchloroaniline)<sup>[17,46]</sup> represent a serious drawback in the arylation process. In order to achieve high yields and selectivity it is mandatory to use high concentrations of trap (around 20 equiv., apart selected cases<sup>[21,35,39]</sup>).

#### 1.4 Generation of novel intermediates from the triplet aryl cation

Owing to high reactivity and short lifetime, **3I** can further evolve to novel high energy intermediates. Indeed, we reasoned to place a suitable electrofugal group on the starting molecule (E, Scheme 1.4). The interaction between the aryl cation and E could in principle lead to the electrofugal group loss with the positive charge. The outcome of the reaction depends on the position of the electrofugal in the molecule, namely phenyl cation may split away directly giving either ortho-benzyne or didehydrotoluenes.<sup>[1,47]</sup>

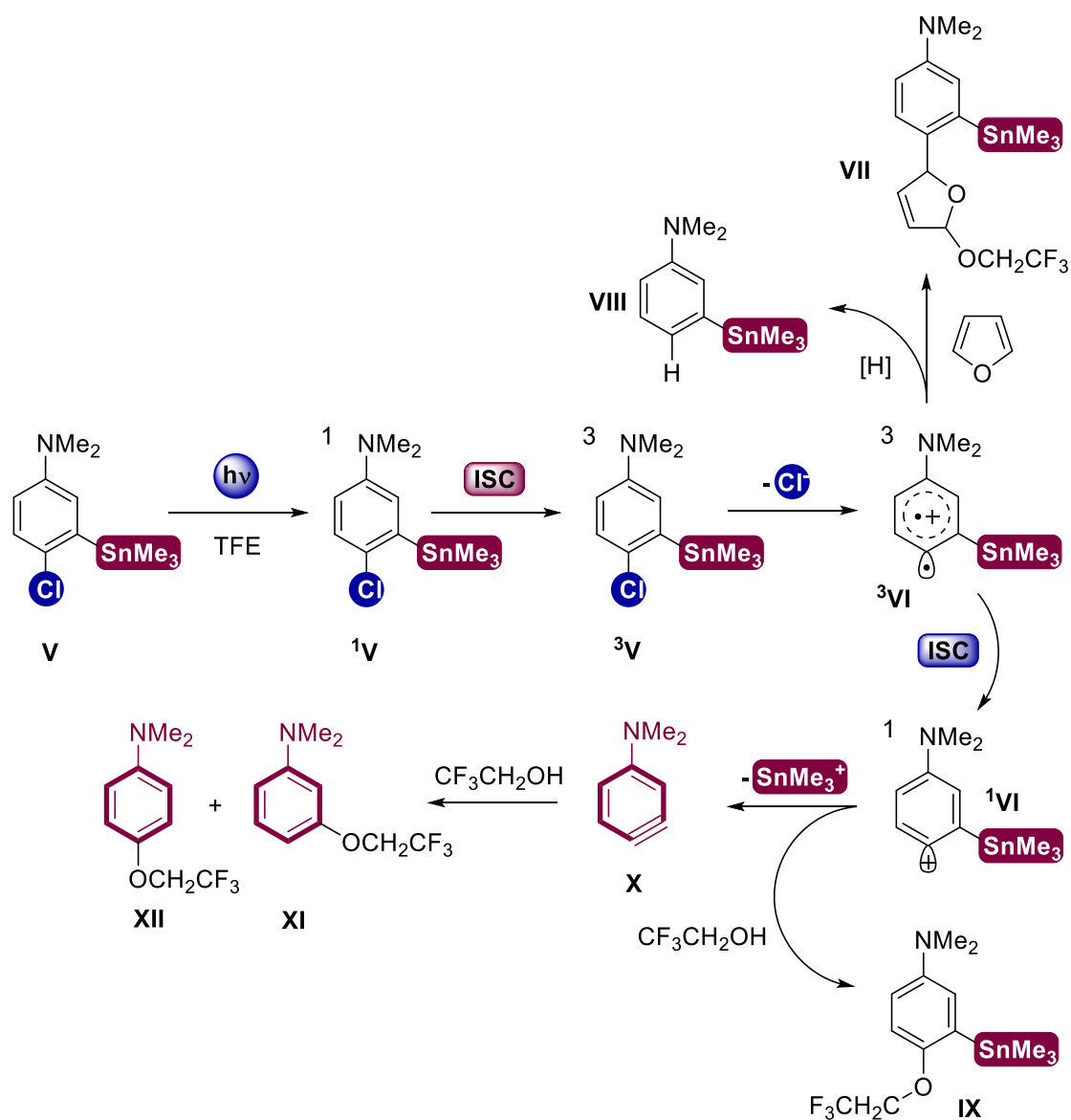


Scheme 1.4

### 1.4.1 From triplet aryl cations to benzyne

Our group demonstrated that irradiation of a compound substituted with a suitable electrofugal group in ortho position to the nucleofugal group (**III**, Scheme 1.4 left) may lead to the photogeneration of ortho-benzyne.<sup>[47]</sup>

An exemplary case is irradiation of 4-dimethylchloroaniline substituted with a  $\text{SnMe}_3$  (**V**, Scheme 1.5) group in ortho position with respect to chlorine. The mechanism beyond this transformation reveals the extreme versatility of the triplet phenyl cation. Actually, after the excitation **V** evolves to the corresponding triplet aryl cation  $^3\text{VI}$ , following the general pattern depicted in Scheme 1.2. ISC to the singlet state is favoured by the heavy atom in  $\beta$  position, that stabilizes the singlet cation  $^1\text{VI}$ . The localized charge of  $^1\text{VI}$  promotes the following demetallation<sup>[28,48]</sup> and allows for benzyne formation. Even though the photogeneration of synthetically appealing ortho-benzyne **X**<sup>[49–53]</sup> is intriguing, the applicability of the aforementioned procedure appears extremely limited, because the  $\pi$ -arynyphiles (*viz.* furan in the reported case) are quenched by the triplet aryl cation and not by benzyne itself, with the formation of **VII**. Benzyne formation was confirmed by solvolysis products **XI** and **XII**, obtained in neat TFE. Furthermore, even in these conditions the intermediates that preclude the formation of benzyne exert their chemistry, lowering the overall yield of benzyne formation.  $^3\text{VI}$  is reduced by the solvent affording **VIII**, while  $^1\text{VI}$  reacts with TFE, forming ether **IX**.

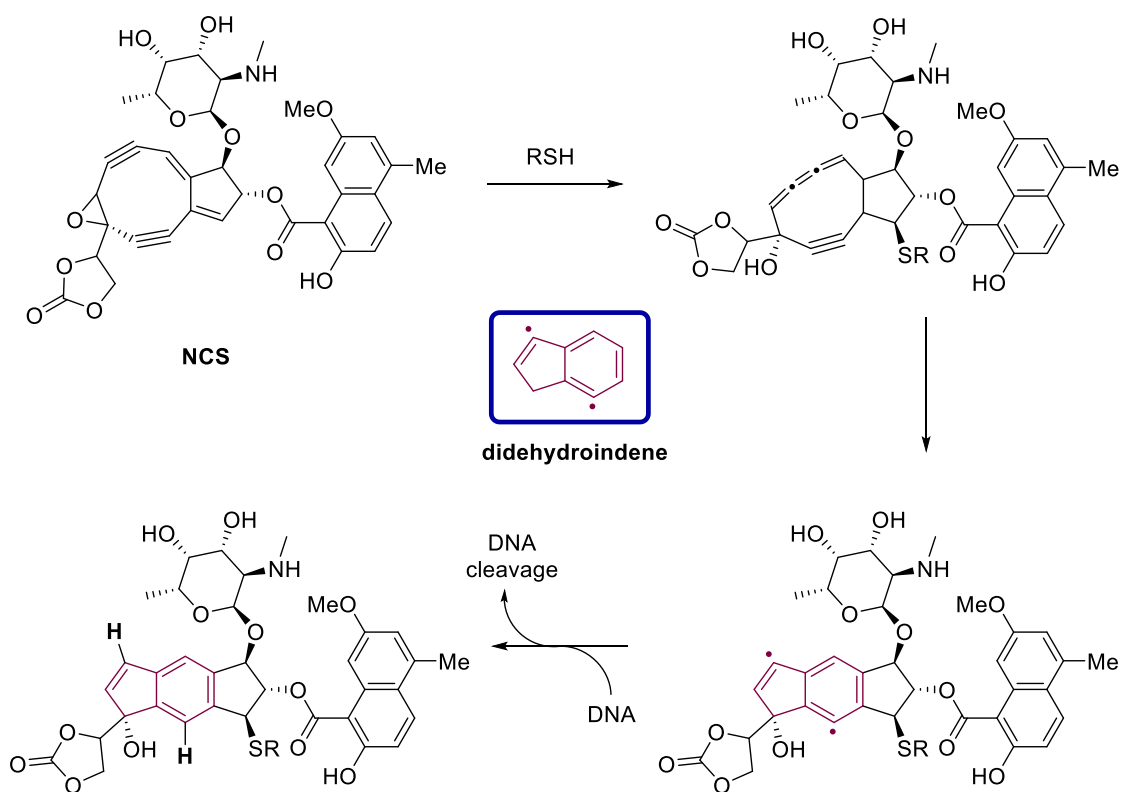


Scheme 1.5

#### 1.4.2 From triplet aryl cations to didehydrotoluenes

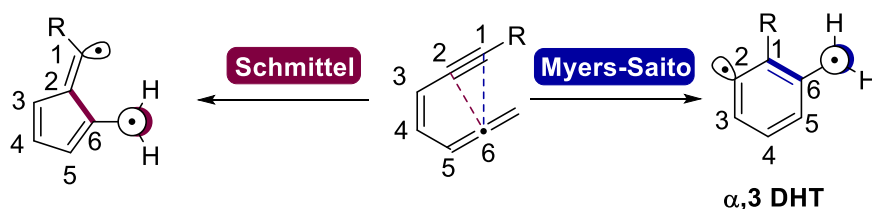
Our group also demonstrated that a  $\sigma,\pi$ -diradical, a didehydrotoluene (DHT), is formed when E is in benzylic position (Scheme 1.4, right side).<sup>[1,3,19]</sup>

The didehydrotoluene is an heterosymmetric diradical<sup>[54,55]</sup> that is used as a simple model for other diradicals such as the didehydroindene (Scheme 1.6),<sup>[56]</sup> the species involved in the antineoplastic action of neocarzinostatin (NCS Scheme 1.6).<sup>[57-64]</sup>



Scheme 1.6

The meta isomer of the didehydrotoluene ( $\alpha,3$  DHT Scheme 1.7) is the only species thermally accessible *via* the Myers–Saito cycloaromatization reaction,<sup>[57,65–67]</sup> that involves a 6–endo–dig ring closure<sup>[68]</sup> involving the C<sub>1</sub> and C<sub>6</sub> carbons of an enyne–allene.

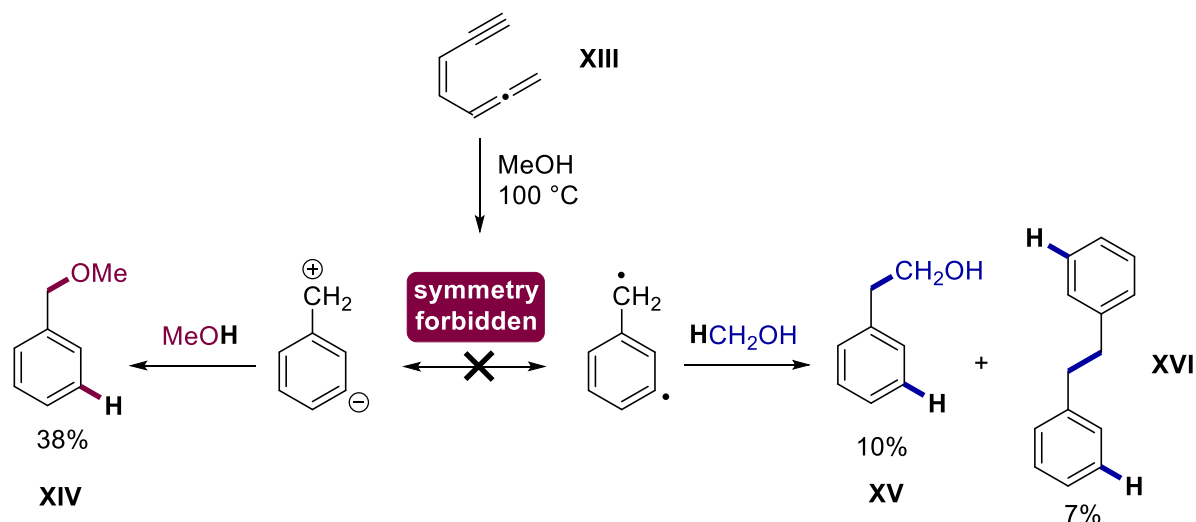


Scheme 1.7

The course of the reaction and the nature and the products obtained strongly depend on the substituent R on the enyne–allene, thus it is found that the 5–exo–dig Schmittel<sup>[69]</sup> cyclization competes with the former transformation.<sup>[54,70–72]</sup>

The DHT has attracted the interest of the theoretical chemists due to its peculiar reactivity. In turn, DHTs undergo a chemical reaction that, in accordance with previous investigations, involves a “radical” path and an “ionic” path. The distribution of the products obtained by Myers *et al.* is strongly influenced by the reaction media; the thermolysis of (Z)–1,2,4–heptatrien–6–yne **XIII** in MeOH afforded methyl benzyl ether (38%, **XIV** Scheme 1.8), generated from an ionic interaction with the solvent, phenethyl

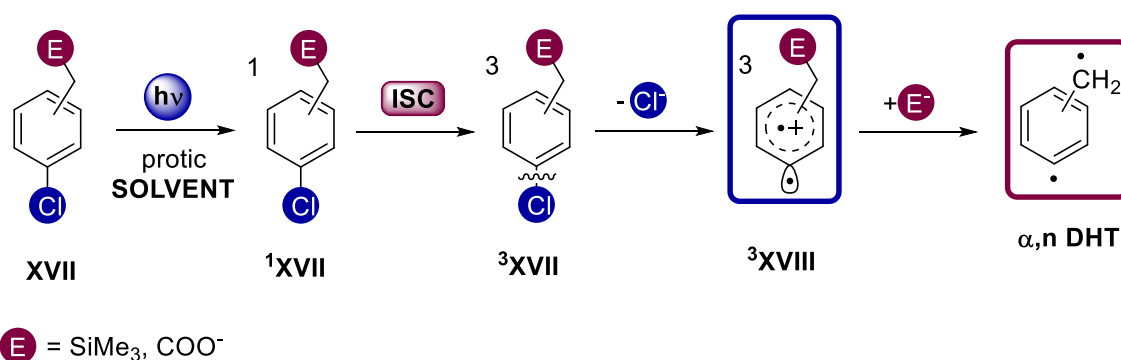
alcohol (10%, **XV** Scheme 1.8) and dibenzyl (10%, **XVI** Scheme 1.8), both originated from a radical-like reactivity.<sup>[66]</sup> The percentage of ether **XIV** and consequently the polar reactivity becomes predominant with the increasing polarity of the medium.<sup>[67]</sup> Nevertheless, adding a radical trap such as 1,4-cyclohexadiene allows the sole formation of the radical-like adducts with the olefin. This multifaceted reactivity led to different interpretation about the nature of the DHT intermediate.<sup>[67]</sup> A resonance between the diradical and the zwitterionic form of the DHT was postulated, even though such interconversion is not symmetry allowed<sup>[56,73]</sup> Carpenter hypothesize that the two reactivities originate from a nonadiabatic transition between the ground state and the excited singlet in a geometry near the transition state along the enyne-allene ring-closure reaction coordinate,<sup>[74]</sup> while our research group suggested the mediation of different spin states of the intermediate (the singlet inducing polar reactivity, the triplet the radical one).<sup>[1]</sup>



However, intrinsic weaknesses are present in the thermal approach to DHTs starting from enyne-allenes. The Myers-Saito cyclization scheme not only competes with the Schmittel cyclization but affords the sole meta  $\alpha,3$  DHT, thus limiting the scope of the reaction and the possibility to study all the three isomers of the diradical. Moreover the reagents are neither stable nor easy to synthesize and modify.<sup>[65]</sup> Therefore, novel methods should be developed in order to use accessible and easy to functionalize reagents that could grant the generation of the three isomeric DHTs.

An alternative to the Myers-Saito cycloaromatization of enyne-allenes based on the irradiation of electron rich aromatic molecules following a one-photon double elimination mechanism was developed by my group.<sup>[1,3,19]</sup> The aromatics have to bear a

nucleofugal group on the ring, namely chloride, and must be substituted with an electrofugal group E (Scheme 1.9) in benzylic position. Noteworthy the process starts from a stable aromatic derivative, rather than from a polyunsaturated compound. Indeed, the chloride **XVII** (Scheme 1.9) under irradiation populates the triplet state  $^3\text{XVII}$  via ISC from the lower excited singlet state  $^1\text{XVII}$  and heterolitically cleaves the aryl–chlorine bond. The presence of a suitable electrofugal group in benzylic position, *viz.* –TMS or –COO<sup>−</sup>, allows the triplet aryl cation  $^3\text{XVIII}$  to break the carbon–E bond either in a solvolytic fashion<sup>[1]</sup> or via an electron transfer process,<sup>[3]</sup> with subsequent formation of the desired  $\alpha,\text{n}$ -didehydrotoluenes. Moreover, it was found that the presence of protic media is mandatory for the second elimination to occur.



Scheme 1.9

Although sparse examples of generation of the three DHTs isomers from aromatics are reported,<sup>[75–78]</sup> the aforementioned method is the only one able to afford all the three  $\alpha,\text{n}$ -didehydrotoluenes isomers in solution under mild conditions.

This approach allows to gain a deeper understanding on DHTs reactivity. The analysis of the of the irradiation products of the three isomeric chlorobenzylsilanes underline a similar product distribution between the meta derivative obtained *via* the enyne–allene chemistry and the photochemical method, highlighting the intermediacy of the same reactive species.

From Table 1.1 the isomer–dependent reactivity of the DHTs can be appreciated. Noteworthy with the meta derivative the ionic pathway is mainly followed, while the para and ortho derivatives generate preferentially radical–like compounds.<sup>[1,79]</sup>

## New Intermediates from Photogenerated Phenyl Cations

		(PhCH <sub>2</sub> ) <sub>2</sub>				
		[%]	[%]	[%]	[%]	
	$\xrightarrow{\Delta}$ MeCN/H <sub>2</sub> O 9:1	47	7	7	1	-
	$\xrightarrow{h\nu}$ MeCN/H <sub>2</sub> O 9:1	38	18	20	2	14
	$\xrightarrow{h\nu}$ MeCN/H <sub>2</sub> O 9:1	4	23	2	4	25
	$\xrightarrow{h\nu}$ MeCN/H <sub>2</sub> O 9:1	2	2	0	14	39

**Table 1.1** Product distribution of the irradiation of the three isomeric chlorobenzylsilanes<sup>[1]</sup> compared to the thermolysis of the (*Z*)-hepta-1,2,4-trien-6-yne.<sup>[66]</sup> The different reactivity are highlighted by different colours, namely DHT ionic (red), DHT diradicalic (blue) and phenyl cationic (green).

The study of the mechanism of action of these diradicals represents a key issue when potential applications of such intermediates are considered.

Thus, in order to widen the scope of photochemical precursors of the didehydrotoluenes, to gain a deeper knowledge on their reactivity and to found potential applications in medicinal chemistry, the development of new nucleofugal and electrofugal groups are deemed worthwhile.



## 1.5 Aim of the Thesis

This thesis is focused on the chemistry of the triplet phenyl cation and on their use in the generation of useful intermediates such as didehydrotoluenes, (DHTs). Therefore, the first part of the thesis will revolve around the study of new nucleofugal and electrofugal groups that are able to afford DHTs following the photochemical strategy developed in my laboratory. Moreover, due to the great limitations on the applicability of the triplet aryl cation chemistry owing to the highly energetic wavelengths needed for its generation, a part of the thesis will be devoted on the study of novel precursors for the solar–light promoted generation of this species. The mechanistical issues underlying the photogeneration of the triplet aryl cation remain, however, partially undisclosed, therefore an in–deep computational approach to the photochemistry of the chloroanilines will be considered to shed more light on the photoreactivity of the chloroaromatics. The last part of the thesis will be focused on the period of the PhD spent at the University of Regensburg under the supervision of Professor Dr. B. König, with the aim of studying novel approaches to different intermediates such as benzyne and aryl radicals by means of photocatalysis.

In particular, the thesis will be divided in the following chapters:

- **Chapter 2 Competing pathways in the photogeneration of didehydrotoluenes from (Trimethylsilylmethyl)aryl sulfonates and phosphates.** The chapter will be devoted on the development of new nucleofugal groups for DHTs photogeneration, namely sulfonates and phosphates.
- **Chapter 3 pH dependent photogeneration of didehydrotoluenes from chlorobenzylphosphonic acids.** The chapter will present the study of a novel electrofugal group for the photochemical strategy towards didehydrotoluenes, *viz.* the phosphonic acid moiety.
- **Chapter 4 Wavelength selective generation of Aryl Radicals and Aryl Cations for metal-free photoarylations.** In the chapter the photochemistry of the arylazosulfones for the photogeneration of synthetically appealing intermediates will be discussed.
- **Chapter 5 Computational study on the excited state deactivation mechanism of the chloroanilines.** In the chapter a computational approach to widen the knowledge of the excited state chemistry of the chloroaromatics will be discussed.
- **Chapter 6 Photocatalytic approach to intermediate generation.** The chapter deals with the period spent Regensburg in Prof König’s group and will be divided into two sections: a first one dedicated to the development of a Photo-Meerwein approach to

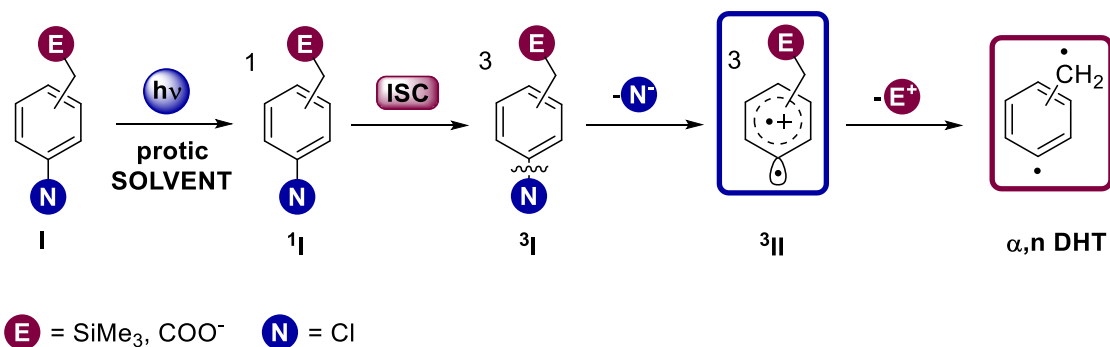
### **New Intermediates from Photogenerated Phenyl Cations**

the synthesis of Isochromanones and Isochromenones, a second one will regard the attempts to generate benzyne by means of photocatalysis.

## 2 COMPETING PATHWAYS IN THE PHOTO GENERATION OF DIDEHYDROTOLUENES FROM (TRIMETHYLSILYLMETHYL) ARYL SULFONATES AND PHOSPHATES

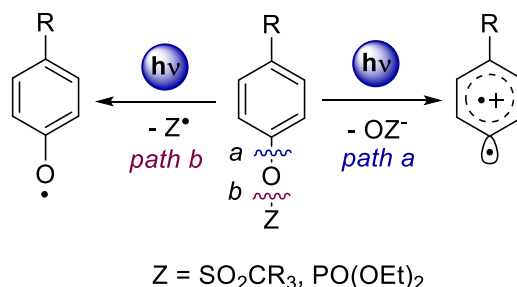
### 2.1 Introduction

In order to widen the scope of DHT precursors we initially focused on the discovery of novel nucleofugal groups (N, Scheme 2.1).



Scheme 2.1

Our attention was thus drawn by the inorganic esters, namely phosphates and sulfonates, known to be potential substrates for the triplet aryl cation photogeneration (<sup>3</sup>II, Scheme 2.1.)<sup>[80]</sup> Indeed, we (and others) have found that those groups of general formula Ar–OZ, operate as nucleofugal leaving groups in place of chlorides (*path a*, Scheme 2.2),<sup>[39,40,81,82]</sup> in competition with ArO–Z homolytical bond cleavage (*path b*).<sup>[83–88]</sup>



Scheme 2.2

The easy availability of such compounds makes the choice appealing, although the scope is little known. As a contribution to the clarification of the matter, we decided to carry out a systematic study of some esters of (trimethylsilylmethyl)phenols, more precisely, mesylates (**1a-c**), triflates (**2a-c**), and diethylphosphates (**3a-c**, Chart 2.1), and to supplement product studies with a computational investigation.

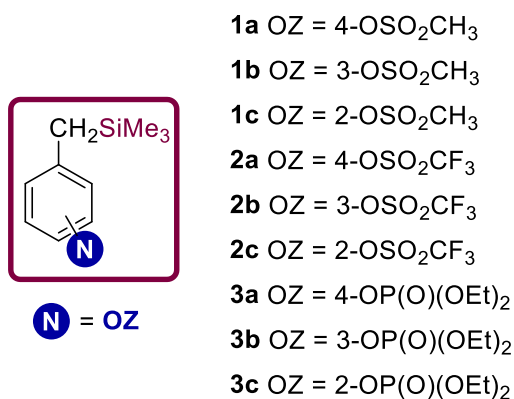
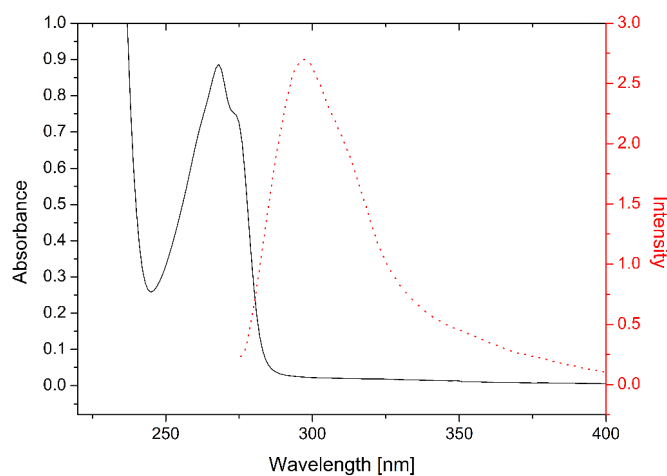


Chart 2.1

## 2.2 Results

### 2.2.1 Experimental studies

The esters used were prepared by known procedures (see Chapter 7.1.1). All of the compounds examined have a large absorption envelope with some vibrational structure ( $\lambda_{\text{max}}$  around 270 nm, see Figure 2.1 for **2a**, Figure 7.1–Figure 7.9 for the others), and a moderate Stoke's shift (20–40 nm, or 3 to 5 · 10<sup>3</sup> cm<sup>-1</sup>).



**Figure 2.1** Absorption (black) and emission (red) spectra of aryl mesylate **2a** ( $2 \times 10^{-3}$  M, MeOH).

<b>Table 2.1 Photophysical data about phenyl esters 1–3</b>				
ArN	Stoke's shift (MeOH, 10 <sup>3</sup> cm <sup>-1</sup> )	$\lambda_F$ , nm ( $\Phi_F$ , MeOH)	$\lambda_F$ , nm ( $\Phi_F$ , C <sub>6</sub> H <sub>12</sub> )	$\Phi_{-1}$ (MeOH)
<b>1a</b>	4.25	305 (0.035)	300 (0.036)	0.61
<b>1b</b>	3.64	297 (0.003)	296(0.009)	0.25
<b>1c</b>	4.83	309 (0.006)	304 (0.005)	0.14
<b>2a</b>	3.74	299 (0.003)	295 (0.003)	0.65
<b>2b</b>	3.84	300 (0.003)	294 (0.004)	0.27
<b>2c</b>	5.14	309 (0.02)	304 (0.03)	0.35
<b>3a</b>	3.73	304 (0.23)	302 (0.28)	0.18
<b>3b</b>	3.24	294 (0.21)	296 (0.27)	0.02
<b>3c</b>	3.63	298 (0.12)	298 (0.13)	0.07

The physical properties of the excited states depended on the structure of the ester, but by no more than an order of magnitude, while the medium (cyclohexane and methanol) had a much smaller influence. The fluorescence quantum yield was found to be very low for sulfonates **1,2**, but up to 28% for the phosphates (Table 2.1).

The photochemical reactions were carried out both by direct irradiation at 254 nm and by acetone sensitization. Previous studies on related compounds suggest that decomposition is faster in water–methanol mixed solvents,<sup>[1]</sup> and this was confirmed for **1a**, but since some of the esters were not sufficiently soluble in that medium, the irradiations in Table 2 were carried out in neat methanol, in order to obtain a sensible comparison. All of the compounds considered were quite photosensitive, with a disappearance quantum yield ( $\Phi_{-1}$ ) higher than 0.6 for the para– mesylate and triflate, somewhat lower for the meta– and ortho– isomers of the same esters, and much lower for the phosphates (0.02 to 0.18, see Table 2.1). The product(s) obtained at elevated ( $\geq 80\%$ ) conversion are gathered in Table 2.2. Upon direct irradiation, a series of products conserving the trimethylsilyl moiety predominated. These included phenol **4**, formed via detachment of the sulfonyl group, and the sulfonylphenol **4'**, (only from triflate **2a**), as well as products where the SO<sub>2</sub> group had been lost, *viz.* the trifluoromethylphenol (**4''**) and the trifluoromethyl ether **4'''**, (Chart 2.2). Anisole (**5**) from the meta-phosphate (**3b**) and benzyltrimethylsilane (**6**, from reductive elimination of the ester), mostly in traces, were likewise formed. Irradiations carried out in other solvents (cyclohexane, CH<sub>2</sub>Cl<sub>2</sub>, ethylacetate, acetonitrile)

## New Intermediates from Photogenerated Phenyl Cations

showed that only TMS-conserving products were formed in the case of triflate **2a** (Table 2.2).

Under acetone sensitization, on the other hand, products resulting from both desilylation and reductive elimination of the ester group predominated (Chart 2.2). These included toluene (**7**), diphenylethane (**7'**), the two alcohols **7''** and **7'''** and benzyl ether **8**. Some of the compounds underwent desilylation only, whether accompanied by hydrolysis of the ester group or not (esters **9aMs**, **9aPhos**, **9c**, phenols **9'** and **9''**). Separate experiments showed that alcohol **9'** resulted from the secondary photoreaction of **4**. Noteworthy, the presence of oxygen in the direct irradiation of **2a** in neat methanol affected only slightly the product distribution whereas the photoreactivity of this triflate was completely suppressed under oxygenated sensitized conditions.

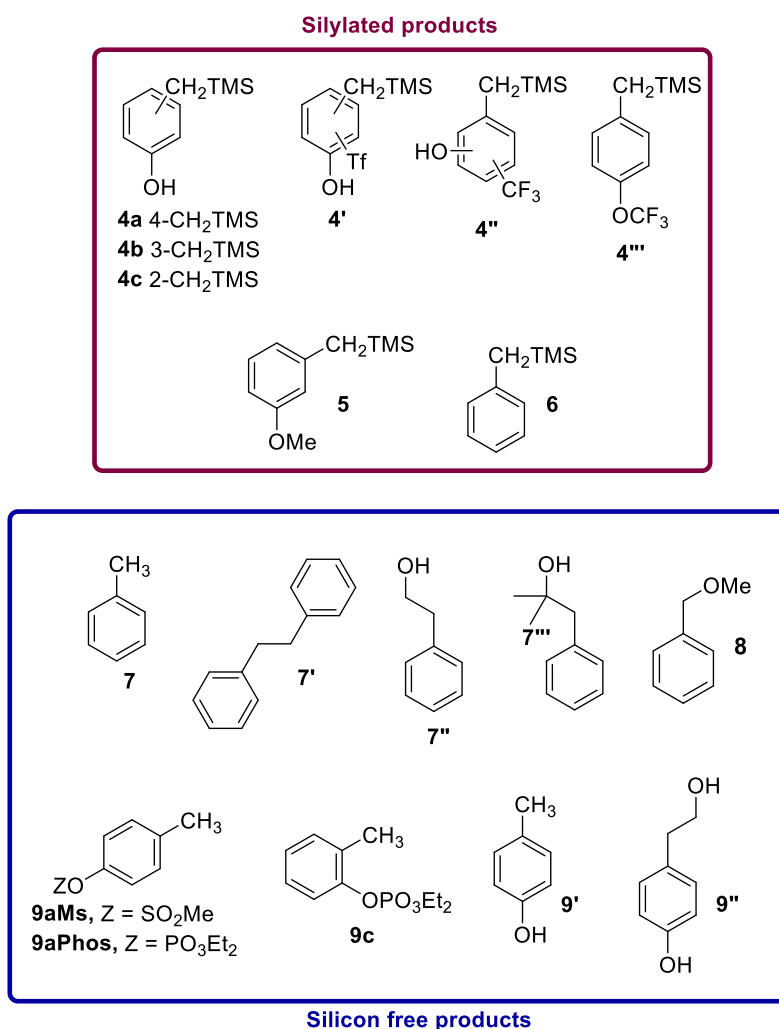


Table 2.2. Products from the irradiation of phenyl esters 1-3 (0.025 M). <sup>[a]</sup>					
ArN	Conditions	Silylated products (% yield)		Silicon-free products (% yield)	
		Ar-O moiety maintained	Ar-O moiety not maintained	Ar-O moiety not maintained	Ar-O moiety maintained
<b>1a</b>	Direct irradiation	<b>4a</b> (38)			
	Sensitized irradiation <sup>[b]</sup>	<b>4a</b> (4)	<b>6</b> (tr)	<b>7''</b> (8), <b>7'''</b> (8)	<b>9aMs</b> (23), <b>9'</b> (6), <b>9''</b> (8)
<b>1b</b>	Direct	<b>4b</b> (44)			
	Sens. <sup>[b]</sup>	<b>4b</b> (93)			
<b>1c</b>	Direct	<b>4c</b> (28)			
	Sens. <sup>[b]</sup>	<b>4c</b> (28)			
<b>2a</b>	Direct	<b>4a</b> (16), <b>4'</b> (9), <b>4''</b> (13), <b>4'''</b> (33)	<b>6</b> (tr)		<b>9'</b> (11)
	Direct <sup>[c,d]</sup>	<b>4'</b> (7), <b>4''</b> (7), <b>4'''</b> (26)			
	Direct <sup>[e]</sup>	<b>4a</b> (7), <b>4'</b> (9), <b>4''</b> (9), <b>4'''</b> (44)	<b>6</b> (tr)		
	Direct <sup>[f,d]</sup>	<b>4'</b> (13), <b>4''</b> (9), <b>4'''</b> (23)			
	Direct <sup>[g,d]</sup>	<b>4'</b> (5), <b>4''</b> (7), <b>4'''</b> (20)			
	Direct <sup>[d,h]</sup>	<b>4'</b> (11), <b>4''</b> (16), <b>4'''</b> (59)			
	Sens. <sup>[b]</sup>		<b>6</b> (tr)	<b>7</b> (8), <b>7'</b> (tr), <b>7''</b> (42), <b>7'''</b> (25)	
Sens. <sup>[b,c,i]</sup>	-	-	-	-	
<b>2b</b>	Direct	<b>4b</b> (27)	<b>6</b> (6)	<b>8</b> (4)	
	Sens. <sup>[b]</sup>	<b>4b</b> (tr)	<b>6</b> (tr)	<b>7''</b> (21), <b>7'''</b> (15) <b>8</b> (51)	
<b>2c</b>	Direct	<b>4c</b> (8), <b>4''</b> (22)	<b>6</b> (tr)		
	Sens. <sup>[b]</sup>		<b>6</b> (tr)	<b>7''</b> (10), <b>7'''</b> (15)	
<b>3a</b>	Direct			<b>7'</b> (1), <b>7''</b> (9)	
	Sens. <sup>[b]</sup>			<b>7''</b> (21), <b>7'''</b> (37)	<b>9aPhos</b> (6)
<b>3b</b>	Direct	<b>4b</b> (23), <b>5</b> (3)	<b>6</b> (5)		
	Sens. <sup>[b,i]</sup>	-	-	-	-
<b>3c</b>	Direct	<b>4c</b> (13)	<b>6</b> (tr)	<b>7'</b> (tr), <b>7''</b> (5)	<b>9c</b> (5)
	Sens. <sup>[b]</sup>			<b>7''</b> (30), <b>7'''</b> (28)	

[a] A 0.025 M solution of 1-3 in MeOH (direct irradiation at  $\lambda = 254$  nm and sensitized irradiation at  $\lambda = 310$  nm) using N<sub>2</sub>-purged solution. Conversion  $\geq 80\%$ . [b] Acetone 10%<sub>v/v</sub> was used as sensitizer. [c] Irradiation carried out in O<sub>2</sub>-saturated solution. [d] Conversion between 50 and 70%. [e] Irradiation in cyclohexane. [f] In CH<sub>2</sub>Cl<sub>2</sub>. [g] In MeCN. [h] In ethyl acetate. [i] No significant reagent consumption was observed.

## 2.2.2 Computational study

Support was sought in computation, by using DFT at the theory level CPCM–B3LYP/6-31G(d), adopting an unrestricted (U) formalism when triplet states were under consideration. The ground state  $S_0$  of benzylsilanes **1-3** is in every case planar, with the ester oxygen lying, as one might expect, in the plane of the aromatic ring (see Figure 2.2a for 4-substituted triflate **2a**, Figure 7.11 Figure 7.13 for the other ones). A deep change was apparent in the triplet states  $T_1$ , which are puckered at the optimized minima, the ring carbon bearing the ester group protruding out of the aromatic plane by *ca.*  $10^\circ$ , while the aryl–O bond is further tilted by *ca.*  $30^\circ$  (Figure 2.2b). The groups present in these molecules further introduce a variety of conformations.

Thus, in puckered triplets the  $\alpha$  conformer has the TMS and the ester moiety protruding out of the plane on the same side, while in the  $\beta$  conformer they are on opposite sides (Figure 2.2b and Figure 7.10). The Ar–OZ bond length was *ca.*  $0.06 \text{ \AA}$  longer than in the ground state and the oxygen atom bears some negative charge ( $-0.23$ , see again Figure 2.2b). The question was whether heterolytic cleavage of the aryl–O bond was a possibility.

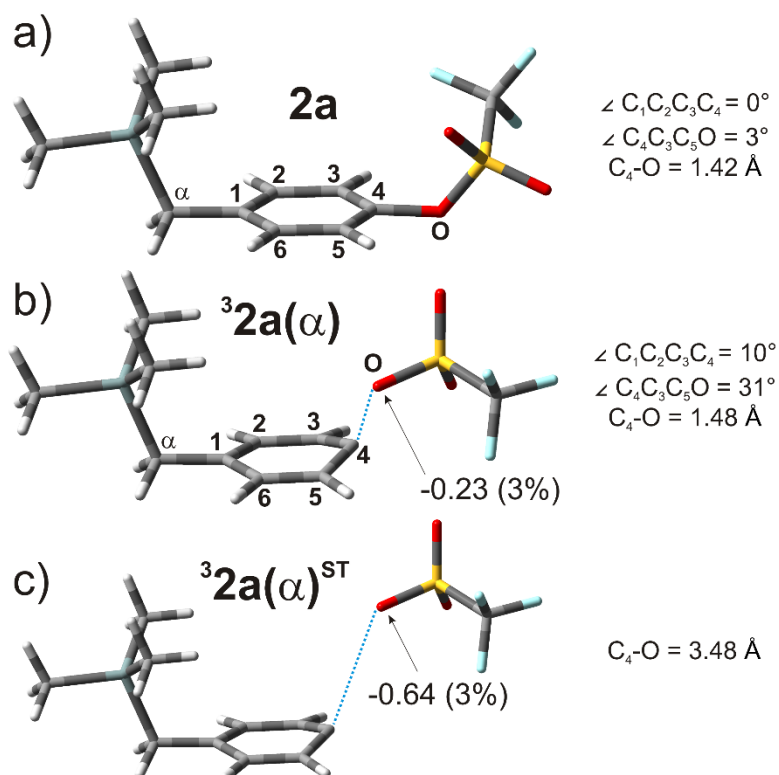


**Figure 2.2** Optimized structures and relevant parameters for: a) ground state **2a**, b) first triplet excited state  $^3\mathbf{2a}$  and c) first triplet excited state  $^3\mathbf{2a}$  upon stretching of the Ar–O bond up to *ca.*  $3.5 \text{ \AA}$  ( $^3\mathbf{2a}^{ST}$ ). The arrows indicate the charge (q<sub>ESP</sub>) on the Ar–O atom (the spin density on the same atom is listed in parentheses).



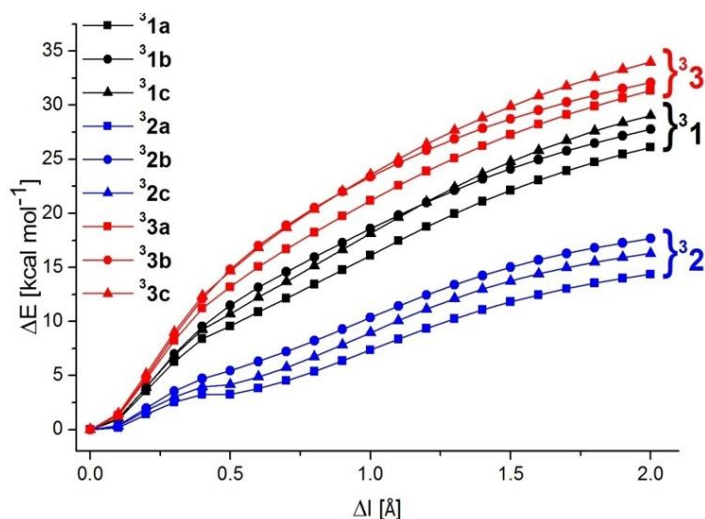


**Figure 2.3** Calculated energy profile related to the elongation of the Ar–OZ bond by *ca.* 2 Å, from the equilibrium value up to *ca.* 3.5 Å in compounds <sup>3</sup>1-<sup>3</sup>3.

This point was answered by calculating the increase in energy related to the elongation of the Ar–OZ bond by *ca.* 2 Å, from the equilibrium value up to *ca.* 3.5 Å (Figure 2.2c). Relevant parameters for the “stretched” structures are reported in Figure 2c for <sup>3</sup>2a( $\alpha$ ) (see <sup>3</sup>2a( $\alpha$ )<sup>ST</sup>), and in Figure 7.11Figure 7.13 for the others. The most telling point was that the negative charge on the oxygen atom more than doubled upon stretching, rising to  $> -0.60$ . By contrast, the spin density on the same atom remained almost unchanged or diminished for triflates (lower than 5%),<sup>[19]</sup> while it increased for mesylates and phosphates, reaching a value in the 15 to 25% range. The energy profile obtained for each of the compounds considered is reported in Figure 2.3, where the energy change ( $\Delta E$ , kcal mol<sup>-1</sup>) associated with the elongation of the title bond with respect to the equilibrium geometry ( $\Delta l$ , Å) is plotted. As can be seen, the energy barrier confronted was 25 to 29 kcal mol<sup>-1</sup> for mesylates, 13 to 19 kcal mol<sup>-1</sup> for triflates and 31 to 34 kcal mol<sup>-1</sup> for phosphates.

## 2.3 Discussion

The lowest singlet excited state in esters **1** to **3** appears to be of  $\pi\pi^*$  character as is almost always true for aromatic molecules. Fluorescence is an important deactivation mechanism for phosphates ( $\Phi_F$  0.12 to 0.28, Table 2.1), which explains the poor reactivity of these compounds, but not for the sulfonates. The photophysical properties in methanol and cyclohexane parallel each other closely, whereas the chemistry changes completely in the polar solvent and proceeds via the triplet. Taken together, these results support the

conclusion that the singlet excited state nature (a  $\pi\pi^*$  state) remains the same in all of the derivatives studied, while a triplet, also  $\pi\pi^*$ , is formed by ISC.

With all of the compounds examined, except for **1a**, two main photochemical processes occur, *viz.* homolytic cleavage of the ArO-Z bond to give a phenoxy and a sulfonyl or phosphonyl radical and heterolytic fragmentation of the Ar-OZ bond. That sulfonate aryl esters, in analogy with acyl aryl esters,<sup>[89]</sup> undergo homolytic cleavage to radical pair **10-O•** **Z** has been previously documented in the literature.<sup>[80]</sup> Phenol **4** and sulfonyl phenol **4'** arise from this path. In a variation of it, the triflyl radical fragments to yield a trifluoromethyl radical, and phenol **4''** as well as trifluoromethyl ether **4'''** from their recombination. The process involves the singlet excited state, apparent from the fact that these compounds predominate by direct irradiation, but not upon acetone sensitization, and further from the lack of a dependence on the polarity of the medium.

With triflates and mesylates, the fluorescence yield decreases by one to two orders of magnitude. As mentioned, the triplet state reactions differ from those of the singlet, as shown by the complete change in the chemistry under sensitized conditions, particularly with the para- derivatives. The first triplet formed is a  $\pi\pi^*$  state and the computational analysis above strongly supports the conclusion that in a polar medium heterolytic cleavage occurs in this case, since stretching of the Ar-OZ bond is accompanied by a marked charge separation. The prediction that this cleavage process is more efficient for triflates than for the other two families studied (compare the energy involved in Figure 2.3) is fully borne out by experiment and the barrier is very close to that calculated for the corresponding chlorides.<sup>[19]</sup> It is thus reasonable that the quantum yields should be of the same order of magnitude. Under sensitized conditions, a triplet state is clearly involved in the process as demonstrated by the efficient quenching with oxygen (Table 2.2).

Ar-O cleavage produces phenyl cations in the triplet state (**<sup>3</sup>11<sup>+</sup>**). In the presence of hydrogen-donating solvents, such as methanol, such species are known to be reduced. In this case, a rudimentary indication of such a process is given by the formation of traces of benzyltrimethylsilane (**6**) in most of the reactions considered. In the absence of a specific trap, however, the fastest reaction is elimination of the trimethylsilyl cation to give didehydrotoluenes **<sup>3</sup>12**. The optimized structure of cation **<sup>3</sup>11<sup>+</sup>** has the CH<sub>2</sub>-SiMe<sub>3</sub> bond perpendicular to the molecular plane and the electronic structure ( $\sigma^1\pi^5$ )<sup>[18,22,90,91]</sup> is similar to that of the benzyltrimethylsilane radical cation ( $\pi^5$ ) produced by electron

transfer. For both intermediates, desilylation is facile and overcomes a modest barrier (18 to 27 kcal mol<sup>-1</sup>).<sup>[19,92,93]</sup>

Previous investigations on DHTs formed from the cycloaromatization of enyne-allenes had evidenced two different chemistries, *viz.* hydrogen abstraction from the solvent to form benzyl radicals (**13**) and an “ionic” path leading to nucleophile addition.<sup>[84,9]</sup> Didehydrotoluenes formed from cations <sup>3</sup>**11**<sup>+</sup> are of triplet multiplicity (<sup>3</sup>**12**) and in accordance with their radical nature, hydrogen abstraction is a favored process and products from benzyl radicals predominate (toluene **7**, diphenylethane **7'**, phenylethanol **7''**).<sup>[1,19]</sup> Particularly convincing are the results in acetone sensitized experiments, where 2-methyl-1-phenylpropane-2-ol **7'''** has been observed. This arises from the competitive trapping of the Me<sub>2</sub>C<sup>•</sup>OH radical (from the photochemical reaction of acetone with MeOH) with radical **13**, and further supports the presence of the latter species.

In the case of meta-triflate **2b**, however, benzyl ether **8** is the main product. This is the expected product from the “ionic” path and it is tempting to attribute this change in reactivity to fast ISC to <sup>1</sup>**12**, actually the ground state in this intermediate.<sup>[19]</sup> The different behaviour of the meta-DHT may be viewed as another manifestation of the ‘meta effect’ in aromatic compounds that has been evidenced in many photochemical reactions.<sup>[20,94-97]</sup> Further notice that in the case of meta-phosphate, a small amount of (m-methoxybenzyl)trimethylsilane **5**, resulting from the trapping of singlet phenyl cation <sup>1</sup>**11b**<sup>+</sup>, was obtained. A further exception to the generalization above is that of mesylate **1a**. This is the fastest reacting substrate, but leads to a complex mixture and degradation. The main product under sensitized conditions is the desilylated ester **9aMs**. In view of the reaction sequence proposed above, this is not unreasonable, since the Ar-OZ cleavage has to confront a high barrier in this case (compare Figure 2.3) and this opens the path to homolytic desilylation to yield radical **14**.<sup>[98,99]</sup>

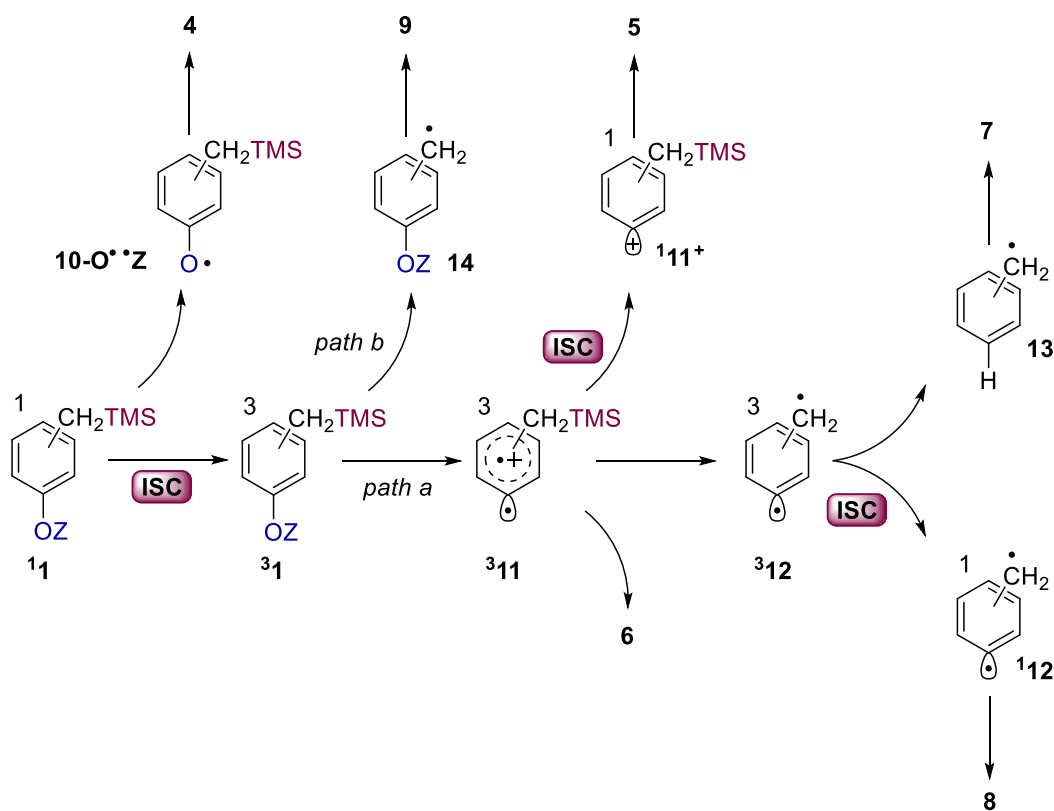
Summing up, this work greatly enlarges the scope of our initial report on chlorobenzylsilanes and clarifies the range of possibilities for photochemical access to DHTs. Thus, aryl sulfonates and, though with a lower efficiency, phosphates can be used in place of halides for the photochemical generation of DHTs via phenyl cation intermediates (*path a* in Scheme 2.3). However, this change may introduce side paths, such as fluorescence (important for phosphates, up to 28% for the para-isomer) and chemical reaction from the singlet state, *viz.* homolytic fragmentation, important for mesylates, up to 20% for the para-isomer (*path b* in Scheme 2.3). *Path a* occurs exclusively on the triplet surface, and triplet sensitization is a useful way to enable this

path, as apparent in particular with the *o*- and *p*-triflates, where acetone sensitization shifts the reaction from almost fully singlet to almost fully triplet. However, in several cases the high energy of such triplets (75–78 kcal mol<sup>-1</sup>, calculated; see Table S3) compared with that of acetone (78.9 kcal mol<sup>-1</sup>, experimental)<sup>[80]</sup> makes this procedure ineffectual under "sensitized conditions".

The trimethylsilyl group is confirmed as an excellent leaving group.<sup>[92,93]</sup> Virtually all of the triplet cations fragmented to give the didehydrotoluene and only traces of **6** were left to indicate the role of the phenyl cation as the intermediate.

The proposed reaction sequence applies regardless of the relative positions of nucleofugal and electrofugal groups, thus giving access to  $\alpha,2$ -,  $\alpha,3$ - and  $\alpha,4$ -DHTs, whereas thermal cycloaromatization is useful only for the  $\alpha,3$ -didehydrotoluenes.

The  $\alpha,2$ - and  $\alpha,4$ -didehydrotoluenes react exclusively by hydrogen abstraction producing the benzyl radical **13**. With the *meta*- isomer, however, > 55% of the products comes from the "ionic" path (ether **8**). Such a manifestation of the "meta" effect finds a parallel in the small amount of singlet phenyl cation product (**5**) from the *meta*-phosphate. When homolytic cleavage of the ArO-Z bond is not favored, other processes intervene, such as desilylation in the case of **1a** (*path c*). This result demonstrates the limits of the photochemical approach.



Scheme 2.3

## 2.4 Conclusions

On the basis of the work described above, the scheme for the generation of didehydrotoluene adducts from the irradiation of **I** in polar media, via triplet  $^3\mathbf{I}$  and phenyl cation  $^3\mathbf{II}$  (Scheme 1) is thus recognized as a general scheme in aromatic photochemistry. Two powerful electrophiles are produced, triplet phenyl cations and didehydrotoluenes, the latter showing distinct diradical reactivity. Applications of these results are underway to exploit (trimethylsilylmethyl)phenyl esters as precursors for the photogeneration of aggressive diradicals for the cleavage of DNA.<sup>[12,13]</sup>

## New Intermediates from Photogenerated Phenyl Cations

# 3 pH DEPENDENT PHOTO GENERATION OF DIDEHYDROTOLUENES FROM CHLORO BENZYLPHOSPHONIC ACIDS

## 3.1 Introduction

After having enlarged the scope of didehydrotoluenes photogenerators with the discovery of a novel potential nucleofugal group X such as the triflate and to a lesser extent also mesylates and diethylphosphates, the aim of the research was shifted toward the investigation of a new electrofugal group E. Hence, the objective of the work herein presented is the pursuit of a group that could be attached to the benzylic position of the aromatic ring of our prototypical DHT precursor and, upon generation of the triplet aryl cation  $^3\text{II}$  should be able to break the E-CH<sub>2</sub>Ar bond in a heterolytic fashion.<sup>[1,100]</sup>

Among the nucleofugal group tested, chlorine atom was shown to be the most versatile and reliable one, both in direct and in sensitized irradiations,<sup>[1,79,101]</sup> thus aryl chlorides were chosen for the following work. It was proven that  $\alpha,n$  DHT generation was preferentially achieved with increased media proticity, for example, by shifting from neat alcohol to aqueous mixtures. Thus, both the fact that the generation of didehydrotoluenes is favoured in the presence of water<sup>[1,3,79,102]</sup> and the obvious interest in this solvent for medicinal application prompted us to find a charged electrofugal group for DHT precursors. In order to improve the DHT precursor solubility in physiological medium, we later found that carbon dioxide can act as an efficient electrofugal group when chlorophenyl acetic acids (COO<sup>-</sup> as the electrofugal group) are irradiated.<sup>[3]</sup> In the latter case, an intramolecular electron transfer between the COO<sup>-</sup> group and the positive charge present on the aromatic ring at the phenyl cation level made the decarboxylation very efficient.<sup>[3]</sup> In particular, upon stretching of the aryl-Cl bond of the anion  $^3\text{III}$  in its triplet state, (Figure 3.1) a zwitterionic species is formed by overcoming a small activation barrier (few kcal mol<sup>-1</sup>).  $^3\text{III}^z$  undergoes a facile intramolecular electron transfer generating a diradical structure  $^3\text{III}^D$  through a surface crossing<sup>[103]</sup> that leads the system energetically downhill to the diradical  $^3\text{IV}$ , with chloride anion detachment. Carbon dioxide loss is equally feasible from both singlet and triplet state of the diradical, thus allowing a facile benzylic bond cleavage with ensuing DHT formation.

## New Intermediates from Photogenerated Phenyl Cations

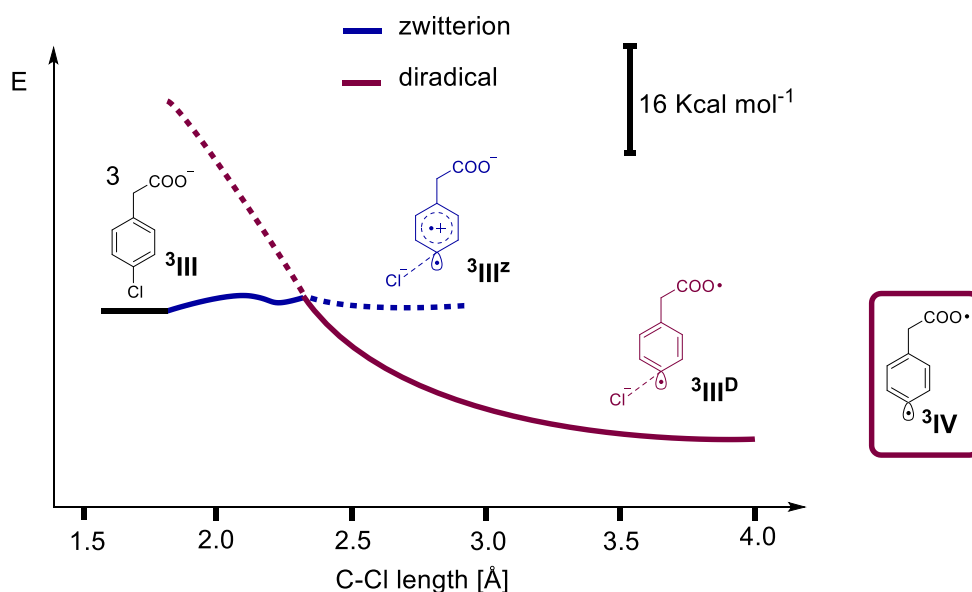
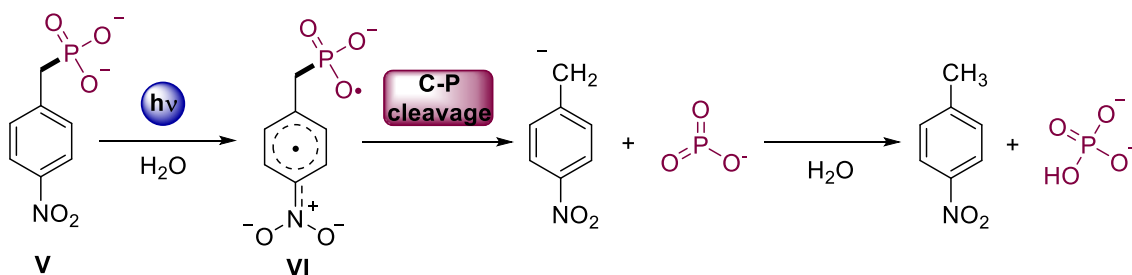


**Figure 3.1** Energy profile upon chloride anion removal from  $^3\text{III}$  obtained at the CASSCF/6-31G(d) level of theory in bulk water. Zwitterionic ( $^3\text{III}^z$ , red) and diradical ( $^3\text{III}^D$ , blue) Potential Energy Surface (PES) are represented.<sup>[3]</sup>

In this study, we focused our attention on the  $-\text{PO}_3^{2-}$  moiety in chlorobenzyl phosphonate due to the intriguing possibility to liberate phosphate anions in solution.<sup>[104–106]</sup> Albeit the photoheterolytic cleavage of the C–O bond in benzyl phosphates ( $\text{ArCH}_2\text{–OPO}_2\text{R}_2$ ) is well documented,<sup>[80]</sup> the analogous liberation of a phosphate group from a benzyl phosphonate is rarely reported.<sup>[107,108]</sup> The process is favoured only when applied to electron-poor aromatics such as nitrobenzylphosphonate ions **V** (Scheme 3.1). In a parallel fashion to the case of chlorophenylacetic acids, an intramolecular electron transfer between the nitro (acceptor) and the  $\text{PO}_3^{2-}$  (donor) group in excited **VI** was found to have a crucial role in the fragmentation of the phosphonate ester.<sup>[107,108]</sup> As a result, C–P bond cleavage produces the benzyl anion and a metaphosphate, that in water media are easily converted in toluene and into the corresponding phosphate (Scheme 3.1).



**Scheme 3.1**

As for the above, we deemed that chlorobenzylphosphonates **1a–c** can be valid candidates for  $\alpha,n$ -DHTs photogeneration (Chart 3.1). Moreover, the presence of two acidic hydrogens in compounds **1a–c** may allow an excited state pH-dependent reactivity. Thus,



different reaction pathways may be tuned at different pHs by the species present in solution, as a consequence of the protonation equilibria.

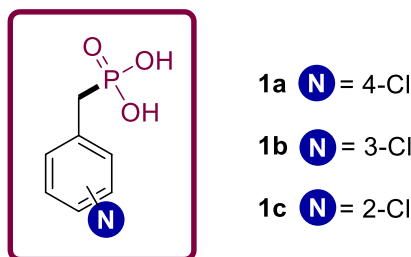
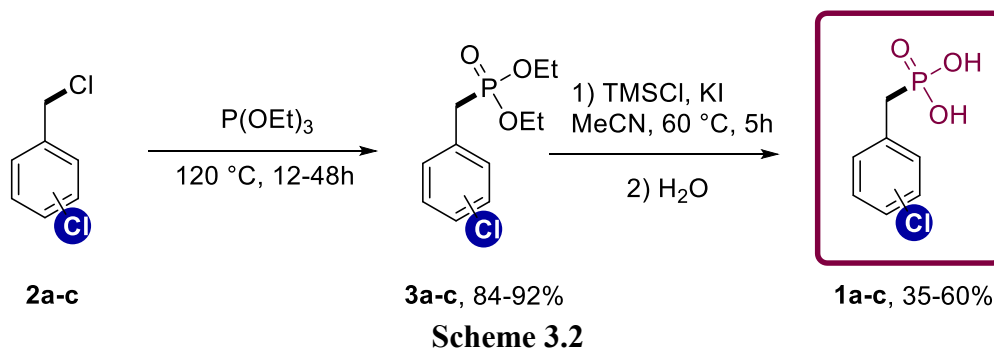


Chart 3.1

## 3.2 Results

### 3.2.1 Experimental studies

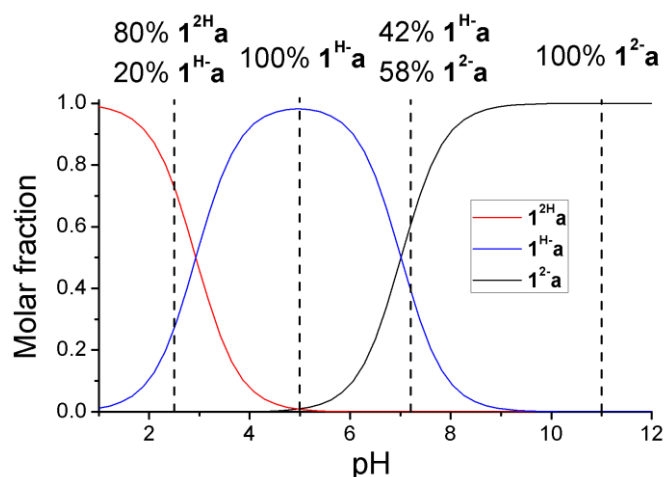
Chlorobenzylphosphonic acids **1a–c** were prepared by a two-step synthesis involving an Arbuzov reaction starting from the corresponding chlorobenzyl chlorides **2a–c** as the first step, followed by the hydrolysis of the diethyl esters **3a–c** with *in situ* generation of TMSI (Scheme 3.2).<sup>[109]</sup>



$pK_{a1}$ s of the three isomeric chlorobenzylphosphonic acids were obtained by means of potentiometric titration (Table 3.1).  $pK_{a1}$  was found to be in 2.32–2.94 range while  $pK_{a2}$  was 7.40–7.46 for **1a–c**. These values are comparable with those reported from similar phosphonic acids.<sup>[110]</sup>

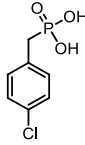
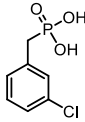
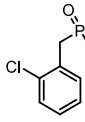
Table 3.1 $pK_a$ values obtained for <b>1a–c</b>		
	$pK_{a1}$	$pK_{a2}$
<b>1a</b>	2.32	7.40
<b>1b</b>	2.88	7.36
<b>1c</b>	2.94	7.46

With the  $pK_a$  in hand it was possible to plot the molar fraction graph of the different protonated species of the phosphonic acids at different pHs (Figure 3.2). In particular, it was found that at pH=2.5 80% of the acid **1a** is present in its fully protonated form (**1<sup>2H</sup>a**, Figure 3.2) while the remnant 20% is represented by the monoprotonated species **1<sup>H</sup>a**. The latter is the only species in solution at pH=5, while at physiological pH = 7.2 42% of **1<sup>H</sup>a** is in equilibrium with 58% of the completely deprotonated species **1<sup>2-</sup>a**, that is the sole form present at pH=11.



**Figure 3.2** Molar fraction vs pH plot for the species **1a**. **1<sup>2H</sup>a** refers to the fully protonated acid, **1<sup>H</sup>a** to the monoprotonated one and **1<sup>2-</sup>a** to the totally dissociated form of **1a**.

The absorption and emission of **1a–c** were studied at three different pHs, namely 2.5, 7.2 and 11 (Table 3.2). The photophysical properties of the chlorobenzylphosphonic acids are modified only to a little extent by pH, in particular the three isomers appear to have higher  $\epsilon$  in the fully deprotonated form at pH=11. The fluorescence quantum yields were found to be very low for the examined compounds, however the para derivative was shown to have higher  $\Phi_F$  than the others. Noteworthy this trend is often found in haloaromatics.<sup>[111,112]</sup>

Table 3.2 Main photophysical properties of compounds 1a–c at pH 2.5, 7 and 11.						
Entry	pH	$\Phi_F$	$\epsilon$ [M <sup>-1</sup> cm <sup>-1</sup> ]	$\lambda_{Abs}$ [nm]	$\lambda_{ex}$ [nm]	$\lambda_{em}$ [nm]
 <b>1a</b>	2.5	0.015	309	268	268	296
	7.2	0.018	270	268	269	298
	11	0.018	447	269	270	300
 <b>1b</b>	2.5	0.012	282	267	268	295
	7.2	0.0094	322	268	268	296
	11	0.0066	418	268	269	297
 <b>1c</b>	2.5	0.0049	269	266	272	298
	7.2	0.0055	340	267	270	296
	11	0.0044	449	268	268	297

The quantum yield of fluorescence  $\Phi_F$ , molar absorptivity  $\epsilon$ , maximum absorption wavelength  $\lambda_{Abs}$ , excitation wavelength  $\lambda_{ex}$  and emission wavelength  $\lambda_{em}$  are reported.

The photochemical reactions were conducted both by direct irradiation at 254 nm or under acetone sensitization. Two main product families were observed (Chart 3.2): a class of molecules containing the phosphorous moiety after loss of the chlorine atom (**4a–c** and **5**), and a further one including chlorine– and phosphorous–free derivatives (**6–12**).

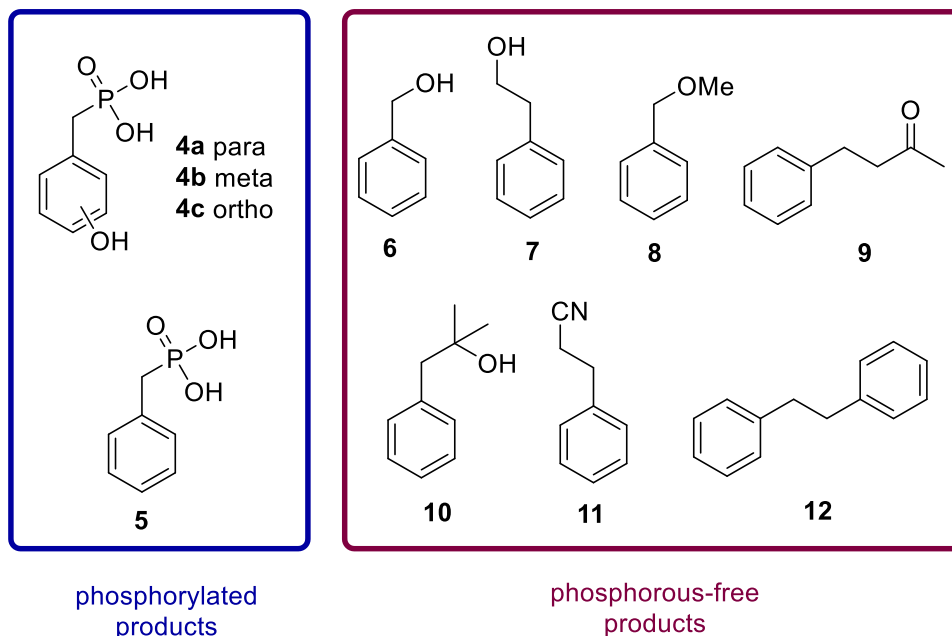
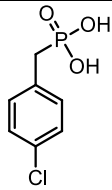


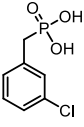
Chart 3.2

**Table 3.3** Products of irradiations and quantum yields of disappearance ( $\Phi_{-1}$ ) of para Chlorobenzylphosphonic acid **1a** (0.005 M) irradiated 1h at 254 nm.

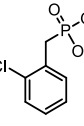
 <b>1a</b>	$\Phi_{-1}$	pH	Conversion [%]	4a [%]	5 [%]	6 [%]	7 [%]	8 [%]	9 [%]	10 [%]	11 [%]	12 [%]
Phosphate buffer <sup>[a]</sup>	0.13	2	74	73		26						
		5	77	58		32						
	0.16	7	100	47		35						
	0.26	11	100			57						
Phosphate buffer <sup>[a]</sup> Sensitized <sup>[b]</sup>		2.5	100						14			3
		7	100						17			6
		11	100						28			9
MeOH			95				32	tr.				2
MeOH–H <sub>2</sub> O 9:1			100	11			33					13
MeOH–H <sub>2</sub> O 1:9			100	35		58		4				
MeOH–H <sub>2</sub> O 1:9 Sens. <sup>[b]</sup>			100			75		5		15		
Buffer <sup>[c]</sup> –MeCN 9:1			94	34	3	30					7	tr.
Buffer <sup>[c]</sup> –MeOH 9:1			98	15			12	4				23
Buffer <sup>[c]</sup> –MGP <sup>[d]</sup>			100	28		50						
Buffer <sup>[c]</sup> –MGP <sup>[e]</sup>			100			66						

[a] 0.05 M. [b] Acetone (10% v/v) used as sensitizer, the irradiation is performed using 310 nm lamps for 1h. [c] Phosphate buffer, pH = 7.2 [d] methylglucopyranoside  $2.5 \times 10^{-3}$ M. [e] methylglucopyranoside  $5.0 \times 10^{-3}$ M.

The photochemical behaviour of compounds **1a–c** in organic media and in aqueous phosphate buffer solution at different pHs, namely 2.5, 5, 7.2 and 11, was tested. Consequently, the choice of the higher and lower pH values was bound to the use of this specific buffer. Moreover, pH 7.2 was screened to establish the reactivity of **1a–c** at physiological pH, while pH 5 was tested for the sole **1a** with the aim to obtain data of the reactivity of the monoprotonated **1<sup>H</sup>a** (see Figure 3.2). Quantum yields of photodecomposition ( $\Phi_{-1}$ ) were measured in aqueous buffer (Table 3.3–5) and the compounds exhibit comparable results ( $\Phi_{-1} = 0.07–0.16$ ) apart from **1a** at pH=11 that shows higher reactivity ( $\Phi_{-1} = 0.26$ ).

Table 3.4 Products of irradiations and quantum yields of disappearance ( $\Phi_{-1}$ ) of meta Chlorobenzylphosphonic acid <b>1b</b> (0.005 M) irradiated 1h at 254 nm									
 <b>1b</b>	$\Phi_{-1}$	pH	Conversion [%]	<b>4b</b> [%]	<b>5</b> [%]	<b>6</b> [%]	<b>8</b> [%]	<b>9</b> [%]	<b>10</b> [%]
	Phosphate buffer <sup>a)</sup>	0.08	2.5	65	89		6		
0.12		7	83	62		6			
0.10		11	68	72					
Phosphate buffer <sup>[a]</sup> Sensitized <sup>[b]</sup>		2.5	100	34	44	7		11	
		7	100	4	39	38		8	
		11	100			43		4	
MeOH			61				11		
MeOH-H <sub>2</sub> O 9:1			95	2	15		71		
MeOH-H <sub>2</sub> O 1:9			100	44		25	5		
MeOH-H <sub>2</sub> O 1:9 sens. <sup>[b]</sup>			100			30	3		5

[a] 0.05 M. [b] Acetone (10% v/v) used as sensitizer, the irradiation is performed using 310 nm lamps for 1h.

Table 3.5 Products of irradiations and quantum yields of disappearance ( $\Phi_{-1}$ ) of meta Chlorobenzylphosphonic acid <b>1b</b> (0.005 M) irradiated 1h at 254 nm									
 <b>1c</b>	$\Phi_{-1}$	pH	Conversion [%]	<b>4c</b> [%]	<b>5</b> [%]	<b>6</b> [%]	<b>9</b> [%]	<b>12</b> [%]	
	Phosphate buffer <sup>[a]</sup>	0.07	2.5	65	56				
0.11		7	83	33		10			
0.11		11	68	38		30			
Phosphate buffer <sup>[a]</sup> Sensitized <sup>[b]</sup>		2.5	100	40	47	3	8	tr.	
		7	100	2	9	12	14	3	
		11	100			13	18	8	

[a] 0.05 M. [b] Acetone (10% v/v) used as sensitizer, the irradiation is performed using 310 nm lamps for 1h.

As apparent from Table 3.3–Table 3.5, a pH and substrate dependent product distribution was observed. More specifically when **1a–c** are irradiated in phosphate buffer at 254 nm two main products are present, *viz.* hydroxybenzylphosphonic acid **4** and benzyl alcohol

6. Under acidic conditions the predominant product is phenol **4** in all chlorophosphonic acid isomers, but shifting towards higher pH values result in the exclusive formation of product **6** for the para derivative, partial for **1c** and negligible for **1b**.

Introduction of a triplet sensitizer such as acetone<sup>[12]</sup> in the buffered solution, dramatically changes the reactivity of compound **1a–c**. Not only the reduced product benzylphosphonic acid **5** is formed, but also **9** and biphenyl **12** are detected. Noteworthy, **9** is generated by loss of both chloride ion and phosphorous groups and subsequent incorporation of the sensitizer. Under these conditions **1a** reacts giving only products belonging to the phosphorous-free family of compounds (see Chart 3.2), though with low mass balance, while **1c** follows a similar trend found in the unsensitized reaction of **1a**, where the products that have lost phosphorous during irradiation become predominant with increased pH. Notably the same behaviour is followed by **1b**, that changes dramatically its reactivity shifting to sensitized conditions from unsensitized ones, where no pH dependent reactivity was found.

A series of irradiations were made for compounds **1a** and **1b** in different MeOH–water mixtures to assess the role of water in product distribution. The reactions in methanol give only products that have lost both nucleofugal and electrofugal groups, while the introduction of water raises the contribution of phenol **4** and benzyl alcohol **6** to the products. Noteworthy the reduction compound **5** is present when **1b** reacts in MeOH–water 1:9, while the main product derived from the loss of phosphorous moiety with no or low concentrations of water is ether **8**. Moreover, **1a** generates phenethyl alcohol **7**. Again, introducing a triplet sensitizer in MeOH–water 1:9 obliterate the contribution of products bearing the electrofugal group, to the benefit of the phosphorous-free ones, allowing to detect a second type of acetone incorporation adduct, alcohol **10**.

In order to test the reactivity of our phosphonic acids in a physiological environment, we decided to examine the reactivity of **1a** at pH 7.2 in media that shows increased hydrogen-atom donating ability. Buffer (pH 7.2)–MeCN 9:1,<sup>[113]</sup> buffer (pH 7.2)–MeOH 9:1,<sup>[114]</sup> buffer (pH 7.2) with  $2.5 \times 10^{-3}$  (1:2 compared to **1a**) and  $5.0 \times 10^{-3}$  M concentration (1:1 compared to **1a**) of methylglucopyranoside (MGP).<sup>[115]</sup> Use of buffer solution with acetonitrile as additive doesn't change remarkably the reactivity of **1a** compared to results obtained with neat phosphate buffer. Notably, products **5** and **11** are present, though in little amount. Methanol allow the system to cleave more easily the electrofugal group and product distribution is shifted toward the loss of both nucleofugal and electrofugal group.

To our delight, introduction in the buffer of a molecule that allows easy H-atom abstraction such as methylglucopyranoside (MGP) allowed to change the reactivity of **1a**, even in low concentrations. When a 1:1 ratio of **1a** and MGP are irradiated no phosphorous-containing products could be detected.

To clarify the fate of the electrofugal group after the detachment, three experiments were conducted at three different pHs (2.5, 7.2 and 11), in order to assess the presence of phosphate anion in solution. For the experiments, no phosphate buffer was used, however the reaction proceeded in a reproducible fashion with the previous results. Thus, we can exclude any type of influence of the buffer on the photochemical reactions. In Table 3.6 data of the tests conducted on **1a** irradiated for one hour at different pHs and subsequently analyzed with an ion chromatograph, are shown. A nice match with the calculated value predicted from the consumption and the product distribution was found.

Table 3.6 Ion chromatography phosphate analysis for <b>1a</b> . <sup>[a]</sup>			
	Conversion	ppm PO <sub>4</sub> <sup>3-</sup> found	ppm PO <sub>4</sub> <sup>3-</sup> calculated
pH=2.5	85%	41.5	46.1
pH=7	89%	40.6	42.6
pH=11	100%	48.8	50.3

[a] pH was corrected using H<sub>2</sub>SO<sub>4</sub> (pH=2.5), HCO<sub>3</sub><sup>3-</sup>/CO<sub>3</sub><sup>2-</sup> buffer (pH=7.2) and NaOH<sub>aq</sub> (pH=11), checking the pH before and after the irradiation.

### 3.2.2 Computational Studies.

Computational studies were devoted to try to find a rationalization between the different behaviour of the species at different pH values and, in particular, to look for a parallelism between the photochemical reactivity of **1a–c** and the chlorophenylacetic acids.<sup>[3]</sup> To have better insight on the mechanisms underlying the reaction, the photochemical cleavages of the aryl–Cl bond and the benzylic C–P bond of **1a** were studied.

In order to fully characterize the diradical species that could arise from the photochemical reaction, CASSCF, a multiconfigurational *ab initio* method, was deemed to be necessary to describe the system. The choice of the active space depended on the structure considered. The protonated species **1<sup>2H</sup>a** was optimized in its ground state and its first triplet and singlet state using a CPCM–CASSCF(10,10)/6–31G(d) level of theory in bulk water, thus comprising the 6 orbitals belonging to  $\pi$  structure of the ring, the  $\sigma/\sigma^*$  pairs of both the C–Cl and C–P bond. While the morphology of the singlets are very similar to

each other, the triplet state adopts the typical puckered structure of the chloroaromatics in their triplet state.<sup>[17,18,22,31]</sup> Elongation of the C–Cl bond furnishes different Potential Energy Surfaces (PESs) that are very similar to the one found for benzyl chlorotrimethylsilanes.<sup>[19]</sup> Cleavage of the chloride anion was confirmed to happen from the lower triplet state with a barrier of 18 kcal mol<sup>-1</sup> affording triplet aryl cation  $^3\mathbf{1}^{2\text{H}}\mathbf{a}^+$  (Figure 3.4a). Heterolytic nature of the cleavage is corroborated by the marked raise of the ESP charge on the heteroatom after stretching (Figure 3.3). Homolytic cleavage that could raise from both the S1 and the S0 is characterized by higher energy barriers and thus is precluded from those states.

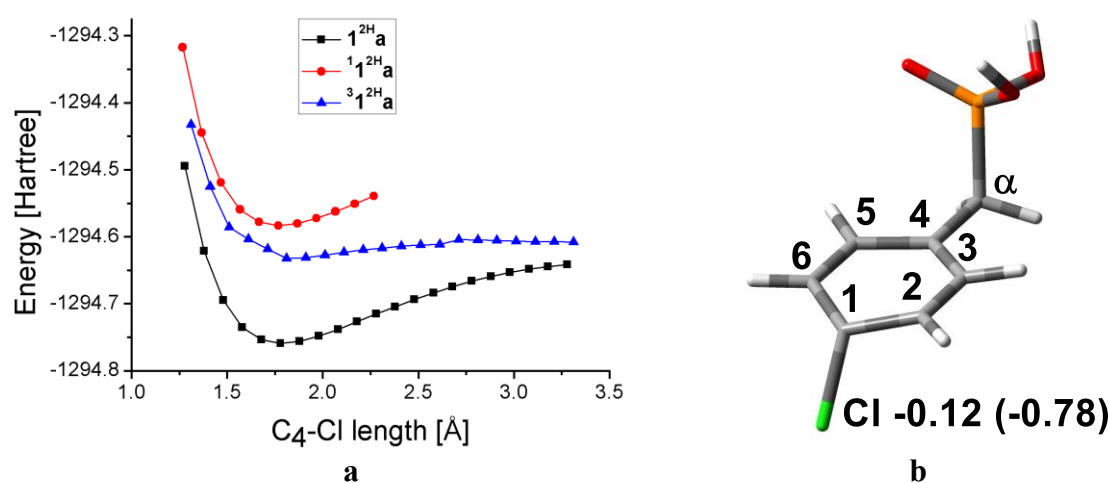


**Figure 3.3** a) Plot of the energy surfaces of the S0, S1 and T1 of  $\mathbf{1}^{2\text{H}}\mathbf{a}$  upon elongation of the C–Cl bond. b). Structure of the puckered triplet state of 1a. On the chlorine atom are reported the ESP charge before and after (in parentheses) elongation.

The monoacidic and the fully deprotonated species of the phosphonic acid case appear to be more difficult to compute, due to the interactions with one of the lone pairs on the oxygen. Consequently a larger active space, *viz.* CPCM–CASSCF(12,11) in bulk water comprising a p orbital on the oxygen, was needed to represent  $\mathbf{1}^{\text{H}}\mathbf{a}$  and  $\mathbf{1}^{2-}\mathbf{a}$ . As for the chlorophenylacetic acids<sup>[3]</sup> two intersecting triplet states were found, one marked by a zwitterionic nature, the second one by a diradical character. The radical cation on the aromatic ring is thus able to abstract an electron from the lone pair on the oxygen originating a diradical with the two spins located on the oxygen itself and on the carbon from which the chlorine is detaching (Figure 3.4b). The diradical state of the monoprotonated species  $\mathbf{1}^{\text{H}}\mathbf{a}^{\text{DCI}}$  intersects the zwitterionic state  $\mathbf{1}^{\text{H}}\mathbf{a}^{\text{Z}}$  at 2.3 Å upon elongation of the Ar–chlorine bond, overcoming a barrier of 5 kcal mol<sup>-1</sup> and proceeds energetically downhill (Figure 3.5a), showing to possess a marked antibonding character. In a parallel fashion, the diradical state of the dideprotonated species  $\mathbf{1}^{2-}\mathbf{a}^{\text{DCI}}$  crosses the



zwitterionic PES of  $1^2\text{-a}^Z$  quite near the equilibrium geometry (C–Cl length of *ca.* 2 Å) after surmounting a barrier of 1.4 kcal mol<sup>-1</sup> (Figure 3.5b). Complete chloride detachment from the monoprotonated and the deprotonated species form the diradical species  $1^{\text{H}}\text{-a}^D$  and  $1^2\text{-a}^D$ , respectively (Scheme 3.3)

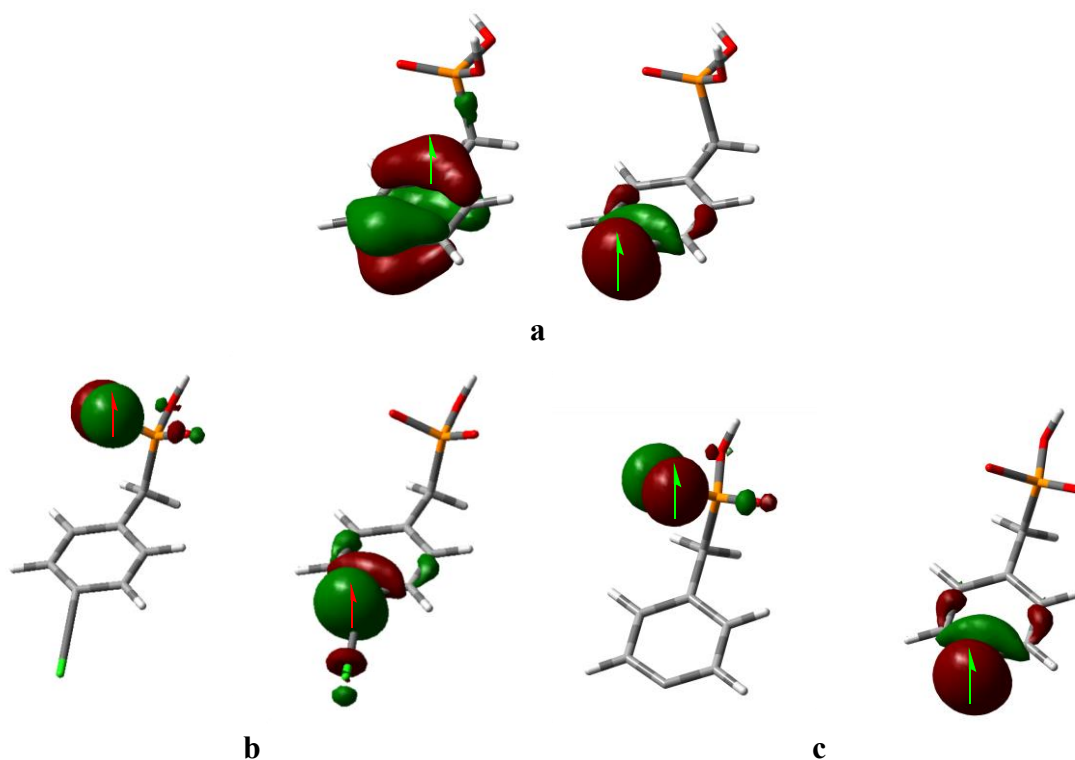


**Figure 3.4** Active orbitals containing the unpaired electron in a) the cationic  $312\text{H}_a^+$  b) the monoprotonated  $1^{\text{H}}\text{-a}^{DCI}$  c) the monoprotonated  $1^{\text{H}}\text{-a}^D$ .

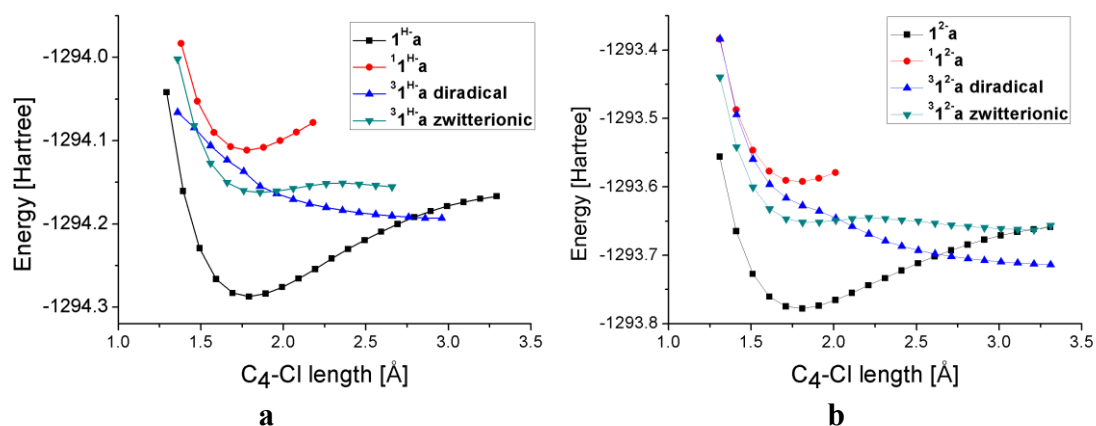
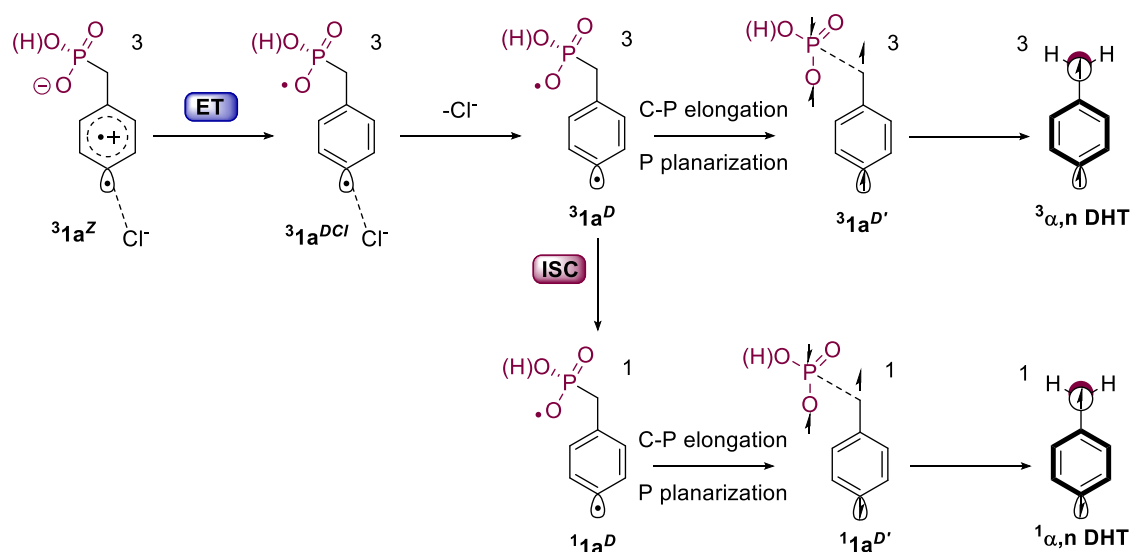


**Figure 3.5** a) Potential energy surfaces PES of  $1^{\text{H}}\text{-a}$  upon elongation of the C–Cl bond. b) Potential energy surfaces PES of  $1^2\text{-a}$  upon elongation of the C–Cl bond.

Phosphorous moiety cleavage was studied at the CPCM–CASCCF (8,9) level of theory for the three different protonated species after chloride loss, both from the triplet and from

the singlet state. Detachment of phosphorous from **1a** generates the cation  $1^{2H}a^+$  with a barrier of *ca.* 36 kcal mol<sup>-1</sup> (Figure 3.6) for the triplet and higher in the singlet (68 kcal mol<sup>-1</sup>, Figure 7.23). The elongation of the C–P bond proceeds energetically in a monotonal fashion. On the other hand, the barriers for the detachment of the electrofugal group from the diradicals  $1^{H-a}D$  and  $1^{2-a}D$  (see Figure 3.5b,c and Scheme 3.3) are characterized by a discontinuity that lowers the activation energy to 14 kcal mol<sup>-1</sup> (see Figure 3.6 for the triplets, Figure 7.23 for the singlets) in both the spin states checked. The discontinuity is due to population of the  $\pi$  bonding orbital between phosphorous and the oxygen that underwent electron transfer with the aromatic ring, ensuing a planarization of the phosphorous group (Scheme 3.3,  $1a^{D'}$  and  $3a^{D'}$ ). In  $1^{H-a}D$  and  $1^{2-a}D$  the singlet and triplet state are almost degenerate in energy, hence C–P cleavage can be equally probable from both the states considered, if populated, generating DHT in both singlet and triplet state (Scheme 3.3).

Dephosphorylation barriers could however be highly overestimated, due to lack of explicit modelling of the solvent assistance in the benzylic bond cleavage.



Scheme 3.3

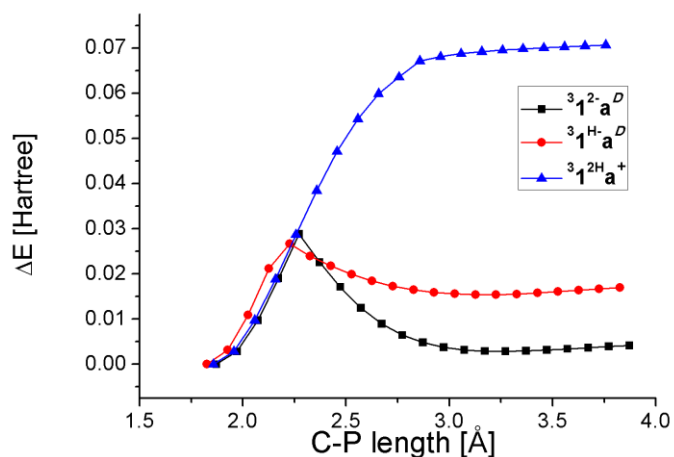


**Figure 3.6** Barriers for the detachment of the electrofugal group from the different protonated species  ${}^3\mathbf{1}^{2H}\mathbf{a}^+$ ,  ${}^3\mathbf{1}^H\mathbf{a}^D$  and  ${}^3\mathbf{1}^{2-}\mathbf{a}^D$  in bulk water. Energies are reported as a difference between the value obtained at a different C–P length and the energy of the system at equilibrium, taken as a reference.

### 3.3 Discussion

All chlorobenzylphosphonic acids tested show an extremely similar photophysics that is almost not dependent on the media analysed if not to a minor extent, while the photochemistry of these derivatives is extremely varied. Scheme 3.4 helps to visualize a generalization of **1a–c** reactivity.

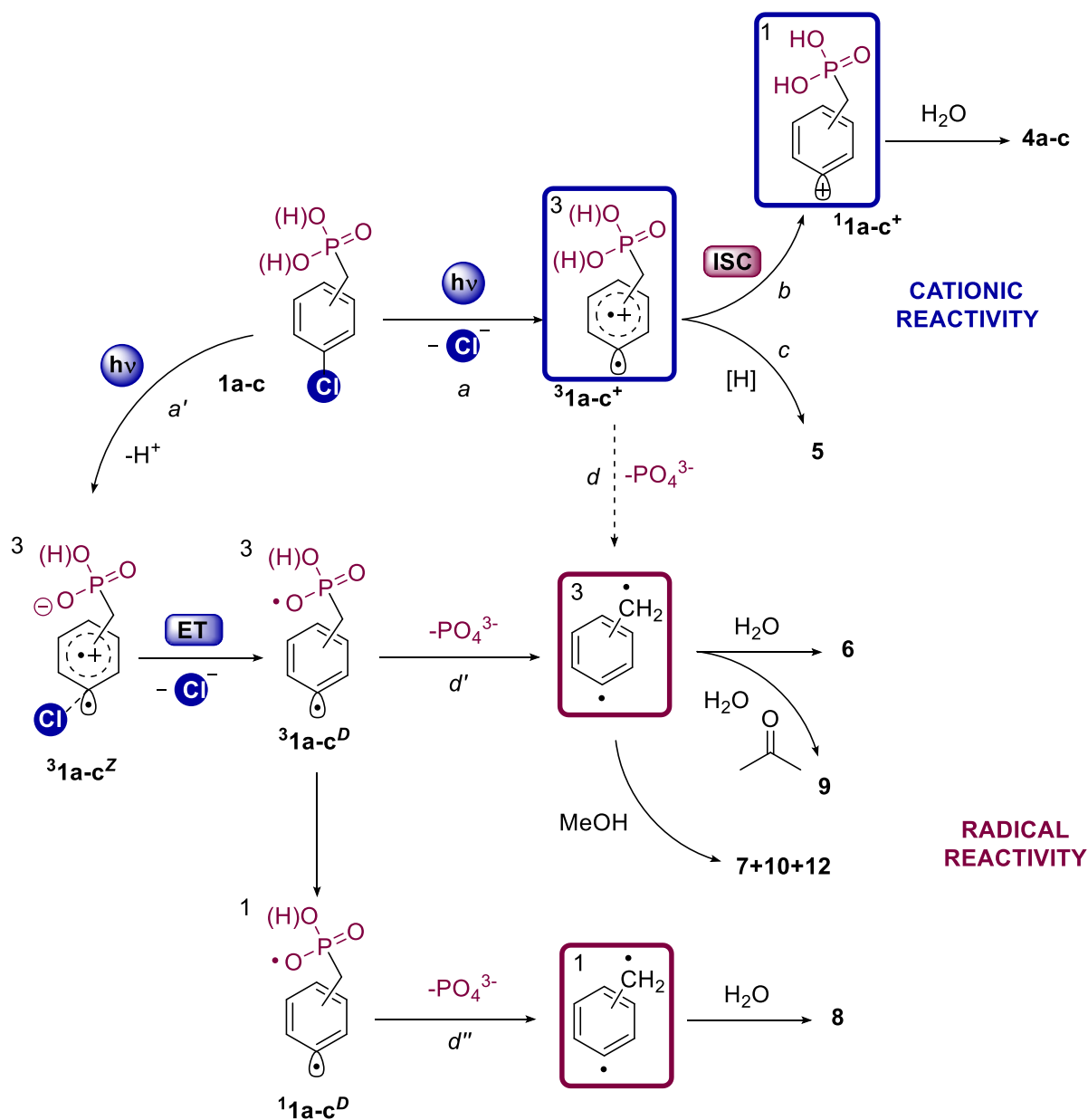
Species **1a–c** after excitation and subsequent ISC generate the triplet phenyl cation  ${}^3\mathbf{1a-c}^+$  (*path a*, Scheme 3.4) via heterolytic loss of the leaving group (chloride anion). This intermediate either reacts with a hydrogen donor (such as acetone, or methanol) and is reduced to phosphonic acid **5** (*path c*) or populates its singlet state  ${}^1\mathbf{1a-c}^+$  through an Intersystem Crossing (ISC).<sup>[116]</sup>  ${}^1\mathbf{1a-c}^+$  is an extremely reactive electrophile that is able to promptly form phenol **4a–c** after reaction with water. Hence, the phosphorylated products of Chart 3.2 could be rationalized on the basis of a cationic reactivity, that prevails in **1b** as previously found for other meta derivatives.<sup>[18]</sup> Presence of higher amounts of water in organic media helps to open *path b* compared to *path c*, as can be reasoned from product distribution in MeOH–water irradiations.

Loss of the phosphorous moiety and DHT formation cannot be achieved directly from  ${}^3\mathbf{1a-c}^+$  (*path d*) due to high energy barriers, however it is feasible by population of the triplet zwitterion  ${}^3\mathbf{1a-c}^Z$ , that can be seen as a triplet aryl cation in its early stage of formation.  ${}^3\mathbf{1a-c}^Z$  easily undergoes a surface crossing with very small barriers that ultimately leads to  ${}^3\mathbf{1a-c}^D$  (*path a'*). Calculations shows this pathway is prerogative of  ${}^1\mathbf{H-}$

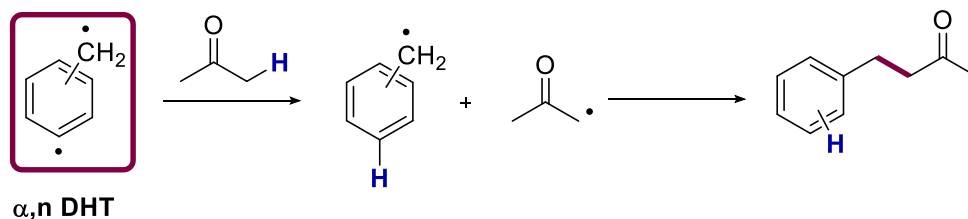
### New Intermediates from Photogenerated Phenyl Cations

and  $1^2$ , because it is the lone pair presence in one of the two oxygens that promotes an internal electron transfer (ET) from the non-bonding orbital on the heteroatom to the radical cation on the aromatic  $\pi$  system. (Scheme 3.4). DHT can be formed in both its spin states after facile C–P bond breaking from  $^31\mathbf{a-c}^D$  (Scheme 3.4). Higher pHs thus help to open *path a'* and allow the internal electron transfer to occur.

Didehydrotoluene in water solvent is known to form benzyl alcohol  $\mathbf{5}^{[3]}$  while in the presence of a molecule such as acetone undergoes a C–H bond insertion, generating  $\mathbf{9}$  after H extraction from the  $\alpha$  carbon and subsequent recombination of the radicals formed (Scheme 3.5).



Scheme 3.4



Scheme 3.5

In a similar fashion products **7** and **11** are generated from the reaction of DHT with the corresponding solvent, either MeOH or MeCN. Intermediacy of radical species is proven by products **10** and **12** presence (see Chapter 2). The benzyl methyl ether **8** was found as predominant product in the sensitized DHT chemistry of the meta isomer, and is ascribed to the so-called ionic pathway of reactivity of the didehydrotoluene, deriving from DHT singlet state.<sup>[74,117]</sup>

From the results, generation of  $\alpha,n$ -DHTs is maximized when the leaving group and the benzylic function are para to each other, as was previously observed in the case of chlorobenzylsilanes and chlorophenylacetic acids.<sup>[1,3,102]</sup> An intriguing selectivity could be found in the para isomer in water buffer. In that case the low pH values allow a cationic type of reactivity to prevail over the radical one. Probably the presence of a lower extent of monoprotonated species at pH 2.5 allowed the DHT to be formed through *path d'*. On the other hand, at higher pH values only the radical reactivity could be detected. Unfortunately, no selective generation of the desired intermediates took place at physiological pH. However, when at the same pH is introduced methylglucopyranoside (MGP) selectivity of DHT formation increases abruptly. Hence, using a stoichiometric amount of methylglucopyranoside shifts para chlorophosphonic acid **1a** to generate only didehydrotoluenes. Use of para-chlorobenzylphosphonic acids seems thus to be promising even at physiological pH.

### 3.4 Conclusions

With the present work, the photochemistry of the three isomers of the chlorobenzylphosphonic acids has been described. A pH selectivity was found for the para- derivative. Noteworthy, at low pH a predominant cationic reactivity is observed whereas under basic conditions a diradical reactivity is exclusive. Introduction of MGP shifts the selectivity towards the diradical formation at physiological pH, paving the way for further studies to unravel the reason of this selectivity and to find potential medicinal applications for the method.

## New Intermediates from Photogenerated Phenyl Cations

# 4 WAVELENGTH SELECTIVE GENERATION OF ARYL RADICALS AND ARYL CATIONS FOR METAL-FREE PHOTOARYLATIONS

## 4.1 Introduction

The use of solar and visible light to promote key photochemical steps in organic synthesis has rapidly grown in recent years.<sup>[118–123]</sup> Two approaches have been followed and in both cases the presence of suitable moieties in the starting compounds has the role of directing the reactivity. In the first case, an organic molecule is activated by a chemical interaction with a visible light absorbing catalyst via an electron<sup>[118–123]</sup> or a hydrogen atom transfer process.<sup>[124]</sup> Transition metal photoredox catalysis has been the most rapidly growing field in the last decade (see a general scheme in Figure 4.1a).<sup>[118–123]</sup> The incorporation in the starting substrates of redox sensitive moieties (X) is required to facilitate the monoelectronic oxidation/reduction step (*path a*). These moieties, known as electroauxiliary groups,<sup>[125]</sup> have the further advantage to be easily eliminated at the end of the process by fragmentation of the resulting radical ions ( $R-X^{\bullet+}$  or  $R-X^{\bullet-}$ , *path b*) to give reactive radicals.

In the second approach a photocleavable coloured moiety (responsible of the absorption of visible light) is introduced in the starting substrate.<sup>[11]</sup> However, this approach is limited to few examples, such as Barton esters<sup>[126]</sup> where stable carboxylic acids are converted into colored photoactive thiohydroxamate esters (Figure 4.1b). Photohomolysis of the labile N–O bond in these esters gave (substituted) carbon-centred (aliphatic) radicals (upon carbon dioxide loss form carbonyloxy radicals).<sup>[11,126]</sup>

In some instances, uncatalyzed processes can be carried out under solar light irradiation even for colourless compounds<sup>[127–129]</sup> or by the in-situ formation of coloured electron donor-acceptor (EDA) complexes.<sup>[130,131]</sup>

Nonetheless, key motivations in devising photolabile visible light absorbing groups are that no need of any (expensive) photocatalysts is required to carry out reactions under solar/visible irradiation.

## New Intermediates from Photogenerated Phenyl Cations

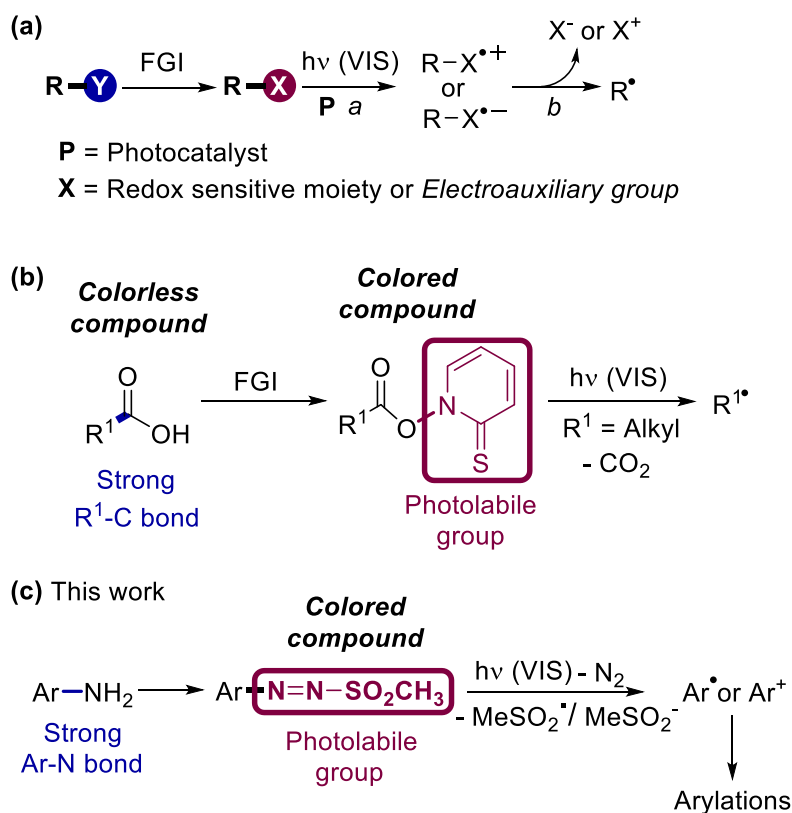


**Figure 4.1** Visible light generation of intermediates. (a) Photoredox catalysis is mainly based on the presence of a redox sensitive moiety (an electroauxiliary group, X) that makes organic molecules more oxidizable and reducible, thus facilitating an electron transfer reaction with a photoexcited photocatalyst. These X groups have the further advantage to be lost in the reaction to give radicals. (b) A coloured moiety could be introduced in an organic compound by a Functional Group Interconversion (FGI) to allow the generation of reactive intermediates by converting a strong bond to a weak photolabile bond. (c) The introduction of an azosulfone group in colourless stable anilines formed colored photolabile arylazo mesylates for the photogeneration of either aryl radicals or aryl cations.

We described herein the application of arylazo sulfones in metal-free photochemical arylations (Figure 4.1c). These substrates were easily prepared from colourless anilines and have been sparsely described<sup>[132]</sup> as suitable precursors of chemical intermediates, including phenyl radicals and cations, upon heating (> 80 °C) or by treatment with a strong acid (e.g. CF<sub>3</sub>COOH) or a base (pyridine as solvent).<sup>[133–137]</sup> Heating of substituted arylazo sulfones in the presence of potassium iodide or *N,N*-dimethylformamide gave iodoarenes and desulfonylated arenes, respectively.<sup>[138]</sup> More attention has been given to the electrophilic character of the N=N bond in the reaction with nucleophiles (e.g. with selenolate ion<sup>[139]</sup> or Grignard reagents<sup>[140]</sup>). Recently, aryl azosulfones have been employed in desulfonylative [3+2] cycloadditions for the synthesis of substituted pyrazoles,<sup>[141]</sup> where, however, the azo-moiety was maintained in the final product.



Little is known on the photoreactivity of arylazo sulfones and arylazo sulfonates.<sup>[133–141]</sup> At least in principle, a phenyl radical<sup>[134,142]</sup> or a phenyl cation may be generated upon irradiation in what it seems to be a solvent dependent process. As an example, the photodecomposition of *p*-alkylphenylazo sulfonates used as photolabile surfactants was investigated in micellar systems.<sup>[143]</sup> A heterolytic cleavage occurred in bulk aqueous phase to yield a phenyl cation, whereas in micelles homolytic cleavage forming the corresponding phenyl radical took place.<sup>[144]</sup> Photolysis of phenylazo-*p*-tolyl sulfones in aromatic solvents under visible light irradiation was suggested to proceed via aryl radicals.<sup>[142]</sup>

As for the above, azosulfones can be viewed as the *coloured* and *stable* form of the corresponding highly reactive and rather unstable aromatic diazonium salts. We reasoned that the use of such azosulfones may widen the application of diazonium salts (recently adopted for the photoredox catalytic generation of aryl radicals)<sup>[145–151]</sup> overcoming, at the same time, their limitations related to their electrophilicity and difficult handling.

## 4.2 Results

We therefore deemed worthwhile to investigate the photochemistry of a set of arylazo mesylates (**1a-h**, **Errore. L'origine riferimento non è stata trovata.**). Compounds **1a-h** were easily obtained as yellow/orange crystalline solids from the corresponding anilines (see Supporting Information for further details). The electronic spectra of azosulfones **1** exhibit a low intensity band in the visible ( $\epsilon = 10^2 \text{ M}^{-1} \text{ cm}^{-1}$ ) and an intense band in the UV region ( $\epsilon = 10^4 \text{ M}^{-1} \text{ cm}^{-1}$ ),<sup>[132]</sup> the latter considerably red shifted when an electron-donating group is present (see Table 7.4 and Figure 7.14–Figure 7.22). These bands were safely attributed to the  $n\pi^*$  and the  $\pi\pi^*$  transitions, respectively.<sup>[132,142]</sup>

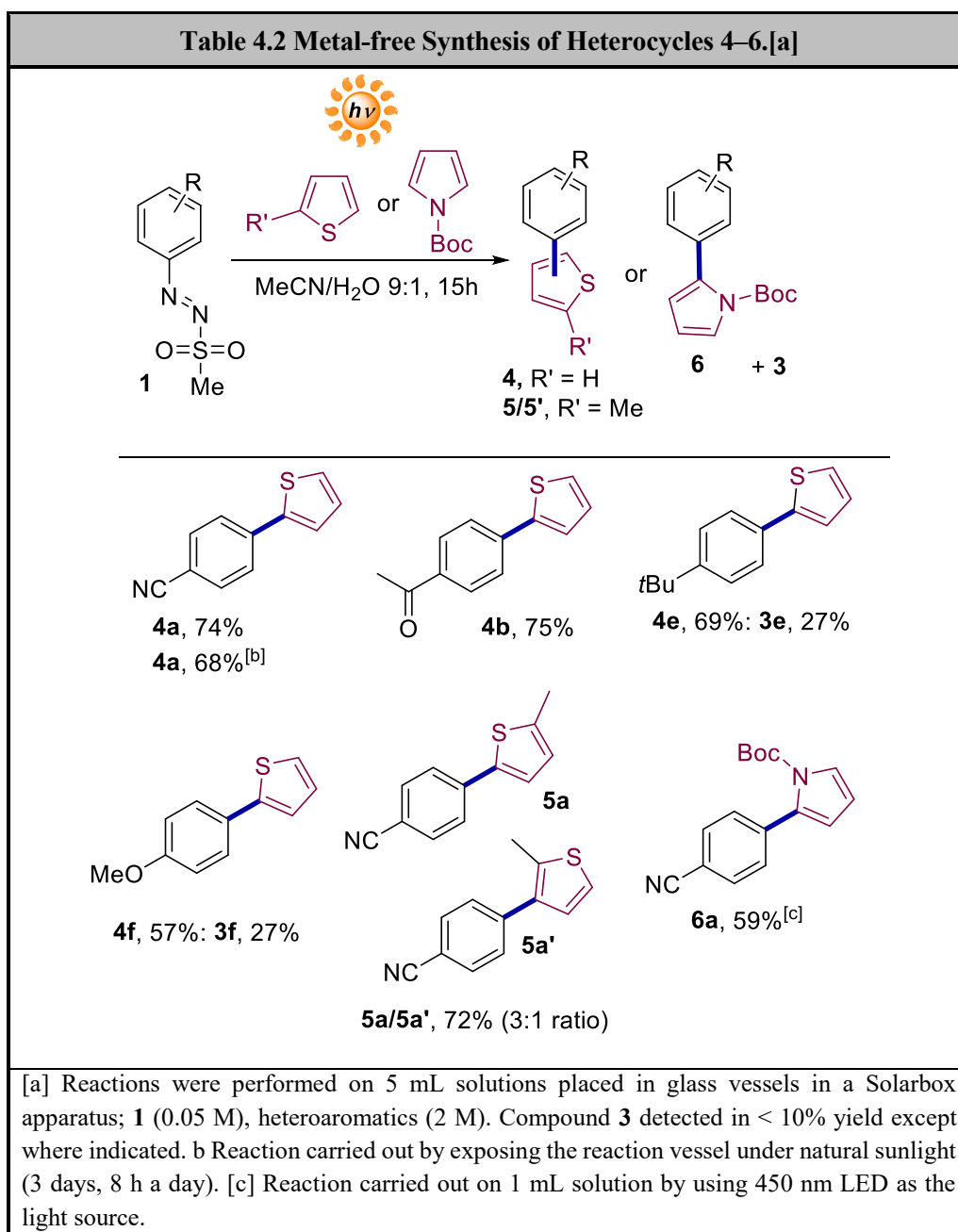
### 4.2.1 Photochemical Arylation of (hetero)Aromatics via Arylazo Mesylates

We carried out preliminary irradiation experiments on **1a** in the presence of furan. We found it convenient to adopt a solar simulator (Solarbox) equipped with a Xe lamp (500 W) as the light source. A MeCN/water 9:1 mixture was found to be the best solvent to obtain the corresponding arylated furan and to minimize the undesired formation of byproducts (mainly benzonitrile, Table 7.5). The reaction was tested on arylazo mesylates **1a-h** and in each case heterobiaryls **2a-h** were obtained in satisfactory yields (Table 4.1). Noteworthy, in the case of **1a** the reaction can be likewise carried out under natural sunlight (3 days irradiation, 56% yield, see further Figure 7.24).

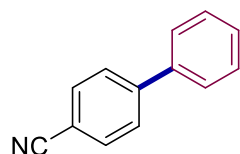
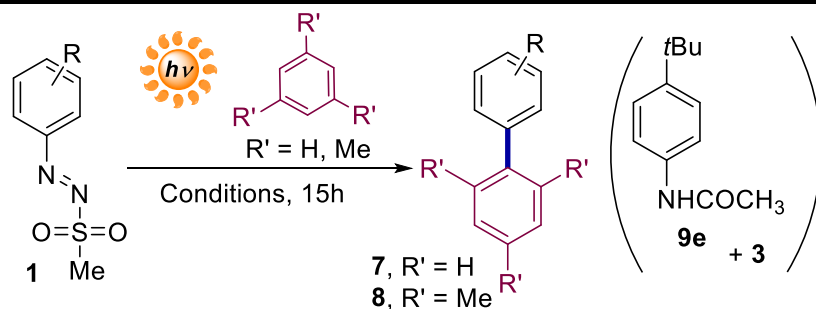
## New Intermediates from Photogenerated Phenyl Cations

We then investigated the arylation of other electron-rich heteroaromatics such as thiophene, 2-methylthiophene and *N*-Boc-pyrrole (Table 4.2). Irradiation of azosulfones **1a,b** in the presence of thiophene led to the corresponding 2-arylthiophenes **4a,b** in more than 70% yield. Sunlight was again convenient to induce the synthesis of **4a**. Azosulfones bearing an electron-donating group on the aromatic ring (**1e,f**) gave again the corresponding arylated products but accompanied by a significant amount of **3e,f** (ca. 30%). Arylation of 2-methylthiophene with **1a** gave a mixture of 2-aryl-5-methylthiophene (**5a**) and 2-methyl-3-arylthiophene (**5a'**) in 72% overall yield (**5a/5a'** 3:1 ratio). In a single case, *N*-Boc-pyrrole was arylated (compound **6a**, isolated as the exclusive isomer, 59% yield) and the use of LED irradiation ( $\lambda = 450$  nm) was found convenient in this case.

Table 4.1 Solar Light Induced Synthesis of 2-Arylfurans 2a-h. <sup>[a]</sup>			
<p><b>1a</b>, R = 4-CN  <b>1b</b>, R = 4-CH<sub>3</sub>CO  <b>1c</b>, R = 4-Cl  <b>1d</b>, R = H  <b>1e</b>, R = 4-<i>t</i>Bu  <b>1f</b>, R = 4-OMe  <b>1g</b>, R = 3-CN  <b>1h</b>, R = 2-CN</p>			
 <b>2a</b> , 70% <b>2a</b> , 56% <sup>[b,c]</sup>	 <b>2b</b> , 62% <b>2b</b> , 87% <sup>[c]</sup>	 <b>2c</b> , 94%	 <b>2d</b> , 70%
 <b>2e</b> , 9%; <b>3e</b> , 59% <b>2e</b> , 71% <sup>[c]</sup>	 <b>2f</b> , 32%; <b>3f</b> , 29% <b>2f</b> , 96% <sup>[c]</sup>	 <b>2g</b> , 68%	 <b>2h</b> , 71%
<p>[a] Reactions were performed on 5 mL solutions placed in glass vessels in a Solarbox apparatus; <b>1</b> (0.1 M), furan (1 M). Letters in the products refer to the same substituents as in compounds <b>1</b>. [b] Reaction carried out by exposing the reaction vessel under natural sunlight (3 days, 8 h a day). [c] <b>1</b> (0.05 M) and furan (2 M).</p>			



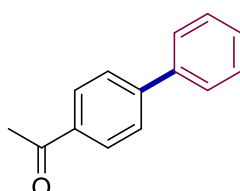
The challenging arylation of unactivated arenes was then tested (Table 3). Arylation of benzene, though satisfactory in some cases, is not a clean process (**3** and acetanilide **9** as the byproducts). However, when photolysis was carried out in neat benzene, or upon sunlight irradiation, biaryls **7** were exclusively formed. Biaryls **8a** and **8b** were obtained in 56% and 32% yields, respectively by the reaction between electron-poor azosulfones **1a,b** and mesitylene. In the latter case, however, the adoption of a 366 nm phosphor coated Hg lamp as the light source improved the arylation yields up to 70% (Table 4.3).

Table 4.3 Synthesis of Biaryls 7,8.<sup>[a]</sup>


**7a**, 74%; **3a**, 14%

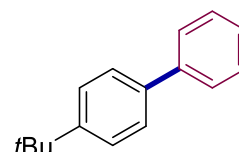
*7a*, 70%<sup>[b]</sup>

*7a*, 72%



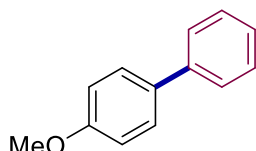
**7b**, 46%; **3b**, 43%

*7b*, 52%



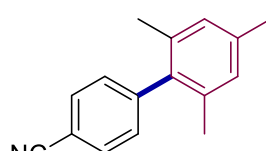
**7e**, 58%; **3e**, 21%; **9e**, 13%

*7e*, 53%



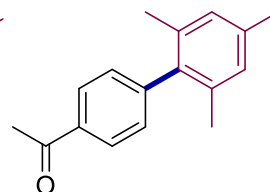
**7f**, 70%<sup>[c]</sup>; **3f**, 12%<sup>[c]</sup>

*7f*, 51%



**8a**, 56%

*8a*, 71%<sup>[d]</sup>



**8b**, 32%

*8b*, 73%<sup>[d]</sup>; **3b**, 10%<sup>[d]</sup>

[a] Conditions (see Table 4.2): **1** (0.05 M), benzene or mesitylene (2 M) irradiated in MeCN-H<sub>2</sub>O 9:1. *In italic: reaction carried out in neat benzene.* [b] Reaction carried out by exposing the reaction vessel under natural sunlight (3 days, 8 h a day). [c] MeCN used as the solvent. [d] The solution was irradiated in a 1 mm quartz cuvette for 5 h by using a 366 nm phosphor coated Hg lamp as the light source (GC yields).

### 4.2.2 Mechanistic Investigations on the Photoreactivity of Azosulfones **1**

Experiments were carried out to investigate the mechanism of the reaction. No appreciable thermal decomposition occurred when the solutions of **1a-h** were irradiated

Table 4.4 Investigation on the Wavelength Dependent Behavior of Azosulfones **1**.<sup>[a]</sup>

Compound	Light source	Additive	100	<b>3</b> [%] <sup>[b]</sup>	<b>9/10</b> [%] <sup>[b]</sup>	Arylated [%] <sup>[b]</sup>
<b>1a</b>	Solarbox <sup>[c]</sup>	-	100	<b>3a</b> , 57	<b>9a</b> , 15; <b>10a</b> , 6	-
<b>1b</b>	Solarbox <sup>[c]</sup>	-	100	<b>3b</b> , 67	-	-
<b>1e</b>	Solarbox <sup>[c]</sup>	-	100	<b>3e</b> , 22	<b>9e</b> , 20; <b>10e</b> , 8	-
<b>1f</b>	Solarbox <sup>[c]</sup>	-	100	<b>3f</b> , 34	<b>9f</b> , 28; <b>10f</b> , 14	-
<b>1f</b>	LED (450 nm) <sup>[d]</sup>	-	70	<b>3f</b> , 56	-	-
<b>1f</b>	Hg (366 nm) <sup>[e]</sup>	-	87	<b>3f</b> , 7	<b>9f</b> , 57; <b>10f</b> , 12	-
<b>1f</b>	LED (450 nm) <sup>[d]</sup>	Ascorbic acid <sup>[f]</sup>	100	<b>3f</b> , 48	-	-
<b>1f</b>	Hg (366 nm) <sup>[e]</sup>	Ascorbic acid <sup>[f]</sup>	100	<b>3f</b> , 50	-	-
<b>1f</b>	LED (450 nm) <sup>[d]</sup>	Furan <sup>[g]</sup>	100	<b>3f</b> , 21	-	<b>2f</b> , 68
<b>1f</b>	Hg (366 nm) <sup>[e]</sup>	Furan <sup>[g]</sup>	100	<b>3f</b> , 16	<b>9f</b> , 5	<b>2f</b> , 58
<b>1f</b>	LED (450 nm) <sup>[d]</sup>	Allyl phenyl sulfone <sup>[h]</sup>	100	<b>3f</b> , 23	-	<b>11f</b> , 48
<b>1f</b>	Hg (366 nm) <sup>[e]</sup>	Allyl phenyl sulfone <sup>[h]</sup>	100	<b>3f</b> , 8	<b>9f</b> , 46	<b>11f</b> , 11
<b>1f</b>	LED (450 nm) <sup>[d]</sup>	TMDD <sup>[i]</sup>	64	<b>3f</b> , 56	-	-
<b>1f</b>	Hg (366 nm) <sup>[e]</sup>	TMDD <sup>[i]</sup>	13	<b>3f</b> , <5	-	-
<b>4-MeOC<sub>6</sub>H<sub>4</sub>N<sub>2</sub>BF<sub>4</sub></b>	Hg (366 nm) <sup>[e]</sup>	Furan <sup>[g]</sup>	100	<b>3f</b> , <5	<b>9f</b> , 25	<b>2f</b> , <5

[a] Conditions: **1** or diazonium salt (0.05 M) in MeCN–H<sub>2</sub>O 9:1. [b] Yields based on the consumption of **1**. [c] 1 mL solution irradiated for 15 h in a vial in the Solarbox. [d] The solution was irradiated in a 1 mm quartz cuvette for 5 h. [e] The solution was irradiated in a 1 mm quartz cuvette for 1.5 h. [f] Ascorbic acid 0.025 M. [g] Furan 2 M. [h] Allyl phenyl sulfone 0.2 M. [i] 4,4–Tetramethyl–1,2–diazetidine dioxide (TMDD) 0.025 M.

in the Solarbox protected from light. Azosulfones **1a,b,e,f** were irradiated in Solarbox in neat MeCN–H<sub>2</sub>O 9:1. Interestingly, along with **3**, solvolysis products namely acetanilide **9** and phenol **10** were obtained in a significant amount except for **1b** where acetophenone **3b** was exclusively formed (Table 4.4). The nature of the products obtained resembles that found previously by our group in the irradiation of benzenediazonium tetrafluoroborate salts.<sup>[152]</sup> Ion chromatograph analyses of the photolysed solutions revealed the presence of methanesulfinic acid (CH<sub>3</sub>SO<sub>2</sub>H, 63% yield in the case of **1a**). We were then interested to ascertain if a wavelength dependent reactivity of the azosulfone exists. Accordingly, we repeated some experiments on sulfone **1f** by using a phosphor coated Hg lamp ( $\lambda = 366$  nm) and a LED ( $\lambda = 450$  nm) in order to reach selectively the  $\pi\pi^*$  and  $n\pi^*$  state, respectively.

Irradiation at these two wavelengths in neat MeCN–H<sub>2</sub>O 9:1 led to a markedly different distribution of products (at 366 nm the main product is acetanilide **9f**) but the presence of ascorbic acid (a reducing agent) led exclusively to anisole **3f** in both cases. Arylation of furan is not wavelength dependent, which is different from the case of allyl phenyl sulfone where estragole **11f** (48%) was isolated as the major product in the irradiation of **1f** at 450 nm but not at 366 nm.

Experiments carried out in the presence of triplet quencher 3,3,4,4-tetramethyl-1,2-diazetidine dioxide (TMDD,  $E_T \leq 42.0$  kcal mol<sup>-1</sup>, 0.025 M)<sup>[153]</sup> demonstrated that while no effect was observed at 450 nm, a dwarfing in the consumption of **1f** (from 86% down to 13%) was apparent at 366 nm. Finally, a comparison with the photoreactivity of 4-methoxyphenyldiazonium tetrafluoroborate (4-MeOC<sub>6</sub>H<sub>4</sub>N<sub>2</sub>BF<sub>4</sub>) was carried out at 366 nm in the presence of furan, but, contrary to what was observed for **1f** under the same conditions, no arylation took place.

### 4.3 Discussion

The obtained data suggest that a wavelength dependent generation of intermediates is involved in the photoreactivity of **1** (Scheme 1). Thus, irradiation at 450 nm populates the  $^1n\pi^*$  state (*path a*) and homolysis of the S-N bond (*path b*) occurs to afford the aryl radical (Ar<sup>•</sup>)/methanesulfonyl radical (CH<sub>3</sub>SO<sub>2</sub><sup>•</sup>) pair. In neat solvent, both radicals undergo hydrogen abstraction from the solvent to give **3**<sup>[154]</sup> and sulfinic acid (CH<sub>3</sub>SO<sub>2</sub>H)<sup>[88]</sup> (*path c*). However, when a radical trap (furan in Scheme 4.1) is present at a sufficient concentration, trapping of Ar<sup>•</sup> (*path d*) to form radical adduct **12**<sup>•</sup> competes efficiently with reduction.<sup>[155]</sup> Hydrogen abstraction from **12**<sup>•</sup> by CH<sub>3</sub>SO<sub>2</sub><sup>•</sup> then affords the heterobiaryl **2**

(*path e*). The intervention of an aryl radical is further supported by the reaction of **1f** with allyl phenyl sulfones (a typical selective trap for aryl radicals<sup>[156]</sup>), that gives estragole **11f** as the main product. On the other hand, irradiation at 366 nm populates the  $^1\pi\pi^*$  state (*path f*). In this case, intersystem crossing to  $^3\pi\pi^*$  (*path g*) is followed by heterolytic cleavage of the S-N bond to generate an excited aryl diazonium salt in the same multiplicity ( $^3\text{ArN}_2^+$ , *path h*). The intermediacy of a triplet state is confirmed here by the efficient quenching observed in the presence of TMDD (*path g'*), not observed upon irradiation at 450 nm (Table 4).

Reduction of  $^3\text{ArN}_2^+$  by ascorbic acid to the corresponding radical, however, leads efficiently to **3** (*path c'*). Heterolysis of the Ar-N bond in  $^3\text{ArN}_2^+$ <sup>[152,157]</sup> generates a triplet aryl cation ( $^3\text{Ar}^+$ , *path i*) that is then reduced to **3** by the solvent (*path j*).<sup>[152,158]</sup> The presence of solvolysis products **9,10** (*path l*) is diagnostic of the formation of a singlet aryl cation  $^1\text{Ar}^+$  (by ISC from  $^3\text{Ar}^+$ , *path k*)<sup>[20,22]</sup> that depends on the nature of the aromatic substituents. A singlet cation reactivity is almost exclusively observed when irradiating the 4-methoxyphenyldiazonium tetrafluoroborate salt evidencing a role of the azosulfone group in the population of  $^3\text{ArN}_2^+$  (Table 4.4). However, in the presence of  $\pi$ -bond nucleophiles, such as (hetero)aromatics, efficient trapping of  $^3\text{Ar}^+$  occurs and heterobiaryls (**2** in Scheme 4.1) are obtained via Wheland intermediate  $12^+$  (*paths m, m'*). In contrast, the presence of a radical trap namely allyl phenyl sulfone, gives allylated **11f** only as a minor product. When using a Xenon lamp (such as that present in the Solarbox apparatus) both  $\text{Ar}^\bullet$  and  $^3\text{Ar}^+$  are generated in solution and this successfully leads to (hetero)aromatics. To improve the yields, however, a more selective generation of one of these intermediates was adopted (see Table 4.2–4.3).

### 4.3.1 Importance of the Method

The development of metal-free arylation procedures for the synthesis of (hetero)biaryls is a pioneering field in organic chemistry.<sup>[155,159–161]</sup> Common strategies involve the generation of reactive intermediates such as aryl cations or radicals. Triplet aryl cations are obtained via UV irradiation of aryl halides (mainly chlorides) and esters in protic solvents,<sup>[158]</sup> but the process is limited to electron-rich substrates. Diazonium salts are likewise used as  $^3\text{Ar}^+$  precursors but in the case of electron-rich substrates, the use of a triplet photosensitizer (e.g. benzophenone) is mandatory.<sup>[152]</sup>

On the other hand, aryl radicals can be formed under metal-free conditions by following either thermal or photochemical approaches. The generation of aryl radicals is reported

via radical mediated halide atom abstraction from aryl iodides taking place at room temperature in the presence of  $(\text{TMS})_3\text{SiH}$  as chain carrier.<sup>[161]</sup> The most recent proposals, however, involve the monoelectronic reduction of aryl halides (mainly iodides and bromides) followed by halide ion loss. The process occurs at  $> 80\text{ }^\circ\text{C}$  in the presence of a strong base (usually *t*BuOK) and organic catalysts such as quinolines,<sup>[162]</sup> phenylhydrazine<sup>[163]</sup> and pyridone based macrocycles.<sup>[164]</sup> The *in situ* generated aryl radical then reacts via  $\text{S}_{\text{RN}}1$  mechanism with an unactivated arene (in most cases, benzene) that acts as reagent and solvent. A milder approach makes use of ascorbic acid to reduce the starting diazonium salts to give aryl radicals.<sup>[155]</sup>

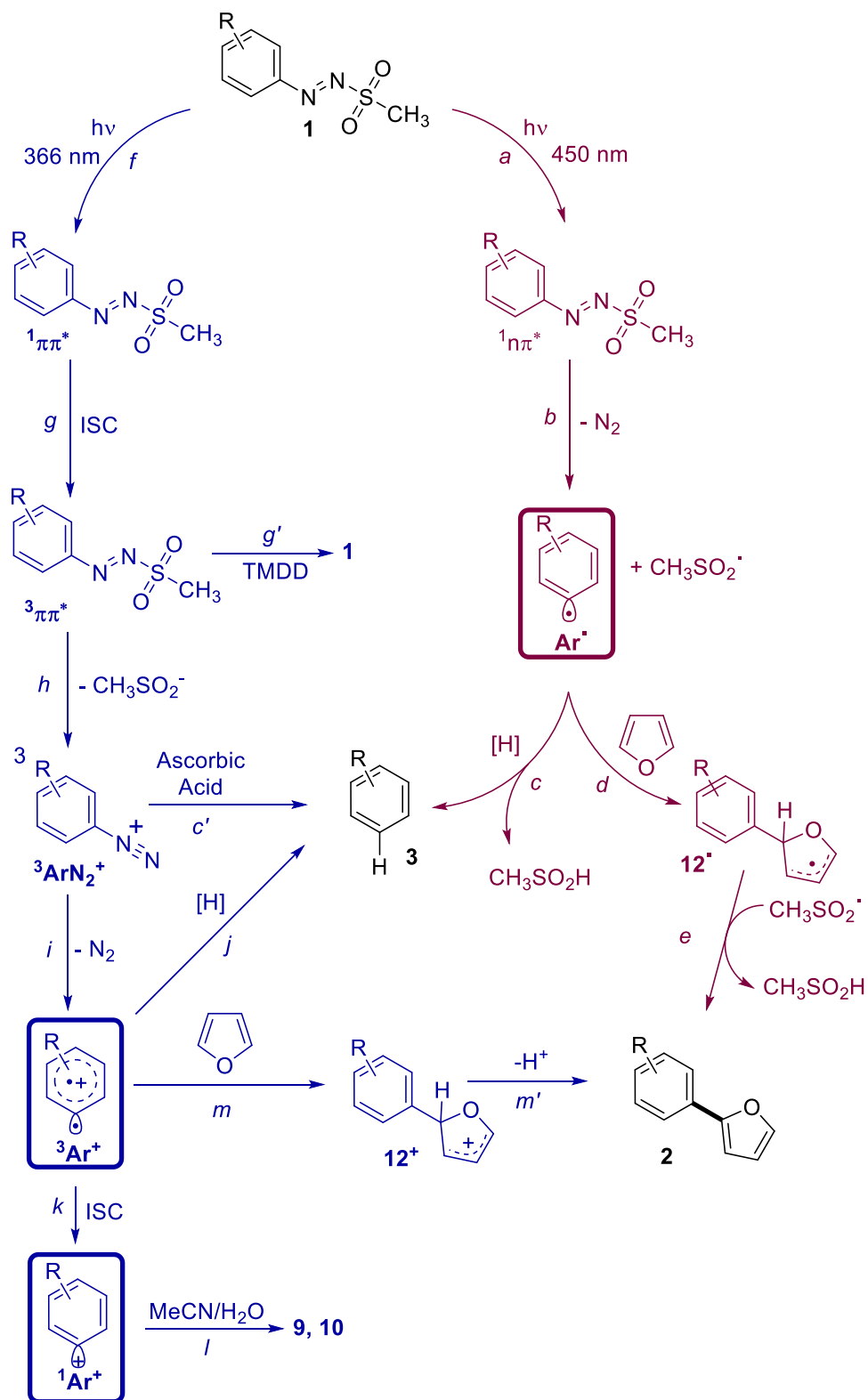
As for metal-free photochemical approaches, aryl radicals can be accessed by Eosin Y photocatalyzed reduction of aryl<sup>[165]</sup> and (hetero)aryl<sup>[166]</sup> diazonium salts or by two photon perylene bisimide photocatalyzed reduction of aryl halides in the presence of triethylamine as the electron donor.<sup>[167]</sup> The uncatalyzed formation of aryl radicals can be promoted by UV irradiation of the *in situ* generated diazo anhydrides.<sup>[168]</sup> Finally, the photoinduced metal-free borylation of aryl halides and ammonium salts was suggested to proceed via either aryl radicals or triplet aryl cations.<sup>[169]</sup>

As a common feature of these processes, the addition of the aryl radical onto a heteroaromatic is particularly successful when the radical bears an electron-withdrawing substituent on the aromatic ring.<sup>[165,167,168,170]</sup> Arylation of simple arenes is likewise feasible but only in the presence of a large excess of the arene.<sup>[151,167]</sup> The same holds even in the present case, as is apparent in Table 4.2–3.

In the present work, we showed that aryl azosulfones are versatile substrates for the uncatalyzed metal-free arylation of heterocycles and unactivated arenes with no need for additives (e.g. bases) at ambient temperature. The introduction of an azosulfone group allows for the wavelength selective formation of aryl radicals and aryl cations albeit both species are generated upon solar light irradiation. Furthermore, aryl azosulfones are not simply a stable coloured form of diazonium salts. The presence of the azosulfonyl group is able to change the photoreactivity of the corresponding salts as shown in the case of **1f** (Table 4.4). This opens the way to the use of such versatile azosulfones in a wide range of metal-free synthetic protocols.



**Chapter 4:** Wavelength Selective Generation of Aryl Radicals and Aryl Cations for Metal-free Photoarylations



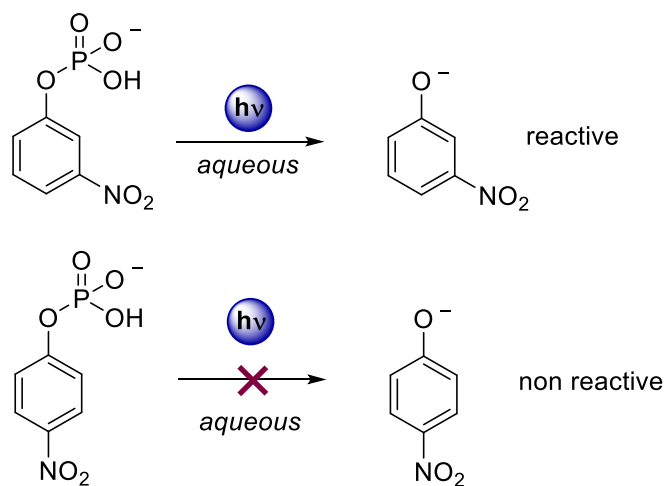
**Scheme 4.1**

## 5 COMPUTATIONAL STUDY ON THE EXCITED STATE DEACTIVATION MECHANISM OF THE CHLOROANILINES

### 5.1 Introduction

Several studies have provided new insights on the theoretical basis that lies beyond the excited state behaviour of the aromatics.<sup>[12,20,171–176]</sup>

A special case is the seminal work of Zimmermann, devoted to rationalize the so-called *meta–ortho effect* of aromatic compounds.<sup>[97,177]</sup> This theoretical work was mainly based on the experimental studies of Havinga (1956) on the nitrophosphate esters photohydrolysis in aqueous solution.<sup>[94]</sup> It was found that irradiating the otherwise thermal stable *m*–nitrophenylphosphate in basic water led to a facile nucleophilic substitution of the ester, while the *para*– derivative remained unreactive (Scheme 5.1).

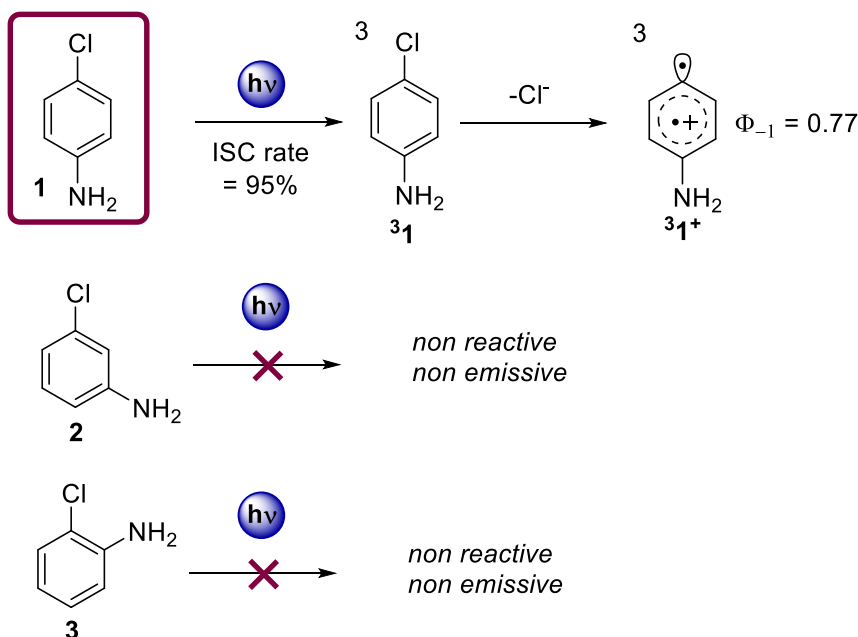


**Scheme 5.1**

Substituent effect in the excited state reactivity of aromatic molecules cannot be explained with the classic and qualitative resonance reasoning. Zimmermann showed by means of computational chemistry that the excited state electron transmission in aromatics follows a *meta–ortho* selectivity, in contrast to the *para–ortho* one that is typical of the ground state.<sup>[178]</sup> Thus the *meta* nitro group stabilizes the charge in benzylic position in the first excited state.

Another curious example is represented by chloroanilines (**1–3** Scheme 5.2).<sup>[17,172,179–185]</sup> This class of compounds was thoroughly studied by my research group as precursors of

the triplet phenyl cation.<sup>[17]</sup> In particular, aryl–chlorine bond is efficiently cleaved from the triplet state of **1** in a heterolytical fashion, affording a triplet aryl cation  $^3\mathbf{1}^+$  (Scheme 5.2), as explained in Chapter 1.



Scheme 5.2

In contrast, meta and ortho derivative **2** and **3** show little to no reactivity compared to the extremely performing para isomer. A quick survey of the quantum yield of disappearance of the three isomers presented in Table 5.1 gives a quantitative flavour to the aforementioned behaviour and confirms the striking difference between the three molecules.

Fluorescence (Table Table 5.1) and phosphorescence intensities follow the same trend, thus  $\mathbf{1} > \mathbf{2} \approx \mathbf{3}$ .<sup>[186]</sup> Notably, lack of phosphorescence in **3** was tentatively attributed to an excited state quenching due to an intramolecular hydrogen–bonding between chlorine and the NH proton.<sup>[186,187]</sup> Noteworthy, the parent compound chlorobenzene (**4**, Chart 5.1) fluoresces weakly. (Table 5.2).<sup>[188]</sup>

Table 5.1 Quantum yields of disappearance ( $\Phi_{\text{Cl}}$ ) and fluorescence ( $\Phi_F$ ) for 1–3.		
	$\Phi_{\text{Cl}}^{-[\text{a}]}$	$\Phi_F$
<b>1</b>	0.72 <sup>[189]</sup> , 0.77 <sup>[b][17]</sup>	0.019 <sup>[b]</sup> , 0.026 <sup>[b][46]</sup>
<b>2</b>	0.014 <sup>[184]</sup>	Very weak Fluorescence <sup>[d][186]</sup>
<b>3</b>	0.03 <sup>[183]</sup>	No emission <sup>[d][186]</sup>

[a] Values obtained in aqueous solutions. [b] Values obtained in MeCN. [c] Values obtained in EtOH. [d] Value obtained in dioxane.

### New Intermediates from Photogenerated Phenyl Cations

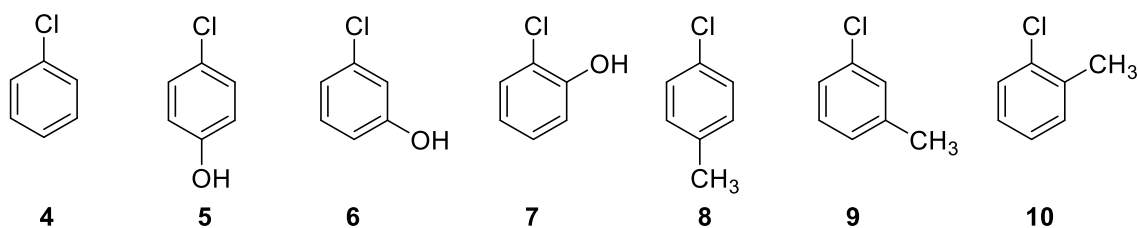


**Chart 5.1**

A nice parallelism with chloroanilines could be found in chlorophenols (**5–7**, Table 5.2, Chart 5.1).<sup>[111]</sup> Actually, the quantum yield of fluorescence in chlorophenols decrease in the order para (**5**) > meta (**6**)  $\approx$  orto (**7**). From a superficial point of view those data could appear an example of meta–ortho selectivity attributable to chloroaromatics, however, in contrast to this behaviour, chlorotoluenes (**8–10**, Chart 5.1) are characterized by similar values of quantum yields of fluorescence (Table 5.2).

<b>Table 5.2 Quantum yields of fluorescence (<math>\Phi_F</math>) for 4–10</b>	
$\Phi_F$	
<b>4</b>	0.007 <sup>a</sup> [188]
<b>5</b>	0.026 <sup>b</sup> [111]
<b>6</b>	0.002 <sup>b</sup> [111]
<b>7</b>	0.002 <sup>b</sup> [111]
<b>8</b>	0.009 <sup>[112]</sup>
<b>9</b>	0.011 <sup>[190]</sup>
<b>10</b>	0.0085 <sup>[190]</sup>
[a] Values obtained in cyclohexane. [b] Value obtained in aqueous solution.	

Hence, the aim of the present chapter is try to rationalize the differences found in the reactivity of the chloroanilines by means of computational chemistry, in order to gain a deeper understanding of the mechanisms that ultimately could lead to the formation of the triplet aryl cation upon irradiation. A sketchy generalization of the phenomenon will be attempted, on the basis of the experimental data previously presented.

To represent the photochemical pathways of **1–3**, the three main decay routes of the first singlet excited state were taken into account,<sup>[12]</sup> namely emission,<sup>[191]</sup> photoreaction via C–Cl detachment. The same three pathways are, almost in principle, accessible from the triplet state of the examined molecules.<sup>[192,193]</sup> In addition, fast Internal Conversion from S1 to S0 through a Conical Intersection was considered. The geometry and nature of this

last species can only be studied by means of computational chemistry due to its intrinsically transient existence (in the sub-picosecond timescale)<sup>[194]</sup>. This so called “Channel 3” is the now well-accepted reason for the disappearance of the S1 fluorescence in benzene, if excited over a critical threshold of  $3000\text{ cm}^{-1}$  (*ca.*  $8.6\text{ kcal mol}^{-1}$ ) above the S1 minimum.<sup>[195–197]</sup> In benzene, the CoIn structure contains a triangular carbon arrangement corresponding to a  $-(\text{CH})_3-$  kink of the carbon skeleton characterized by weak interacting electrons in a triangular shape, loosely coupled with an allylic moiety (Figure 5.1). This particular Conical Intersection is dubbed as *Prefulvenic*, due to the system could either collapse to the ground state minimum or populate a short lived intermediate, namely prefulvene itself, that spontaneously rearranges giving the products of benzene photolysis, *viz.* benzvalene and fulvene (Figure 5.1).<sup>[198]</sup>

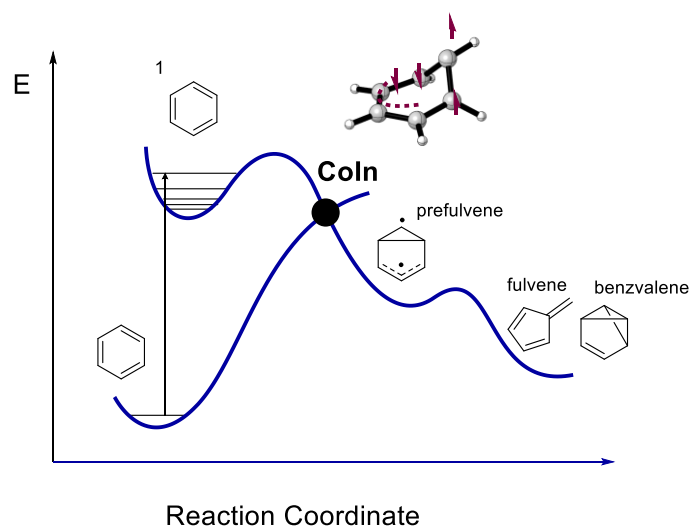


Figure 5.1

This funnel is found in different aromatic molecules, presenting a topology and an electronic distribution similar to the one typical of benzene.<sup>[199–204]</sup>

## 5.2 Results and Discussion

A first approach to tackle the problem from a computational point of view is to investigate if a difference between the rates of fluorescence deactivation could exist between the three chloroanilines. A rough estimate of such a data is obtained through comparison of the S0S1 oscillator strength of **1–3**. Therefore, the program RASSI (as implemented in MOLCAS<sup>[205]</sup>) to the optimized structures of the chloroanilines was applied. In all the cases considered the software calculated the interactions between the 12 lower singlet and 12 lower triplet states at the SA12-CASSCF(12,10)/ANO-S-VDZP level of theory (see Chapter 7.4 for further details). The active space comprises the 6  $\pi$  orbitals of the aromatic

## New Intermediates from Photogenerated Phenyl Cations

ring, the  $p_z$  lone pair on Cl, the N lone pair and  $\sigma/\sigma^*$  C–Cl bonds. Contribute of spin-orbit coupling was explicitly included. The approach herein presented must be addressed as merely qualitative, due to the lack of the dynamical correction accounted by the CASPT2 procedure, that wasn't applied owing to the high computational costs. No difference between the oscillator strength values computed was found and the para derivative possesses the lower value for the transition between S1 and S0, as is represented in Table 5.3.

<b>Table 5.3 Oscillator Strength of the S0S1 radiative transition at the CASSCF(12,10)/ANO–S–VDZP level for 1–3</b>			
	<b>1</b>	<b>2</b>	<b>3</b>
Osc. Strength	4.28E–03	7.55E–03	1.10E–02

The same procedure was applied on the lower triplet state, to measure the differences between the rates of phosphorescence among 1–3, hence considering the S0T1 transition. To our surprise also these values of Oscillator Strength for the meta and ortho isomer were higher than the one from 1 (Table 5.4).

<b>Table 5.4 Oscillator Strength of the S0T1 radiative transition at the CASSCF(12,10)/ANO–S–VDZP level for 1–3</b>			
	<b>1</b>	<b>2</b>	<b>3</b>
Osc. Strength	8.26E-08	1.26E-07	1.99E-07

Computational results obtained from this approach seems to disprove the experimental data, where the para- derivative is found to be the most emissive.

Approximate values of the Spin Orbit Coupling (SOC) between the singlet S1 and the triplet states could be computed using the functionalities of the RASSI program, to evaluate the possibility of an Inter System Crossing near the region of the optimized S1 state. However, no values greater than a threshold of  $1.000 \text{ cm}^{-1}$ <sup>[206,207]</sup> could be found, discarding the possibility to directly populate a  $T_n$  state directly from the S1 more stable geometry.

Photochemistry of 1–3 was analysed computing the energies of the first 10 singlets and triplets along the C–Cl elongation coordinate at the SA10–CASSCF(12,10)/ANO–S–VDZP level. The plots represented in Figure 5.2 presents a qualitative overview of the lower states of the para and meta chloroanilines for the sake of comparison, however no particular differences could be found between the energy barriers of Cl detachment either

from the lower singlet or triplet excited states of **1** and **2**, as can be fully appreciated in Figure 5.2e and Figure 5.2f.

As a parallelism with benzene,<sup>[195]</sup> the S1–S0 funnelling deactivation pathway was deemed necessary to be explored for **1–3**, hence a conical intersection between the first excited singlet state and the ground state was searched for the three chloroanilines. A minimal set of 6 electrons in 6 orbitals belonging to the aromatic ring  $\pi$  framework was chosen to minimize the computational effort. Albeit the introduction of the lone pair on nitrogen in the active space seems to be a necessary prerequisite to the analysis of the chloroanilines, all the attempts to include it in the active space in a geometry different from the equilibrium were unsuccessful, up to SA10–CASSCF level. Moreover, the chlorine  $p_z$  orbital perpendicular to the aromatic ring is characterized by an occupancy  $> 1.99$ , thus it was discarded from the active space.<sup>[208]</sup> The C–Cl  $\sigma$  and  $\sigma^*$  orbitals are not taken into account because the S1 excited state along the prefulvenic coordinate is known to possess only  $\pi\pi^*$  nature.<sup>[195]</sup> All the calculations were optimized with the 6–31G\* at the CASSCF level and subsequently the energies obtained were refined at the MS–CASPT2 level. Energies of the two lower singlets were furtherly evaluated using the MS–CASPT2//SA2–CASSCF(6,6)/ANO–S–VDZP level of theory. Due to Atomic Natural Orbitals basis sets are known to perform extremely well with excited state calculations,<sup>[209]</sup> this choice allowed to compare the goodness of the results obtained with Pople’s basis.

To our delight a prefulvenic–like crossing between the S1 and S0 Potential Energy Surfaces was located for the three isomers (**1–3coin**). Those geometries deserve some comment. In all the cases studied the carbon bearing the chlorine atom (C1) is puckered out–of–plane while C2 and C6 (Figure 5.3) are forming the typical prefulvene cyclopropylic structure. The chlorine atom follows the distortion of the ring translating upward from its original position. Substituent position seems to affect only slightly the conical intersection geometry. Most notably the distance between C1 and C6 is longer only in the meta isomer while the ortho substitution modifies the C3–C2–C1–Chlorine dihedral angle from  $167^\circ$  to  $163^\circ$  in respect of the two other anilines. The C–N and C–Cl don’t undergo major changes between the three isomers.

## New Intermediates from Photogenerated Phenyl Cations

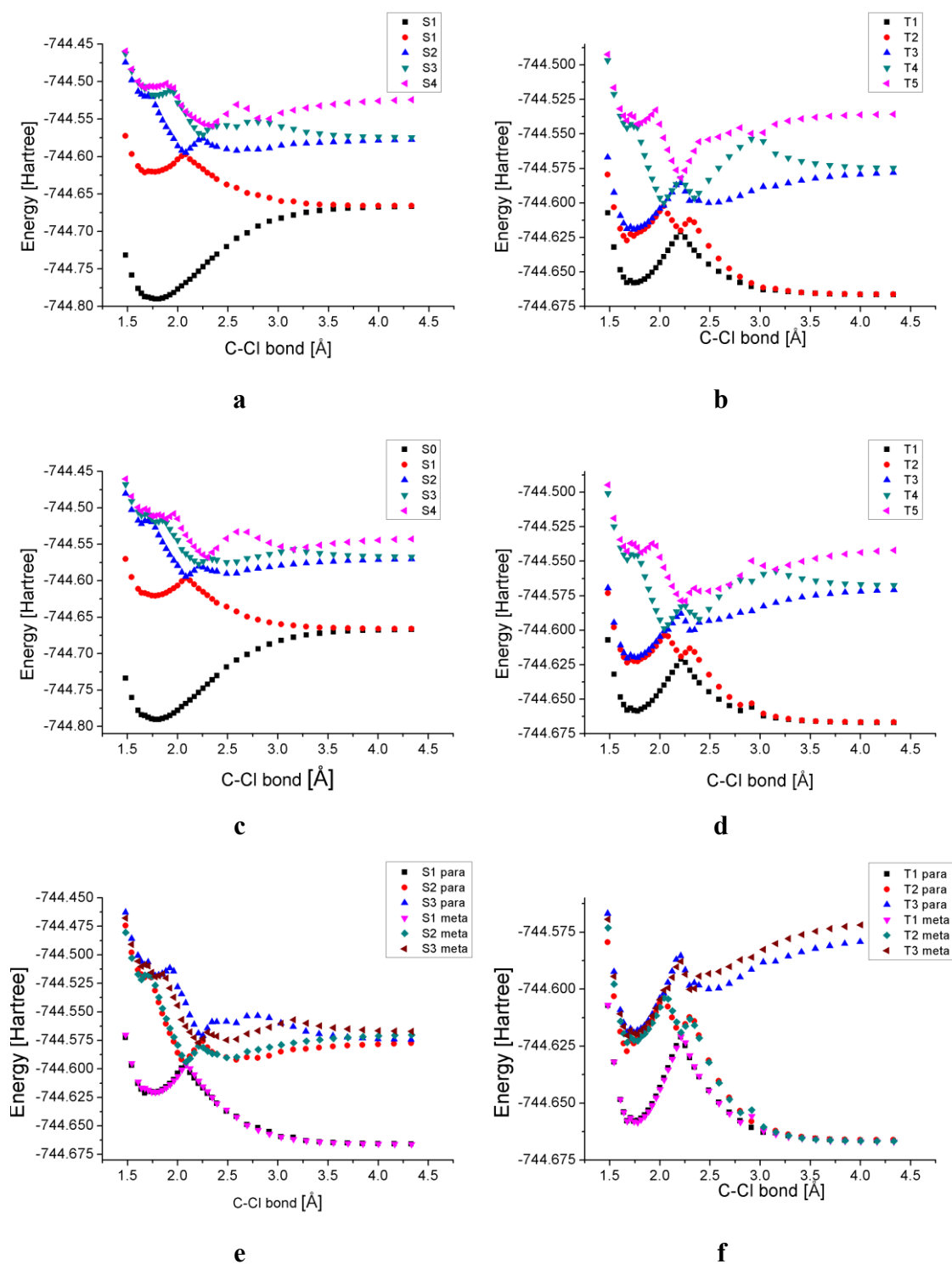


**Figure 5.2** Energy at the SA10–CASSCF(12,10)/ANO–S–VDZP level of theory along the C–Cl stretching coordinate of a) five lower singlet states of **1**; b) five lower triplet states of **1**; c) five lower singlet states of **2**; d) five lower triplet states of **2**; e) three lower singlet states of **1** superimposed to the three lower singlet states of **2**; f) three lower triplet states of **1** superimposed to the three lower triplet states of **2**.



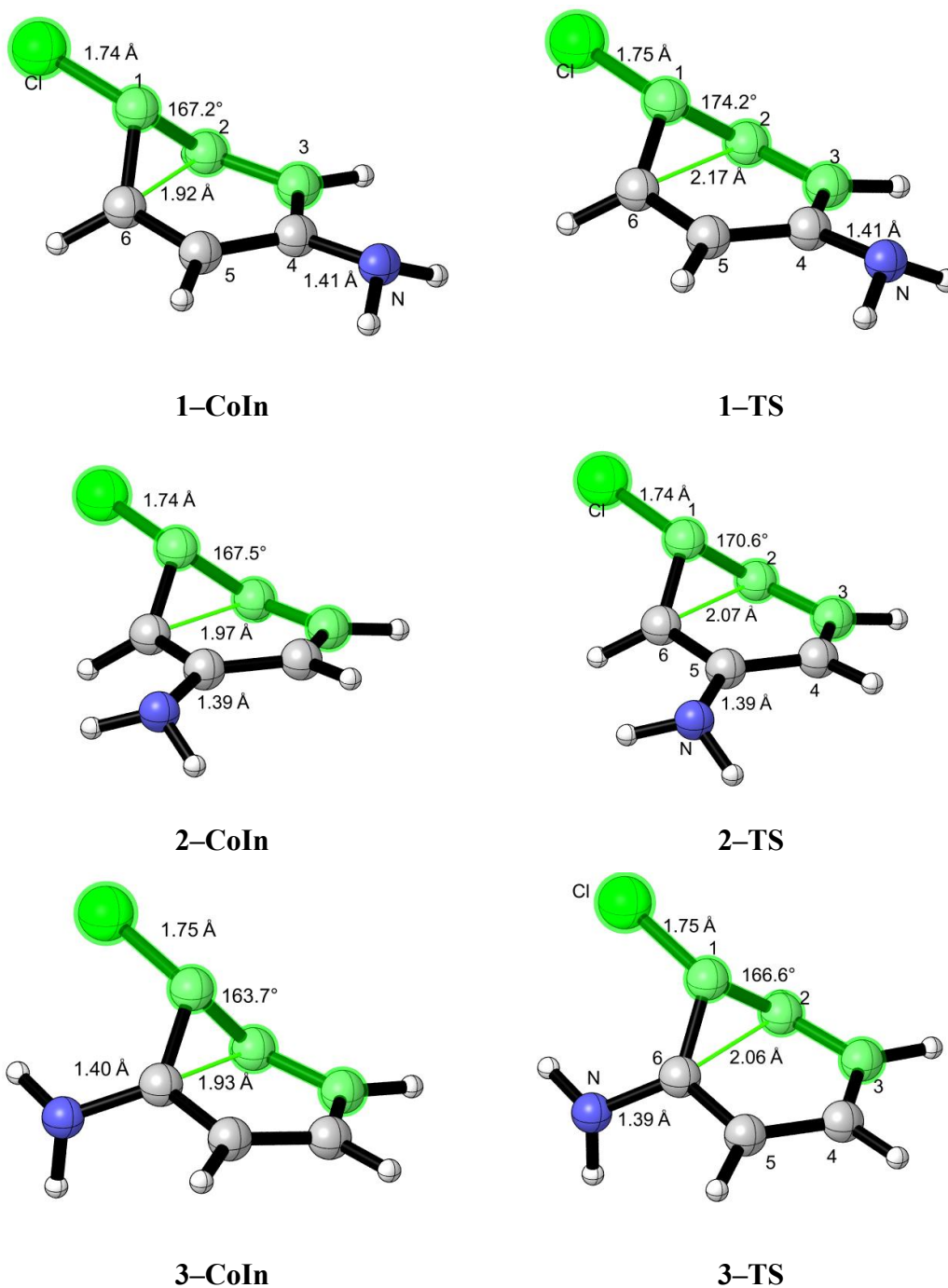


**Figure 5.3**

Transition State structures (**1–3 TS**, Figure 5.3) connecting S1 minima to the conical intersection were found. The geometries thus optimized resemble those of the corresponding conical intersection. The C2–C6 bond in the TS of the para derivative is appreciably longer than the one in the two other isomers (*ca.* 0.1 Å more) while the C–Cl and C–N bonds remains unchanged. A displacement of the geometry at which the S1/S0 minimal energy crossing point (MECP) occurs in **2** is also observed after the introduction of the perturbational correction of MS–CASPT2 (**2 MECP-PT2**, Table 5.5).

This minor inconsistency could be ascribed to the use of two different software packages to optimize the geometries and subsequently calculate the perturbational corrected energies (see Chapter 7.4).<sup>[210,211]</sup> On the other hand, it is known that the introduction of PT2 correction to CASSCF energies could be the source of minor modifications of the PES.<sup>[212]</sup>

The photochemical process was explored by means of an Intrinsic Reaction Coordinate analysis from the optimized geometry of the transition states on the S1.<sup>[191,211]</sup>

Energies of the S1 state at the geometries belonging to the conical intersections and to the stationary points calculated using 6-31G\* and ANO-S-VDZP basis sets are reported in Table 5.5, while the energy differences between the optimized first excited state and the transition state towards the conical intersection are presented in Table 5.6.

The energy gap to overcome to reach the geometry of the conical intersection is quite high when the CASSCF results are considered, *viz.* between 15 and 21 kcal mol<sup>-1</sup>, with the para derivative possessing a slightly steeper barrier compared to the meta and ortho one (*ca.* 4 kcal mol<sup>-1</sup> higher, Table 5.6). The MS-CASPT2 correction, however, influences greatly the energy of the transition structure of **2** and **3**, lowering the energy gap to *ca.* 8 kcal mol<sup>-1</sup>, while in **1** the barrier remains almost unaffected. S1 PESs of **1–3** at the different level of theory are depicted in Figure 5.4.

The difference in energy barriers confirms the existence of a discrepancy between the non-radiative deactivation pathway following the so-called “Channel 3”.

Table 5.5 Energy of the stationary points and conical intersections of 1–3					
	C2–C6 length [Å]	CASSCF Energy [Hartree]		MS-CASPT2 Energy [Hartree]	
		6-31G*	ANO–S–VDZP	6-31G*	ANO–S–VDZP
<b>1 CoIn</b>	1.92	-744.4998	-744.5820	-745.4880	-745.6035
<b>1 TS</b>	2.17	-744.4962	-744.5790	-745.4805	-745.59682
<b>1 S1</b>	2.50	-744.5297	-744.6114	-745.5097	-745.6256
<b>2 CoIn</b>	1.97	-744.5037	-744.5860	-745.4918	-745.6069
<b>2 MECP-PT2</b>	1.98	-744.5035	-744.5859	-745.4948	-745.6100
<b>2 TS</b>	2.07	-744.5033	-744.5860	-745.4946	-745.6102
<b>2 S1</b>	2.49	-744.5289	-744.6104	-745.5080	-745.6235
<b>3 CoIn</b>	1.93	-744.5039	-744.5851	-745.4967	-745.6118
<b>3 TS</b>	2.06	-744.50389	-744.5853	-745.4961	-745.6110
<b>3 S1</b>	2.50	-744.5284	-744.6096	-745.5085	-745.6235

Consequently, we can reason that the meta and ortho isomers **2** and **3** possess in their excited state S1 a preferential funnel to the ground state with energy barriers comparable

with benzene,<sup>[195,198]</sup> thus assessing the nature of their photostability and low emission values.

Table 5.6 S1-TS energy difference of 1-3. <sup>[a]</sup>				
	6-31G*		ANO-S-VDZP	
	CASSCF	MS-CASPT2	CASSCF	MS-CASPT2
<b>1</b>	21.0	18.3	20.3	18.1
<b>2</b>	16.0	8.4	15.3	8.3
<b>3</b>	15.4	7.8	15.2	7.9

[a] All the  $\Delta E$  are expressed in kcal mol<sup>-1</sup>

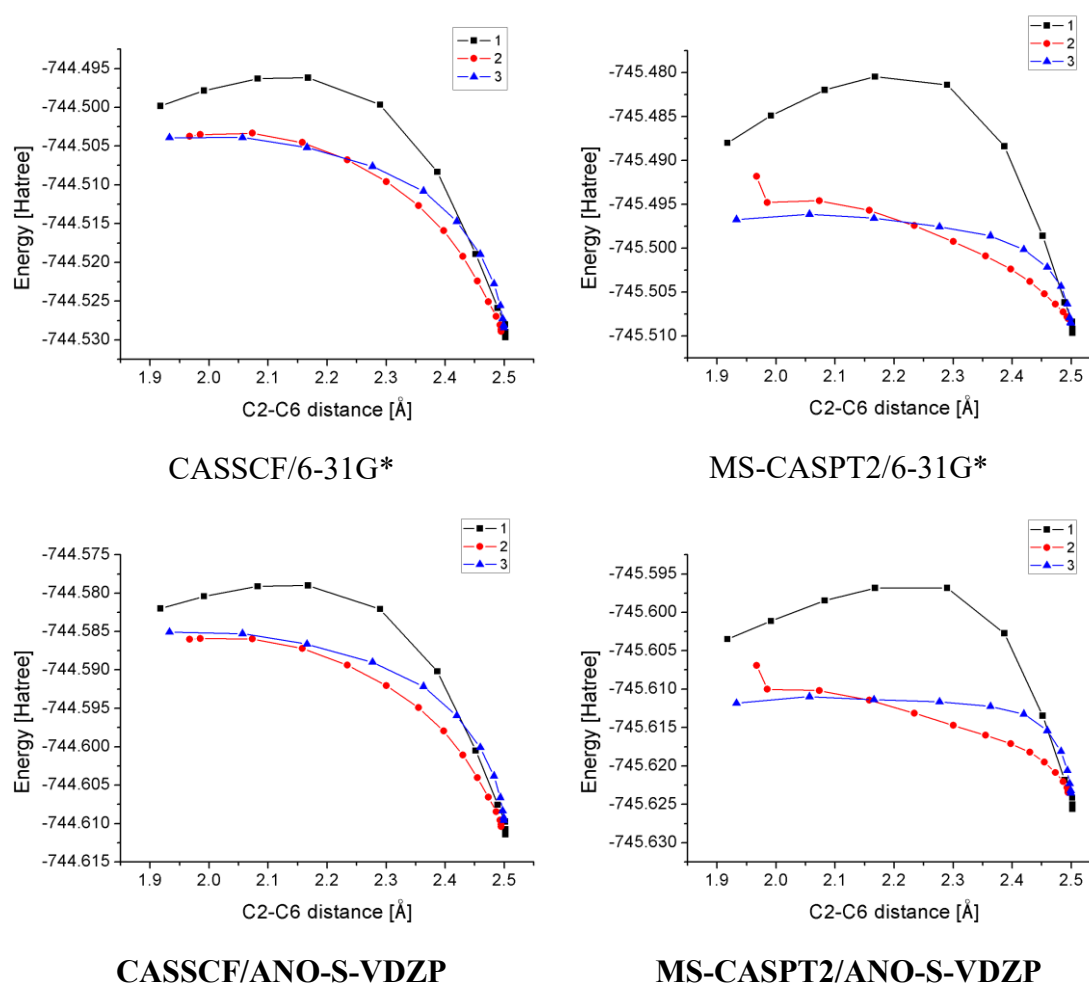


**Figure 5.4** Comparison between the first excited singlet state S1 surfaces of the three isomers **1** (■), **2** (●) and **3** (▲) are plotted.

To provide a generalization of the results obtained with **1-3**, the prefulvenic conical intersection, the S1 minimum and the TS for chlorobenzene **4**, the three isomers of chlorophenol **5-7** and chlorotoluene **8-10** were computed with SA2-CASSCF(6,6)/6-31G\*, averaging the two lower singlets. Albeit this computational scheme lacks the

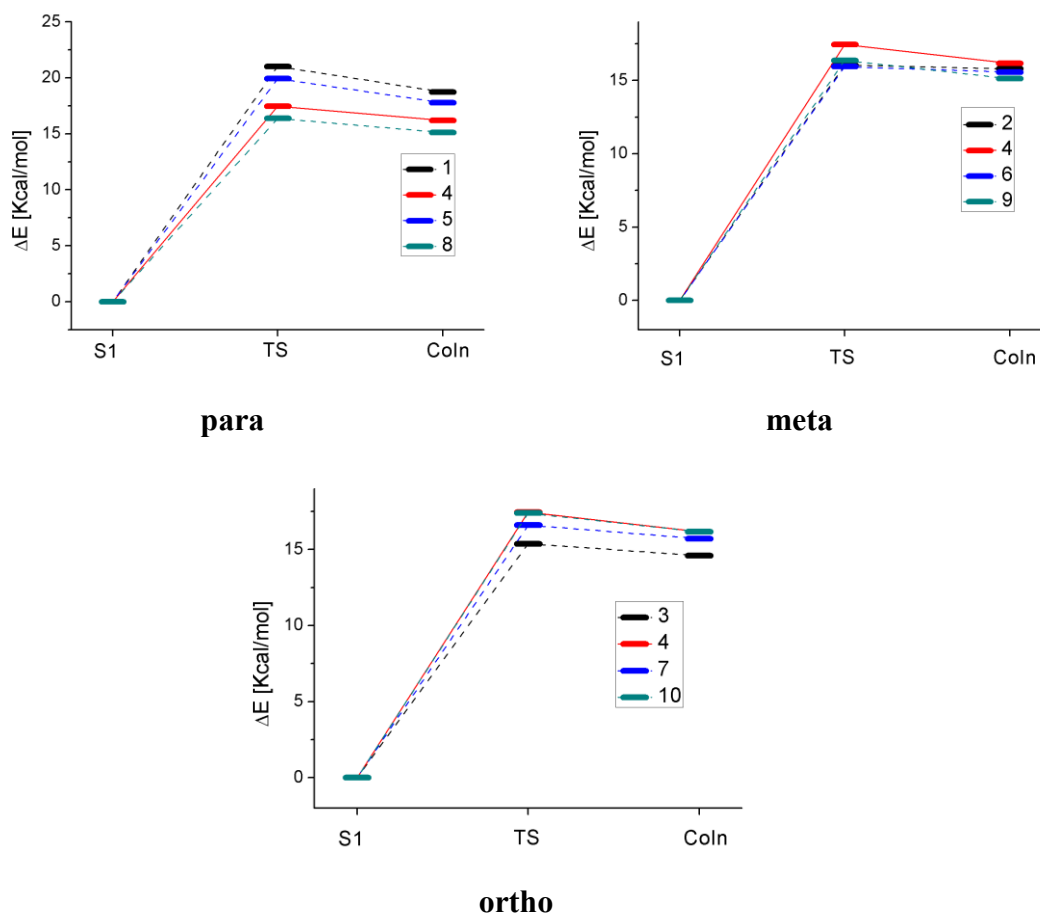
dynamical correlation furnished by PT2 correction, it should be considered correct from a qualitative standpoint. Moreover, it allows a fast correlation between the barriers of the different compounds, without worrying about any morphological change of the shape of the PES introduced by MS-CASPT2.<sup>[212]</sup> The results are presented in Table 5.7 while a comparison of the para, meta and ortho isomers referred to chlorobenzene is depicted in Figure 5.5.

Table 5.7 Energy of the stationary points and conical intersections of 1–10						
		S1 [Hartree]	TS [Hartree]	CoIn [Hartree]	$\Delta E$ S1–TS [kcal mol <sup>-1</sup> ]	$\Delta E$ S1–CoIn [kcal mol <sup>-1</sup> ]
	<b>para 1</b>	-744.5297	-744.4962	-744.4998	21.0	18.7
	<b>meta 2</b>	-744.5289	-744.5033	-744.5037	16.1	15.8
	<b>ortho 3</b>	-744.5284	-744.5039	-744.5052	15.4	14.6
	<b>4</b>	-689.5016	-689.4738	-689.4758	17.5	16.2
	<b>para 5</b>	-764.3547	-764.3229	-764.3264	19.9	17.8
	<b>meta 6</b>	-764.3538	-764.3284	-764.3290	15.9	15.6
	<b>ortho 7</b>	-764.3505	-764.3240	-764.3254	16.6	15.7
	<b>para 8</b>	-728.5393	-728.5114	-728.5140	17.5	15.9
	<b>meta 9</b>	-728.5393	-728.5132	-728.5152	16.4	15.1
	<b>ortho 10</b>	-728.5385	-728.5107	-728.5127	17.4	16.2

Presence of an electron-donating group on the aromatic ring weakly stabilizes the transition state in respect of the chlorobenzene, at least if the substituent is in ortho or meta position compared to chlorine (that's the case of  $-\text{NH}_2$ ,  $-\text{OH}$  and  $-\text{CH}_3$ ). However, the nature of the substituent in para position seems to deeply modify the height of the barrier. In particular nitrogen and oxygen, destabilize the transition state of the prefulvenic pathway, while the methyl group doesn't behave in a similar fashion, even though it is weakly electron-donating for hyperconjugation effect.<sup>[213]</sup> It seems that all the effects that regulate this type of selectivity between the regioisomers cannot be ascribed to mere resonance, due to the impossibility to include the lone pair of the heteroatom inside the active space.

An evidence of such a destabilization could be given introducing a rough approximation. The prefulvenic conical intersection and the TS electronic configuration are characterized by an allyl moiety weakly interacting with the other three electrons positioned in the puckered cyclopropyl,<sup>[198]</sup> thus these structures can be approximated as the sum of two isolated allyl systems. A correlation between simpler allyl radicals differently substituted

with nitrogen could be proposed as a comparison for the stability of the TS (Scheme 5.3a). Due to the chlorine is always placed on the puckered carbon it could be considered a constant variable of the three systems that does not interfere (if not minimally) with the relative stabilization of **1–3**. Thus, to simplify the model further, chlorine can be substituted with hydrogen. Under these premises, meta and ortho aniline are the sum of an allyl radical and a 1–amino radical, while **3** is the sum of an allyl radical and a 2–amino radical.



**Figure 5.5** Comparison between the TS and CoIn  $\Delta E$  S1–TS and  $\Delta E$  S1–CoIn of the para (**1,5** and **8**), meta (**2, 6** and **9**) and ortho (**3, 7** and **10**) isomers of chloroaniline, chlorophenol and chlorotoluene referred to the energies of chlorobenzene **4** reported in Table 5.7.

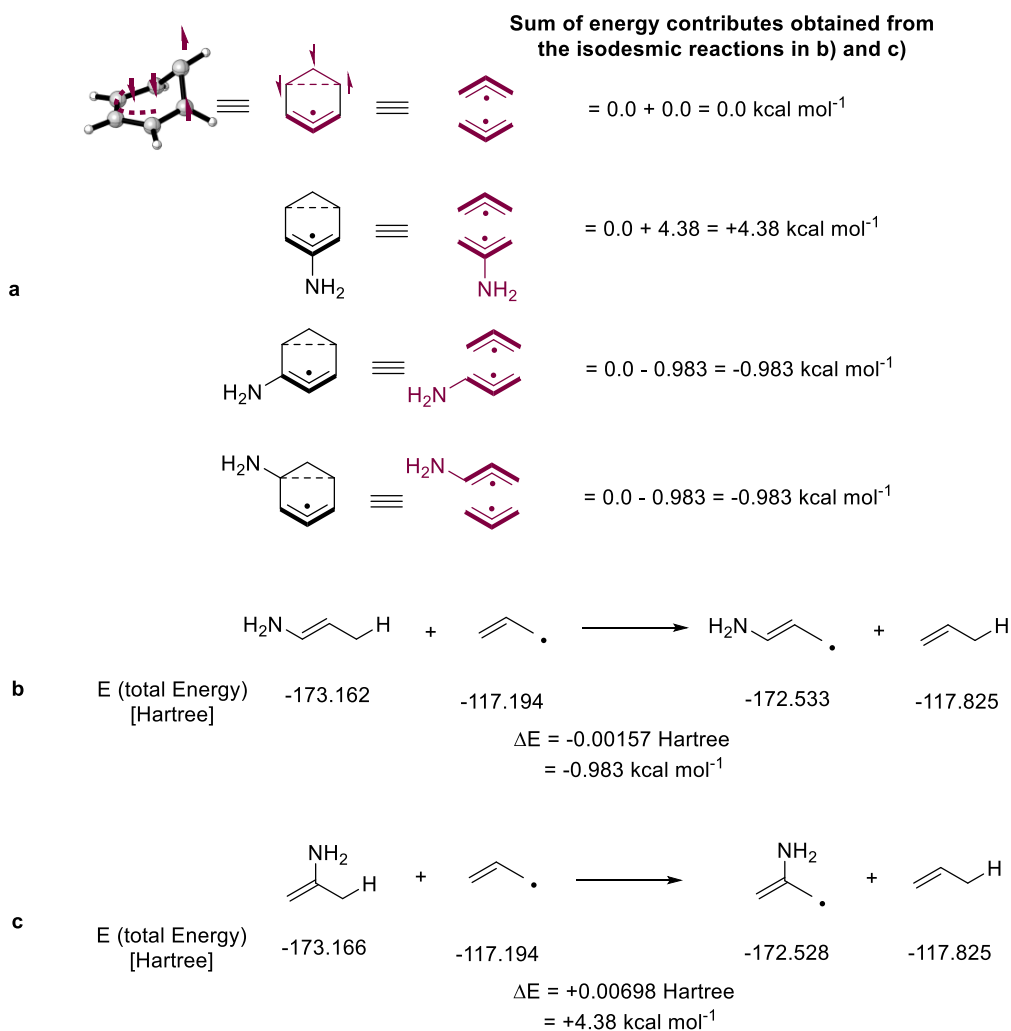
Hence an isodesmic reaction is obtained using density functional theory at the UB3LYP/6–31G(d) level. In Scheme 5.3b is presented the isodesmic equation that represents the stabilization of the 1–substituted allyl radical compared to allyl radical itself, while in Scheme 5.3c the same reasoning is made for the allyl radical substituted with the heteroatom at the central carbon. It appears clear from the calculations presented that if the 1–substituted allyl radical is slightly more stable than the parent allylic one (*ca.* 1 kcal mol<sup>-1</sup>), although the 2–substituted one is destabilized by 4.4 kcal mol<sup>-1</sup>. Summing

### New Intermediates from Photogenerated Phenyl Cations

the contributes for **1–4**, **3** appears to be destabilized in respect of **2** and **3** that on the other hand are weakly stabilized in respect of **4**, following the same trend found in the IRC calculations.

Differences between the chloroanilines can be ascribed to the position of the amino group in para position to the chlorine atom, that destabilizes the allyl radical formed in the transition state (further analysis of the frontier orbitals involved in the excited state is reported in Chapter 7.4).

A generalization of this reasoning lead to explain the similar morphology of the phenol excited state path to the S0S1 funnel and thus the lower emission found in **7** and **8**. The orbitals of toluene are less affected by substitution due to the apolar nature of the methyl, thus only minor differences can be found in the values of fluorescence emission of **8–10**.



**Scheme 5.3**

### 5.3 Conclusions

The results of this study confirm that the meta and ortho anilines are less reactive than their para isomer. Hence **1** is less prone to deactivate nonradiatively through the “Channel 3” in respect of the two other anilines, consequently it can either react populating the lower triplet state and form the triplet aryl cation, or to a smaller extent fluoresce. The generalization of this consideration could be applied to all the other systems bearing a strong electron rich polarizing group ( $-\text{OH}$ , for the case herein analysed, but as a major approximation also  $-\text{NMe}_2$  or  $\text{OMe}$ ), if a destabilizing interaction between the substituent placed on position 2 of the allylic moiety of the conical intersection is hypothesized. In this case the reported values of higher reactivity of the para isomers of the electron rich compounds<sup>[39,46]</sup> could be ascribed to a difficult funnelling through the prefulvenic conical intersection that depopulates the excited state.

With this study, no other differences were found both in the photophysics and in the photochemistry of chloroanilines. Further computational studies should be devoted to rationalize both the geometries at which the Intersystem Crossing to the triplet state occurs and the role of the substituents on this mechanism.

## 6 PHOTOCATALYTIC APPROACH TO INTERMEDIATE GENERATION

### 6.1 Photo-Meerwein approach to the synthesis of Isochromanones and Isochromenones

#### 6.1.1 Introduction

The isochromanone moiety (A, Chart 6.1) is a recurrent structure in a huge number of molecules recognized to have biological and pharmacological activity.<sup>[214–217]</sup> 3,4-Dihydroisocoumarins are commonly isolated from a wide variety of natural sources such as plant, insects and microbes and their activity spans from antifungal<sup>[218,219]</sup> to cytotoxic,<sup>[220]</sup> antimalarial<sup>[221]</sup> and antiallergical<sup>[222,223]</sup> properties.

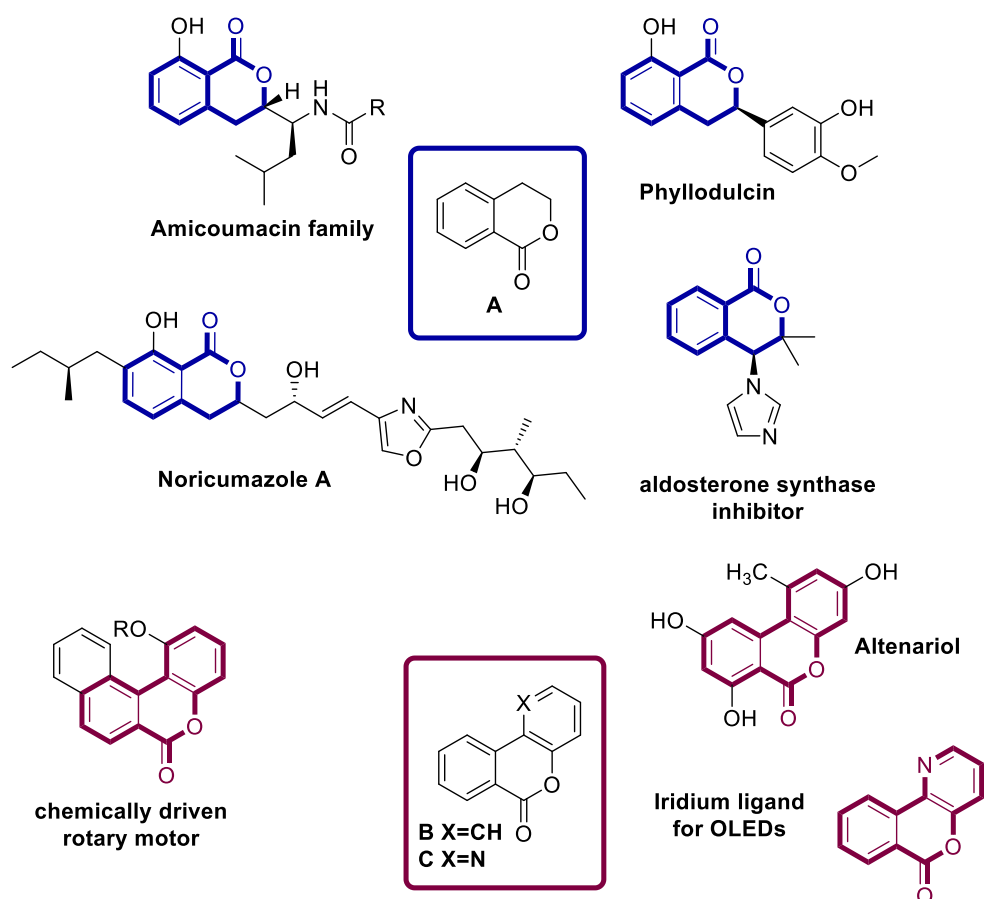


Chart 6.1

The interest on these molecules is clearly witnessed by the recent isolation of Icumazole A and by the total synthesis of Noricumazole A (Chart 6.1), two molecules characterised

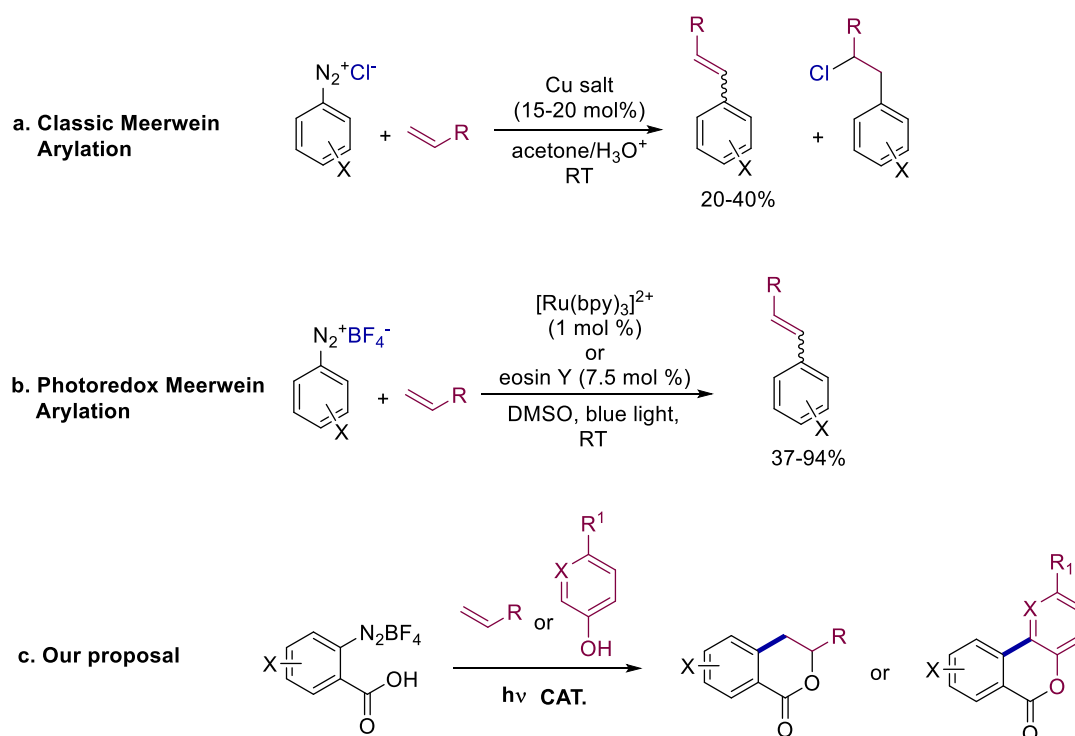


by a marked activity against various fungi and yeasts.<sup>[218]</sup> Moreover (S)-4-(1H-imidazol-1-yl)-3,3-dimethylisochroman-1-one was discovered as a significant aldosterone inhibitor.<sup>[224]</sup> Noteworthy, Amicoumacins (Chart 6.1) belong to an interesting family of antibiotics bearing the isochromanone core that are currently under study for their antibacterial antiinflammatory, antiulcer and antineoplastic action.<sup>[225,226]</sup> An interesting case is Phyllostulcin (Chart 6.1), principal constituent of *Hydrangeae Dulcis Folium*, a natural medicine belonging to the Japanese heritage and its traditional pharmacopoeia. Phyllostulcin not only possesses antimicrobial activity, but has a well-known sweetening effect, 600–800 times as sweet as sucrose.<sup>[219,227–229]</sup>

A structurally related family of compounds is represented by molecules possessing the isochromenone moiety (**B**, Chart 6.1) that, as the isochromanones, belongs to the bigger isocoumarin-like product family.<sup>[230]</sup> Molecules bearing an isochromenone functionality possess various biological activities,<sup>[230]</sup> thus they have found application in material chemistry, in liquid crystals and in the construction of molecular machine.<sup>[231,232]</sup> In particular, heterosubstituted derivatives **C** (Chart 6.1) emerged as a class of iridium ligands in strongly emitting organometallic complexes, that could find application in the development of tunable OLEDs.<sup>[233]</sup>

The large number of applications triggered the development of various synthetic routes for compounds **A–C**. The synthesis of dihydroisocoumarins comprises ortho lithiation of aromatic compounds,<sup>[234]</sup> oxidation of isochromane moiety,<sup>[141,235]</sup> NHC,<sup>[236]</sup> rhodium<sup>[237–239]</sup> or palladium<sup>[240]</sup> catalysed reactions, or procedures based either on rearrangements of isobenzofurans,<sup>[241]</sup> or Passerini–aldol sequence.<sup>[224]</sup> Besides, isochromenone tricyclics are synthesized by metal-catalysed and metal free oxidative lactonization.<sup>[242–245]</sup> On the other hand the derivatives **C** can be synthesized following a free radical pathway starting from ortho-bromobenzoic acids<sup>[246]</sup>, through a rearrangement of isoindolones<sup>[247]</sup> or by treating the diazonium salt of the anthranilic acid in the presence of TiCl<sub>3</sub> and 3-hydroxypyridines in aqueous hydrochloric acid.<sup>[248]</sup>

## New Intermediates from Photogenerated Phenyl Cations



**Scheme 6.1**

Herein we report the preparation of isochromanone and isochromenone by the photo-Meerwein reaction using the diazonium salt of different substituted anthranilic acid as the source of aryl radicals.<sup>[30,155,249]</sup> The classic Meerwein arylation scheme reported by Hans Meerwein in 1939 involves the copper catalysed addition of an aryl diazonium salt to an electron-poor alkene,<sup>[250]</sup> however the yields of this reaction are rather poor (only around 20–40%) with high catalyst loadings (Scheme 6.1a).<sup>[145]</sup> The use of an organometallic ( $[\text{Ru}(\text{bpy})_3]^{2+}$ ) or an organic (Eosin Y) photocatalyst allows the generation of aryl radicals from aryl diazonium salts under visible light irradiation by loss of molecular nitrogen. The radicals thus generated can be trapped by a suitable unsaturated compound forming a styrene in good yields (37–94%) by an addition–elimination reaction making use of low catalyst loadings (Scheme 6.1b).<sup>[145]</sup> We reasoned that the presence of an acidic moiety diazonium salt is crucial for cyclization step to occur and subsequently form the desired bi(tri)cyclic compound (Scheme 6.1c).

### 6.1.2 Results and Discussion

In order to develop a photo-Meerwein arylation for isochroma(e)none synthesis, we first investigated a series of different reaction conditions. The model reaction chosen for the optimization was the one between diazonium salt **1a**, thoroughly studied in the past as aryne source,<sup>[251,252]</sup> and styrene **2**. First, a set of different solvents was tested by using

$\text{Ru}(\text{bpy})_3\text{Cl}_2 \cdot 6\text{H}_2\text{O}$  (2 mol%, Entries 1–5) as the photocatalyst, and a ratio of **2/1a** of 5. Solvents spanning from MeCN and MeCN/water (9:1, volume ratio), to the protic (EtOH), polar aprotic (dry dimethylsulfoxide, DMSO) and non-polar (dichloromethane, DCM) were tested. Irradiations were carried out by using 455 nm blue LEDs under inert atmosphere at 23 °C for 2 h. Dry MeCN (entry 1) was identified as the best reaction medium and isochromanone **3** was obtained in 40% GC yield (37% isolated yield). The same reaction in dry MeCN any replacing the metal complex photocatalyst by Eosin Y (7.5 mol%, Entry 6) gave a lower yield of **3**. Next, the reaction was further optimized using dry MeCN as the solvent and  $\text{Ru}(\text{bpy})_3\text{Cl}_2 \cdot 6\text{H}_2\text{O}$  as the catalyst, varying the proportion of the diazonium salt and the olefin. We observed that a combination of **1a** and **2** in a 1:3 ratio gave a significant increase in the yield of the reaction (Entry 10, Table 6.1), giving up to 90% of compound **3** (GC yield). Interestingly, higher amounts of **2** were found to be detrimental for the overall yield, probably due to polymerization reactions as indicated by the presence of a thick insoluble precipitate. The catalyst loading was tested and further experiments confirmed that the maximum conversion is obtained with 2 mol% of  $\text{Ru}(\text{bpy})_3\text{Cl}_2 \cdot 6\text{H}_2\text{O}$  (Table 6.1, entries 10–12). Two control experiments were also carried out in order to assess the role of the catalyst and the effect of air on the reaction. Thus, irradiating the diazonium salt and the olefin under uncatalyzed conditions led only to a small amount of **3** (6% yield, Table 6.1, entry 13). Furthermore, degassing was proven to be necessary for the outcome of the reaction since the irradiation in the presence of air leads to a significant yield drop (55% yield, entry 14). Moreover, the reaction time was optimized and 2 h were sufficient to obtain a complete conversion of the diazonium salt (see Table 7.6). Therefore, after the evaluation of various reaction parameters, the optimum conditions were those reported in entry 10.

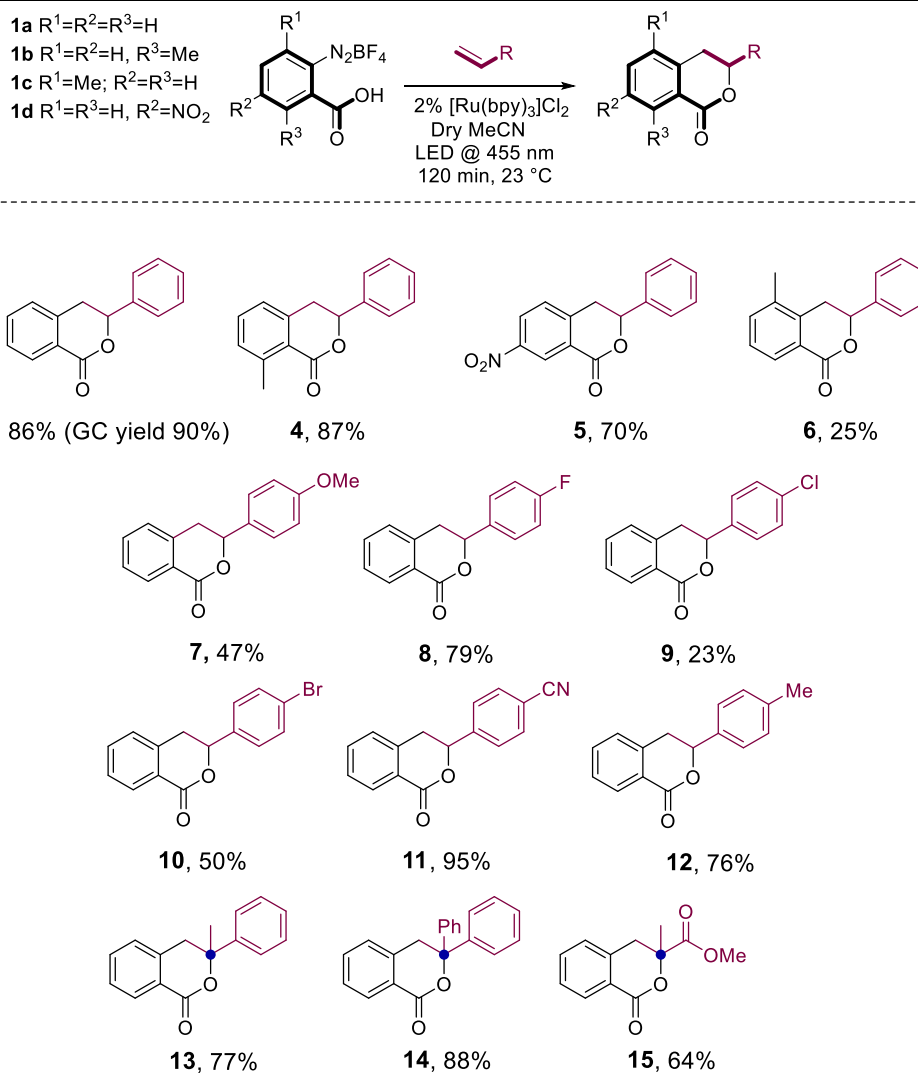
Having optimized the reaction conditions, we decided to investigate the reaction scope by using a series of diazonium salts of different benzoic acids and different substituted styrenes (Table 6.2). The photo-Meerwein reaction was found to occur in moderate to good yields (23–95%) affording a small library of 3,4-dihydroisocoumarins. Both the presence of different substituents on the ring of the diazonium salt and modifications of the electron demanding nature of the substituents on styrenes do not affect the reaction outcome. Both electron withdrawing and electron donating groups on the aromatic ring give acceptable yields of compounds **3-14**.

Table 6.1 Optimization of the Photo-Meerwein reaction of **1** with **2**.<sup>[a]</sup>

Entry	Solvent <sup>[a]</sup>	Catalyst (mol%)		<b>1a</b> <sup>[b]</sup>	<b>2</b> <sup>[b]</sup>	<b>3</b> [%] <sup>[c]</sup>
1	Dry MeCN	[Ru(bpy) <sub>3</sub> ] <sup>2+</sup>	(2)	1 equiv.	5 equiv.	40 (37) <sup>[d]</sup>
2	MeCN/water 9:1	[Ru(bpy) <sub>3</sub> ] <sup>2+</sup>	(2)	1 equiv.	5 equiv.	17
3	Dry DMSO	[Ru(bpy) <sub>3</sub> ] <sup>2+</sup>	(2)	1 equiv.	5 equiv.	35
4	DCM	[Ru(bpy) <sub>3</sub> ] <sup>2+</sup>	(2)	1 equiv.	5 equiv.	10
5	EtOH	[Ru(bpy) <sub>3</sub> ] <sup>2+</sup>	(2)	1 equiv.	5 equiv.	21
6	Dry MeCN	Eosin Y	(2)	1 equiv.	5 equiv.	34
7	Dry MeCN	[Ru(bpy) <sub>3</sub> ] <sup>2+</sup>	(2)	1 equiv.	1 equiv.	54
8	Dry MeCN	[Ru(bpy) <sub>3</sub> ] <sup>2+</sup>	(2)	5 equiv.	1 equiv.	30
9	Dry MeCN	[Ru(bpy) <sub>3</sub> ] <sup>2+</sup>	(2)	2 equiv.	1 equiv.	61
10	Dry MeCN	[Ru(bpy) <sub>3</sub> ] <sup>2+</sup>	(2)	1 equiv.	3 equiv.	90 (86) <sup>[d]</sup>
11	Dry MeCN	[Ru(bpy) <sub>3</sub> ] <sup>2+</sup>	(1)	1 equiv.	3 equiv.	78
12	Dry MeCN	[Ru(bpy) <sub>3</sub> ] <sup>2+</sup>	(3)	1 equiv.	3 equiv.	87
13	Dry MeCN	–		1 equiv.	3 equiv.	6
14	Dry MeCN <sup>[e]</sup>	[Ru(bpy) <sub>3</sub> ] <sup>2+</sup>	(2)	1 equiv.	3 equiv.	55

[a] The reactions are conducted under inert conditions (N<sub>2</sub>) for 120 min at 23°C. [b] The limiting reagent concentration is 0.25M. [c] GC yields. [d] Isolated yields. [e] Reaction conducted under air.

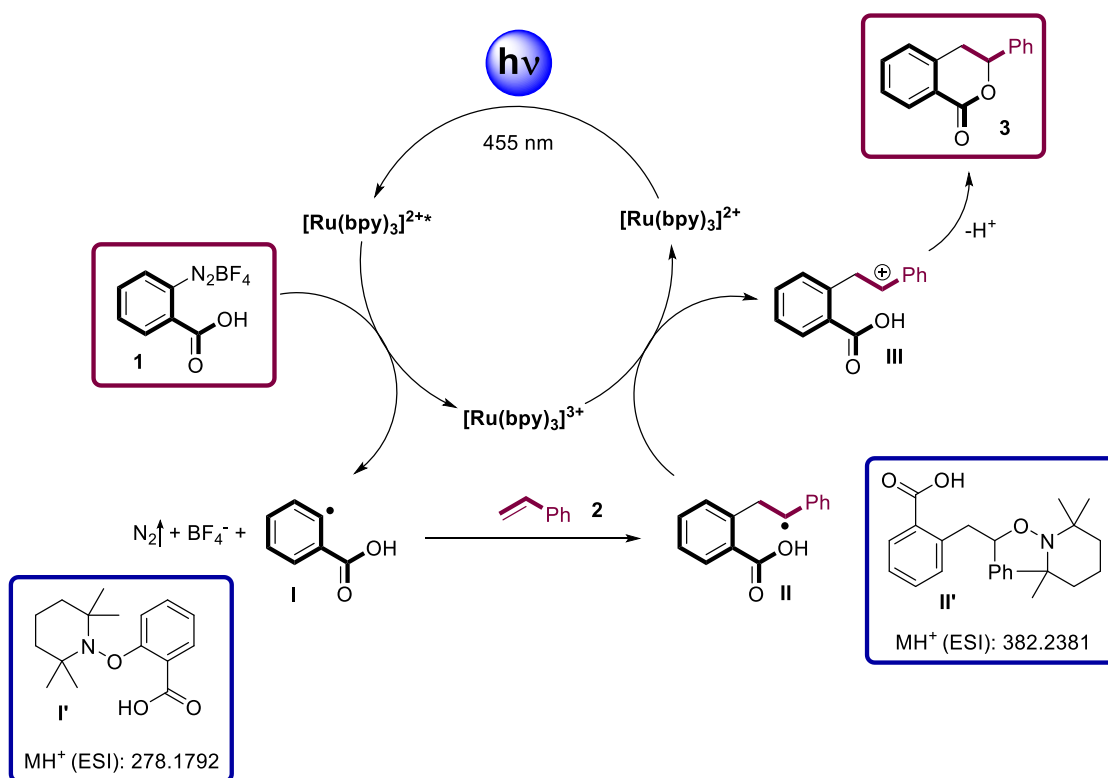
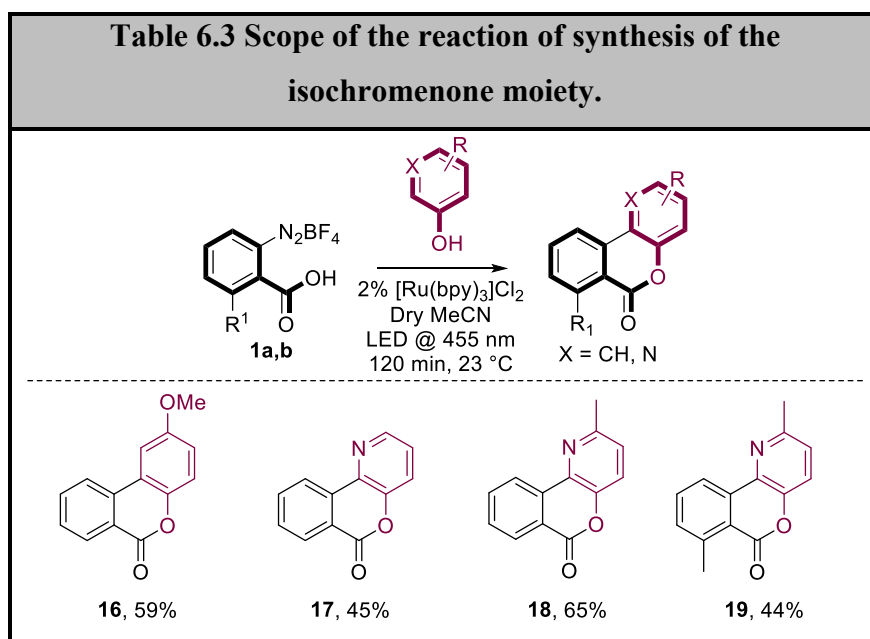
To extend the scope of the reaction methyl methacrylate was used as olefin giving product **15** in 64% yield. The formation of quaternary carbons is possible by the transformation and illustrated by the synthesis of compounds **13–15** that were obtained in good yields.

**Table 6.2 Scope of the reaction of synthesis of the isochromanone moiety.**

In order to broaden the scope of the reaction, (hetero)aromatic compounds were tested as trapping agents of the aryl radicals, in order to extend our protocol to isochromanones (Table 6.3).

Hydroxy substituted (hetero)aromatics were chosen due to the known ortho directing effect of the hydroxyl group on the regioselectivity of the radical attack.<sup>[248,253]</sup> Moreover, the presence of the hydroxy group allows the one-pot condensation of the carboxyl group with the alcohol, affording the tricyclic compounds **16–19** in yields comparable with those achievable with thermal methods.<sup>[248]</sup>

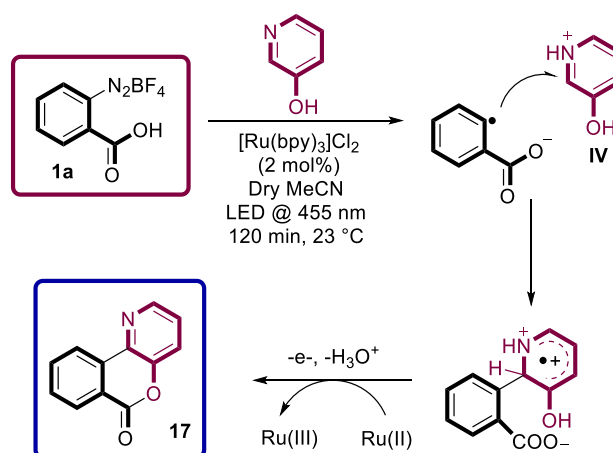
A plausible mechanism of the reactions presented is shown in Scheme 6.2 for the reaction of **1a** and styrene. Experiments in the presence of TEMPO support a photo-Meerwein radical reaction pathway (see Chapter 7.5.4).<sup>[254]</sup>



Scheme 6.2

Oxidative quenching of the photoexcited Ru catalyst by diazonium salt **1** followed by loss of N<sub>2</sub> leads to the aryl radical **I** that in the presence of styrene gives radical **II**. The catalytic cycle is closed by the electron transfer from **II** to the oxidised form of the catalyst that generates the benzyl cation **III**. Branched π nucleophiles like diphenylethylene or methyl methacrylate promote a better stabilization of the cationic intermediate allowing the formation of quaternary carbon centres in high yield, as demonstrated by products **13-**

15. The final product **3** is obtained from ring closure and subsequent proton loss of the cation **III** (Scheme 6.2). Both radical intermediates **I** and **II** were trapped by TEMPO to give **I'** ( $\text{MH}^+$  (ESI-MS): 278.1792) and **II'** ( $\text{MH}^+$  (ESI-MS): 382.2381), respectively. On the other hand, the selectivity of the attack in position 2 of the pyridine and phenolic ring can be explained on the basis of cases previously reported in the literature.<sup>[248,253]</sup> In particular for the hydroxypyridine reaction we propose the intermediacy of the 3-hydroxypyridinium cation **IV**, generated *in situ* from the interaction of the heterocyclic nitrogen and the carboxylic acid proton (Scheme 6.3).<sup>[248,253,255]</sup>



Scheme 6.3

### 6.1.1 Conclusion

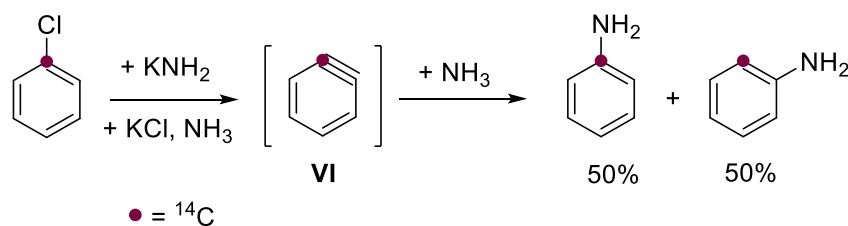
In conclusion, we optimized and developed a photo-Meerwein procedure giving access to structurally diverse isochromanone derivatives bearing the dihydroisocoumarin core and to the (hetero)biaryl tricyclic isochromenones. The reported method is reliable and affords the desired products in good yields with high selectivity under mild conditions.

## 6.2 Study on the photocatalytic generation of benzyne

## 6.2.1 Introduction

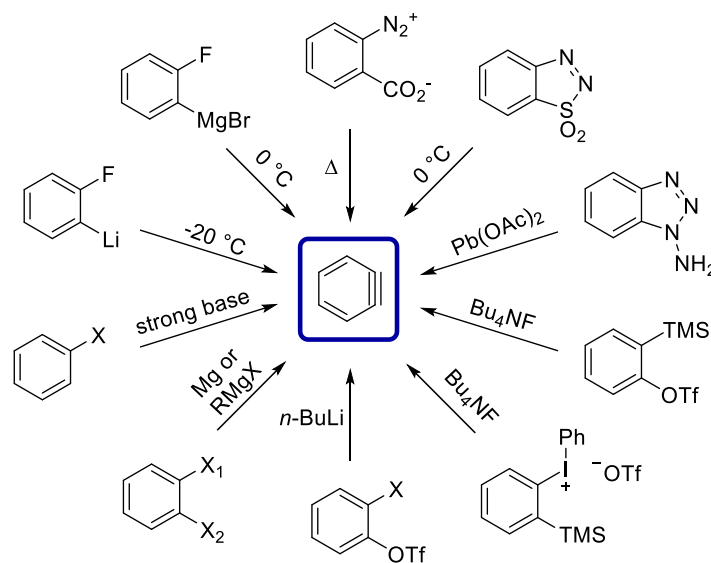
We then focused on the generation of an orthobenzyne biradical by means of photocatalysis.

The existence of ortho-benzyne **VI** was firstly postulated in 1927<sup>[256]</sup> by Bachmann *et al.* and its role as intermediate was corroborated by the work of Wittig<sup>[257]</sup> and confirmed by Roberts *et al.* with the work on the reaction of <sup>14</sup>C-labelled chlorobenzene with sodium amide (Scheme 6.4).



Scheme 6.4

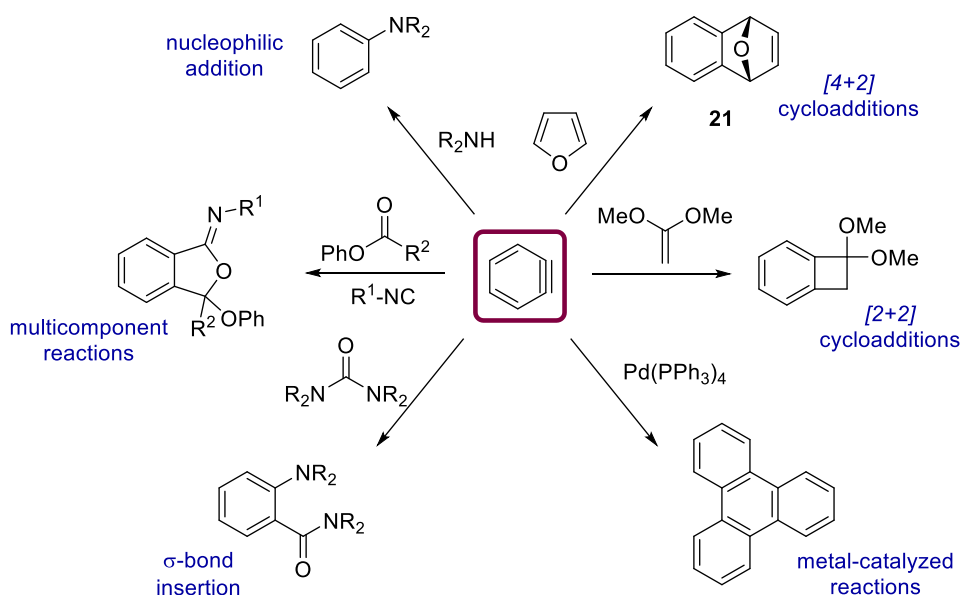
Its synthetic scope was initially limited due to the harsh conditions required.<sup>[49,251,258]</sup> The classical ways of benzyne formation comprises at the moment a plethora of different approaches, (see exemplary in Scheme 6.5<sup>[50]</sup>) most of them need the presence of strong bases such as alkyl lithium species, nevertheless the development of precursors that requires milder reaction conditions such as the ortho silyl triflates belonging to the so-called Kobayashi protocol<sup>[259,260]</sup> and similar reagents,<sup>[261]</sup> allowed the benzyne chemistry to be smoothly used in almost neutral conditions. Noteworthy, a benzyne chemistry step is applied in the synthesis of more than 75 natural polycyclic compounds.<sup>[50]</sup>



Scheme 6.5



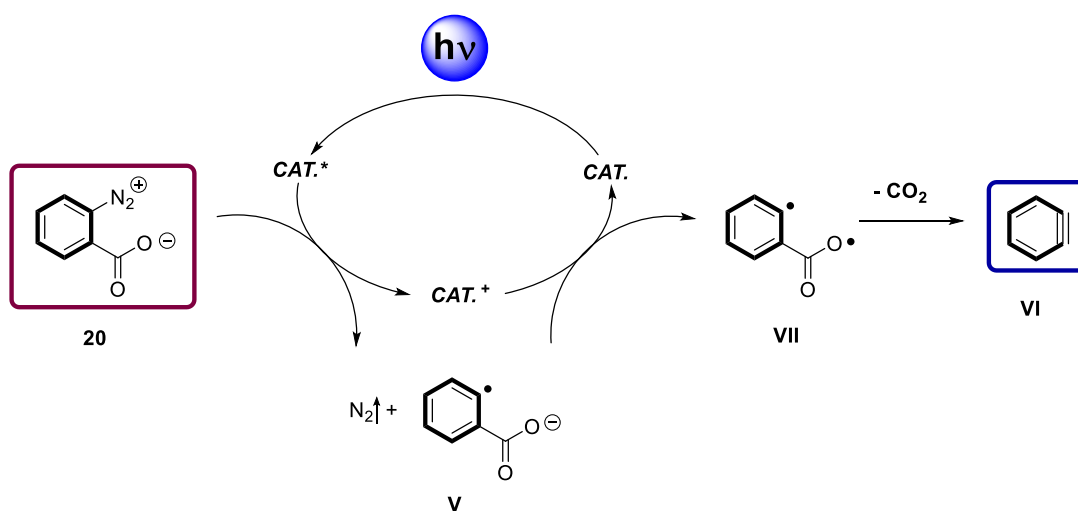
The reactions the benzyne can undergo are indeed various<sup>[51]</sup> and include [4+2]<sup>[262]</sup> or [2+2]<sup>[263]</sup> cycloadditions, metal-catalyzed reactions,<sup>[264]</sup>  $\sigma$ -bond insertions,<sup>[265]</sup> multicomponent reactions<sup>[266]</sup> and nucleophilic additions<sup>[267]</sup> (Scheme 6.6).



Scheme 6.6

Remarkably, also the photochemists undertook the challenge of discovering new precursors for the benzyne generation,<sup>[47,52,53]</sup> however to the best of our knowledge no photocatalytic approach for this task was attempted yet.

We reasoned that the diazonium salt of the anthranilate **20** could be a potential reagent for benzyne formation. A photocatalyst in its excited state could be able to donate an electron to the  $N_2^+$  group, forming **V**. At this point the oxidized form of the catalyst should be able to abstract an electron from the lone pair on the carboxylate affording the diradical **VII**. The carboxyl radical spontaneously eliminates carbon dioxide generating the aryne **VI** (Scheme 6.7).



Scheme 6.7

Hence, it is compulsory for this approach that the diazonium salt should be in its deprotonated form, otherwise the catalytic cycle could not be closed due to the extremely high oxidation potentials of the carboxylic acid species itself (oxidation potential  $> +1.85\text{V vs. Ag/AgCl}$ )<sup>[268]</sup>.

### 6.2.2 Results and Discussion

To develop a photocatalytic approach for the generation of the benzyne the catalyst chosen for the tests is the  $[\text{Ru}(\text{bpy})_3]^{2+}$  complex previously used efficiently for the synthesis of isochromanones and isochromenones via a photoredox–Meerwein approach. The ruthenium (II) catalyst can efficiently donate an electron to the  $\text{N}_2^+$  group<sup>[119]</sup> while its oxidized state is potentially able to abstract an electron from the carboxylate **20** ( $\text{Ru}^{3+}/\text{Ru}^{2+}=1.29\text{V vs. SHE}$ ,<sup>[119]</sup> while the potential of oxidation of the carboxylate is reported to be  $1.24\text{V vs. SHE}$ )<sup>[269]</sup>. The short lifetime of the ortho–benzyne, which decay was studied by Zewail *et al.* and deemed to be in the range of  $400\text{ ps}$ ,<sup>[270]</sup> imparts an intrinsic difficulty to the direct detection of the presence of the intermediate formation in solution. Furan was consequently used as a convenient trap for the aryne, due to the ability of the latter to undergo facile  $[4+2]$  click reactions with this heterocyclic aromatic compound, that is considered one of the prototypical “arynophiles”.<sup>[261]</sup> The formation of 1,4-dihydro-1,4-epoxynaphthalene (**21**, Scheme 6.6) was followed by means of GC analysis.

In order to make **20** to react, two approaches were followed for its generation in solution. The first one consisted in its synthesis starting from the anthanilic acid in the presence of

a suitable nitrite reactant, while the second choice was based on the deprotonation of the anthranilic acid diazonium salt with suitable bases.

Hence the first part of the study was mainly based on the generation of **20** starting from the anthranilic acid **22**. The procedure were derived from the seminal work of Friedman and Logullo<sup>[258]</sup> and of Ried and Schön,<sup>[271]</sup> though different variations of the experimental procedures were explored.

The protocol to synthesize the anthranilate **20** was characterized by the reaction between isoamyl nitrite (1.5 equiv.) and **22** (1 equiv.) in various media and trichloroacetic acid (1 mol%) (see Table 6.4). Irradiations were conducted using LEDs emitting at 455 nm at different temperatures with  $[\text{Ru}(\text{bpy}_3)]^{2+}$  and Eosin Y as photocatalysts. Irradiation was kept for 30 mins, even though in the majority of the cases gas evolution stopped after a few minutes the LED was turned on, with complete consumption of **22**. All the solutions were kept under inert atmosphere inside a Schlenk tube with an additional cone for addition of the reagents with a quick fit septum equipped with a quartz rod, that allowed the light of the LED mounted on top of it to be transmitted to the solution. The apparatus thus constructed, granted the temperature to be controlled precisely during the irradiation. In all the tested conditions (Table 6.4), no [4+2] adduct with furan was detected.

In all these cases an unknown peak at the GC was found. The signal was attributed to 3a,9b-dihydro-5H-furo[3,2-c]isochromen-5-one (Figure 6.1), but all the attempts to isolate the compound failed.

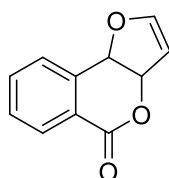
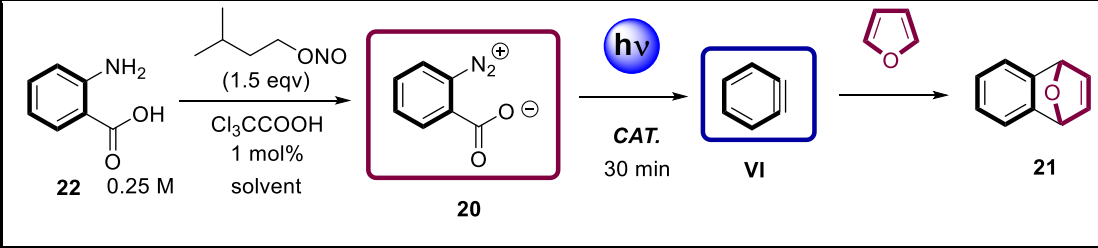


Figure 6.1

Following the negative results obtained with the first method, the generation of the anthranilate diazonium salt was done through the deprotonation of the anthranilic acid diazonium salt. All the reactions were conducted in acetonitrile, evaluating the effect of different carbonates, *viz.* Li, Na and Ca salts. Three sets of experiments were designed: the first one comprised the irradiation of the diazonium salt with the different bases in the presence of the  $[\text{Ru}(\text{bpy})_3] \cdot 3\text{H}_2\text{O}$  catalyst (Table 6.5 entries 1–3). The second and the third one consisted of the reaction of the mixture in absence of irradiation, with (Table 6.5 entries 4–6), or without (Table 6.5 entries 7–9) the photocatalyst.

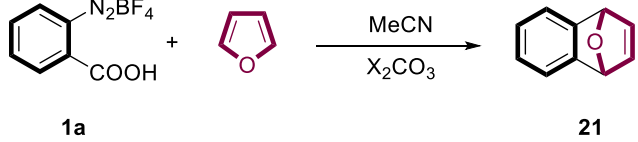
**Table 6.4 Screening of conditions for in situ generation of benzyne from 22**


Solvent and conditions <sup>[a]</sup>	Catalyst (mol %)	Furan [eqv]	T [°C]	21 [%]
THF	[Ru(bpy <sub>3</sub> )] <sup>2+</sup> (2)	5	0	0
THF	[Ru(bpy <sub>3</sub> )] <sup>2+</sup> (2)	5	0→RT	0
THF <sup>[b]</sup>	[Ru(bpy <sub>3</sub> )] <sup>2+</sup> (2)	5	0→RT	0
THF <sup>[c]</sup>	[Ru(bpy <sub>3</sub> )] <sup>2+</sup> (2)	5	0	0
THF <sup>[d]</sup> (dropping 1 in the dark)	[Ru(bpy <sub>3</sub> )] <sup>2+</sup> (2)	5	0	0
THF/DCM 1:1 <sup>[c]</sup>	[Ru(bpy <sub>3</sub> )] <sup>2+</sup> (2)	5	0	0
THF/DCM 1:1 <sup>[c]</sup>	[Ru(bpy <sub>3</sub> )] <sup>2+</sup> (2)	5	23	0
MeCN	[Ru(bpy <sub>3</sub> )] <sup>2+</sup> (2)	10	0	0
MeCN/water 9:1	[Ru(bpy <sub>3</sub> )] <sup>2+</sup> (2)	10	0	0
MeCN/water 8:2	[Ru(bpy <sub>3</sub> )] <sup>2+</sup> (2)	10	0	0
MeCN/water 1:1	[Ru(bpy <sub>3</sub> )] <sup>2+</sup> (2)	5	0	0
DCM/Acetone 8:2	[Ru(bpy <sub>3</sub> )] <sup>2+</sup> (2)	10	0	0
DMSO	[Ru(bpy <sub>3</sub> )] <sup>2+</sup> (2)	5	23	0
DMIM BTI <sup>[e]</sup>	[Ru(bpy <sub>3</sub> )] <sup>2+</sup> (2)	5	0	0
DMIM BTI <sup>[e]</sup>	[Ru(bpy <sub>3</sub> )] <sup>2+</sup> (2)	5	23	0
MeCN/water 1:1	Eosin Y (5)	5	0	0
DMSO	Eosin Y (5)	5	23	0
DMIM BTI <sup>[e]</sup>	Eosin Y (5)	5	0	0
DMIM BTI <sup>[e]</sup>	Eosin Y (5)	5	23	0

[a] 30 minutes irradiation using blue LEDs at 455 nm. [b] 30 min stirring in the dark than 10 min irradiation. [c] **22** added dropwise during irradiation. [d] **22** added dropwise in 5 min before irradiation [e] 1-Decyl-3-methylimidazolium bis(trifluoromethylsulfonyl)imide.

Quite surprisingly, all the entries where the irradiation occurred didn't generate the benzyne adduct, while the peak assigned to 3a,9b-dihydro-5H-furo[3,2-c]isochromen-5-one was found. Furthermore, the thermal reactions in the presence of a base afforded the desired product in average to high yields, with an increase that followed the solubility of

the base in acetonitrile. Presence of the photocatalyst was found unfavourable for the reaction even in the absence of light, probably as a consequence of secondary reactions that involved the Ruthenium.

<b>Table 6.5 Screening of different conditions for in situ generation of benzyne from 1a</b>		
		
<b>1a</b>		<b>21</b>
<b>Conditions<sup>[a]</sup></b>	<b>X<sub>2</sub>CO<sub>3</sub><sup>[b]</sup></b>	<b>21<sup>[c]</sup></b>
<b>LED @ 455 nm with Cat.</b>	K	0
<b>LED @ 455 nm with Cat.</b>	Na	0
<b>LED @ 455 nm with Cat.</b>	Li	0
<b>No irradiation with Cat.</b>	K	63
<b>No irradiation with Cat.</b>	Na	45
<b>No irradiation with Cat.</b>	Li	11
<b>No irradiation No Cat.</b>	K	71
<b>No irradiation No Cat.</b>	Na	50
<b>No irradiation No Cat.</b>	Li	10
[a] <b>1</b> (0.25 M) and furan (5 eqv) under inert conditions (N <sub>2</sub> ) for 120 min at 23°C. Catalyst is [Ru(bpy) <sub>3</sub> ] <sup>2+</sup> [b] Concentration of the base is 0.25 M. [c] GC yields.		

The results thus obtained demonstrate the impossibility to generate the benzyne intermediate by using the [Ru(bpy)<sub>3</sub>] or Eosin Y catalyst under irradiation. This failure is probably related both to the catalyst, that promotes the Meerwein arylation in a faster way than the elimination of CO<sub>2</sub> from the carboxylate, and presumably to the oxidation potentials of the CO<sub>2</sub><sup>-</sup> group in the anthranilic acid that could be higher than expected, consequently the [Ru(bpy)<sub>3</sub>] photocatalyst in its oxidized form could not be able to abstract an electron from the radical anion (**V**) promoting the cleavage of carbon dioxide and subsequent generation of benzyne.

However, this results confirms that a side thermal reaction that actually generates benzyne could be present, but the presence of the photocatalyst inhibits this pathway. Those conclusions are an evidence in favour of the proposed mechanism of the photo-Meerwein generation of isochromenones, where the **V** is postulated to exist as an intermediate. The

coupling between the **V** and the pyridinium cation is faster than the abstraction of an electron from the carboxylate group induced by the catalyst (Scheme 6.3).

### 6.2.3 Conclusion and future perspectives

Even though a photocatalytical approach to the generation of benzyne could not be discovered, the results obtained gave a deeper insight on the mechanism of action of the ruthenium catalyst, allowing to unravel the mechanism of formation of the isochromenones via a Photo–Meerwein protocol. Future improvements of the methods could be achieved screening a wider range of photocatalysts, possessing higher oxidation potential in their oxidized state, allowing a feasible electron transfer from the carboxylate (*i.e.*  $[\text{Ru}(\text{bpz})_3]^{2+}$ , which oxidation potential for the redox couple Ru(III)/Ru(II) is +1.86 V<sup>[119,272,273]</sup>).

## 7 EXPERIMENTAL SECTION

### 7.1 Experimental details relative to Chapter 2

#### 7.1.1 Synthetic procedures

$^1\text{H}$  and  $^{13}\text{C}$  NMR spectra were recorded on a 200, 300 or 400 MHz spectrometer. The attributions were made on the basis of  $^1\text{H}$  and  $^{13}\text{C}$  NMR, as well as DEPT-135 experiments; chemical shifts are reported in ppm downfield from TMS. UV and fluorescence spectra were recorded on a Jasco V-550 UV spectrophotometer and a PerkinElmer LS55 luminescence spectrometer, respectively.

The photochemical reactions were performed by using nitrogen-purged solutions in quartz tubes. Irradiations were performed in a multilamp reactor fitted with ten 15 W phosphor coated lamps (maximum of emission at 310 nm) or with four low pressure Hg lamps (maximum of emission at 254 nm). Workup of the photolytes involved concentration in vacuo and chromatographic separation by using silica gel. Solvent of HPLC purity were employed in the photochemical reactions. Quantum yields were measured at 254 nm (1 Hg lamp, 15W).

The reaction course was followed by GC analyses and the products formed were identified and quantified by comparison with authentic samples. GC-MS analyses were carried out using a Thermo Scientific DSQII single quadrupole GC/MS system. A Restek Rtx-5MS (30 m  $\times$  0.25 mm  $\times$  0.25  $\mu\text{m}$ ) capillary column was used for analytes separation with helium as carrier gas at 1 mL  $\text{min}^{-1}$ . The injection in the GC system was performed in split mode and the injector temperature was 250  $^\circ\text{C}$ . The GC oven temperature was held at 80  $^\circ\text{C}$  for 2 min, increased to 220  $^\circ\text{C}$  by a temperature ramp of 10  $^\circ\text{C min}^{-1}$  and held for ten min. The transfer line temperature was 250  $^\circ\text{C}$  and the ion source temperature 250  $^\circ\text{C}$ . Mass spectral analyses were carried out in full scan mode.

Benzyltrimethylsilane (**6**), toluene (**7**), bibenzyl (**7'**), 2-phenylethanol (**7''**), 2-methyl-1-phenylpropan-2-ol (**7'''**), benzyl methyl ether (**8**), p-cresol (**9'**), 2-(4-hydroxyphenyl)ethanol (**9''**), were commercially available and used as received. The structure of compounds **4'** and **4''** has been determined by GC-MS analyses.

**4'**: GC-MS (m/z) 73 (100), 106 (25), 137 (22), 153 (33), 163 (28), 179 (72), 227 (29), 243 (22), 258 (39).

**4''**: GC-MS (m/z) 73 (100), 156 (77), 233 (4), 248 (2).

#### 7.1.1.1 General procedure for the irradiation of compounds **1–3**

A solution (2 mL) of the substrate (**1–3**, 0.025 M) in the chosen medium was poured into quartz tubes, purged with nitrogen and irradiated using a multilamp reactor fitted with four low pressure Hg lamps (emission maximum at 254 nm) or ten 15 W phosphor-coated lamps (emission maximum at 310 nm) for the sensitized photoreactions. The solution was then analyzed by GC/MS. The photoproducts were identified by comparison with authentic samples and quantified by using calibration curves.

#### 7.1.1.2 General procedure for the synthesis of n-(trimethylsilylmethyl) phenols **4a–c**

The compounds **4a–c** were prepared from the corresponding anisoles by following a known procedure under anhydrous conditions.<sup>[28]</sup> Into a three-necked round-bottom flask, a solution of the n-(trimethylsilylmethyl) anisole (2.2 g, 11 mmol) in anhydrous CH<sub>2</sub>Cl<sub>2</sub> (23 mL) was cooled at -78 °C. Then a BBr<sub>3</sub> solution in CH<sub>2</sub>Cl<sub>2</sub> (12 mL, 1M) was added dropwise, while maintaining vigorous stirring. The resulting mixture was then allowed to reach room temperature and further stirred for 3h, then poured into a water/ice mixture (20 mL). The aqueous layer was separated and extracted with 2×20 mL of CH<sub>2</sub>Cl<sub>2</sub>. The organic phases were collected, dried over Na<sub>2</sub>SO<sub>4</sub> and the solvent evaporated. The obtained residue was purified by column chromatography (eluant: cyclohexane:ethyl acetate 99:1).

**4-(Trimethylsilylmethyl)phenol (4a)**. Obtained in 94% yield from 4-(trimethylsilylmethyl) anisole<sup>[274,275]</sup> as a colorless solid, mp. 89.7–92.6 °C. <sup>1</sup>H-NMR (CDCl<sub>3</sub>):<sup>[276]</sup> δ 6.70-6.85 (AA'BB', 4H), 2.00 (s, 2H), 0.00 (s, 9H); <sup>13</sup>C-NMR (CDCl<sub>3</sub>): δ 151.9, 132.2, 128.6 (CH), 114.8 (CH), 25.4 (CH<sub>2</sub>), -2.3 (CH<sub>3</sub>); IR (neat, v/cm<sup>-1</sup>): 3200, 1598, 1508, 849; Anal. Calcd. for C<sub>10</sub>H<sub>16</sub>OSi: C, 66.61; H, 8.94. Found: C, 66.6; H, 8.9.

**3-(Trimethylsilylmethyl)phenol (4b)**. Obtained in 97% yield from 3-(trimethylsilylmethyl)anisole (**5**,<sup>[277]</sup>) as an oil. <sup>1</sup>H-NMR (CDCl<sub>3</sub>):<sup>[276]</sup> δ 7.08 (t, 1H, *J* = 7.8 Hz), 6.58 (d, 1H), 6.55 (d, 1H, *J* = 7,8 Hz), 6.49 (s, 1H), 4.80 (s, 1H), 2.04 (s, 2H), 0.00 (s, 9H); <sup>13</sup>C-NMR (CDCl<sub>3</sub>): δ 155.0, 142.6, 129.3 (CH), 120.9 (CH), 115.1 (CH), 111.1 (CH), 27.1 (CH<sub>2</sub>), -1.9 (CH<sub>3</sub>); IR (neat, v/cm<sup>-1</sup>): 3340, 1586, 1249, 943, 849; Anal. Calcd. for C<sub>10</sub>H<sub>16</sub>OSi: C, 66.61; H, 8.94. Found: C, 66.7; H, 9.0.



**2-(Trimethylsilylmethyl)phenol (4c).** Obtained in 95% yield from 2-(trimethylsilylmethyl)anisole<sup>[278]</sup> as an oil. <sup>1</sup>H-NMR (CDCl<sub>3</sub>):<sup>[276]</sup>  $\delta$  7.01-6.99 (m, 2H), 6.85 (m, 1H), 6.77 (m, 1H), 2.10 (s, 2H), 0.06 (s, 9H); <sup>13</sup>C-NMR (CDCl<sub>3</sub>):  $\delta$  152.3, 129.9 (CH), 126.6, 125.1 (CH), 120.6 (CH), 114.9 (CH), 26.8 (CH<sub>2</sub>), -1.7 (CH<sub>3</sub>); IR (neat, v/cm<sup>-1</sup>): 3393, 2955, 1590, 1500, 1454, 1247, 859, 751; Anal. Calcd. for C<sub>10</sub>H<sub>16</sub>OSi: C, 66.61; H, 8.94. Found: C, 66.7; H, 8.8.

#### 7.1.1.3 General procedure for the synthesis of aryl methanesulfonates **1a–c** and **9Ms**

The procedure is a modification of a synthesis found in the literature.<sup>[279]</sup> To a cooled (10 °C) solution of the chosen phenol **4a–c** (1 g, 5.6 mmol, 0.2 M), Et<sub>3</sub>N (1.2 mL, 8.3 mmol) in CH<sub>2</sub>Cl<sub>2</sub> (28 mL), methansulfonyl chloride (820  $\mu$ L, 6.1 mmol) was added dropwise. After ten minutes the temperature was allowed to raise to room temperature and stirred for 3h. The reaction mixture was then poured into a of water/ice mixture (20 mL), the organic layer was washed with brine (20 mL) and water (20 mL), dried over Na<sub>2</sub>SO<sub>4</sub> and the solvent evaporated. The obtained residue was purified by column chromatography (stationary phase: alumina, eluant: cyclohexane/ethyl acetate 99:1 + 0.2% Et<sub>3</sub>N).

**4-(Trimethylsilylmethyl)phenyl methanesulfonate (1a).** Obtained in 84% yield from **4a**, colorless solid, mp. 45.1-46.9 °C. <sup>1</sup>H-NMR (CDCl<sub>3</sub>):  $\delta$  7.00-7.15 (AA'BB', 4H), 3.15 (s, 3H), 2.10 (s, 2H), 0.00 (s, 9H); <sup>13</sup>C-NMR (CDCl<sub>3</sub>):  $\delta$  145.9, 140.1, 129.0 (CH), 121.5 (CH), 36.9 (CH<sub>3</sub>), 26.5 (CH<sub>2</sub>), -2.1 (CH<sub>3</sub>); IR (neat, v/cm<sup>-1</sup>): 2955, 1500, 1368, 1155, 970; Anal. Calcd. for C<sub>11</sub>H<sub>18</sub>O<sub>3</sub>SSi: C, 51.13; H, 7.02. Found: C, 51.1; H, 7.1.

**3-(Trimethylsilylmethyl)phenyl methanesulfonate (1b).** Obtained in 73% yield from **4b**, oil. <sup>1</sup>H-NMR (CDCl<sub>3</sub>):  $\delta$  7.30-7.25 (m, 1H), 7.05-6.95 (m, 3H), 3.15 (s, 3H), 2.10 (s, 2H), 0.00 (s, 9H); <sup>13</sup>C-NMR (CDCl<sub>3</sub>):  $\delta$  151.0, 145.1, 131.2 (CH), 128.7 (CH), 123.0 (CH), 118.9 (CH), 38.9 (CH<sub>3</sub>), 28.9 (CH<sub>2</sub>), -0.3 (CH<sub>3</sub>); IR (neat v/cm<sup>-1</sup>): 2955, 1607, 1581, 1369, 1182, 824; Anal. Calcd. for C<sub>11</sub>H<sub>18</sub>O<sub>3</sub>SSi: C, 51.13; H, 7.02. Found: C, 51.0; H, 7.0.

**2-(Trimethylsilylmethyl)phenyl methanesulfonate (1c).** Obtained in 34% yield from **4c**, colorless solid. mp. 45.8-47.9 °C. <sup>1</sup>H-NMR (CDCl<sub>3</sub>):  $\delta$  7.00-7.14 (m, 4H), 3.20 (s, 3H), 2.20 (s, 2H), 0.05 (s, 9H); <sup>13</sup>C-NMR (CDCl<sub>3</sub>):  $\delta$  146.6, 133.8, 130.6 (CH), 126.9 (CH), 125.4 (CH), 121.7 (CH), 38.0 (CH<sub>3</sub>), 21.3 (CH<sub>2</sub>), -1.7 (CH<sub>3</sub>); IR (neat v/cm<sup>-1</sup>): 2955, 1578, 1487, 1365, 970. Anal. Calcd. for C<sub>11</sub>H<sub>18</sub>O<sub>3</sub>SSi: C, 51.13; H, 7.02. Found: C, 51.1; H, 7.1

**4-Methyphenyl methanesulfonate (9Ms).** was obtained in 81% yield from p-cresol, colorless solid. mp 45-47 °C (lit. 44–45<sup>[280]</sup>). IR (neat  $\nu/\text{cm}^{-1}$ ): 3035, 2941, 1506, 1372, 1361, 1199, 1174, 1148, 972, 871; Anal. Calcd. for  $\text{C}_8\text{H}_{10}\text{O}_3\text{S}$ : C, 51.60; H, 5.41. Found: C, 51.7; H, 5.5. The spectroscopic data of **9Ms** were in accordance with the literature.<sup>[280]</sup>

#### 7.1.1.4 General procedure for the synthesis of aryl trifluoromethanesulfonates **2a–c**

The procedure was adapted from that found in the literature.<sup>[281]</sup> In a round-bottom flask a bilayer system composed by a solution of the chosen phenol **4a–c** (2 g, 12 mmol) in  $\text{CH}_2\text{Cl}_2$  (0.3 M solution) and a 20% aq. LiOH solution is cooled down to -10 °C. 2 mL (12 mmol) of  $\text{Tf}_2\text{O}$  were added dropwise under stirring, then the reaction mixture was kept at -10 °C for 10 min and later stirred for 3h at room temperature. The organic layer was separated, washed with  $2 \times 10$  mL of water and dried over  $\text{MgSO}_4$ . The solvent was evaporated and the obtained residue purified by column chromatography (stationary phase: neutral alumina; eluant: cyclohexane/ethyl acetate 99:1 + 0.2%  $\text{Et}_3\text{N}$ ).

**4-(Trimethylsilylmethyl)phenyl trifluoromethanesulfonate (2a).** Obtained in 72% yield from **4a**, colorless oil.  $^1\text{H-NMR}$  ( $\text{CDCl}_3$ ):  $\delta$  7.15-7.00 (AA'BB', 4H), 2.10 (s, 2H), 0.00 (s, 9H);  $^{13}\text{C-NMR}$  ( $\text{CDCl}_3$ ):  $\delta$  146.4, 141.3, 129.1 (CH), 125.0 (q,  $J = 315$  Hz,  $\text{CF}_3$ ), 120.8 (CH), 26.6 ( $\text{CH}_2$ ), -2.2 ( $\text{CH}_3$ ); IR (neat,  $\nu/\text{cm}^{-1}$ ): 2958, 1499, 1425, 1251, 1211, 1143, 891, 852; Anal. Calcd. for  $\text{C}_{11}\text{H}_{15}\text{F}_3\text{O}_3\text{SSi}$ : C, 42.29; H, 4.84. Found: C, 42.2; H, 4.9.

**3-(Trimethylsilylmethyl)phenyl trifluoromethanesulfonate (2b).** Obtained in 79% yield from **4b**, colorless oil.  $^1\text{H-NMR}$  ( $\text{CDCl}_3$ ):  $\delta$  7.00-7.05 (m, 1H), 6.90-6.95 (m, 2H), 6.90-6.95 (m, 1H), 2.15 (s, 2H), 0.00 (s, 9H);  $^{13}\text{C-NMR}$  ( $\text{CDCl}_3$ ):  $\delta$  146.4, 141.3, 129.5 (CH), 127.7 (CH), 120.3 (CH), 119 (q,  $J = 317$  Hz,  $\text{CF}_3$ ), 116.4 (CH), 27.1 ( $\text{CH}_2$ ), -2.3 ( $\text{CH}_3$ ); IR (neat  $\nu/\text{cm}^{-1}$ ): 2957, 1612, 1425, 1216, 1144, 942, 840; Anal. Calcd. for  $\text{C}_{11}\text{H}_{15}\text{F}_3\text{O}_3\text{SSi}$ : C, 42.29; H, 4.84. Found: C, 42.3; H, 4.9

**2-(Trimethylsilylmethyl)phenyl trifluoromethanesulfonate (2c).** Obtained in 79% yield from **4c**, after stirring the reaction mixture at 60 °C for two days, colorless oil.  $^1\text{H-NMR}$  ( $\text{CDCl}_3$ ):  $\delta$  7.29-7.14(m, 4H), 2.22 (s, 2H), 0.04 (s, 9H);  $^{13}\text{C-NMR}$  ( $\text{CDCl}_3$ ):  $\delta$  147.0, 133.8, 130.9 (CH), 127.9 (CH), 125.7 (CH), 121.2 (CH), 118.5 (q,  $J = 318$  Hz,  $\text{CF}_3$ ), 116.4 (CH), 21.2 ( $\text{CH}_2$ ), -1.7 ( $\text{CH}_3$ ); IR (neat  $\nu/\text{cm}^{-1}$ ): 2958, 1420, 1216, 1142, 897; Anal. Calcd. for  $\text{C}_{11}\text{H}_{15}\text{F}_3\text{O}_3\text{SSi}$ : C, 42.29; H, 4.84. Found: C, 42.1; H, 5.0.

7.1.1.5 General procedure for the synthesis of aryl phosphates **3a–c**, **9Phos**, **9c**.

The synthesis was carried out by modifying a known procedure.<sup>[282]</sup> In a round-bottom flask a bilayer system composed by a solution of the chosen phenol **4a–c** (550 mg, 3 mmol, 1M) in toluene (3 mL) and NaOH 20%<sub>aq</sub> (3 mL) was cooled at -10 °C. A solution of diethyl phosphorylchloride (4.6 mmol, 3M) in toluene (4.6 mL) was added dropwise. The resulting solution was stirred at 60°C overnight. The organic layer was washed with water (2×20 mL), and the aqueous phase extracted with toluene (20 mL). The organic phases were reunited, dried over MgSO<sub>4</sub> and the solvent evaporated. The purification of the crude oil was carried out by column chromatography (stationary phase: silica gel, eluant cyclohexane/acetate 9:1).

**4-(Trimethylsilylmethyl)phenyl diethylphosphate (3a)**. Obtained in 86% yield from **4a**, oil. <sup>1</sup>H-NMR (CDCl<sub>3</sub>): δ 7.23-6.90 (AA'BB', 4H), 4.15-4.30 (q, 4H, *J* = 7Hz), 2.05 (s, 2H), 1.30-1.40 (t, 6H, *J* = 7 Hz), 0.00 (s, 9H); <sup>13</sup>C-NMR (CDCl<sub>3</sub>): δ 147.2, 136.8, 128.5 (CH), 119.2 (CH), 64.1(CH<sub>2</sub>), 25.8 (CH<sub>2</sub>), 15.7 (CH<sub>3</sub>), -2.4 (CH<sub>3</sub>); IR (neat, v/cm<sup>-1</sup>): 2956, 1505, 1207, 1034, 964; Anal. Calcd. for C<sub>14</sub>H<sub>25</sub>O<sub>4</sub>PSi: C, 53.14; H, 7.96. Found: C, 53.0; H, 8.0.

**3-(Trimethylsilylmethyl)phenyl diethylphosphate (3b)**. Obtained in 79% yield from **4b**, oil. <sup>1</sup>H-NMR (CDCl<sub>3</sub>): δ 7.20-7.12 (t, 1H, *J* = 7.8 Hz), 6.95-6.77 (m, 3H), 4.20 (dq, 4 H, *J* = 7 and 1 Hz), 2.08 (s, 2H), 1.34 (dt, 6 H, *J* = 7 and 1 Hz), 0.01 (s, 9H); <sup>13</sup>C-NMR (CDCl<sub>3</sub>): δ 150.4, 142.6, 129.0 (CH), 124.5 (CH), 119.2 (CH), 115.2 (CH), 64.2 (CH<sub>2</sub>), 26.9 (CH<sub>2</sub>), 15.9 (CH<sub>3</sub>), -2.1(CH<sub>3</sub>); IR (neat v/cm<sup>-1</sup>): 2956, 1607, 1538, 1484, 1249, 1158, 1033, 980, 851; Anal. Calcd. for C<sub>14</sub>H<sub>25</sub>O<sub>4</sub>PSi: C, 53.14; H, 7.96. Found: C, 53.1; H, 8.1.

**2-(Trimethylsilylmethyl)phenyl diethylphosphate (3c)**. Obtained in 27% yield from **4c**, oil. <sup>1</sup>H-NMR (CDCl<sub>3</sub>): δ 7.30-7.29 (m, 1H), 7.06-7.02 (m, 3H), 4.20 (m, 4H), 2.16 (s, 2H), 1.35 (m, 6H), 0.01 (s, 9H); <sup>13</sup>C-NMR (CDCl<sub>3</sub>): δ 147.9, 131.5, 130.1 (CH), 125.0 (CH), 124.5 (CH), 119.3 (CH), 64.3 (CH<sub>2</sub>), 20.6 (CH<sub>2</sub>), 16.0 (CH<sub>3</sub>), -1.7 (CH<sub>3</sub>); IR (neat v/cm<sup>-1</sup>): 3488, 2955, 1582, 1490, 1273, 1228, 1036, 965, 853; Anal. Calcd. for C<sub>14</sub>H<sub>25</sub>O<sub>4</sub>PSi: C, 53.14; H, 7.96. Found: C, 53.0; H, 7.9.

**4-Methyphenyl diethylphosphate (9Phos)**. Obtained in 84% yield from p-cresol, colorless oil. <sup>1</sup>H-NMR (CDCl<sub>3</sub>): δ 7.13-7.07 (m, 4H), 4.20 (m, 4H), 2.30 (s, 3H), 1.33 (m, 6H); <sup>13</sup>C-NMR (CDCl<sub>3</sub>): δ 148.4, 134.4, 130.0 (CH), 119.6 (CH), 64.3 (CH<sub>2</sub>), 20.6 (CH<sub>3</sub>), 16.0 (CH<sub>3</sub>); Anal. Calcd. for C<sub>11</sub>H<sub>17</sub>O<sub>4</sub>P: C 54.10; H, 7.02. Found: C, 54.0; H, 7.0. The spectroscopic data of **9Phos** were in accordance with the literature.<sup>[283]</sup>

**2-Methyphenyl diethylphosphate (9c)**. was obtained in 58% yield from ortho-cresol, colorless oil.  $^1\text{H-NMR}$  ( $\text{CDCl}_3$ ):  $\delta$  7.28-7.26 (m, 1H), 7.19-7.02 (m, 3H), 4.20 (m, 4H), 2.30 (s, 3H), 1.33 (m, 6H);  $^{13}\text{C-NMR}$  ( $\text{CDCl}_3$ ):  $\delta$  149.0, 131.2, 129.1 (CH), 126.9 (CH), 124.8 (CH), 119.6 (CH), 64.4 ( $\text{CH}_2$ ), 20.6 ( $\text{CH}_3$ ), 16.0 ( $\text{CH}_3$ ); Anal. Calcd. for  $\text{C}_{11}\text{H}_{17}\text{O}_4\text{P}$ : C 54.10; H, 7.02. Found: C, 54.2; H, 7.1. The spectroscopic data of **9c** were in accordance with the literature.<sup>[247]</sup>

#### 7.1.1.6 Irradiation of **2a** in cyclohexane.

An argon saturated solution of **2a** (424 mg, 1.4 mmol) in cyclohexane (50 mL) was irradiated for 6h at 254 nm. The photolyzed mixture was evaporated and the resulting residue purified by column chromatography (eluant: neat cyclohexane) to give 90 mg of 4-trifluoromethylbenzyltrimethylsilane (**4'''**; oil, 26% yield).

**4'''**:  $^1\text{H-NMR}$ , ( $\text{CD}_3\text{COCD}_3$ )  $\delta$ : 7.15 (s, 4H), 2.20 (s, 2H), 0.05 (s, 9H);  $^{13}\text{C-NMR}$ , ( $\text{CD}_3\text{COCD}_3$ )  $\delta$ : 147.4, 147.1, 130.5 (CH), 122.0 (CH), 120.0 (q,  $\text{CF}_3$ ,  $J = 252$  Hz), 27.0 ( $\text{CH}_2$ ), -1.6 ( $\text{CH}_3$ ); GC-MS (m/z): 73 (100), 77 (10), 90 (85), 156 (6), 139 (3), 148 (3), 156 (6), 233 (4). Anal. Calcd. for  $\text{C}_{11}\text{H}_{15}\text{F}_3\text{OSi}$ : C, 53.21; H, 6.09. Found: C, 53.3; H, 6.1.

## 7.1.2 Photophysical parameters for compounds 1–3.

<b>Table 7.1 Absorption parameters measured for compounds 1–3.</b>		
<b>Compound</b>	$\lambda_{\max}$ [nm]	$\varepsilon$ [mol L <sup>-1</sup> cm <sup>-1</sup> ]
<b>1a</b>	270	419
<b>1b</b>	268	516
<b>1c</b>	268.5	620
<b>2a</b>	268.5	644
<b>2b</b>	269	534
<b>2c</b>	267	567
<b>3a</b>	273	682
<b>3b</b>	268	500
<b>3c</b>	268.5	734

<b>Table 7.2 Emission parameters measured for compounds 1–3.</b>						
<b>Compound</b>	<b>MeOH</b>			<b>Cyclohexane</b>		
	$\Phi_F \times 10^{-2}$	$\lambda_{em}$ [nm]	$\Delta E S_1/S_0$ , kcal mol <sup>-1</sup>	$\Phi_F \times 10^{-2}$	$\lambda_{em, nm}$	$\Delta E S_1/S_0$ , kcal mol <sup>-1</sup>
<b>1a</b>	3.43	305	104	3.6	300	104
<b>1b</b>	0.29	297	104	0.86	295.5	104
<b>1c</b>	0.62	308.5	101	0.53	304	104
<b>2a</b>	0.26	298.5	103	0.32	295	104
<b>2b</b>	0.29	300	103	0.4	294	105
<b>2c</b>	1.9	309.5	100	3.14	304	102
<b>3a</b>	22.8	304	102	27.6	302	102
<b>3b</b>	20.6	293.5	105	27.2	296	105
<b>3c</b>	11.4	297.5	104	13.1	297.5	104

### New Intermediates from Photogenerated Phenyl Cations

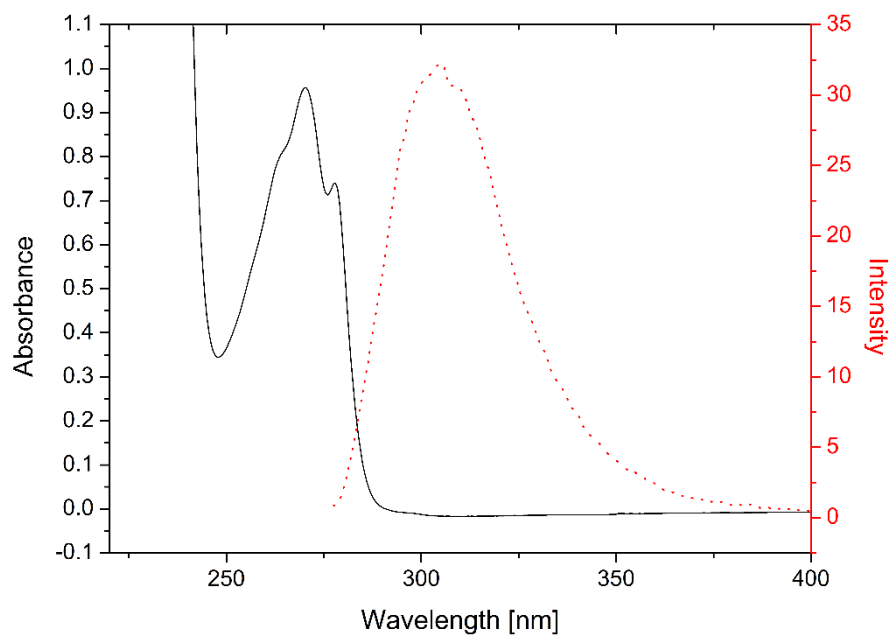


**Figure 7.1** Absorption (black) and emission (red) spectra of aryl mesylate **1a** ( $2 \times 10^{-3}$  M, MeOH).

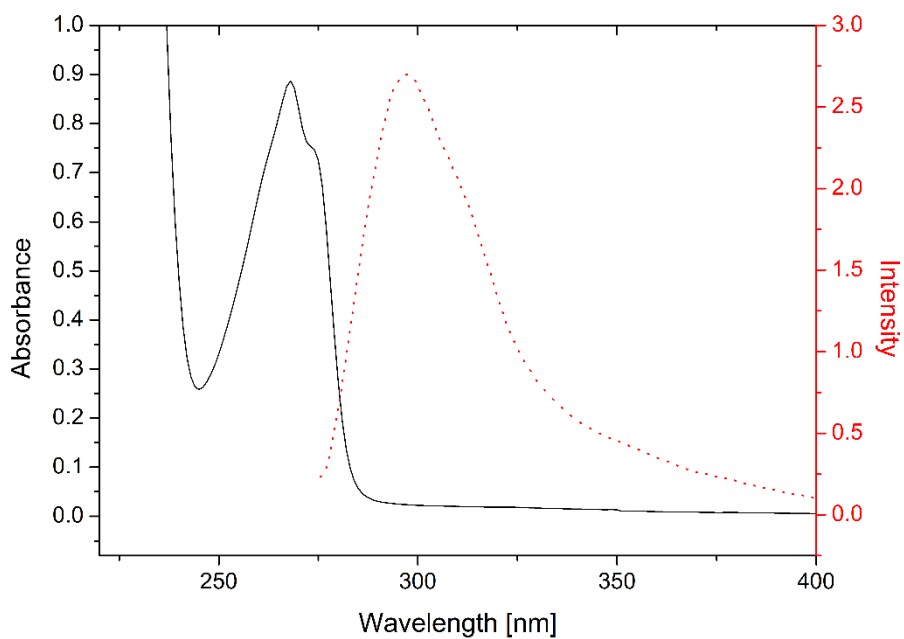


**Figure 7.2** Absorption (black) and emission (red) spectra of aryl mesylate **1b** ( $2 \times 10^{-3}$  M, MeOH).

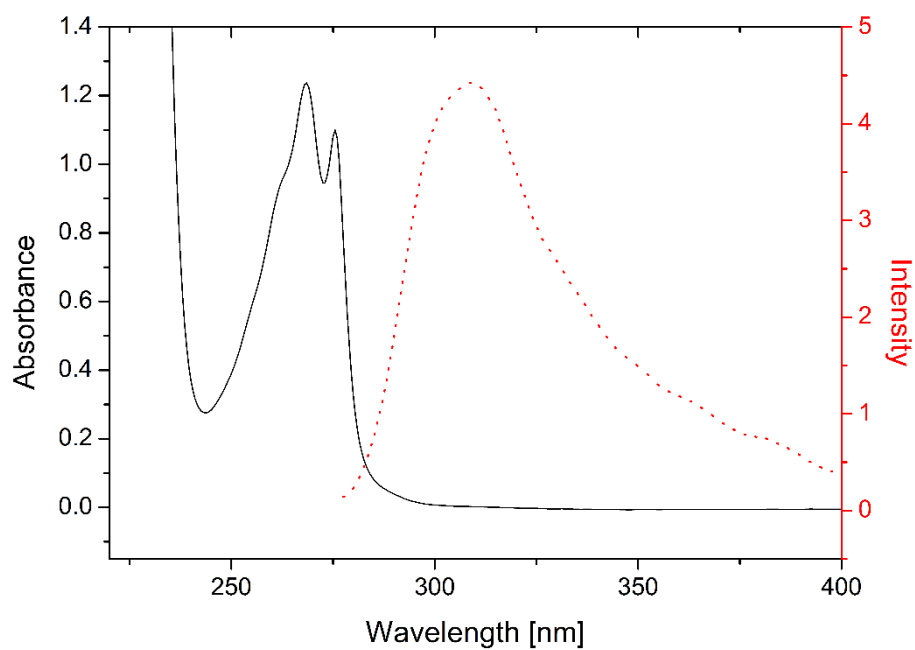


**Figure 7.3** Absorption (black) and emission (red) spectra of aryl mesylate **1c** ( $2 \times 10^{-3}$  M, MeOH).

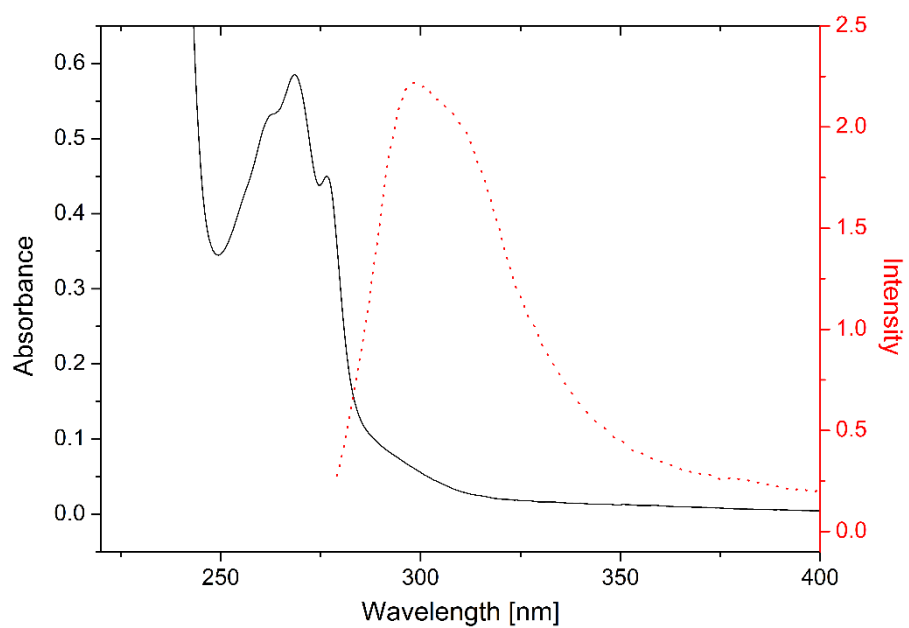


**Figure 7.4** Absorption (black) and emission (red) spectra of aryl mesylate **2a** ( $2 \times 10^{-3}$  M, MeOH).

### New Intermediates from Photogenerated Phenyl Cations

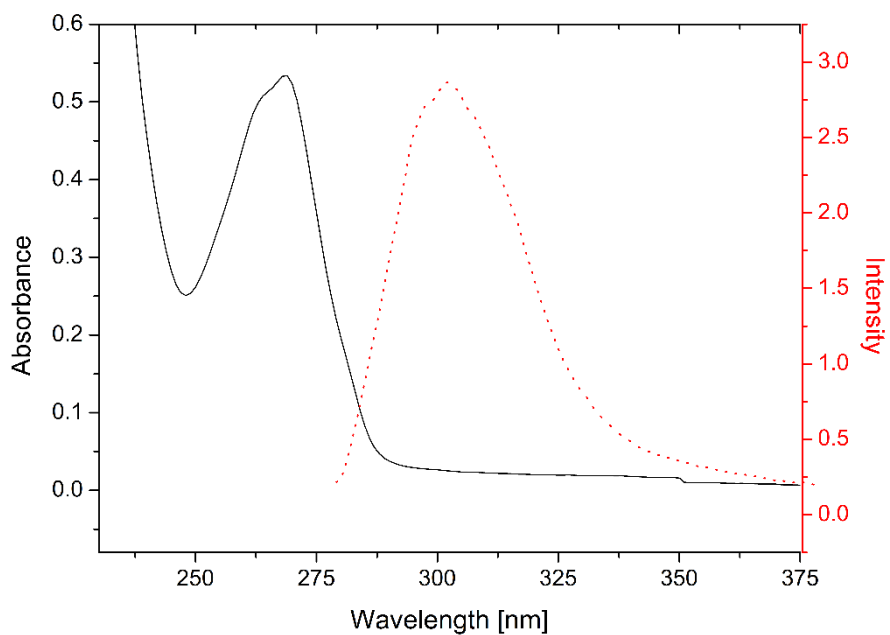


**Figure 7.5** Absorption (black) and emission (red) spectra of aryl mesylate **2b** ( $2 \times 10^{-3}$  M, MeOH).

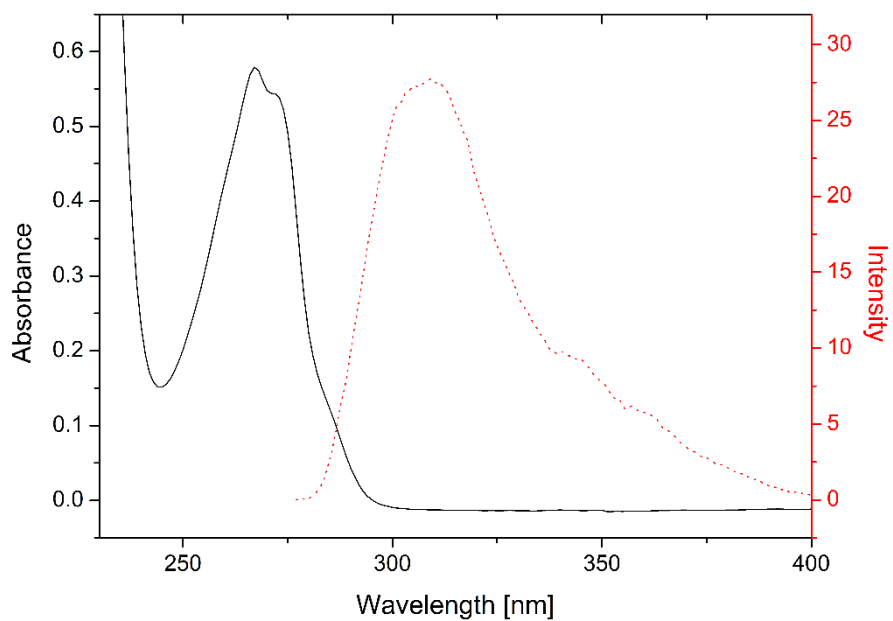


**Figure 7.6** Absorption (black) and emission (red) spectra of aryl mesylate **2c** ( $2 \times 10^{-3}$  M, MeOH).



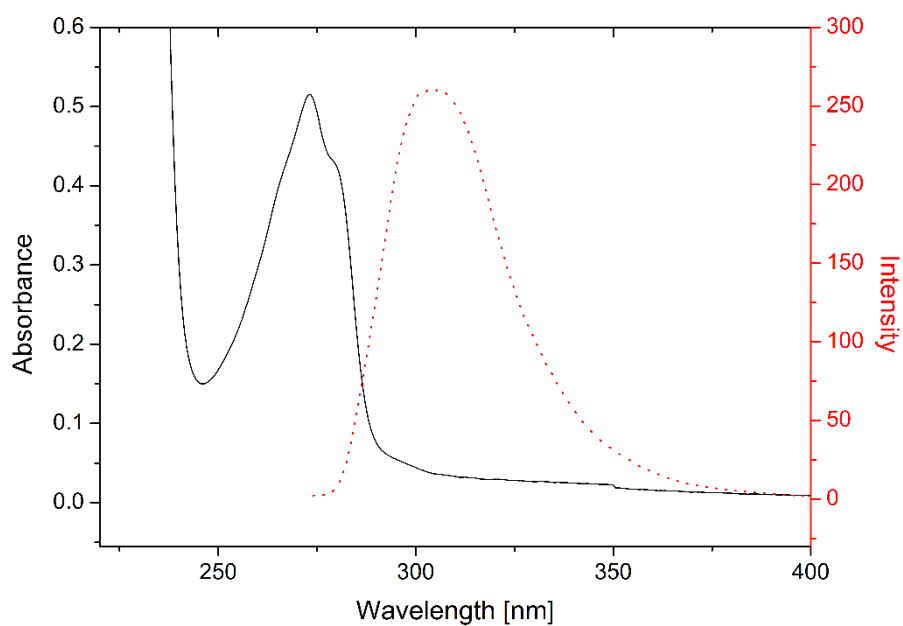


**Figure 7.7** Absorption (black) and emission (red) spectra of aryl mesylate **3a** ( $2 \times 10^{-3}$  M, MeOH).

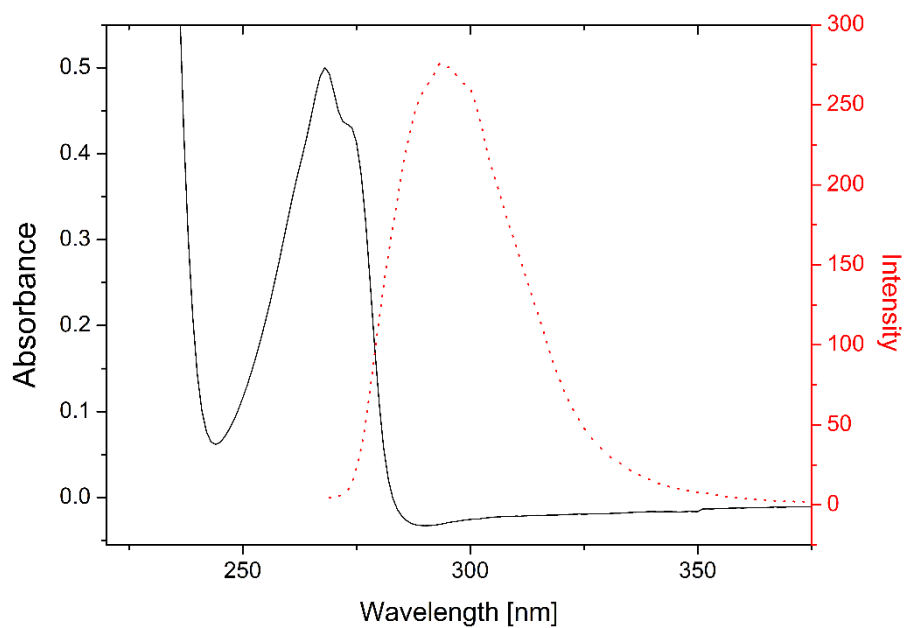


**Figure 7.8** Absorption (black) and emission (red) spectra of aryl mesylate **3b** ( $2 \times 10^{-3}$  M, MeOH).

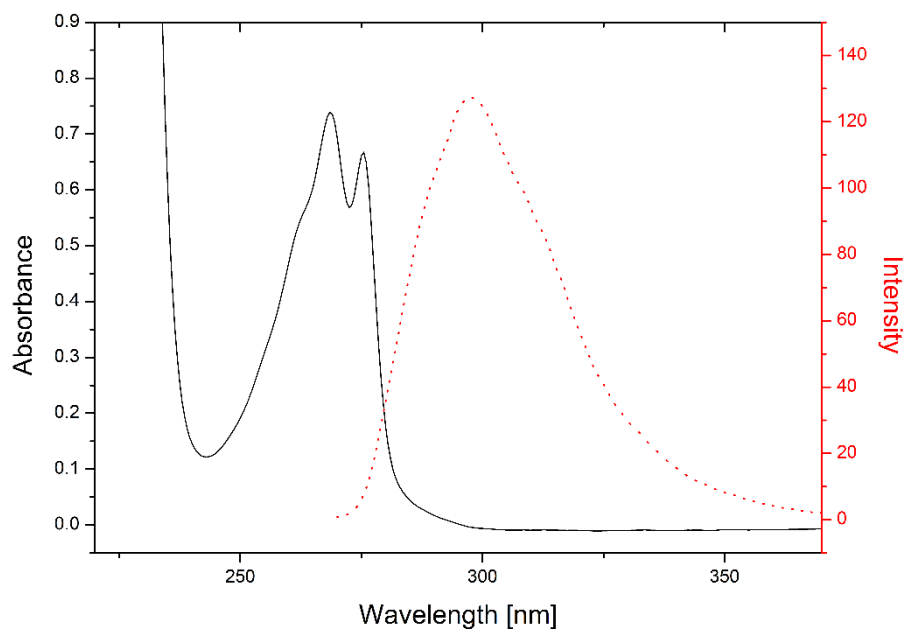


**Figure 7.9** Absorption (black) and emission (red) spectra of aryl mesylate **3c** ( $2 \times 10^{-3}$  M, MeOH).

### 7.1.3 Computational Details

All the calculations were carried out using the Gaussian 09 program package.<sup>[284]</sup> In our investigation, the level of theory chosen for the optimization of all of the stationary points was DFT (Density Functional Theory) by using the B3LYP functional<sup>[179,285–287]</sup> and the standard 6–31G(d) basis set. No symmetry constraint was applied to the structures investigated. Frequency calculations were performed in vacuo to check that minima had no imaginary frequencies.

Solvent effect was included by single-point calculations at the CPCM-B3LYP/6–31G(d) method (methanol bulk) on the optimized geometries obtained in vacuo.<sup>[288]</sup> The solvent cavity was calculated using the united atom topological model applied on radii optimized for the HF/6-31G(d) level of theory (RADII = UAHF option). Atomic charges have been calculated in solvent bulk according to the Merz-Singh-Kollman scheme,<sup>[289,290]</sup> via the POP = MK keyword and have been labeled in the text as “qESP”.

In order to simplify and to speed up the modeling of compounds **3**, the corresponding dimethyl derivatives, *viz.* dimethyl n-(trimethylsilylmethyl)phenyl phosphates (n = 2 - 4), have been considered and are labeled in the following as: **3-Me<sub>2</sub>**. This enabled us to avoid the optimization of a large number of conformers related to the degrees of freedom of the ethyl moieties.

As mentioned in the text, two different minima were located for the lowest-energy triplet states of compounds **1-3**, *viz.* a geometry with the ester moiety and the -SiMe<sub>3</sub> group on the same side (hereafter tagged as geometry "**α**") or opposite (hereafter tagged as geometry "**β**") with respect to the plane of the aromatic ring (see Figure 7.10 for compound **2a**, taken as an example).

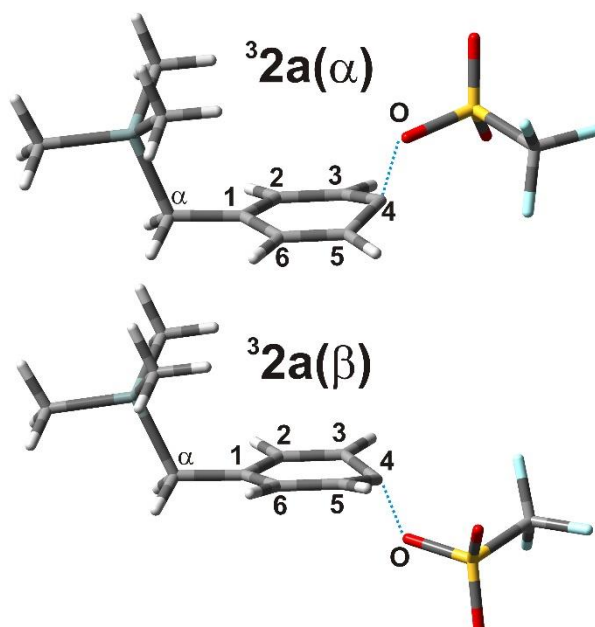


Figure 7.10  $\alpha$  (upper side) and  $\beta$  (lower side) structures for  $^32a$ , taken as an example.

The B3LYP/6-31G(d) Gibbs free energies ( $G_{\text{DFT}}$ ) reported in the text have thus been calculated by means of Eq. 1 reported below.

$$G_{\text{DFT}} = E_{0(\text{DFT,CPCM})} + \Delta G_{\text{CORR}} \quad (1)$$

Where: -  $E_{0(\text{DFT,CPCM})}$  is the total electronic energy calculated at the CPCM–B3LYP level (methanol bulk);

-  $\Delta G_{\text{CORR}}$  is the unscaled thermal correction to Gibbs Free Energy as from the output of the frequency calculation in vacuo, also including the zero-point vibrational energy (ZPVE).

When structures not corresponding to stationary points have been considered (e.g. when stretching a bond), energies have been expressed simply by considering the first term of Eq. 1, that is  $E_{0(\text{DFT,CPCM})}$ , since frequency calculations (needed for determining  $\Delta G_{\text{CORR}}$ ) were carried out exclusively on stationary points.

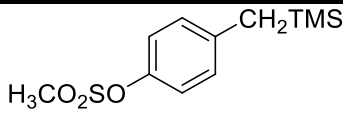
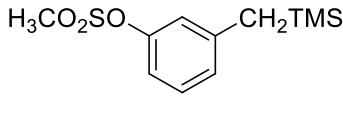
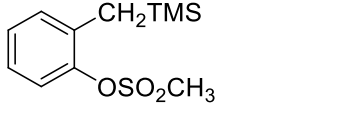
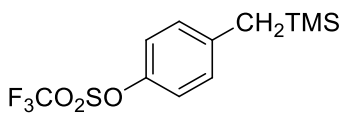
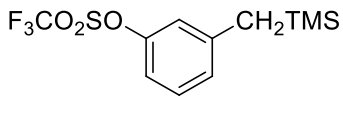
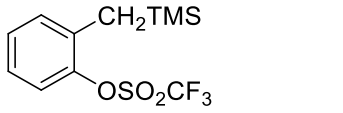
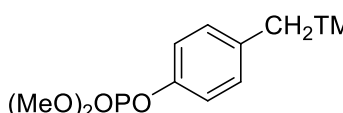
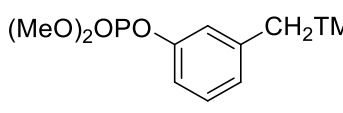
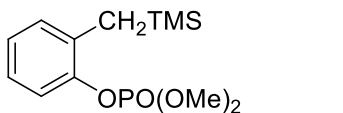
When evaluating the energy change related to the elongation of the Ar–O bond in  $^31a-c$  (see Figure 2.3), the variations observed for each point with respect to the equilibrium geometry have been considered, resulting in a  $\Delta E_{(\text{DFT,CPCM})}$  vs  $\Delta l$  plot, where:

$$\Delta E_{0(\text{DFT,CPCM})} [\text{kcal mol}^{-1}] = E_{0(\text{DFT,CPCM})} - E_{0(\text{DFT,CPCM})}(\text{equilibrium})$$

$$\Delta l [\text{\AA}] = \text{Ar-O bond length} - \text{Ar-O bond length (equilibrium)}$$

Optimized geometry listed in cartesian format (coordinates are given in Å) are reported below. The conversion factor between Hartree and kcal mol<sup>-1</sup> has been: 1 Hartree = 627.509 kcal mol<sup>-1</sup>. When summing the data for calculating G<sub>DFT</sub> (see Eq. 1), all the digits available from the calculations were used; nevertheless, the energy values reported below (in Hartree units, **Table 7.3**) have been rounded considering 6 significant digits after the unit.

**Table 7.3** Gibbs free energies of the stationary points described in the text for the three isomers of the compounds 1–3 calculated at the CPCM-(U)B3LYP/6-31G(d) level of theory in methanol bulk.

Species	G <sub>DFT</sub> [Hartree]		
	1–3a–c	<sup>3</sup> 1–3a–c(α)	<sup>3</sup> 1–3a–c(β)
 <b>1a</b>	-1343.145804	-1343.023220	-1343.021446
	ΔG(α vs β) = -1.11 kcal mol <sup>-1</sup> (α more stable)		
	ΔG( <sup>3</sup> 1a(α)-1a) = 76.92 kcal mol <sup>-1</sup>		
 <b>1b</b>	-1343.145143	-1343.019991	-1343.020035
	ΔG(α vs β) = 0.03 kcal mol <sup>-1</sup> (β more stable)		
	ΔG( <sup>3</sup> 1a(β)-1a) = 78.04 kcal mol <sup>-1</sup>		
 <b>1c</b>	-1343.143020	-1343.016661	-1343.021218
	ΔG(α vs β) = 2.86 kcal mol <sup>-1</sup> (β more stable)		
	ΔG( <sup>3</sup> 1a(β)-1a) = 76.43 kcal mol <sup>-1</sup>		
 <b>2a</b>	-1640.860278	-1640.740327	-1640.739921
	ΔG(α vs β) = -0.26 kcal mol <sup>-1</sup> (α more stable)		
	ΔG( <sup>3</sup> 1a(α)-1a) = 75.27 kcal mol <sup>-1</sup>		
 <b>2b</b>	-1640.858635	-1640.737490	-1640.737965
	ΔG(α vs β) = 0.30 kcal mol <sup>-1</sup> (β more stable)		
	ΔG( <sup>3</sup> 1a(β)-1a) = 75.72 kcal mol <sup>-1</sup>		
 <b>2c</b>	-1640.858106	[a]	-1640.738426
	ΔG( <sup>3</sup> 1a(β)-1a) = 75.10 kcal mol <sup>-1</sup>		
 <b>3a-Me<sub>2</sub></b> <sup>[b]</sup>	-1401.540121	-1401.418882	-1401.417488
	ΔG(α vs β) = -0.87 kcal mol <sup>-1</sup> (α more stable)		
	ΔG( <sup>3</sup> 1a(α)-1a) = 76.08 kcal mol <sup>-1</sup>		
 <b>3b-Me<sub>2</sub></b> <sup>[b]</sup>	-1401.540979	-1401.416855	-1401.416701
	ΔG(α vs β) = -0.10 kcal mol <sup>-1</sup> (α more stable)		
	ΔG( <sup>3</sup> 1a(α)-1a) = 77.89 kcal mol <sup>-1</sup>		
 <b>3c-Me<sub>2</sub></b> <sup>[b]</sup>	-1401.538415	-1401.414128	-1401.416996
	ΔG(α vs β) = 1.80 kcal mol <sup>-1</sup> (β more stable)		
	ΔG( <sup>3</sup> 1a(β)-1a) = 76.19 kcal mol <sup>-1</sup>		

[a] No α conformer was found in the case of **2c**. [b] As mentioned above, the dimethyl esters of **3a-c** have been modeled computationally.

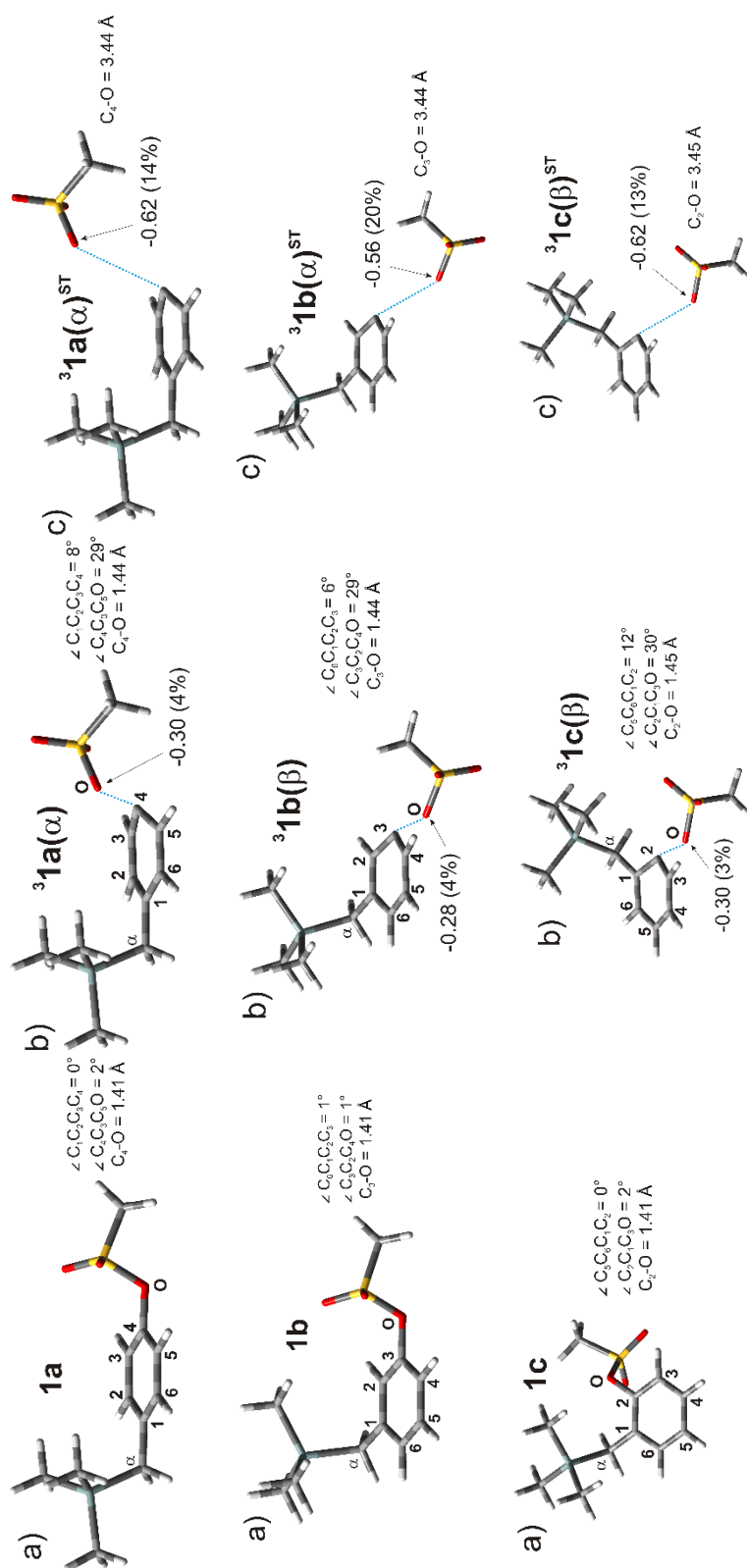


**Figure 7.11** Optimized structures and relevant parameters for: a) ground state **1a–c**, b) first triplet excited state **31a–c** and c) first triplet excited state **31a–c<sup>ST</sup>**. The arrows indicate the charge (qESP) on the Ar-O atom (the spin density on the same atom is listed in parentheses).

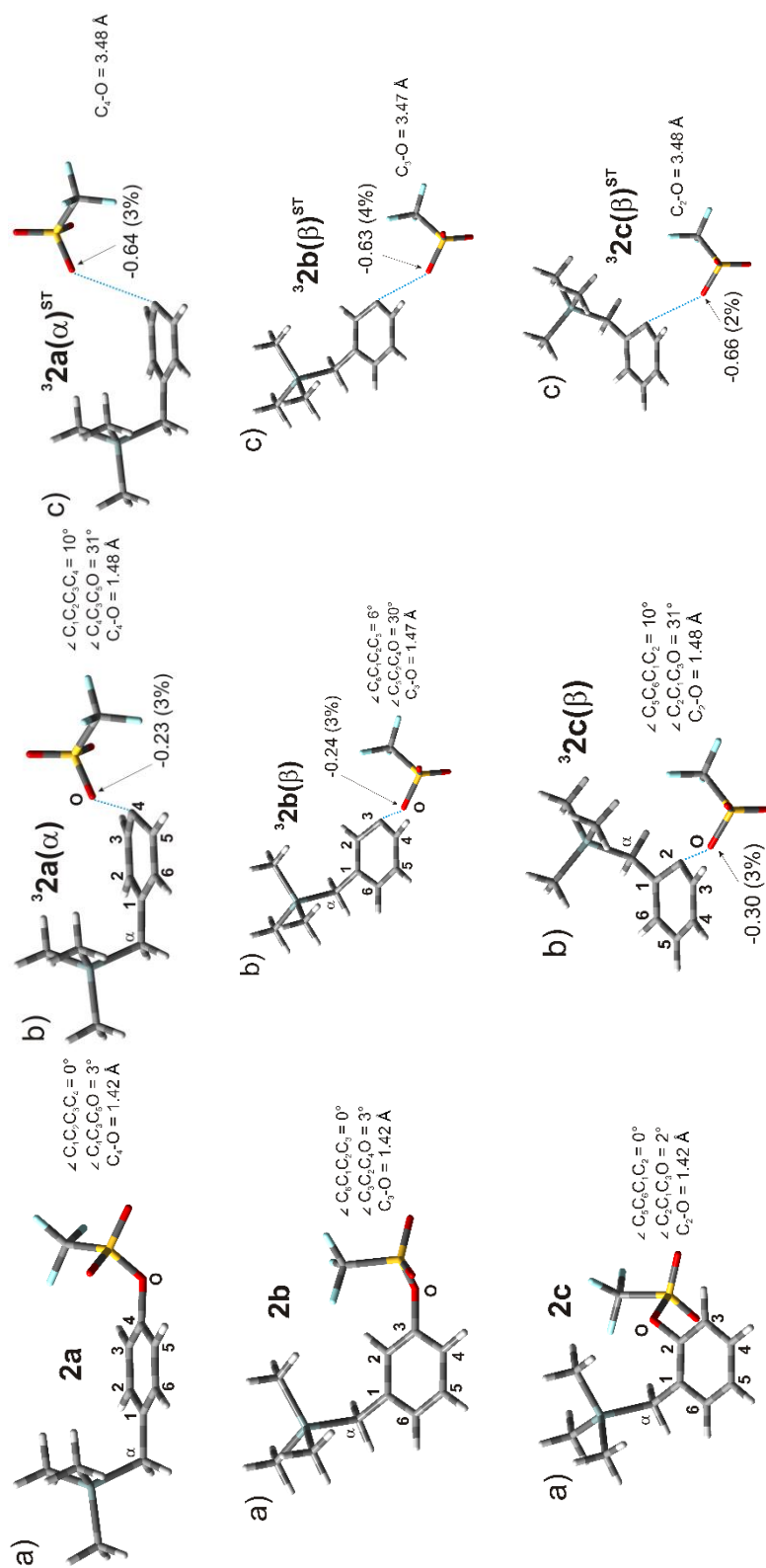


**Figure 7.12** Optimized structures and relevant parameters for: a) ground state **2a-c**, b) first triplet excited state  **$^32a-c$**  and c) first triplet excited state  **$^32a-c^{ST}$**  upon stretching of the Ar-O bond ( **$^32a-c^{ST}$** ). The arrows indicate the charge (qESP) on the Ar-O atom (the spin density on the same atom is listed in parentheses).



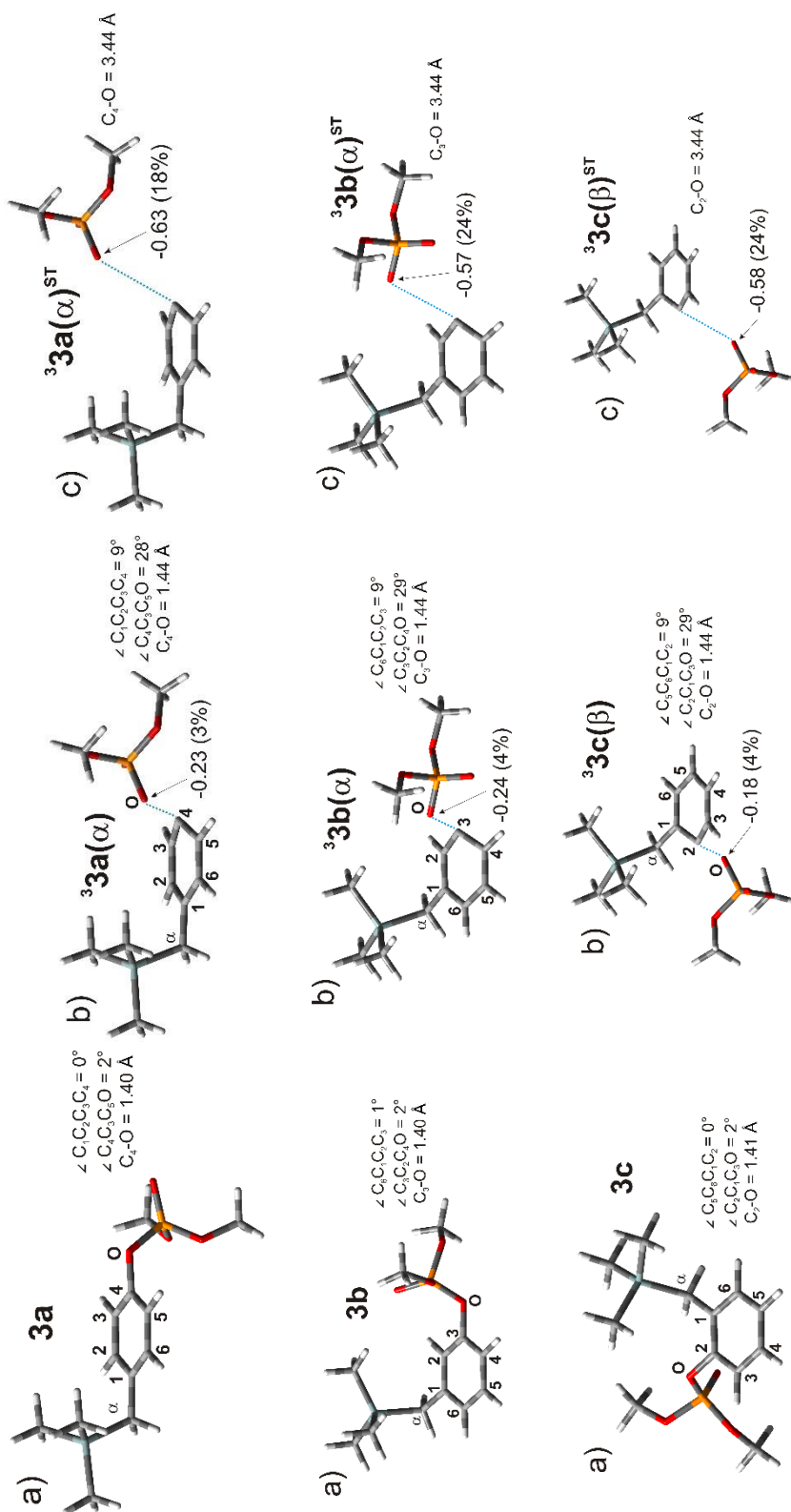


**Figure 7.13** Optimized structures and relevant parameters for: a) ground state **3a-c**, b) first triplet excited state **3a-c** and c) first triplet excited state **3a-c** upon stretching of the Ar-O bond (**3a-c<sup>ST</sup>**). The arrows indicate the charge (qESP) on the Ar-O atom (the spin density on the same atom is listed in parentheses).

## New Intermediates from Photogenerated Phenyl Cations

### 7.1.3.1 Cartesian coordinates for 1–3.

1a				<sup>3</sup> 1a(α)				<sup>3</sup> 1a(β)			
C	0.5797	-1.0485	-1.2678	C	-0.7019	-1.8104	0.6813	C	-0.6498	1.3891	-0.3868
C	1.3169	-1.1786	-0.0792	C	-1.3310	-1.2168	-0.4733	C	-1.2021	0.0811	-0.6459
C	-0.8098	-0.9377	-1.2552	C	0.6489	-1.8257	0.8342	C	0.5800	1.5538	0.1684
C	0.6079	-1.1944	1.1335	C	-0.4858	-0.7436	-1.5330	C	-0.4610	-1.0632	-0.1962
C	-0.7810	-1.0827	1.1660	C	0.8740	-0.7503	-1.4350	C	0.7688	-0.9527	0.3818
C	-1.4766	-0.9592	-0.0333	C	1.4828	-1.0609	-0.1169	C	1.4456	0.3699	0.3592
H	-1.3264	-1.0953	2.1036	H	1.5119	-0.4770	-2.2678	H	1.2920	-1.8111	0.7875
H	1.1018	-1.0410	-2.2215	H	-1.3370	-2.3086	1.4126	H	-1.2657	2.2600	-0.6053
H	-1.3764	-0.8396	-2.1748	H	1.1199	-2.3341	1.6714	H	0.9673	2.5412	0.4053
H	1.1518	-1.3016	2.0687	H	-0.9572	-0.4348	-2.4653	H	-0.9305	-2.0427	-0.2743
C	2.8216	-1.2703	-0.1028	C	-2.8131	-1.1394	-0.5786	C	-2.5666	-0.0666	-1.2290
H	3.1570	-1.7585	-1.0275	H	-3.2915	-1.9722	-0.0440	H	-2.6491	-1.0021	-1.7983
H	3.1765	-1.9001	0.7240	H	-3.1356	-1.1943	-1.6279	H	-2.7857	0.7529	-1.9267
C	3.3051	1.2611	1.6582	C	-2.8652	1.9759	-0.7835	C	-4.0008	1.5415	1.0379
H	2.2294	1.4544	1.7386	H	-1.7750	2.0292	-0.6868	H	-3.0529	1.6933	1.5666
H	3.6003	0.6507	2.5206	H	-3.1033	1.9352	-1.8534	H	-4.1583	2.4045	0.3794
H	3.8218	2.2247	1.7460	H	-3.2796	2.9124	-0.3904	H	-4.8030	1.5491	1.7860
C	3.2452	1.5220	-1.4300	C	-3.1683	0.6059	1.9876	C	-3.7732	-1.5443	1.2501
H	3.7512	2.4933	-1.3697	H	-3.5982	1.5171	2.4213	H	-4.5789	-1.5724	1.9939
H	3.5150	1.0705	-2.3927	H	-3.5748	-0.2465	2.5455	H	-3.7869	-2.5016	0.7151
H	2.1658	1.7111	-1.4416	H	-2.0868	0.6346	2.1616	H	-2.8230	-1.4791	1.7920
C	5.5979	0.0530	-0.0422	C	-5.4472	0.3895	-0.1083	C	-5.6234	-0.2691	-0.8903
H	5.8782	-0.4470	-0.9773	H	-5.8802	-0.4736	0.4116	H	-5.6446	-1.2013	-1.4675
H	6.1831	0.9783	0.0244	H	-5.9424	1.2890	0.2777	H	-6.4842	-0.2828	-0.2104
H	5.9108	-0.5944	0.7860	H	-5.7056	0.3016	-1.1704	H	-5.7716	0.5598	-1.5928
Si	3.7380	0.4137	0.0226	Si	-3.5717	0.4880	0.1438	Si	-4.0011	-0.0841	0.0700
O	-2.8843	-0.9248	-0.0105	O	2.0760	0.0646	0.5650	O	2.5750	0.4576	-0.5341
S	-3.5880	0.5868	0.0180	S	3.5258	0.6575	0.0333	S	4.0019	-0.2605	-0.1035
O	-3.2462	1.2525	1.2718	O	3.6261	0.5380	-1.4189	O	3.7518	-1.4620	0.6885
O	-3.3480	1.2536	-1.2591	O	3.6656	1.9432	0.6995	O	4.7786	-0.3107	-1.3325
C	-5.2790	-0.0132	0.0835	C	4.6526	-0.5310	0.7820	C	4.6793	1.0068	0.9818
H	-5.4070	-0.6018	0.9925	H	4.4129	-1.5229	0.3944	H	3.9893	1.1490	1.8156
H	-5.4724	-0.6126	-0.8068	H	4.5315	-0.4898	1.8652	H	4.8010	1.9263	0.4079
H	-5.9221	0.8690	0.1013	H	5.6660	-0.2421	0.4953	H	5.6450	0.6448	1.3409

Chapter 7: Experimental Section

<b>1b</b>				<b><sup>3</sup>1b(α)</b>			<b><sup>3</sup>1b(β)</b>				
C	1.0491	2.4106	-0.0073	C	-1.1681	1.0274	-0.7547	C	1.0584	0.3405	-0.6532
C	1.1141	1.1951	-0.7085	C	-0.0563	0.3811	-1.2124	C	0.0347	-0.4428	-0.2118
C	-0.1697	2.9338	0.4261	C	0.2899	2.6876	0.4229	C	-0.1666	2.3848	0.1224
C	-1.2945	1.0564	-0.5265	C	1.4216	2.0674	-0.0366	C	-1.1868	1.6162	0.6213
H	1.9679	2.9549	0.1972	H	1.2698	0.7275	-0.6715	C	-1.2208	0.1716	0.2473
H	-0.1910	3.8771	0.9649	H	2.4104	2.4922	0.0912	H	-1.9832	2.0293	1.2293
C	2.4338	0.6048	-1.1338	C	-0.1408	-0.4546	-1.9033	H	0.0906	-1.5268	-0.2824
H	3.1784	1.4004	-1.2674	H	0.3662	3.6288	0.9635	H	-0.1579	3.4588	0.2974
H	2.3333	0.1073	-2.1078	H	1.7560	-0.3651	0.1352	O	-2.2900	-0.1789	-0.6494
C	2.0413	-2.1962	0.1951	C	3.3895	-0.5963	0.2840	S	-3.8350	-0.2838	-0.0600
H	1.0228	-1.9415	0.5097	H	4.0919	0.6840	0.2531	O	-4.0398	0.6856	1.0135
H	1.9706	-2.7020	-0.7761	H	3.5325	-1.5129	1.4044	O	-4.6816	-0.2957	-1.2426
H	2.4369	-2.9251	0.9134	H	3.7270	-1.4690	-1.2543	C	-3.7871	-1.9325	0.6620
C	3.3535	0.1150	1.8039	C	3.4461	-0.8192	-2.0852	H	-3.0164	-1.9455	1.4349
H	3.7738	-0.5984	2.5232	H	3.1494	-2.3942	-1.2628	H	-3.5672	-2.6511	-0.1285
H	4.0207	0.9853	1.7751	H	4.7979	-1.6817	-1.2785	H	-4.7702	-2.1250	1.0968
H	2.3862	0.4496	2.1950	H	-3.3939	-0.5867	0.1303	Si	3.7708	-0.3956	0.0769
C	4.8687	-1.1877	-0.5674	C	-5.1258	-0.9835	-0.5287	C	5.2702	-1.0893	-0.8510
H	5.5463	-0.3285	-0.6420	H	-3.5297	0.2439	1.8260	C	3.2444	-1.5887	1.4471
H	5.3439	-1.9259	0.0902	H	-2.3637	-2.1673	0.2580	C	4.2084	1.2904	0.8197
H	4.7927	-1.6377	-1.5649	H	-5.7382	-0.0784	-0.6210	H	5.0487	-2.0635	-1.3034
Si	3.1669	-0.6791	0.0963	Si	-5.0811	-1.4563	-1.5174	H	5.5910	-0.4158	-1.6550
O	-2.4901	0.3811	-0.8464	O	-5.6550	-1.6719	0.1414	H	6.1239	-1.2259	-0.1760
S	-2.9998	-0.7639	0.2518	S	-4.0104	-0.4269	2.5487	H	4.0274	-1.6807	2.2094
O	-2.0111	-1.8378	0.3203	O	-2.5444	0.5080	2.2265	H	2.3314	-1.2440	1.9460
O	-3.4463	-0.0974	1.4716	O	-4.1303	1.1607	1.7809	H	3.0487	-2.5929	1.0519
C	-4.4200	-1.3014	-0.7061	C	-1.3300	-1.9476	0.5484	H	3.3618	1.7300	1.3591
H	-4.0699	-1.6988	-1.6592	H	-2.7831	-2.8515	1.0055	H	5.0394	1.1947	1.5296
H	-5.0850	-0.4495	-0.8525	H	-2.3345	-2.7036	-0.6986	H	4.5190	2.0045	0.0472
H	-4.9141	-2.0797	-0.1210	H	-0.9951	2.1721	0.1217	C	0.9322	1.7887	-0.5384
C	-1.3631	2.2566	0.1750	C	-1.8787	2.6979	0.4713	H	1.7411	2.4115	-0.9083
H	-2.3225	2.6373	0.5066	H	-2.5607	0.6031	-1.1317	C	2.3403	-0.2276	-1.1981
C	-0.0890	0.5224	-0.9693	C	-2.5473	0.0836	-2.0988	H	2.7035	0.3941	-2.0279
H	-0.0963	-0.4172	-1.5119	H	-3.2106	1.4808	-1.2544	H	2.1656	-1.2292	-1.6120

**New Intermediates from Photogenerated Phenyl Cations**

<b>1c</b>				<b><sup>3</sup>1c(α)</b>				<b><sup>3</sup>1c(β)</b>			
C	-0.8920	2.3725	-0.7628	C	-0.8111	2.5827	0.0765	C	0.8824	2.3966	-1.0291
C	-0.4465	1.0618	-0.5211	C	-0.4885	1.3720	-0.5019	C	0.5970	1.0846	-0.7226
C	0.9401	3.3209	0.4987	C	1.5732	3.2554	0.1680	C	-0.7175	3.2225	0.6785
C	1.4086	2.0355	0.7631	C	1.9630	2.0819	-0.4007	C	-1.0513	1.9500	1.0325
C	0.7162	0.9378	0.2550	C	0.9567	0.9993	-0.4904	C	-0.5965	0.8558	0.1447
H	2.3042	1.8689	1.3508	H	2.9874	1.8840	-0.6981	H	-1.6991	1.7237	1.8729
H	1.4751	4.1826	0.8867	H	2.2997	4.0450	0.3495	H	-1.1105	4.0683	1.2392
O	1.1697	-0.3577	0.5948	O	1.2039	-0.0860	0.4370	O	-1.6636	0.2613	-0.6353
S	2.4886	-0.9492	-0.2340	S	2.1840	-1.2973	-0.1244	S	-2.4282	-1.0234	0.0711
O	2.1049	-1.2249	-1.6164	O	1.3924	-2.1903	-0.9698	O	-1.5652	-2.2005	-0.0301
O	3.6571	-0.1214	0.0520	O	3.4345	-0.7343	-0.6291	O	-2.9739	-0.6294	1.3683
C	2.5960	-2.4863	0.6889	C	2.4654	-2.0737	1.4708	C	-3.7525	-1.1454	-1.1366
H	1.6680	-3.0435	0.5564	H	1.5031	-2.3683	1.8910	H	-3.3144	-1.3143	-2.1209
H	2.7705	-2.2520	1.7396	H	2.9801	-1.3628	2.1180	H	-4.3305	-0.2209	-1.1138
H	3.4400	-3.0398	0.2720	H	3.0900	-2.9503	1.2854	H	-4.3701	-1.9954	-0.8387
C	-0.2153	3.4857	-0.2668	C	0.1907	3.5040	0.4648	C	0.2117	3.4686	-0.3857
H	-0.5895	4.4827	-0.4827	H	-0.0979	4.4576	0.8962	H	0.4709	4.4915	-0.6411
C	-1.2018	-0.1289	-1.0481	H	-1.8548	2.8846	0.1449	H	1.6900	2.6204	-1.7245
Si	-2.5959	-0.7865	0.0957	C	-1.4750	0.4457	-1.1397	C	1.3704	-0.0948	-1.1992
H	-0.5143	-0.9522	-1.2663	Si	-2.5854	-0.6226	0.0234	Si	2.5709	-0.8530	0.1101
H	-1.6738	0.1389	-2.0027	H	-0.9530	-0.2477	-1.8109	H	1.9773	0.1708	-2.0750
C	-3.9395	0.5357	0.2782	H	-2.1874	1.0171	-1.7532	H	0.6884	-0.9025	-1.4974
C	-1.9098	-1.2327	1.8024	C	-3.6694	0.5200	1.0765	C	1.6523	-1.2595	1.7097
C	-3.3246	-2.3290	-0.7303	C	-3.6777	-1.6726	-1.1135	C	3.2846	-2.4342	-0.6510
H	-3.5331	1.4636	0.6969	C	-1.5698	-1.7518	1.1477	C	3.9588	0.3910	0.4461
H	-4.3993	0.7792	-0.6876	H	-4.2922	1.1753	0.4553	H	0.7906	-1.9086	1.5184
H	-4.7394	0.1936	0.9463	H	-4.3428	-0.0672	1.7130	H	2.3151	-1.7741	2.4170
H	-2.7027	-1.6256	2.4508	H	-3.0649	1.1555	1.7337	H	1.2813	-0.3536	2.2032
H	-1.1249	-1.9944	1.7335	H	-4.3605	-2.3017	-0.5295	H	4.0063	-2.9064	0.0268
H	-1.4751	-0.3587	2.3006	H	-4.2886	-1.0495	-1.7776	H	2.4937	-3.1661	-0.8534
H	-2.5688	-3.1146	-0.8508	H	-3.0718	-2.3362	-1.7419	H	3.8031	-2.2316	-1.5960
H	-4.1452	-2.7483	-0.1353	H	-0.9395	-1.1681	1.8271	H	3.5577	1.3450	0.8078
H	-3.7234	-2.0997	-1.7260	H	-2.2290	-2.3861	1.7533	H	4.6504	0.0119	1.2083
H	-1.7862	2.5126	-1.3652	H	-0.9180	-2.4018	0.5537	H	4.5453	0.5971	-0.4577

Chapter 7: Experimental Section

<b>2a</b>				<b><sup>3</sup>2a(α)</b>				<b><sup>3</sup>2a(β)</b>			
C	-1.3440	-1.8167	-0.0318	C	-1.3204	-1.8385	0.3161	C	-1.3035	1.1206	-0.6720
C	-1.9945	-0.8996	-0.8740	C	-2.0700	-1.1329	-0.6936	C	-1.9635	-0.1609	-0.6336
C	0.0461	-1.8835	0.0412	C	0.0403	-1.8311	0.3356	C	-0.0490	1.2985	-0.1762
C	-1.1958	-0.0429	-1.6501	C	-1.3448	-0.5155	-1.7674	C	-1.3075	-1.2385	0.0511
C	0.1956	-0.0880	-1.5848	C	0.0191	-0.4941	-1.7992	C	-0.0558	-1.1066	0.5776
C	0.7986	-1.0090	-0.7352	C	0.7465	-0.9316	-0.5906	C	0.7133	0.1125	0.2495
H	0.8098	0.5711	-2.1892	H	0.5723	-0.1192	-2.6540	H	0.4078	-1.8899	1.1675
H	-1.9358	-2.5011	0.5705	H	-1.8715	-2.4362	1.0403	H	-1.8543	1.9711	-1.0697
H	0.5399	-2.6014	0.6866	H	0.6089	-2.4190	1.0505	H	0.4267	2.2749	-0.1547
H	-1.6700	0.6674	-2.3225	H	-1.9115	-0.1170	-2.6077	H	-1.8574	-2.1669	0.1963
C	-3.4983	-0.8198	-0.9235	C	-3.5547	-1.0867	-0.6418	C	-3.3457	-0.3169	-1.1658
H	-3.9366	-1.8069	-0.7253	H	-3.9621	-1.9912	-0.1691	H	-3.5187	-1.3445	-1.5118
H	-3.8300	-0.5313	-1.9297	H	-3.9838	-1.0177	-1.6508	H	-3.5099	0.3449	-2.0266
C	-3.6743	2.1707	-0.0579	C	-3.7099	2.0264	-0.4681	C	-4.5868	1.8599	0.7109
H	-2.5837	2.2441	0.0227	H	-2.6176	2.1084	-0.5007	H	-3.6277	2.0261	1.2143
H	-3.9567	2.4863	-1.0698	H	-4.0814	2.1012	-1.4973	H	-4.6604	2.5786	-0.1144
H	-4.1069	2.8944	0.6436	H	-4.0908	2.8953	0.0822	H	-5.3824	2.1010	1.4265
C	-3.8196	-0.0660	2.0866	C	-3.6279	0.3379	2.1371	C	-4.6539	-1.1238	1.5593
H	-4.2589	0.6306	2.8110	H	-4.0244	1.1728	2.7278	H	-5.4521	-0.9215	2.2840
H	-4.1796	-1.0711	2.3386	H	-3.9337	-0.5903	2.6350	H	-4.7641	-2.1649	1.2326
H	-2.7336	-0.0549	2.2335	H	-2.5343	0.3942	2.1775	H	-3.6978	-1.0389	2.0882
C	-6.1644	0.3322	0.0951	C	-6.1472	0.2685	0.3230	C	-6.3982	-0.1461	-0.8138
H	-6.5474	-0.6764	0.2920	H	-6.4857	-0.6690	0.7802	H	-6.5119	-1.1683	-1.1944
H	-6.6748	1.0178	0.7825	H	-6.6143	1.0924	0.8764	H	-7.2478	0.0544	-0.1496
H	-6.4621	0.6066	-0.9242	H	-6.5361	0.2984	-0.7019	H	-6.4792	0.5372	-1.6677
Si	-4.2852	0.4188	0.3185	Si	-4.2599	0.4178	0.3572	Si	-4.7562	0.0771	0.1022
O	2.2099	-1.1098	-0.7579	O	1.3281	0.1855	0.1840	O	1.7995	-0.1198	-0.7250
S	3.1063	-0.5945	0.5183	S	2.7088	0.8708	-0.3270	S	3.1795	-0.8180	-0.2297
O	2.3116	-0.5542	1.7350	O	2.9389	0.6261	-1.7438	O	2.9861	-1.5908	0.9893
O	4.3727	-1.2929	0.4166	O	2.7643	2.1984	0.2567	O	3.8231	-1.3656	-1.4094
C	3.4126	1.1778	-0.0040	C	3.9235	-0.1985	0.6140	C	4.1262	0.7232	0.2529
F	2.2538	1.8387	-0.0499	F	3.7449	-0.0413	1.9233	F	3.4371	1.4044	1.1722
F	4.2171	1.7485	0.8896	F	5.1606	0.1682	0.2826	F	5.3027	0.3580	0.7600
F	3.9838	1.2015	-1.2054	F	3.7373	-1.4812	0.2914	F	4.3179	1.4924	-0.8159

**New Intermediates from Photogenerated Phenyl Cations**

<b>2b</b>				<b><sup>3</sup>2b(α)</b>			<b><sup>3</sup>2b(β)</b>				
C	1.6192	2.5266	0.1905	C	1.6448	0.6875	0.5762	C	1.7110	0.5611	-0.6420
C	1.6124	1.3794	-0.6203	C	0.5879	-0.1098	0.1099	C	0.5945	-0.1111	-0.2394
C	0.4320	3.1215	0.6177	C	0.4416	2.6581	-0.2170	C	0.7601	2.6949	0.2707
C	-0.8030	1.4502	-0.5437	C	-0.6115	1.8650	-0.6725	C	-0.3490	2.0304	0.7311
H	2.5709	2.9646	0.4803	C	-0.5112	0.4896	-0.4935	C	-0.5619	0.6372	0.2607
H	0.4675	4.0137	1.2363	H	-1.4857	2.2886	-1.1546	H	-1.0781	2.4938	1.3867
C	2.8964	0.7291	-1.0662	H	0.6130	-1.1879	0.2252	H	0.5054	-1.1869	-0.3690
H	3.6973	1.4782	-1.1145	H	0.3933	3.7364	-0.3402	H	0.9099	3.7442	0.5158
H	2.7872	0.3282	-2.0827	O	-1.5413	-0.3149	-1.0389	O	-1.6639	0.5221	-0.7054
C	2.3150	-2.1643	-0.0396	S	-2.6028	-1.1033	-0.0685	S	-3.1992	0.5497	-0.1673
H	1.3054	-1.8889	0.2831	O	-3.2429	-2.0872	-0.9191	O	-3.3046	1.2111	1.1257
H	2.2437	-2.5587	-1.0609	O	-2.0040	-1.4277	1.2158	O	-4.0337	0.9056	-1.2994
H	2.6540	-2.9854	0.6040	C	-3.8501	0.2634	0.2316	C	-3.4321	-1.2828	0.1402
C	3.6807	-0.1005	1.8374	Si	4.2513	-0.4411	-0.0103	Si	4.2753	-0.5966	0.0558
H	4.0155	-0.9108	2.4963	C	5.6706	-1.1655	1.0146	C	5.7200	-1.3452	-0.9137
H	4.4111	0.7135	1.9217	C	4.8503	1.0882	-0.9507	C	3.5709	-1.8649	1.2679
H	2.7247	0.2693	2.2250	C	3.5985	-1.7379	-1.2230	C	4.8587	0.9439	0.9876
C	5.2119	-1.2414	-0.6083	H	6.0617	-0.4334	1.7314	H	5.4093	-2.2292	-1.4835
H	5.9370	-0.4194	-0.5716	H	5.3480	-2.0463	1.5830	H	6.1427	-0.6244	-1.6240
H	5.6227	-2.0690	-0.0172	H	6.5042	-1.4754	0.3727	H	6.5278	-1.6554	-0.2398
H	5.1478	-1.5811	-1.6491	H	5.6410	0.8247	-1.6637	H	4.3129	-2.1369	2.0283
Si	3.5190	-0.7066	0.0525	H	4.0366	1.5565	-1.5163	H	2.6892	-1.4739	1.7885
O	-2.0206	0.9059	-1.0240	H	5.2611	1.8442	-0.2702	H	3.2723	-2.7871	0.7548
S	-3.0599	0.1427	-0.0148	H	2.7579	-1.3530	-1.8117	H	4.0410	1.4122	1.5472
O	-3.0884	0.7724	1.2951	H	4.3819	-2.0446	-1.9267	H	5.6462	0.6864	1.7066
O	-4.2492	-0.0971	-0.8074	H	3.2546	-2.6396	-0.7018	H	5.2720	1.6978	0.3064
C	-2.1882	-1.5064	0.1948	C	1.5500	2.0781	0.3999	C	1.7695	2.0033	-0.4368
C	-0.8054	2.5922	0.2489	H	2.3560	2.7136	0.7580	H	2.6531	2.5386	-0.7717
H	-1.7388	3.0427	0.5639	C	2.8573	0.0610	1.2149	C	2.9118	-0.1313	-1.2235
C	0.3680	0.8424	-0.9828	H	2.5684	-0.8387	1.7739	H	3.3750	0.4996	-1.9940
H	0.3009	-0.0384	-1.6139	H	3.2961	0.7521	1.9464	H	2.6113	-1.0630	-1.7191
F	-1.1287	-1.3559	0.9934	F	-4.2261	0.7924	-0.9315	F	-4.6528	-1.4761	0.6371
F	-3.0416	-2.3658	0.7442	F	-3.3044	1.2111	0.9941	F	-2.5206	-1.7117	1.0165
F	-1.7878	-1.9641	-0.9908	F	-4.9056	-0.2586	0.8517	F	-3.3000	-1.9549	-1.0005

Chapter 7: Experimental Section

<b>2c</b>				<b><sup>3</sup>2c(β)</b>			
C	-2.4541	1.9723	-0.7517	C	1.8109	2.2490	-1.1158
C	-1.4252	1.0401	-0.5357	C	1.2030	1.0767	-0.7189
C	-1.2923	3.6800	0.5115	C	0.5576	3.5589	0.5716
C	-0.2557	2.7806	0.7542	C	-0.0856	2.4397	1.0135
C	-0.3440	1.4944	0.2306	C	0.0270	1.2241	0.1834
H	0.6116	3.0572	1.3449	H	-0.7266	2.4380	1.8883
H	-1.2389	4.6884	0.9103	H	0.4240	4.5062	1.0895
O	0.6794	0.5652	0.5556	O	-1.1788	0.9468	-0.6241
S	2.1214	0.6838	-0.2200	S	-2.5168	0.3570	0.0813
O	1.9251	0.9002	-1.6456	O	-2.5261	0.6015	1.5161
O	3.0474	1.4907	0.5594	O	-3.6337	0.6939	-0.7809
C	2.5675	-1.1162	0.0463	C	-2.1859	-1.4719	-0.1515
C	-2.3934	3.2687	-0.2418	C	1.4726	3.4917	-0.5265
H	-3.2077	3.9608	-0.4377	H	1.9791	4.3941	-0.8544
C	-1.4964	-0.3605	-1.0777	H	2.6172	2.2120	-1.8464
Si	-2.2441	-1.6874	0.0972	C	1.6217	-0.2891	-1.1404
H	-0.5026	-0.7060	-1.3791	Si	2.7244	-1.2090	0.1555
H	-2.1116	-0.3627	-1.9867	H	2.2019	-0.2430	-2.0713
C	-4.0920	-1.3370	0.3195	H	0.7435	-0.9173	-1.3343
C	-1.3942	-1.6797	1.7871	C	2.0348	-1.0043	1.9041
C	-1.9902	-3.3647	-0.7446	C	2.7489	-3.0390	-0.3289
H	-4.2605	-0.3470	0.7595	C	4.4668	-0.4760	0.0636
H	-4.6291	-1.3726	-0.6362	H	1.0077	-1.3748	1.9846
H	-4.5550	-2.0759	0.9848	H	2.6479	-1.5597	2.6247
H	-1.8275	-2.4531	2.4336	H	2.0330	0.0472	2.2140
H	-0.3189	-1.8722	1.7098	H	3.3989	-3.6162	0.3400
H	-1.5193	-0.7172	2.2963	H	1.7450	-3.4764	-0.2725
H	-0.9233	-3.5805	-0.8783	H	3.1177	-3.1820	-1.3517
H	-2.4194	-4.1781	-0.1471	H	4.4533	0.6037	0.2536
H	-2.4619	-3.3980	-1.7341	H	5.1274	-0.9343	0.8094
H	-3.3127	1.6684	-1.3454	H	4.9199	-0.6365	-0.9222
F	1.7501	-1.8946	-0.6664	F	-1.9734	-1.7384	-1.4393
F	2.4690	-1.4301	1.3356	F	-1.1053	-1.8328	0.5528
F	3.8204	-1.2914	-0.3666	F	-3.2418	-2.1558	0.2817

**New Intermediates from Photogenerated Phenyl Cations**

<b>3a-Me2</b>				<b><sup>3</sup>3a(α)-Me2</b>			<b><sup>3</sup>3a(β)-Me2</b>				
C	-1.6891	-0.1739	-0.6130	C	-0.1185	-1.2618	-1.6313	C	-0.0398	-0.7783	1.2804
C	-1.0055	1.0505	-0.5487	C	1.0585	-1.5462	0.9396	C	1.0487	0.5467	-0.9864
C	0.8698	0.0047	0.5328	C	-0.3014	-1.5508	0.8694	C	-0.1821	0.9447	-0.5608
H	-1.4715	1.9445	-0.9564	C	-0.9462	-1.1595	-0.4102	C	-0.8797	0.1289	0.4674
O	2.1142	0.1036	1.1680	H	-0.9228	-1.7639	1.7330	H	-0.7004	1.7882	-1.0046
C	0.2640	1.1479	0.0202	H	-0.6047	-1.2791	-2.6033	H	-0.4456	-1.1925	2.1995
H	0.7827	2.0998	0.0683	H	1.5516	-1.7528	1.8889	H	1.5346	1.0814	-1.8014
C	0.2204	-1.2257	0.4887	O	-1.6368	0.0983	-0.3648	O	-2.0420	-0.5578	-0.0185
H	0.7140	-2.1039	0.8908	C	1.8834	-1.3592	-0.2236	C	1.7700	-0.5238	-0.3524
O	4.6758	0.0652	1.3411	O	-3.1314	-0.3555	1.7959	O	-3.3006	1.5257	-1.1063
P	3.5320	-0.0494	0.4160	C	-3.1390	2.5848	-0.7776	C	-4.4300	-2.1714	-0.5373
O	3.3228	-1.4286	-0.3755	H	-3.8175	2.1950	-1.5429	H	-4.8210	-2.1165	0.4835
O	3.5282	1.0151	-0.8005	H	-3.4209	3.6069	-0.5192	H	-5.1452	-2.6869	-1.1805
C	4.0989	2.3192	-0.5843	H	-2.1110	2.5630	-1.1494	H	-3.4743	-2.7023	-0.5392
H	4.1862	2.7816	-1.5691	C	-5.3660	-0.7815	-0.2038	C	-5.0447	1.3847	1.3667
H	3.4410	2.9253	0.0478	H	-5.9798	0.0893	0.0505	H	-5.9810	1.0830	0.8847
H	5.0813	2.2361	-0.1132	H	-5.8181	-1.3155	-1.0414	H	-5.1889	1.4332	2.4474
C	4.3890	-1.9235	-1.2063	H	-5.2847	-1.4385	0.6654	H	-4.7321	2.3583	0.9818
H	4.0824	-2.9169	-1.5370	O	-4.0598	-0.3678	-0.6487	O	-4.0187	0.3992	1.1417
H	4.5268	-1.2696	-2.0727	O	-3.2466	1.8206	0.4357	O	-4.2685	-0.8544	-1.0920
H	5.3192	-1.9925	-0.6347	P	-3.0294	0.2307	0.4456	P	-3.3947	0.2650	-0.3453
C	-1.0489	-1.3054	-0.0821	Si	4.0539	0.5019	0.1223	Si	4.5735	0.0893	0.0224
H	-1.5500	-2.2697	-0.1224	C	3.5864	1.5548	-1.3787	C	4.3729	1.9345	-0.3426
C	-3.0727	-0.2660	-1.2084	C	5.9397	0.3733	0.2603	C	6.1988	-0.5444	-0.7179
H	-3.2253	-1.2568	-1.6571	C	3.3359	1.2564	1.7004	C	4.5568	-0.2099	1.8911
H	-3.1813	0.4592	-2.0263	H	4.0125	1.1496	-2.3047	H	4.4106	2.1389	-1.4195
Si	-4.5142	0.0365	0.0213	H	2.4995	1.6073	-1.5072	H	3.4190	2.3184	0.0361
C	-4.3880	1.7812	0.7457	H	3.9590	2.5804	-1.2668	H	5.1761	2.5134	0.1299
C	-6.1363	-0.1384	-0.9446	H	6.3929	1.3638	0.3895	H	7.0601	-0.0252	-0.2798
C	-4.4573	-1.2433	1.4150	H	6.2395	-0.2401	1.1186	H	6.3327	-1.6173	-0.5345
H	-4.4570	2.5484	-0.0354	H	6.3798	-0.0755	-0.6384	H	6.2354	-0.3857	-1.8025
H	-5.1987	1.9671	1.4608	H	3.6217	0.6811	2.5894	H	4.6969	-1.2711	2.1310
H	-3.4393	1.9284	1.2744	H	3.6987	2.2818	1.8425	H	5.3646	0.3468	2.3820
H	-7.0043	0.0256	-0.2944	H	2.2413	1.2921	1.6662	H	3.6110	0.1122	2.3412



## Chapter 7: Experimental Section

<b>3b-Me<sub>2</sub></b>				<b><sup>3</sup>3b(α)-Me<sub>2</sub></b>				<b><sup>3</sup>3b(β)-Me<sub>2</sub></b>			
C	1.7477	2.5072	-0.1510	C	1.6438	2.2637	0.0885	C	-1.5848	0.3738	0.6309
C	1.6582	1.2446	-0.7585	C	1.6967	1.0937	-0.6867	C	-0.5234	-0.3286	0.1450
C	0.6023	3.2012	0.2411	C	0.4287	2.7446	0.5741	C	-0.4998	2.5149	-0.0986
C	-0.7490	1.3980	-0.5548	C	-0.7128	0.9157	-0.4561	C	0.5581	1.8316	-0.6335
H	2.7267	2.9520	0.0101	H	2.5619	2.8061	0.3005	C	0.6837	0.3774	-0.3203
H	0.6960	4.1801	0.7037	H	0.4076	3.6575	1.1633	H	1.3322	2.3170	-1.2181
C	2.8931	0.4684	-1.1414	C	3.0080	0.5517	-1.1996	H	-0.5138	-1.4162	0.1611
H	3.7453	1.1502	-1.2598	H	3.6957	1.3776	-1.4256	H	-0.5790	3.5920	-0.2332
H	2.7508	-0.0210	-2.1146	H	2.8519	0.0144	-2.1445	O	1.8094	0.0679	0.5095
C	2.1427	-2.3004	0.1172	C	2.8000	-2.1195	0.3984	Si	-4.2546	-0.5126	-0.0883
H	1.1264	-1.9648	0.3531	H	1.8707	-1.7941	0.8799	C	-5.6923	-1.3449	0.8243
H	2.1059	-2.7966	-0.8609	H	2.5313	-2.6803	-0.5052	C	-3.6706	-1.6139	-1.5111
H	2.4205	-3.0622	0.8565	H	3.3023	-2.8157	1.0810	C	-4.8170	1.1666	-0.7601
C	3.5512	-0.1345	1.8456	C	4.3718	0.2665	1.5946	H	-5.3977	-2.3180	1.2356
H	3.8484	-0.8928	2.5803	H	4.8600	-0.4114	2.3055	H	-6.0531	-0.7288	1.6570
H	4.3015	0.6651	1.8754	H	5.0649	1.0944	1.4011	H	-6.5406	-1.5161	0.1503
H	2.5975	0.2928	2.1751	H	3.4852	0.6824	2.0866	H	-4.4561	-1.7277	-2.2681
C	5.0943	-1.5572	-0.4337	C	5.4883	-1.2441	-0.8712	H	-2.7884	-1.1917	-2.0056
H	5.8549	-0.7669	-0.4454	H	6.1510	-0.4081	-1.1258	H	-3.4041	-2.6177	-1.1583
H	5.4489	-2.3457	0.2414	H	6.0563	-1.9310	-0.2319	H	-4.0105	1.6787	-1.2971
H	5.0465	-1.9858	-1.4423	H	5.2547	-1.7767	-1.8010	H	-5.6538	1.0434	-1.4587
Si	3.4049	-0.8921	0.1168	Si	3.9153	-0.6421	-0.0018	H	-5.1568	1.8309	0.0440
O	-2.0257	0.8631	-0.7931	O	-1.8575	0.2008	-0.8262	C	-1.5508	1.8272	0.5607
C	-0.6645	2.6500	0.0472	C	-0.7705	2.0823	0.3053	H	-2.3891	2.3877	0.9642
H	-1.5700	3.1652	0.3490	H	-1.7217	2.4581	0.6637	C	-2.8216	-0.2937	1.1734
C	0.3817	0.7006	-0.9669	C	0.4937	0.4242	-0.9509	H	-3.2109	0.2757	2.0288
H	0.2620	-0.2712	-1.4334	H	0.4800	-0.4752	-1.5600	H	-2.5758	-1.2943	1.5523
C	-4.0020	-1.4449	-1.8903	P	-3.1451	-0.0023	0.1368	O	3.6943	1.3150	-0.9056
H	-5.0544	-1.6506	-2.0915	C	-5.4218	-0.8968	-0.8163	C	3.9191	-1.0116	2.2262
H	-3.5777	-0.8584	-2.7114	H	-5.7844	-1.4689	0.0438	H	3.9468	-2.0006	1.7582
H	-3.4501	-2.3818	-1.7752	H	-5.7784	0.1333	-0.7487	H	4.7091	-0.9344	2.9751
C	-3.2719	-0.5895	2.5579	H	-5.7717	-1.3606	-1.7398	H	2.9437	-0.8504	2.6928
H	-3.2942	0.0650	3.4305	C	-1.9289	-2.1831	1.0418	C	4.4598	-1.4849	-1.7886
H	-4.2480	-1.0680	2.4302	H	-1.8443	-2.7114	1.9928	H	5.4304	-1.5659	-1.2875

**New Intermediates from Photogenerated Phenyl Cations**

<b>3c-Me2</b>				<b><sup>3</sup>3c(α)-Me2</b>				<b><sup>3</sup>3c(β)-Me2</b>			
C	-1.0554	3.6199	-0.2105	C	1.3079	1.3229	0.4823	C	-1.1212	1.1107	0.6559
C	0.0829	3.5964	0.5964	C	-0.1270	3.7047	-0.2323	C	-0.2669	3.4004	-0.8545
C	0.2008	1.2088	0.3050	C	-0.8373	2.7030	0.3540	C	0.2860	2.1995	-1.1820
H	-1.5556	4.5606	-0.4242	C	-0.1873	1.3748	0.4942	C	0.0595	1.0589	-0.2598
H	0.4791	4.5139	1.0220	H	-1.8816	2.8117	0.6256	H	0.9517	2.0722	-2.0292
O	0.8208	-0.0078	0.6506	H	-0.6021	4.6614	-0.4403	H	-0.0483	4.2837	-1.4512
C	0.7144	2.3811	0.8549	O	-0.7273	0.3650	-0.3696	O	1.2262	0.6646	0.4779
H	1.6014	2.3226	1.4763	C	1.2691	3.5474	-0.5184	C	-1.1965	3.5106	0.2307
C	-0.9431	1.1915	-0.5075	H	1.8198	4.3694	-0.9653	H	-1.6322	4.4769	0.4656
O	1.9249	-0.8033	-1.6110	O	-3.2837	0.7283	0.2421	O	2.8839	0.3176	-1.5824
P	2.0985	-0.5740	-0.1586	C	-3.5643	-1.7794	-1.6951	C	3.2957	-0.4230	2.2333
O	3.2463	0.4598	0.2739	H	-4.4190	-1.1028	-1.6051	H	2.8496	-1.4196	2.3097
O	2.4646	-1.8731	0.7133	H	-3.4940	-2.1577	-2.7157	H	4.2584	-0.4084	2.7469
C	1.8742	-3.1430	0.3809	H	-3.6718	-2.6152	-0.9966	H	2.6245	0.3184	2.6749
H	2.4867	-3.9031	0.8689	C	-2.2896	-1.1027	2.3969	C	2.4467	-2.6457	-1.0372
H	0.8513	-3.1945	0.7680	H	-2.3154	-2.0651	2.9115	H	3.4367	-2.8990	-0.6431
H	1.8730	-3.2975	-0.7014	H	-1.5004	-0.4769	2.8272	H	1.8005	-3.5242	-0.9948
C	4.4858	0.4670	-0.4615	H	-3.2524	-0.5946	2.4909	H	2.5406	-2.2933	-2.0672
H	5.0156	1.3706	-0.1568	O	-1.9996	-1.3912	1.0166	O	1.8173	-1.6420	-0.2154
H	5.0804	-0.4147	-0.2023	O	-2.3335	-1.0757	-1.4440	O	3.5692	-0.0909	0.8607
H	4.2930	0.4856	-1.5371	P	-2.2056	-0.2300	-0.0922	P	2.4209	-0.1376	-0.2581
Si	-2.8114	-0.9601	0.0273	Si	2.6249	-1.2550	-0.0775	Si	-2.7851	-1.1515	0.0058
C	-3.1997	-2.6344	-0.7744	C	1.2117	-2.2604	-0.8206	C	-4.3858	-0.1743	-0.2492
C	-4.3873	0.0898	0.0963	C	3.6996	-2.3835	1.0053	C	-3.1653	-2.8190	0.8232
C	-2.1561	-1.2214	1.7830	C	3.6821	-0.5002	-1.4544	C	-1.9173	-1.4315	-1.6507
H	-3.5721	-2.5120	-1.7988	H	0.5388	-2.6462	-0.0461	H	-4.9380	-0.0548	0.6910
H	-2.3081	-3.2714	-0.8224	H	0.6046	-1.6605	-1.5047	H	-4.1798	0.8275	-0.6436
H	-3.9650	-3.1790	-0.2081	H	1.6099	-3.1181	-1.3777	H	-5.0499	-0.6813	-0.9597
H	-5.1470	-0.3825	0.7312	H	4.1303	-3.2004	0.4132	H	-3.8366	-3.4211	0.1985
H	-4.1866	1.0861	0.5075	H	4.5312	-1.8356	1.4648	H	-2.2500	-3.4022	0.9809
H	-4.8271	0.2222	-0.8999	H	3.1150	-2.8386	1.8143	H	-3.6496	-2.6910	1.7990
H	-1.9405	-0.2650	2.2728	H	4.5473	0.0425	-1.0543	H	-0.9385	-1.9045	-1.5116
H	-2.8934	-1.7518	2.3983	H	4.0650	-1.2821	-2.1220	H	-2.5174	-2.0784	-2.3029
H	-1.2288	-1.8047	1.7899	H	3.1004	0.2007	-2.0636	H	-1.7510	-0.4864	-2.1798

## 7.2 Experimental details relative to Chapter 3

$^1\text{H}$  and  $^{13}\text{C}$  NMR spectra were recorded on a 300 and 75 MHz spectrometer. The attributions were made on the basis of  $^1\text{H}$  and  $^{13}\text{C}$  NMR, as well as DEPT-135 experiments; chemical shifts are reported in ppm downfield from TMS. UV and fluorescence spectra were recorded on a Jasco V-550 UV spectrophotometer and a PerkinElmer LS55 luminescence spectrometer, respectively.

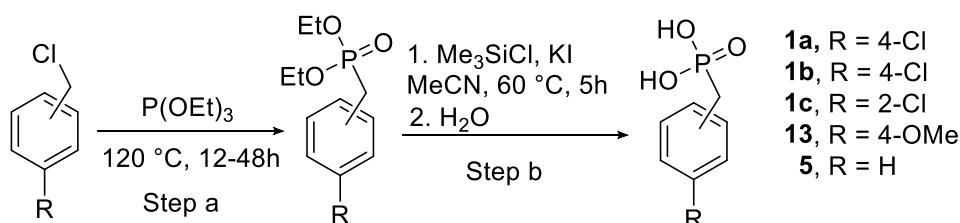
The acidity released was determined from 5 mL of the photolyzed solutions by dilution with water (25 mL) and titration with aqueous 0.1 M NaOH by means of a potentiometer equipped with a pH glass combined electrode module. Phosphate anion was determined via HPLC ion chromatography and quantified by means of a calibration curve obtained with commercially available samples.

The photochemical reactions were performed by using nitrogen-purged solutions in quartz tubes. Irradiations were performed in a multilamp reactor fitted with ten 15 W phosphor coated Hg lamps (maximum of emission at 310 nm) or with four 15 W low pressure Hg lamps (maximum of emission at 254 nm). Solvent of HPLC purity were employed in the photochemical reactions. Quantum yields were measured at 254 nm (1 Hg lamp, 15W). The reaction course was followed by GC, and HPLC analyses. Compounds **4a–c** and **5** were identified and quantified via HPLC analyses. Compounds **6**,<sup>[1]</sup> **7**,<sup>[1]</sup> **8**,<sup>[1]</sup> **9** (MS (m/z): 148 ( $\text{M}^+$ , 88), 133 (19), 105 (83), 91 (89), 43 (100)) **10**,<sup>[2]</sup> **11** (MS (m/z): 131 ( $\text{M}^+$ , 18), 91 (100), 65 (15)) and **12**<sup>[1]</sup> were identified by means of GC-MS analyses and quantified by comparison with authentic samples.

GC-MS analyses were carried out using a Thermo Scientific DSQII single quadrupole GC-MS system. A Restek Rtx-5MS (30 m  $\times$  0.25 mm  $\times$  0.25  $\mu\text{m}$ ) capillary column was used for analytes separation with helium as carrier gas at 1 mL  $\text{min}^{-1}$ . The injection in the GC system was performed in split mode and the injector temperature was 250  $^\circ\text{C}$ . The GC oven temperature was held at 80  $^\circ\text{C}$  for 2 min, increased to 220  $^\circ\text{C}$  by a temperature ramp of 10  $^\circ\text{C min}^{-1}$  and held for ten min. The transfer line temperature was 250  $^\circ\text{C}$  and the ion source temperature 250  $^\circ\text{C}$ . Mass spectral analyses were carried out in full scan mode. HPLC analyses were carried out using a Supelco Discovery C18 HPLC Column (25cm  $\times$  4.6mm, 5 $\mu\text{m}$  particle size). Solvents used for the gradient elution process were  $\text{H}_2\text{O}$  (in the presence of 0.1%  $\text{HCOOH}$ , A) and MeCN (B). The gradient is set to start at 90% A and 10% B at 8 min to 10% A and 90% B after 60 min at a flow rate of 0.5 mL  $\text{min}^{-1}$ . The UV-detector is set to operate at 230 or 240 nm.

7.2.1 Synthesis of compounds **1a–c**, **5** and **13**

Benzylphosphonic acids **1a–c**, **5** and **15** were obtained from the corresponding benzylchlorides through a two-step synthesis (see Scheme 7.1) previously described in literature.<sup>[109]</sup>



Scheme 7.1

7.2.1.1 Step a. General procedure for the synthesis of benzyldiethylphosphonates<sup>[109]</sup>

A mixture of the appropriate chosen benzyl chloride (1 equiv.) with triethylphosphite (1.2 equiv.) is kept refluxing under a constant stream of nitrogen for 12-48 hours at 120 °C. The crude mixture was then distilled in vacuo ( $3 \times 10^{-2}$  Torr) at 90 °C in order to remove the unreacted phosphite, and the desired product was used for the next step without any further purification.

**Diethyl 3-chlorobenzylphosphonate (3b).** From from 3-chlorobenzylchloride (2,53 mL, 20 mmol) and triethylphosphite (4.12 mL, 24 mmol). Removal of the unreacted phosphite afforded the desired product (4.4 g, 84% yield) as a colorless oil. <sup>1</sup>H NMR (300 MHz, CDCl<sub>3</sub>)<sup>[291]</sup>  $\delta$  7.33 – 7.15 (m, 4H), 4.10 – 3.97 (m, 4H), 3.12 (d,  $J = 21.7$  Hz, 2H), 1.26 (t,  $J = 7.1$  Hz, 6H). <sup>13</sup>C NMR (75 MHz, CDCl<sub>3</sub>)  $\delta$  134.1 (d,  $J = 3.5$  Hz), 133.6 (d,  $J = 9.1$  Hz), 129.7 (dd,  $J = 7.4, 4.9$  Hz, CH), 127.8 (d,  $J = 6.5$  Hz, CH), 127.0 (d,  $J = 3.6$  Hz, CH), 62.1 (d,  $J = 6.8$  Hz, CH<sub>2</sub>), 33.3 (d,  $J = 138.6$  Hz, CH<sub>2</sub>), 16.2 (d,  $J = 6.0$  Hz, CH<sub>3</sub>). IR (KBr,  $\nu/\text{cm}^{-1}$ ): 3063, 2983, 2908, 1597, 1573, 1477, 1432, 1393, 1250, 1026, 879, 803. Anal. Calcd. for C<sub>11</sub>H<sub>16</sub>ClO<sub>3</sub>P: C, 50.30; H, 6.14; Cl, 13.50; O, 18.27; P, 11.79

**Diethyl 2-chlorobenzylphosphonate (3c).** From 2-chlorobenzylchloride (2.5 mL, 20 mmol) and triethylphosphite (4.12 mL, 24 mmol). Removal of the unreacted phosphite afforded the desired product (4.8 g, 92% yield) as a colorless oil.

Spectroscopic data were in accordance with literature.<sup>[292]</sup> <sup>1</sup>H NMR (300 MHz, CDCl<sub>3</sub>) δ 7.52 – 7.09 (m, 4H), 4.05 (dq, J = 14.2, 7.1 Hz, 4H), 3.37 (d, J = 22.0 Hz, 2H), 1.25 (t, J = 7.1 Hz, 6H). <sup>13</sup>C NMR (75 MHz, CDCl<sub>3</sub>) δ 134.1 (d, J = 8.3 Hz), 131.6 (d, J = 5.2 Hz), 129.9 (d, J = 9.1 Hz), 129.5 (d, J = 3.0 Hz), 128.2 (d, J = 3.6 Hz), 126.7 (d, J = 3.4 Hz), 62.1 (d, J = 6.7 Hz), 30.6 (d, J = 139.2 Hz), 16.2 (d, J = 6.1 Hz). IR (KBr, v/cm<sup>-1</sup>) 3064, 2984, 2908, 1478, 1443, 1253, 1029, 967, 754. Anal. Calcd. for C<sub>11</sub>H<sub>16</sub>ClO<sub>3</sub>P: C, 50.30; H, 6.14; Cl, 13.50; O, 18.27; P, 11.79

**Diethyl 4-methoxybenzylphosphonate(14).** From 4-methoxybenzylchloride (2.70 mL, 20 mmol) and triethylphosphite (4.12 mL, 24 mmol). Removal of the unreacted phosphite afforded the desired product (4.2 g, 81% yield) as a colorless oil. Spectroscopic data were in accordance with literature.<sup>[293]</sup> <sup>1</sup>H NMR (300 MHz, CDCl<sub>3</sub>) δ 7.23 – 6.80 (AA'BB', 4H), 4.13 – 3.90 (m, 4H), 3.78 (s, 3H), 3.08 (d, J = 21.1 Hz, 2H), 1.24 (t, J = 7.1 Hz, 6H). <sup>13</sup>C NMR (75 MHz, CDCl<sub>3</sub>) δ 158.4 (d, J = 3.5 Hz), 130.6 (d, J = 6.5 Hz), 123.3 (d, J = 9.3 Hz), 113.9 (d, J = 3.0 Hz), 61.9 (d, J = 6.8 Hz), 55.1 (s), 32.6 (d, J = 139.0 Hz), 16.3 (d, J = 6.0 Hz). IR (KBr v/cm<sup>-1</sup>): 2983, 2838, 1612, 1585, 1515, 1250, 1030, 965, 853, 787. Anal. Calcd. for C<sub>12</sub>H<sub>19</sub>O<sub>4</sub>P: C, 55.81; H, 7.42; O, 24.78; P, 11.99.

**Diethyl benzylphosphonate(15).** From benzyl chloride (1.15 mL, 10 mmol) and triethylphosphite (2.06 mL, 12 mmol). Removal of the unreacted phosphite afforded the desired product (1.5 g, 66% yield) as a colorless oil. Spectroscopic data were in accordance with literature.<sup>[294,295]</sup> <sup>1</sup>H NMR (300 MHz, CDCl<sub>3</sub>) δ 7.38 – 7.16 (m, 5H), 4.12 – 3.92 (m, 4H), 3.16 (d, J = 21.6 Hz, 2H), 1.25 (t, J = 7.1 Hz, 6H). <sup>13</sup>C NMR (75 MHz, CDCl<sub>3</sub>) δ 131.5 (d, J = 9.1 Hz), 129.6 (d, J = 6.6 Hz), 128.4 (d, J = 3.1 Hz), 126.7 (d, J = 3.6 Hz), 62.0 (d, J = 6.8 Hz), 33.7 (d, J = 138.1 Hz), 16.2 (d, J = 6.0 Hz). IR (KBr v/cm<sup>-1</sup>): 3064, 3032, 2983, 2908, 1604, 1496, 1456, 1391, 1250, 1098, 1027, 965, 828, 699. Anal. Calcd. For C<sub>11</sub>H<sub>17</sub>O<sub>3</sub>P: C, 57.89; H, 7.51; O, 21.03; P, 13.57

#### 7.2.1.2 Step b. General procedure for the synthesis of benzylphosphonic acids **1a–c**, **5** and **13**

To a 2 M solution of the chosen diethylphosphonate (1 equiv.) and KI (3 equiv.) in anhydrous MeCN freshly distilled trimethylsilylchloride (TMSCl, 3 equiv.) was added. The obtained mixture was thus stirred for 5h at 60°C. The solid was subsequently filtered off and the solvent removed in vacuo. The crude residue was treated with a few drops of HPLC-grade water, and the resulting precipitate purified via recrystallization from acidic water (HCl 1M).

**4-chlorobenzylphosphonic acid (1a).** From commercially available diethyl 4-chlorobenzylphosphonate (2 g, 7.6 mmol), KI (1.34 g, 22.8 mmol) and TMSCl (2.90 mL, 22.8 mmol) in MeCN (10 mL). Purification afforded **1a** (940 mg, 59% yield) as a white solid, m.p. 172-173 °C (lit. 168-171 °C<sup>[296]</sup>). <sup>1</sup>H NMR (300 MHz, DMSO):  $\delta$  8.66 (s, 1H), 7.30 (AA'BB', 4H), 2.96 (d,  $J = 21.4$  Hz, 2H). <sup>13</sup>C NMR (75 MHz, DMSO)  $\delta$  133.4 (d,  $J = 8.7$  Hz), 131.5 (d,  $J = 6.1$  Hz; CH), 130.6 (d,  $J = 3.9$  Hz), 127.9 (d,  $J = 2.3$  Hz; CH), 34.7 (d,  $J = 131.6$  Hz, CH<sub>2</sub>). <sup>31</sup>P NMR (121 MHz, DMSO)  $\delta$  20.51 (t,  $J = 19.3$  Hz). IR (KBr,  $\nu$  cm<sup>-1</sup>): 2854 (br), 1596, 1490, 1413, 1264, 1213, 1142, 1017, 947, 929, 752, 713. Anal. Calcd. for C<sub>7</sub>H<sub>8</sub>ClO<sub>3</sub>P: C, 40.70; H, 3.90; Cl, 17.16; O, 23.24; P, 14.99.

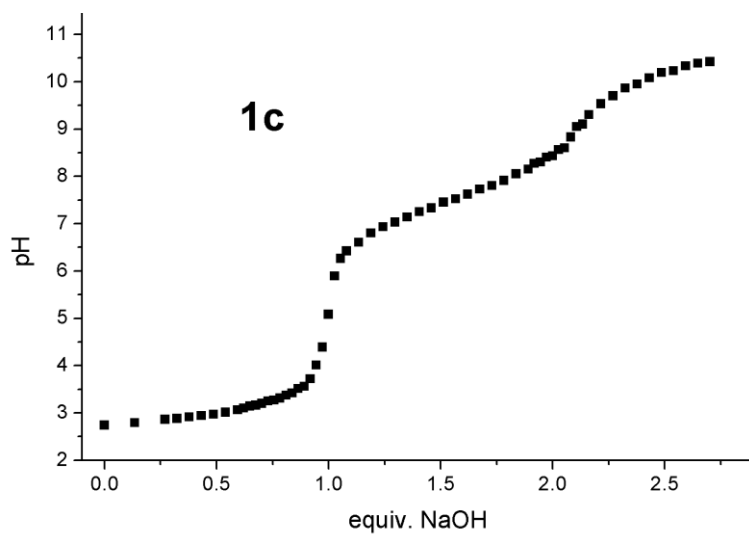
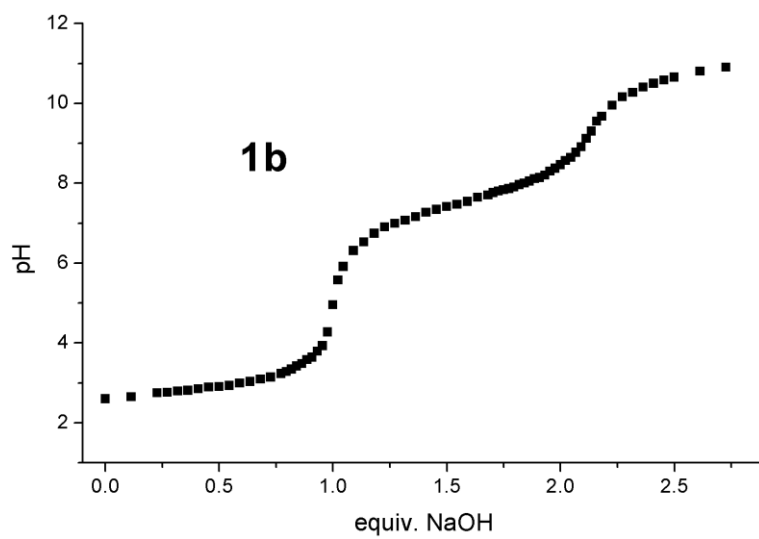
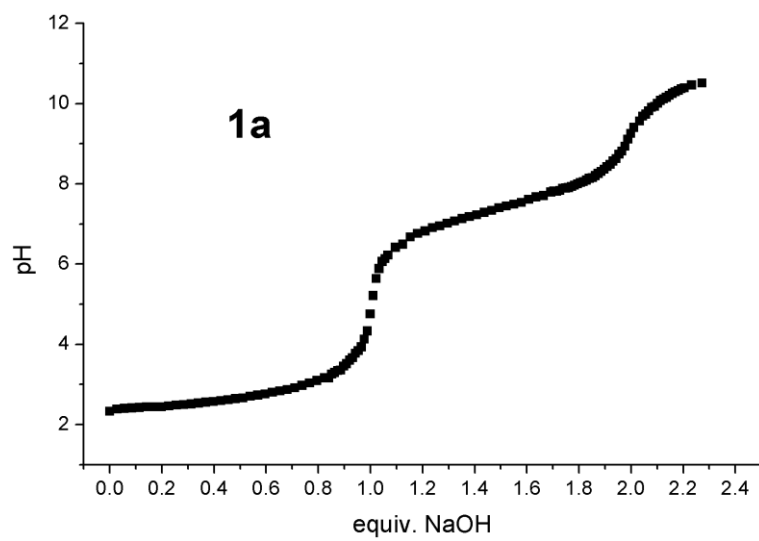
**3-chlorobenzylphosphonic acid (1b).** From diethyl 3-chlorobenzylphosphonate (1.5 g, 5 mmol) KI (2.49 g, 15 mmol) and TMSCl (1.90 mL, 15 mmol) in MeCN (8 mL). Purification afforded **1b** (350 mg, 34% yield) as a white solid, m.p. 178-179 °C. <sup>1</sup>H NMR (300 MHz, DMSO)  $\delta$  7.31 – 7.17 (m, 4H), 2.96 (d,  $J = 21.4$  Hz, 2H). <sup>13</sup>C NMR (75 MHz, DMSO)  $\delta$  137.0 (d,  $J = 8.6$  Hz), 132.5 (d,  $J = 3.1$  Hz), 130.0 (d,  $J = 2.5$  Hz, CH), 129.4 (d,  $J = 6.1$  Hz, CH), 128.5 (d,  $J = 6.4$  Hz, CH), 125.9 (d,  $J = 3.1$  Hz, CH), 34.9 (d,  $J = 131.3$  Hz, CH<sub>2</sub>). <sup>31</sup>P NMR (121 MHz, DMSO)  $\delta$  20.00 (t,  $J = 21.0$  Hz). IR (KBr,  $\nu$  cm<sup>-1</sup>): 2923 (br), 1596, 1570, 1428, 1410, 1270, 1190, 1049, 991, 950, 884, 739, 698, 678. Anal. Calcd. for C<sub>7</sub>H<sub>8</sub>ClO<sub>3</sub>P: C, 40.70; H, 3.90; Cl, 17.16; O, 23.24; P, 14.99.

**Synthesis of 2-chlorobenzylphosphonic acid (1c):** From diethyl 2-chlorobenzylphosphonate (2 g, 7.6 mmol), KI (1.34 g, 22.8 mmol) and TMSCl (2.90 mL, 22.8 mmol) in MeCN (10 mL). Purification afforded **1c** (575 mg, 37% yield) as a white solid, m.p. 184-185 °C (lit. 183 °C<sup>[297]</sup>). <sup>1</sup>H NMR (300 MHz, DMSO)  $\delta$  7.42 (t,  $J = 6.9$  Hz, 2H), 7.25 (dq,  $J = 14.9, 7.3$  Hz, 2H), 3.14 (d,  $J = 21.7$  Hz, 2H). <sup>13</sup>C NMR (75 MHz, DMSO)  $\delta$  133.3 (d,  $J = 7.9$  Hz), 132.3 (d,  $J = 8.6$  Hz), 131.9 (d,  $J = 4.9$  Hz, CH), 129.1 (d,  $J = 2.8$  Hz, CH), 127.8 (d,  $J = 3.3$  Hz, CH), 126.7 (d,  $J = 3.2$  Hz, CH), 32.5 (d,  $J = 132.4$  Hz, CH<sub>2</sub>). <sup>31</sup>P NMR (121 MHz, DMSO)  $\delta$  19.99 (t,  $J = 21.0$  Hz). IR (KBr  $\nu$  cm<sup>-1</sup>): 2923 (br), 1413, 1265, 1096, 1016, 929, 833, 814, 712, 655. Anal. Calcd. for C<sub>11</sub>H<sub>16</sub>ClO<sub>3</sub>P: C, 50.30; H, 6.14; Cl, 13.50; O, 18.27; P, 11.79.

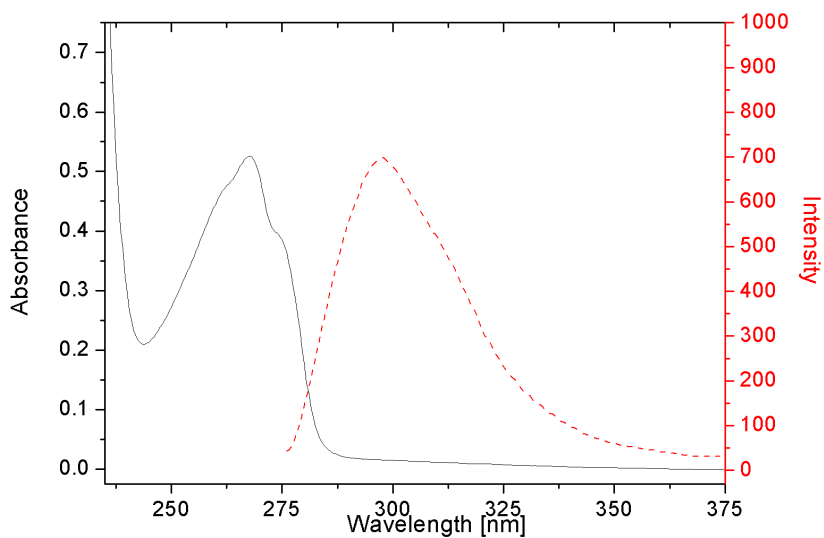
**4-hydroxybenzylphosphonic acid (2a).**

m.p. 211-212 °C. <sup>1</sup>H NMR (300 MHz, DMSO)  $\delta$  8.78 (s, 1H), 7.15 – 6.48 (AA' BB', 4H), 2.82 (d,  $J = 20.9$  Hz, 2H). <sup>13</sup>C NMR (75 MHz, DMSO)  $\delta$  155.9 (d,  $J = 3.0$  Hz), 130.9 (d,  $J = 6.3$  Hz), 124.4 (d,  $J = 8.8$  Hz), 115.2 (d,  $J = 2.3$  Hz), 34.7 (d,  $J = 133.6$  Hz). IR (KBr,  $\nu$  cm<sup>-1</sup>): 2929 (br), 1616, 1604, 1515, 1404, 1312, 1242, 1178, 1152, 1117, 1096, 988, 929, 841, 824, 785, 721. Anal. Calcd. for C<sub>7</sub>H<sub>9</sub>O<sub>4</sub>P: C, 44.69; H, 4.82; O, 34.02; P, 16.47

**Benzylphosphonic acid (5). From diethyl benzylphosphonate (15).** (1.6 g, 6.6 mmol) KI (3.29 g, 19.8 mmol) and TMSCl (2.51 mL, 19.8 mmol) in MeCN (10 mL). In this case the crude residue was purified twice by crystallization with acidic water to furnish **5** (221 mg, 20% yield) as a white solid, (m.p. 168-169 °C, lit. 169-173 °C<sup>[298]</sup>) The spectral data are in accordance with the literature.<sup>[299]</sup> <sup>1</sup>H NMR (300 MHz, DMSO)  $\delta$  7.41 – 7.06 (m, 5H), 2.95 (d, J = 20.8 Hz, 2H). <sup>13</sup>C NMR (75 MHz, DMSO)  $\delta$  133.4 (d, J = 120.4 Hz), 129.3 (d, J = 63.7 Hz), 128.2 (d, J = 34.3 Hz), 125.8 (s), 35.4 (d, J = 131.4 Hz). IR (KBr  $\nu$  cm<sup>-1</sup>): 2923 (br), 1604, 1265, 1560, 1496, 1262, 1074, 992, 942, 738, 722, 693. Anal. Calcd. for C<sub>7</sub>H<sub>9</sub>O<sub>3</sub>P C, 48.85; H, 5.27; O, 27.89; P, 18.00

7.2.2 Potentiometric Titration of **1a–c**



7.2.3 Absorption and emission spectra of compound **1-c**

**Figure 7.14** Absorption (black) and emission (red) spectra of **1a** (pH=2.5,  $5 \times 10^{-3}$  M).

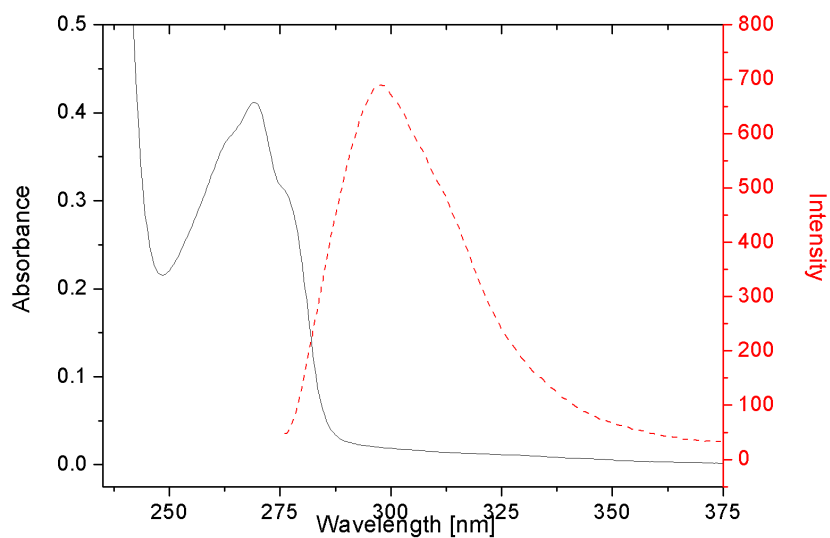


**Figure 7.15** Absorption (black) and emission (red) spectra of **1a** (pH=7.2,  $5 \times 10^{-3}$  M).

## New Intermediates from Photogenerated Phenyl Cations

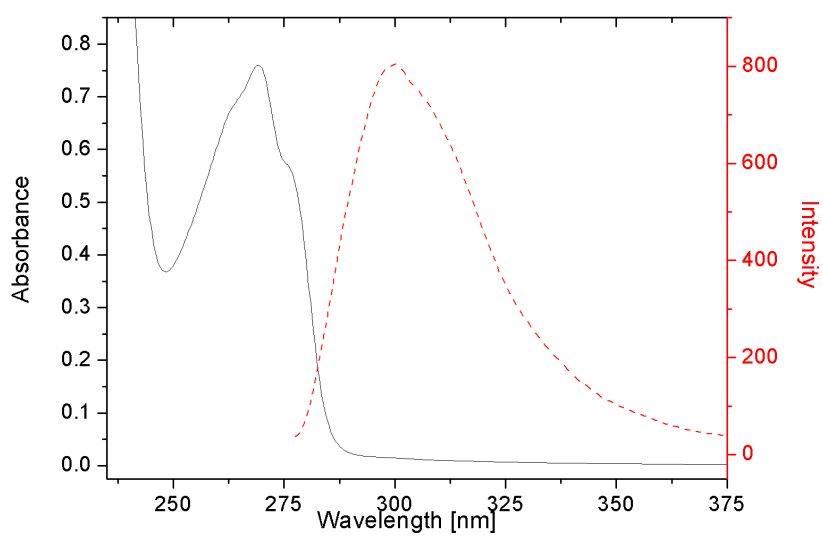


**Figure 7.16** Absorption (black) and emission (red) spectra of **1a** (pH=11,  $5 \times 10^{-3}$  M).

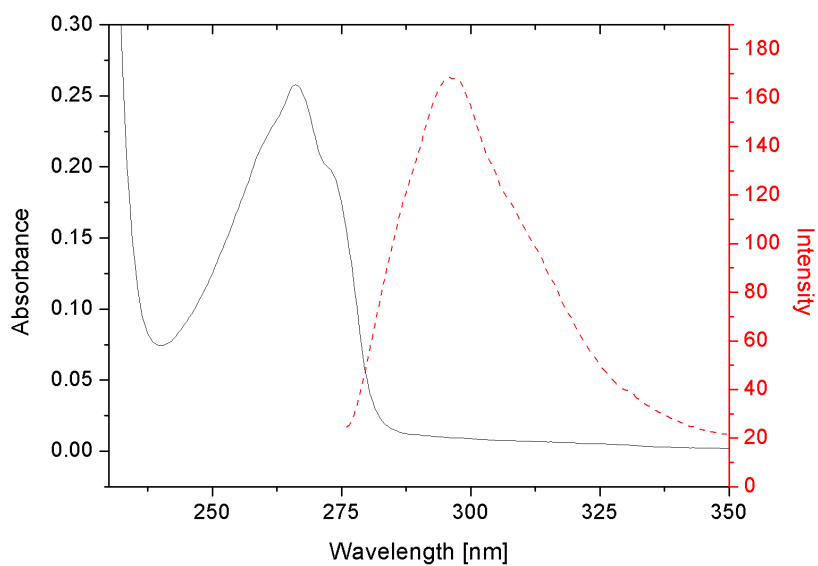


**Figure 7.17** Absorption (black) and emission (red) spectra of **1b** (pH=2.5,  $5 \times 10^{-3}$  M).

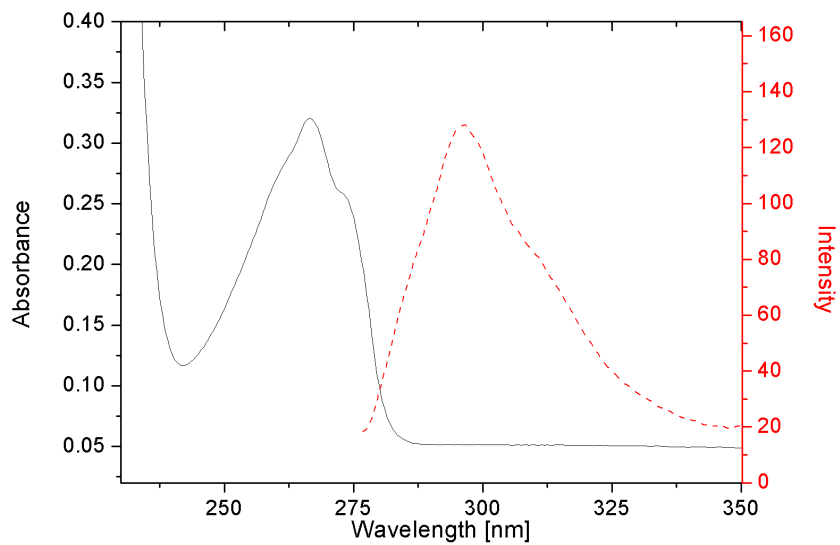


Figure 7.18 Absorption (black) and emission (red) spectra of **1b** (pH=7.2,  $5 \times 10^{-3}$  M).

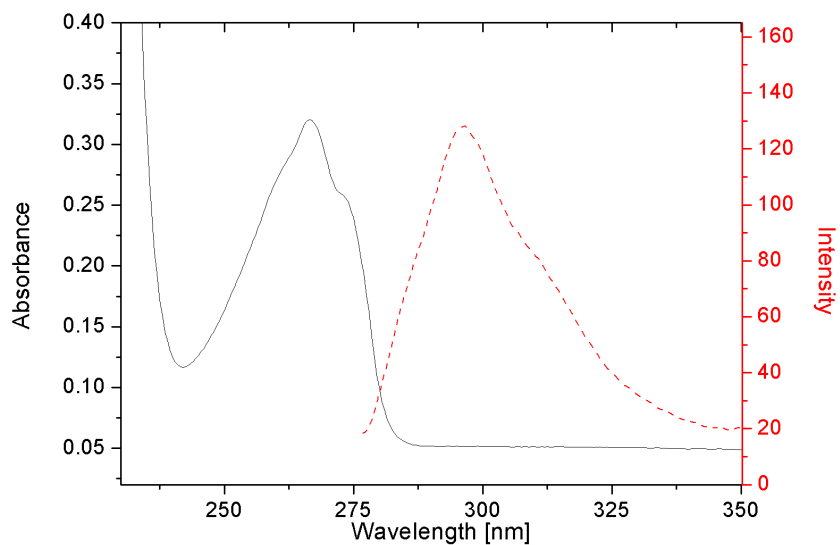
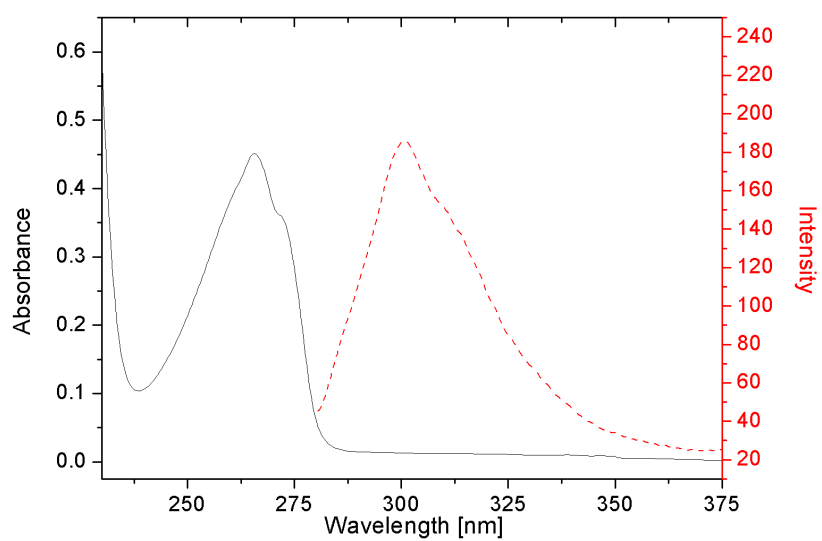
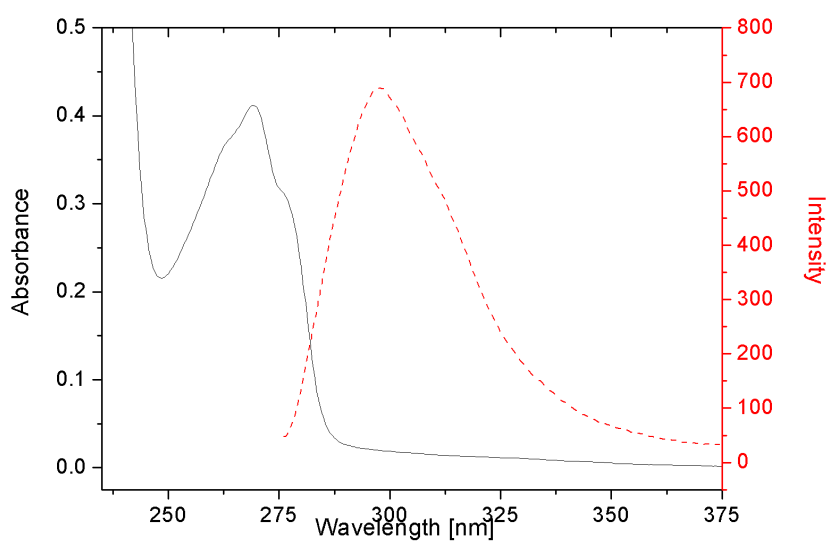


Figure 7.19 Absorption (black) and emission (red) spectra of **1b** (pH=11,  $5 \times 10^{-3}$  M).

## New Intermediates from Photogenerated Phenyl Cations



**Figure 7.20** Absorption (black) and emission (red) spectra of **1c** (pH=2.5,  $5 \times 10^{-3}$  M).



**Figure 7.21** Absorption (black) and emission (red) spectra of **1c** (pH=7.2,  $5 \times 10^{-3}$  M).

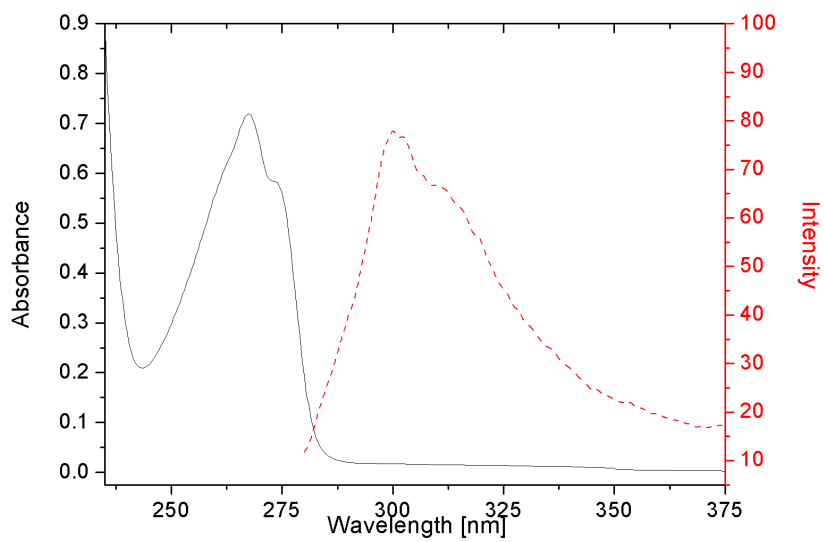


**Figure 7.22** Absorption (black) and emission (red) spectra of **1c** (pH=11,  $5 \times 10^{-3}$  M).

#### 7.2.4 Computational Details

All the calculations were carried out using the Gaussian 09 program package,<sup>[284]</sup> except where otherwise stated. In our investigation, the level of theory chosen for the optimization of all of the stationary points was CASSCF (Complete Active Space Self-Consistent Field) by using the standard 6-31G(d) basis set. This is a multiconfiguration method (MC-SCF), which makes use of all the configurations involving a set of molecular orbitals (MOs, the so-called “active space”) and a given number of electrons. Thus, this set of configurations is indicated as CASSCF( $n,m$ ), where  $n$  is the number of electrons and  $m$  is the number of MOs of the active space (both occupied and virtual). All the Potential Energy Surfaces were calculated using State-Specific CASSCF, apart from **11-2-a** that was computed with State-Averaged SA2-CASSCF(12,11)<sup>[300]</sup>. No symmetry constraint was applied to the structures investigated. Frequency calculations were performed in vacuo to check that minima had 0 imaginary frequencies. The occupancies of the orbitals included in the active space were carefully checked, and the values observed were always higher than 0.01 and lower than 1.99 for all of the stationary points reported, as recommended. Solvent effect was included by single-point calculations at the CPCM-CASSCF/6-31G(d) method (water bulk) on the optimized geometries obtained in vacuo.<sup>[288]</sup> The solvent cavity was calculated using the united atom topological model applied on radii optimized for the HF/6-31G(d) level of theory (RADII = UAHF option). Potential Energy Surfaces were constructed through constrained optimization, freezing the scanned coordinate (either C-Cl or C-P) at different bond lengths. Atomic charges have been calculated in solvent bulk according to the Merz-Singh-Kollman scheme,<sup>[286,287]</sup> via the POP = MK keyword and have been labelled in the text as “qESP”.

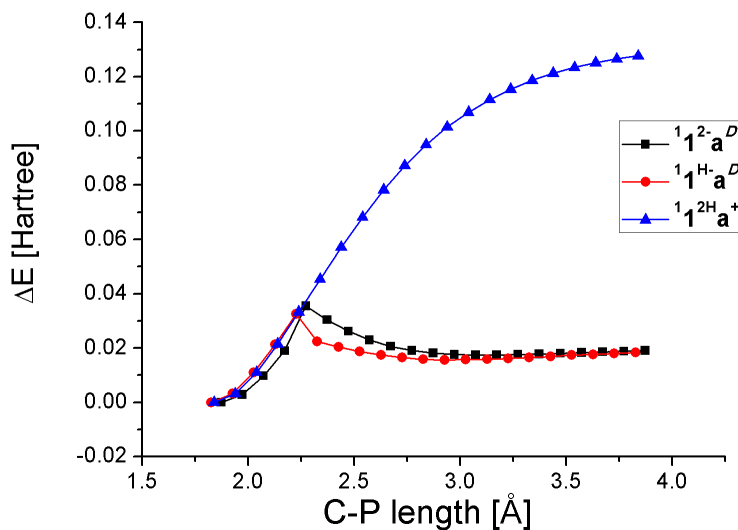


**Figure 7.23** Barriers for the detachment of the electrofugal group from the different protonated species  $1^{12}\text{H}_a^+$ ,  $1^{1\text{H}}\text{-a}^D$  and  $1^{12}\text{-a}^D$  in bulk water. Energies are reported as a difference between the value obtained at a different C–P length and the energy of the system at equilibrium, taken as a reference.

#### 7.2.4.1 Cartesian Coordinates for $1\text{a}$

$1^{12}\text{H}_a$				$3^{12}\text{H}_a$				$1^{12}\text{H}_a$			
C	-0.6072	1.0324	-0.6593	C	0.7032	1.1720	0.1050	C	-0.6138	1.1177	-0.6475
C	-1.9479	1.1547	-0.2977	C	1.9314	1.2466	-0.4734	C	-1.9924	1.2094	-0.2645
C	-2.6824	0.0052	-0.0220	C	2.7514	0.0195	-0.6011	C	-2.7215	0.0069	-0.0168
C	-2.1032	-1.2561	-0.0971	C	2.0395	-1.2754	-0.4834	C	-2.1103	-1.2783	-0.1335
C	-0.7597	-1.3635	-0.4594	C	0.8099	-1.3093	0.1001	C	-0.7317	-1.3568	-0.5155
C	0.0005	-0.2266	-0.7497	C	0.1259	-0.0992	0.4788	C	0.0242	-0.1639	-0.7863
H	-0.0325	1.9184	-0.8582	H	0.1157	2.0625	0.2375	H	-0.0472	2.0148	-0.8037
H	-2.4100	2.1209	-0.2305	H	2.3501	2.1826	-0.7912	H	-2.4715	2.1615	-0.1586
H	-2.6835	-2.1325	0.1198	H	2.5379	-2.1701	-0.8050	H	-2.6790	-2.1650	0.0613
H	-0.3089	-2.3380	-0.5157	H	0.3096	-2.2510	0.2415	H	-0.2614	-2.3176	-0.5988
Cl	-4.3955	0.1529	0.4367	Cl	4.3111	0.0805	0.3178	Cl	-4.4213	0.1108	0.4548
C	1.4578	-0.3505	-1.1389	C	-1.2296	-0.1555	1.1304	C	1.4763	-0.2500	-1.1696
H	1.7047	-1.3704	-1.4108	H	-1.3969	-1.1142	1.6087	H	1.7295	-1.2407	-1.5307
H	1.6899	0.2764	-1.9936	H	-1.3293	0.6085	1.8951	H	1.7158	0.4543	-1.9606
P	2.6006	0.1532	0.1971	P	-2.6071	0.1153	-0.0468	P	2.6143	0.1343	0.2139
O	4.0008	-0.2855	-0.4187	O	-3.8688	-0.1843	0.8762	O	4.0198	-0.2496	-0.4286
H	4.7359	0.1923	-0.0490	H	-4.6522	0.2762	0.5942	H	4.7477	0.2185	-0.0333
O	2.3429	-0.8986	1.3694	O	-2.5239	-1.1343	-1.0359	O	2.3402	-1.0153	1.2865
H	2.0605	-0.4737	2.1719	H	-2.4893	-0.8648	-1.9474	H	2.1044	-0.6587	2.1360
O	2.5371	1.5356	0.6533	O	-2.6594	1.3909	-0.7493	O	2.5558	1.4711	0.7909

### New Intermediates from Photogenerated Phenyl Cations

$1^{\text{H}}\text{-a}$			
C	0.2053	0.2436	-0.0693
C	0.1132	0.1250	1.3159
C	1.2525	-0.1980	2.0472
C	2.4765	-0.3943	1.4245
C	2.5497	-0.2733	0.0341
C	1.4250	0.0380	-0.7368
H	-0.6564	0.5261	-0.6442
H	-0.8220	0.2890	1.8182
H	3.3492	-0.6333	2.0036
H	3.4987	-0.4212	-0.4505
Cl	1.1387	-0.3607	3.8288
C	1.5055	0.1205	-2.2444
H	2.5369	0.0216	-2.5669
H	0.9515	-0.7077	-2.6800
P	0.8191	1.6968	-2.9923
O	1.0667	1.3387	-4.5833
H	0.2075	1.2204	-4.9654
O	1.6863	2.8215	-2.5993
O	-0.6559	1.6940	-2.8068

$3^{\text{H}}\text{-a}^{\text{ZCl}}$			
C	0.6081	-1.0405	0.0380
C	1.8503	-1.1884	0.5693
C	2.7555	-0.0259	0.6257
C	2.1346	1.3085	0.5069
C	0.8897	1.4124	-0.0402
C	0.1068	0.2552	-0.3710
H	-0.0657	-1.8747	-0.0235
H	2.2114	-2.1409	0.9113
H	2.7023	2.1725	0.7997
H	0.4487	2.3830	-0.1840
Cl	4.2755	-0.2203	-0.4268
C	-1.2442	0.3739	-1.0110
H	-1.4059	1.3846	-1.3709
H	-1.3098	-0.2943	-1.8665
P	-2.6580	-0.0646	0.1478
O	-3.9182	0.1690	-0.8882
H	-4.2812	-0.6883	-1.0655
O	-2.7025	0.9487	1.2168
O	-2.6059	-1.5275	0.3988

$3^{\text{H}}\text{-a}^{\text{DC[a]}}$			
C	0.0044	-0.0049	0.0011
C	0.0043	-0.0047	1.4013
C	1.2196	-0.0113	2.0664
C	2.4337	-0.0122	1.3931
C	2.4236	-0.0064	-0.0028
C	1.2100	-0.0109	-0.7086
H	-0.9308	-0.0079	-0.5354
H	-0.9216	-0.0090	1.9479
H	3.3495	-0.0325	1.9514
H	3.3531	-0.0044	-0.5476
C	1.2023	-0.0413	-2.2240
H	1.9939	-0.6757	-2.6121
H	0.2654	-0.4371	-2.6035
P	1.4438	1.5825	-3.0173
O	1.0679	1.2472	-4.5344
H	1.3596	1.9251	-5.1348
O	2.6907	2.3036	-2.8329
O	0.1814	2.5200	-2.5800
Cl	1.9942	-0.6612	4.7418
C	0.0044	-0.0049	0.0011

[a] Optimization conducted freezing the C–Cl bond to 2.86 Å

$1^{\text{H}}\text{-a}$			
C	0.1516	0.2128	-0.0815
C	0.0653	0.0918	1.3467
C	1.2509	-0.1974	2.0839
C	2.5172	-0.3588	1.4481
C	2.5861	-0.2384	0.0223
C	1.4090	0.0344	-0.7612
H	-0.7064	0.5070	-0.6524
H	-0.8637	0.2387	1.8609
H	3.3923	-0.5588	2.0345
H	3.5360	-0.3410	-0.4667
Cl	1.1521	-0.3647	3.8531
C	1.4753	0.1027	-2.2608
H	2.4977	-0.0340	-2.5983
H	0.8809	-0.7007	-2.6931
P	0.8359	1.7056	-3.0019
O	1.0815	1.3530	-4.5952
H	0.2209	1.2628	-4.9817
O	1.7329	2.8025	-2.5963
O	-0.6396	1.7435	-2.8253
C	0.1516	0.2128	-0.0815



Chapter 7: Experimental Section

<b>1<sup>2</sup>-a</b>			
C	0.2916	0.2596	-0.0348
C	0.1950	0.1739	1.3509
C	1.3153	-0.2020	2.0913
C	2.5253	-0.4795	1.4781
C	2.5994	-0.3931	0.0819
C	1.4981	-0.0373	-0.7069
H	-0.5305	0.5952	-0.6460
H	-0.7267	0.4089	1.8534
H	3.3840	-0.7569	2.0643
H	3.5397	-0.6091	-0.3977
Cl	1.1923	-0.3261	3.8924
C	1.5598	0.0074	-2.2131
H	2.6004	-0.0108	-2.5341
H	1.0907	-0.8966	-2.6023
P	0.6508	1.4812	-3.1020
O	0.9263	1.1633	-4.5530
O	1.3251	2.7132	-2.5472
O	-0.7904	1.2761	-2.6556
C	0.2916	0.2596	-0.0348

<b>1<sup>1</sup>2-a<sup>[a]</sup></b>			
C	0.2112	0.4086	-0.0263
C	0.1146	0.3229	1.3594
C	1.2350	-0.0530	2.0998
C	2.4450	-0.3305	1.4866
C	2.5190	-0.2441	0.0904
C	1.4177	0.1117	-0.6985
H	-0.6108	0.7442	-0.6376
H	-0.8071	0.5579	1.8619
H	3.3037	-0.6080	2.0728
H	3.4594	-0.4601	-0.3892
Cl	1.1119	-0.1772	3.9009
C	1.4794	0.1564	-2.2047
H	2.5201	0.1381	-2.5257
H	1.0104	-0.7477	-2.5939
P	0.5704	1.6302	-3.0936
O	0.8459	1.3122	-4.5446
O	1.2447	2.8622	-2.5387
O	-0.8707	1.4251	-2.6471
C	0.2112	0.4086	-0.0263

[a] Geometry Optimized at the SA2-CASSCF(12,11) level of theory

<b>3<sup>1</sup>2-aZC<sup>[a]</sup></b>			
C	0.0142	0.0481	-0.0054
C	0.0069	0.0172	1.3519
C	1.2783	-0.0400	2.0915
C	2.4925	0.3316	1.3371
C	2.4569	0.3254	-0.0267
C	1.2522	0.0851	-0.7695
H	-0.8899	0.1374	-0.5808
H	-0.9118	0.0280	1.9142
H	3.3926	0.5553	1.8845
H	3.3537	0.5429	-0.5826
Cl	1.4772	-1.4859	3.1621
C	1.2151	0.0002	-2.2443
H	2.2196	-0.0560	-2.6568
H	0.6643	-0.8825	-2.5635
P	0.2510	1.4862	-3.1364
O	0.4057	1.0912	-4.5838
O	1.0087	2.7113	-2.6919
O	-1.1403	1.3214	-2.5561
C	0.0142	0.0481	-0.0054

[a] Optimization conducted freezing the C-Cl bond to 1.87 Å

<b>3<sup>1</sup>2-aDC<sup>[a]</sup></b>			
C	0.1132	0.1467	0.0075
C	0.1232	-0.0021	1.3808
C	1.3388	-0.0137	2.1549
C	2.5390	0.0189	1.3651
C	2.5091	0.1624	-0.0121
C	1.3084	0.2426	-0.7540
H	-0.8299	0.2356	-0.5064
H	-0.8214	-0.0560	1.9047
H	3.4962	-0.0187	1.8676
H	3.4508	0.2441	-0.5403
Cl	1.3577	-1.1746	3.5451
C	1.3234	0.2703	-2.2697
H	2.3528	0.3187	-2.6182
H	0.9220	-0.6601	-2.6807
P	0.4283	1.5970	-3.2332
O	0.8933	1.5004	-4.6403
O	1.1252	3.0095	-2.6785
O	-1.0037	1.6574	-2.8650
C	0.1132	0.1467	0.0075

[a] Optimization conducted freezing the C-Cl bond to 1.86 Å

### New Intermediates from Photogenerated Phenyl Cations

$1^1\text{H}_a^+$			
C	-0.0342	-0.0142	0.0163
C	0.0073	-0.0204	1.4361
C	1.3090	0.0405	1.7276
C	2.5540	-0.0162	1.2546
C	2.3975	-0.0077	-0.1613
C	1.1351	-0.0154	-0.7713
H	-1.0053	0.0336	-0.4402
H	-0.8417	-0.0155	2.0890
H	3.4839	-0.0348	1.7858
H	3.2992	0.0001	-0.7444
C	1.0197	-0.0193	-2.2810
H	1.9943	-0.0784	-2.7478
H	0.4481	-0.8805	-2.6101
P	0.1434	1.4686	-2.9146
O	0.1396	1.2848	-4.4850
H	-0.7308	1.2688	-4.8725
O	1.2339	2.5809	-2.6343
H	0.9664	3.4777	-2.8160
O	-1.1716	1.6709	-2.3245

$3^1\text{H}_a^+$			
C	-0.0029	-0.0188	0.0007
C	-0.0023	-0.0060	1.3721
C	1.2549	0.0112	2.0065
C	2.5066	0.0246	1.3491
C	2.4886	0.0123	-0.0213
C	1.2400	-0.0222	-0.7226
H	-0.9220	-0.0032	-0.5524
H	-0.9097	-0.0019	1.9445
H	3.4209	0.0440	1.9106
H	3.4018	0.0269	-0.5849
C	1.2170	-0.0294	-2.2140
H	2.1826	-0.2770	-2.6339
H	0.4827	-0.7420	-2.5756
P	0.6770	1.6243	-2.8643
O	0.7682	1.4664	-4.4294
H	-0.0570	1.5939	-4.8903
O	1.9427	2.4794	-2.4603
H	1.8964	3.4153	-2.6408
O	-0.6130	2.0426	-2.3485

$1^1\text{H}_a^D$			
C	-0.0004	-0.0015	0.0005
C	-0.0001	-0.0015	1.3984
C	1.2278	-0.0002	2.0380
C	2.4450	0.0048	1.3814
C	2.4227	0.0063	-0.0179
C	1.2073	-0.0027	-0.7134
H	-0.9342	0.0103	-0.5325
H	-0.9218	-0.0013	1.9498
H	3.3751	0.0067	1.9188
H	3.3498	0.0133	-0.5635
C	1.1932	-0.0017	-2.2286
H	2.1632	-0.2755	-2.6297
H	0.4725	-0.7147	-2.6160
P	0.7330	1.6115	-2.9505
O	1.9658	2.5282	-2.5584
H	1.7870	3.4613	-2.6239
O	-0.5924	2.1388	-2.6846
O	0.9266	1.4065	-4.5574

$3^1\text{H}_a^D$			
C	0.1563	0.3080	-0.0659
C	0.0934	0.3483	1.3299
C	1.2405	0.0196	2.0320
C	2.4370	-0.3402	1.4391
C	2.4794	-0.3729	0.0407
C	1.3446	-0.0567	-0.7165
H	-0.7103	0.5689	-0.6465
H	-0.8140	0.6262	1.8330
H	3.3038	-0.5867	2.0237
H	3.3938	-0.6452	-0.4564
C	1.4000	-0.0958	-2.2302
H	2.2703	-0.6433	-2.5763
H	0.5255	-0.5879	-2.6437
P	1.4480	1.5602	-2.9988
O	2.8706	2.1034	-2.5569
H	2.9654	3.0470	-2.6436
O	0.3160	2.4481	-2.8095
O	1.6458	1.2610	-4.5902

Chapter 7: Experimental Section

	$1^2\text{-a}^D$		
C	-0.0001	-0.0001	0.0001
C	0.0000	-0.0003	1.4023
C	1.2262	-0.0002	2.0394
C	2.4385	0.0087	1.3663
C	2.4133	0.0114	-0.0309
C	1.1936	0.0011	-0.7333
H	-0.9401	0.0015	-0.5248
H	-0.9231	0.0010	1.9551
H	3.3734	0.0237	1.8981
H	3.3283	0.0597	-0.5900
C	1.1685	-0.0386	-2.2457
H	1.6066	-0.9713	-2.5951
H	0.1438	-0.0269	-2.6027
P	2.0885	1.3059	-3.1684
O	1.7043	1.1851	-4.5863
O	3.4762	1.3614	-2.6677
O	1.3379	2.6778	-2.6074

	$3^2\text{-a}^D$		
C	0.0001	0.0003	0.0000
C	0.0001	0.0003	1.4021
C	1.2263	-0.0001	2.0394
C	2.4386	0.0083	1.3663
C	2.4135	0.0109	-0.0309
C	1.1938	0.0010	-0.7334
H	-0.9399	0.0022	-0.5250
H	-0.9230	0.0021	1.9549
H	3.3735	0.0228	1.8981
H	3.3285	0.0586	-0.5900
C	1.1687	-0.0390	-2.2458
H	1.6065	-0.9719	-2.5950
H	0.1440	-0.0269	-2.6028
P	2.0891	1.3054	-3.1681
O	1.7052	1.1852	-4.5861
O	3.4768	1.3605	-2.6673
O	1.3383	2.6771	-2.6069

### 7.3 Experimental details relative to Chapter 4

Aromatics used in the experiments (furan, thiophene, 2-methyl thiophene, *N*-Boc Pyrrole, benzene and mesitylene) were commercially available and used as received, except for furan, which was freshly distilled before use. Compounds **3**, **9**, **10** and **11f** have been characterized by comparison with authentic samples, and their yields calculated by means of GC calibration curves. The reaction course was followed by means of TLC and HPLC analyses (C18 column, Eluent: MeOH/Water mixture).  $^1\text{H}$  and  $^{13}\text{C}$  NMR spectra were recorded on a 300 MHz spectrometer. The attributions were made on the basis of  $^1\text{H}$  and  $^{13}\text{C}$  NMR, as well as DEPT-135 experiments; chemical shifts are reported in ppm downfield from TMS. Ion chromatography analyses were performed by means of an instrument equipped with a conductimetric detector and an electrochemical suppressor by using the following eluant:  $\text{NaHCO}_3$  0.8 mM +  $\text{Na}_2\text{CO}_3$  4.5 mM, flux:  $1\text{ mL min}^{-1}$ ; current imposed at detector: 50 mA.

#### 7.3.1 General procedure for the synthesis of arylazo sulfones **1a–h**.

Diazonium salts were synthesized by following a known procedure<sup>[301]</sup> and purified by dissolving in acetone and precipitation by adding cold diethyl ether before use. For the synthesis of **1a–h** we adapted a procedure previously described.<sup>[140]</sup> To a cooled ( $0\text{ }^\circ\text{C}$ ) suspension of the appropriate diazonium salt (1 equiv., 0.3 M) in  $\text{CH}_2\text{Cl}_2$  sodium methanesulfinate (1 equiv. except where indicated) was added in one portion. The temperature was allowed to rise to room temperature and the solution stirred overnight. The resulting mixture was then filtered and the obtained solution evaporated. The raw solid was purified by dissolution in cold  $\text{CH}_2\text{Cl}_2$  and precipitation by adding *n*-hexane.

**4-Cyanophenylazo mesylate (1a).** From 840 mg (3.87 mmol) of 4-cyanobenzenediazonium tetrafluoroborate<sup>[302]</sup> and 395 mg (3.87 mmol) of sodium methanesulfinate in  $\text{CH}_2\text{Cl}_2$  (13 mL). Compound **1a** was obtained in 52% yield (421 mg, yellow crystalline solid, mp  $114.5\text{--}115.6\text{ }^\circ\text{C}$  dec.).  $^1\text{H}$  NMR (300 MHz,  $\text{CDCl}_3$ )  $\delta$ : 8.08–7.90 (AA'BB', 4H), 3.28 (s, 3H).  $^{13}\text{C}$  NMR (75 MHz,  $\text{CDCl}_3$ )  $\delta$ : 150.6, 133.6 (CH), 124.6 (CH), 118.0, 117.2, 34.9 ( $\text{CH}_3$ ). IR (KBr,  $\nu\text{ cm}^{-1}$ ): 2922, 2232, 1344, 1334, 1169, 1145, 957. Anal. Calcd. for  $\text{C}_8\text{H}_7\text{N}_3\text{O}_2\text{S}$ : C, 45.92; H, 3.37; N, 20.08. Found: C, 46.1; H, 3.1; N, 19.8.

**4-Acetylphenylazo mesylate (1b).** From 1 g (4.27 mmol) of 4-acetylbenzenediazonium tetrafluoroborate<sup>[303]</sup> and 436 mg (4.27 mmol) of sodium methanesulfinate in  $\text{CH}_2\text{Cl}_2$  (14 mL). Compound **1b** was obtained in 87% yield (840 mg, orange crystalline solid, mp

120.5-120.9 °C dec.). <sup>1</sup>H NMR (300 MHz, CDCl<sub>3</sub>) δ: 8.18–8.02 (AA'BB', 4H), 3.27 (s, 3H), 2.70 (s, 3H). <sup>13</sup>C NMR (75 MHz, CDCl<sub>3</sub>) δ: 196.6, 151.1, 141.4, 129.5 (CH), 124.4 (CH), 34.8 (CH<sub>3</sub>), 26.8 (CH<sub>3</sub>). IR (KBr, ν cm<sup>-1</sup>): 1688. Anal. Calcd. for C<sub>9</sub>H<sub>10</sub>N<sub>2</sub>O<sub>3</sub>S: C, 47.78; H, 4.45; N, 12.38. Found: C, 47.9; H, 4.4; N, 12.5.

**4-Chlorophenylazo mesylate (1c).** From 1.2 g (5.30 mmol) of 4-chlorobenzenediazonium tetrafluoroborate<sup>[147]</sup> and 541 mg (5.30 mmol) of sodium methanesulfinate in CH<sub>2</sub>Cl<sub>2</sub> (17.5 mL). Compound **1c** was obtained in 50% yield (577 mg, yellow solid, mp 120.1-120.4 °C dec.). <sup>1</sup>H NMR (300 MHz, CDCl<sub>3</sub>) δ: 7.92–7.55 (AA'BB', 4H), 3.22 (s, 3H). <sup>13</sup>C NMR (75 MHz, CDCl<sub>3</sub>) δ: 147.2, 141.7, 130.0 (CH), 125.7 (CH), 34.8 (CH<sub>3</sub>). IR (KBr, ν cm<sup>-1</sup>): 3052, 2950, 1489, 1345, 1265, 954. Anal. Calcd. for C<sub>7</sub>H<sub>7</sub>ClN<sub>2</sub>O<sub>2</sub>S: C, 38.45; H, 3.23; N, 12.81. Found: C, 38.4; H, 3.1; N, 12.7.

**Phenylazo mesylate (1d).** From 1.2 g (6.25 mmol) of benzenediazonium tetrafluoroborate<sup>[302]</sup> and 638 mg (6.25 mmol) of sodium methanesulfinate in CH<sub>2</sub>Cl<sub>2</sub> (21 mL). Compound **1d** was obtained in 55% yield (633 mg, orange solid, mp 72.7-73.1 °C dec.).<sup>[304]</sup> <sup>1</sup>H NMR (300 MHz, CDCl<sub>3</sub>) δ: 8.00-7.95 (m, 2H), 7.70-7.65 (m, 1H), 7.60-7.55 (m, 2H), 3.24 (s, 3H). <sup>13</sup>C NMR (75 MHz, CDCl<sub>3</sub>) δ: 148.9, 135.1 (CH), 129.6 (CH), 124.5 (CH), 34.6 (CH<sub>3</sub>). IR (KBr, ν cm<sup>-1</sup>): 3057, 1345, 1266, 1146, 905. Anal. Calcd. for C<sub>7</sub>H<sub>8</sub>N<sub>2</sub>O<sub>2</sub>S: C, 45.64; H, 4.38; N, 15.21. Found: C, 45.5; H, 4.2; N, 15.1.

**4-tert-Butylphenylazo mesylate (1e).** From 958 mg (3.99 mmol) of 4-tert-butylbenzenediazonium tetrafluoroborate<sup>[302]</sup> and 407 mg (3.99 mmol) of sodium methanesulfinate in CH<sub>2</sub>Cl<sub>2</sub> (13 mL). Compound **1e** was obtained in 40% yield (383 mg, orange needles, mp 70.3–71.0 °C dec.). <sup>1</sup>H NMR (300 MHz, CDCl<sub>3</sub>) δ: 7.92–7.59 (AA'BB', 4H), 3.22 (s, 3H), 1.39 (s, 9H). <sup>13</sup>C NMR (75 MHz, CDCl<sub>3</sub>) δ: 159.7, 146.9, 126.6 (CH), 124.4 (CH), 35.4, 34.6 (CH<sub>3</sub>), 30.9 (CH<sub>3</sub>). IR (KBr, ν cm<sup>-1</sup>): 3055, 2969, 1344, 1265, 1150, 955. Anal. Calcd. for C<sub>11</sub>H<sub>16</sub>N<sub>2</sub>O<sub>2</sub>S: C, 54.98; H, 6.71; N, 11.66. Found: C, 55.2; H, 6.5; N, 11.4.

**4-Methoxyphenylazo mesylate (1f).** From 890 mg (4.01 mmol) of 4-methoxybenzenediazonium tetrafluoroborate<sup>[305]</sup> and 409 mg (4.01 mmol) of sodium methanesulfinate in CH<sub>2</sub>Cl<sub>2</sub> (14 mL). Compound **1f**<sup>[141]</sup> was obtained in 44% yield (378 mg, yellow needles, mp 81.5-82.6 °C dec.). <sup>1</sup>H NMR (300 MHz, CDCl<sub>3</sub>) δ: 7.97–7.06 (AA'BB', 4H), 3.96 (s, 3H), 3.21 (s, 3H). <sup>13</sup>C NMR (75 MHz, CDCl<sub>3</sub>) δ: 165.6, 143.1, 127.3 (CH), 114.8 (CH), 55.8 (CH<sub>3</sub>), 34.8 (CH<sub>3</sub>). IR (KBr, ν cm<sup>-1</sup>): 3038, 2934, 1603, 1147, 1028. Anal. Calcd. for C<sub>8</sub>H<sub>10</sub>N<sub>2</sub>O<sub>3</sub>S: C, 44.85; H, 4.70; N, 13.08. Found: C, 44.7; H, 4.9; N, 13.3.

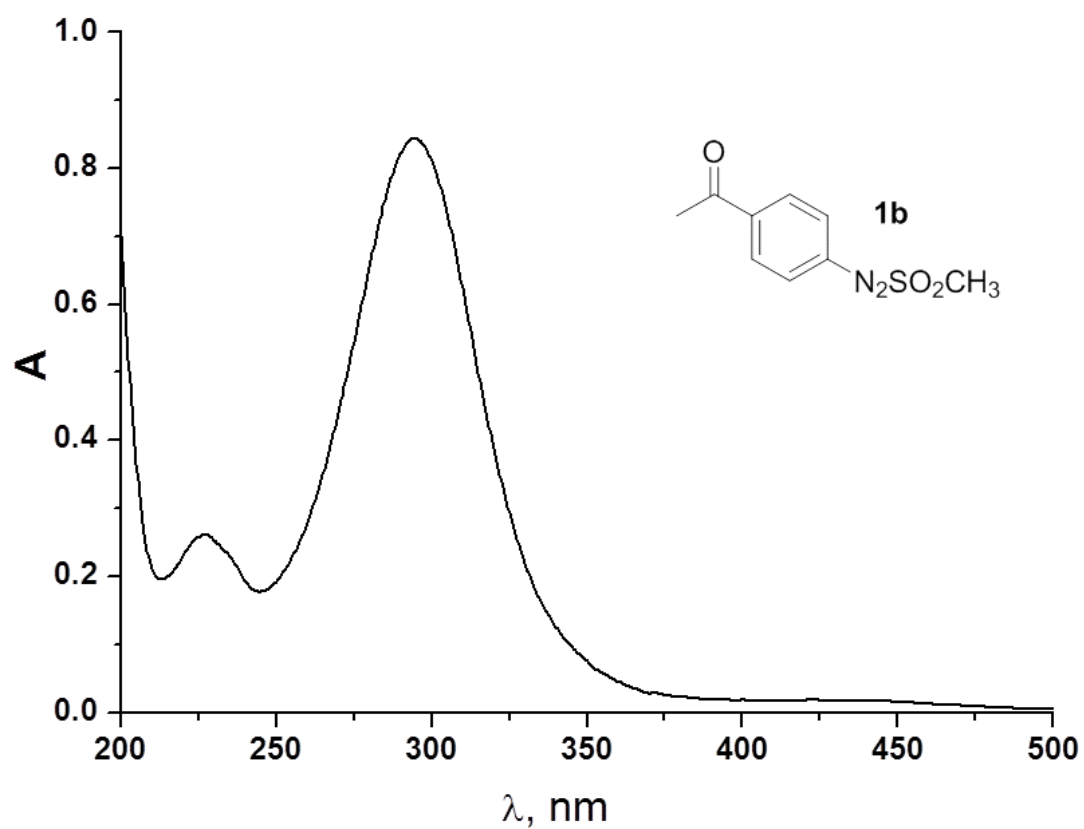
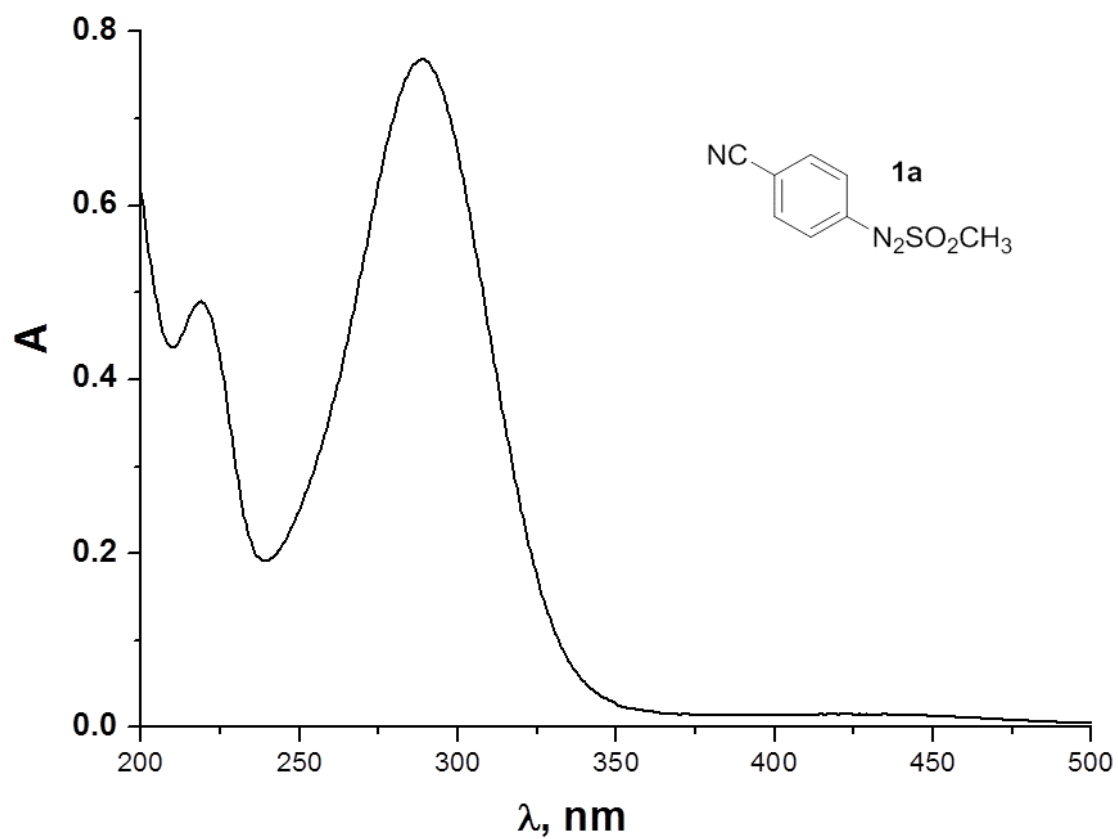
**3-Cyanophenylazo mesylate (1g).** From 960 mg (4.42 mmol) of 3-cyanobenzenediazonium tetrafluoroborate<sup>[306]</sup> and 496 mg (4.86 mmol, 1.1 equiv.) of sodium methanesulfinate in CH<sub>2</sub>Cl<sub>2</sub> (15 mL). Compound **1g** was obtained in 34% yield (314 mg, orange solid, mp 121.9–122.1 °C dec.). <sup>1</sup>H NMR (300 MHz, CDCl<sub>3</sub>) δ: 8.27 (s, 1H), 8.21 (dd, *J* = 7.9, 1.0 Hz, 1H), 7.97 (dd, *J* = 7.9, 1.0 Hz, 1H), 7.77 (t, *J* = 7.9 Hz, 1H), 3.28 (s, 3H). <sup>13</sup>C NMR (75 MHz, CDCl<sub>3</sub>) δ: 148.9, 137.5 (CH), 130.8 (CH), 128.2 (CH), 127.6 (CH), 116.9, 114.3, 34.9 (CH<sub>3</sub>). IR (KBr, ν cm<sup>-1</sup>) 3039, 2229, 1337, 1197, 965. Anal. Calcd. for C<sub>8</sub>H<sub>7</sub>N<sub>3</sub>O<sub>2</sub>S: C, 45.92; H, 3.37; N, 20.08. Found: C, 45.8; H, 3.4; N, 20.3.

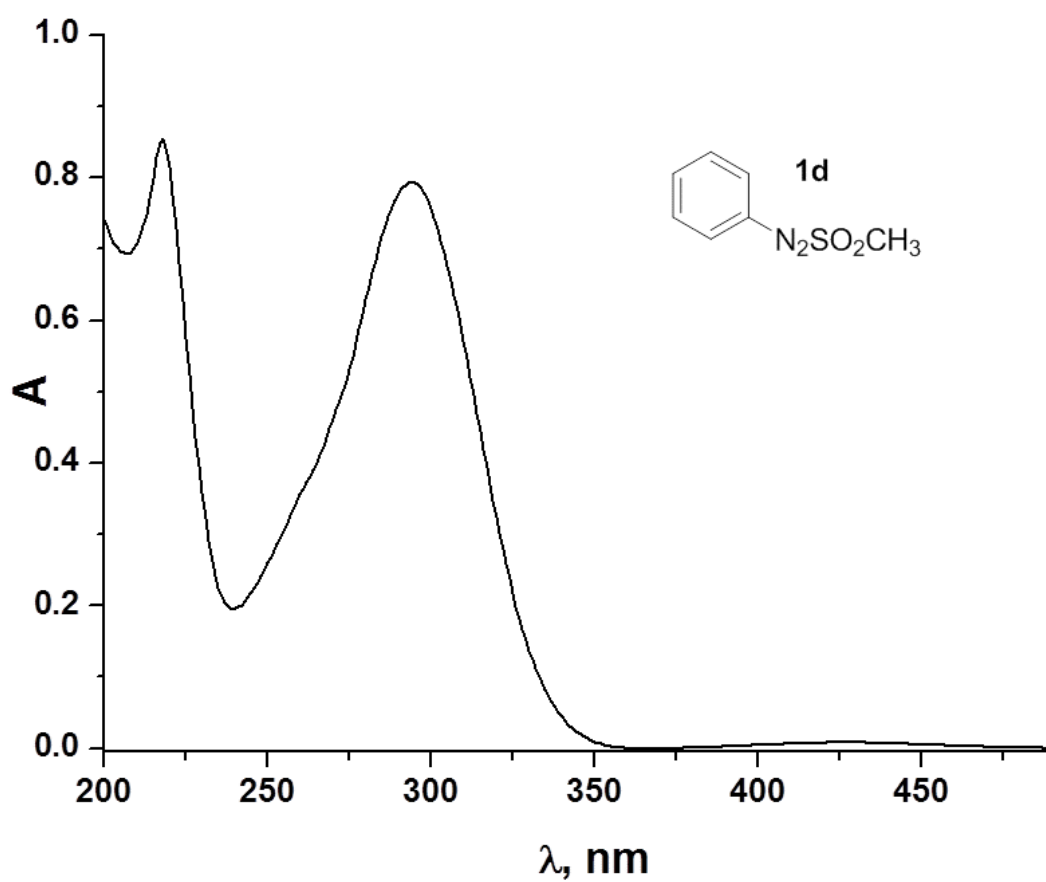
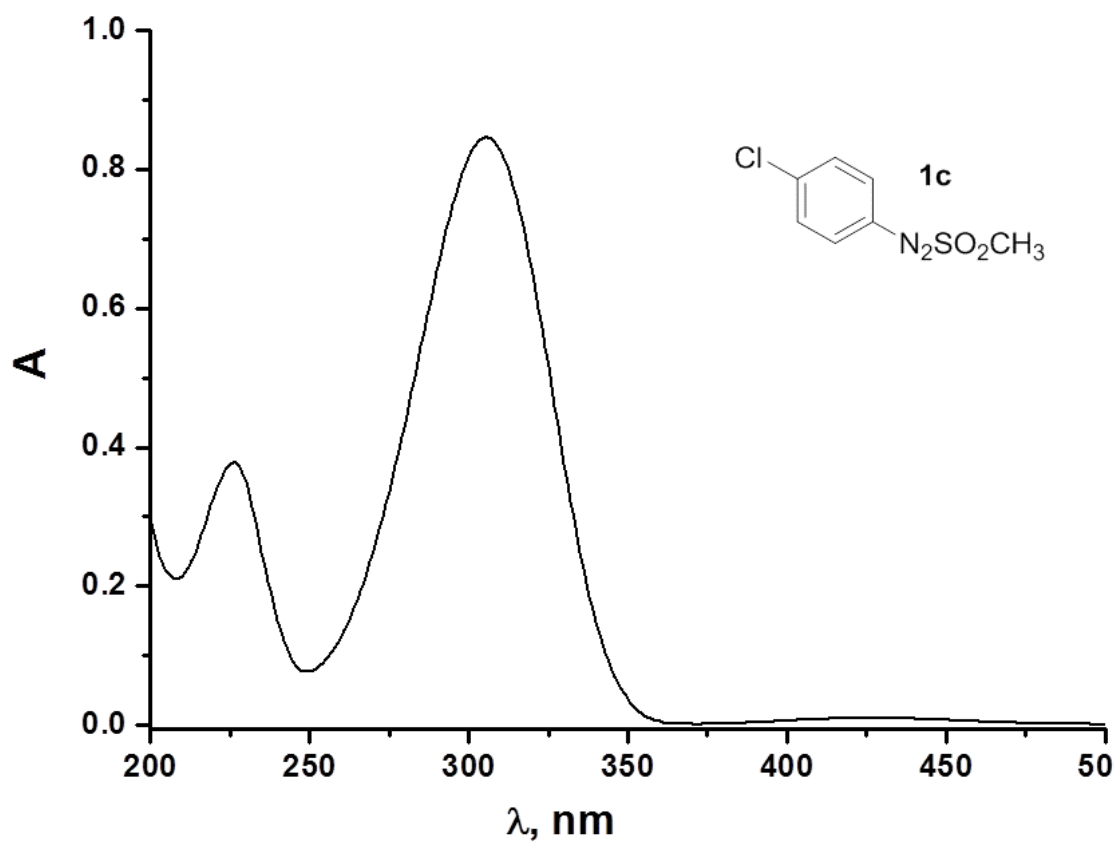
**2-Cyanophenylazo mesylate (1h).** From 1.56 g (7.19 mmol) of 2-cyanobenzenediazonium tetrafluoroborate<sup>[307]</sup> and 808 mg (7.91 mmol, 1.1 equiv.) of sodium methanesulfinate in CH<sub>2</sub>Cl<sub>2</sub> (24 mL). Compound **1h**<sup>[139]</sup> was obtained in 60% yield, (902 mg, orange solid, mp 117.7–118.4 °C dec.). <sup>1</sup>H NMR (300 MHz, CDCl<sub>3</sub>) δ: 8.02–7.92 (m, 2H), 7.87–7.79 (m, 2H), 3.31 (s, 3H). <sup>13</sup>C NMR (75 MHz, CDCl<sub>3</sub>) δ: 149.1, 135.0 (CH), 134.0 (CH), 133.8 (CH), 117.2 (CH), 115.9, 115.1, 34.5 (CH<sub>3</sub>). IR (KBr, ν cm<sup>-1</sup>) 3050, 2234, 1341, 1158, 963. Anal. Calcd. for C<sub>8</sub>H<sub>7</sub>N<sub>3</sub>O<sub>2</sub>S: C, 45.92; H, 3.37; N, 20.08. Found: C, 45.7; H, 3.6; N, 20.2.

### 7.3.2 Photophysical data of arylazo sulfones 1a-h

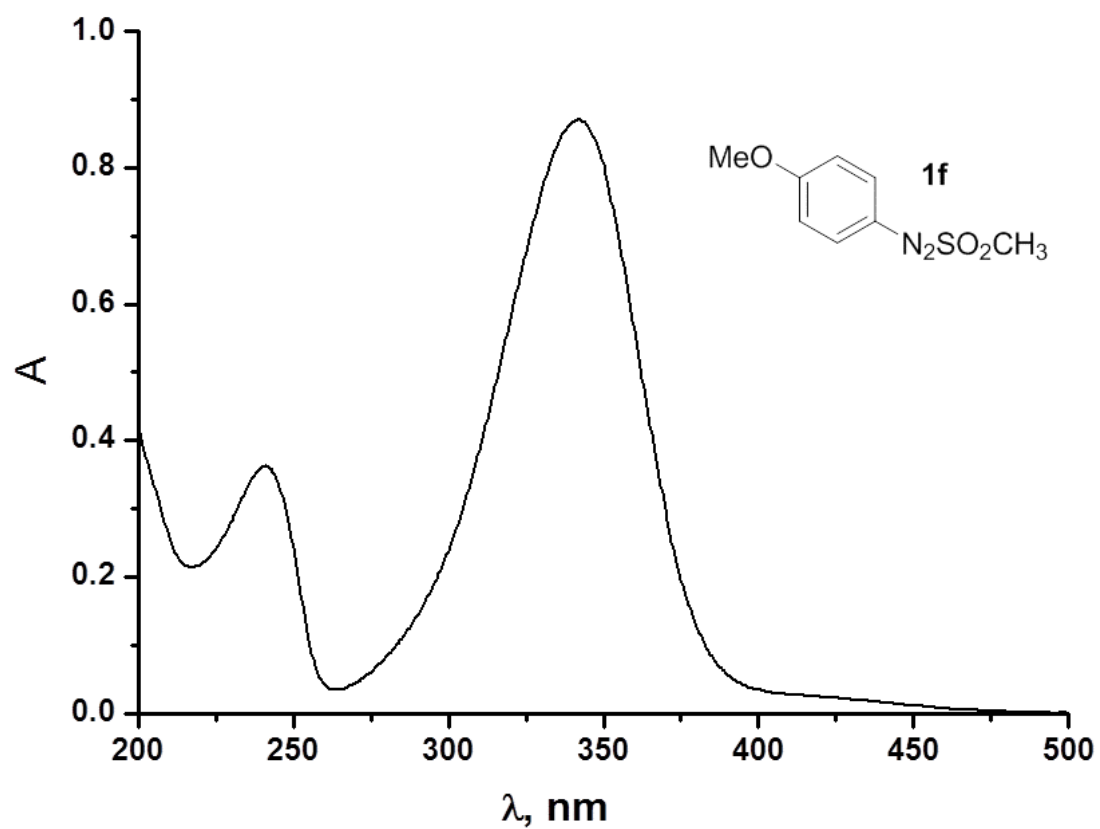
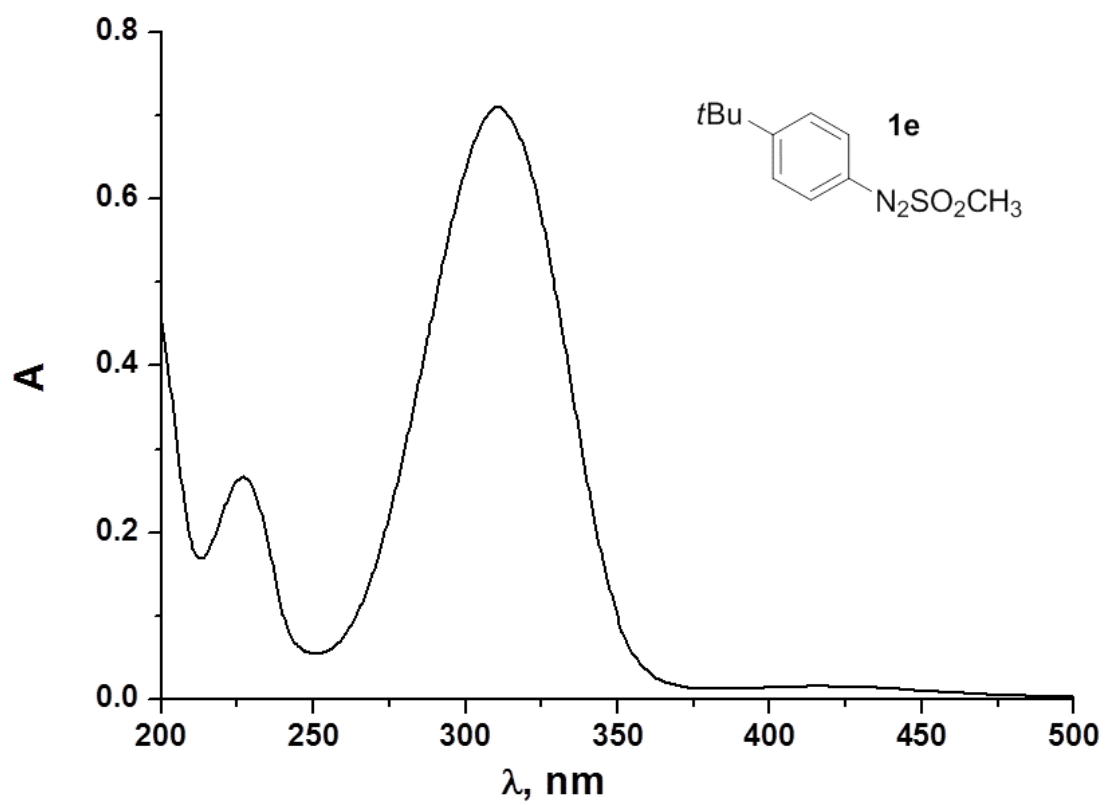
Table 7.4 Photophysical data of compounds 1a-h. <sup>[a]</sup>	
Compound	$\lambda_{\text{abs}}$ , nm ( $\epsilon$ , M <sup>-1</sup> cm <sup>-1</sup> )
<b>1a</b>	435 (155); 288.5 (15360)
<b>1b</b>	424 (215) 294 (16870)
<b>1c</b>	425 (170) 305 (17000)
<b>1d</b>	427 (135) 294 (14530)
<b>1e</b>	421.5 (255) 310.5 (14190)
<b>1f</b>	425 (230) 342 (17405)
<b>1g</b>	439 (160) 289 (17230)
<b>1h</b>	437 (95) 293 (10045)

[a] The  $\epsilon$  value related to the low intensity band in the visible was determined by using  $5 \times 10^{-4}$  M solutions of **1a-h** in neat acetonitrile, whereas  $5 \times 10^{-5}$  M solutions were used to determine the  $\epsilon$  value in the UV region.

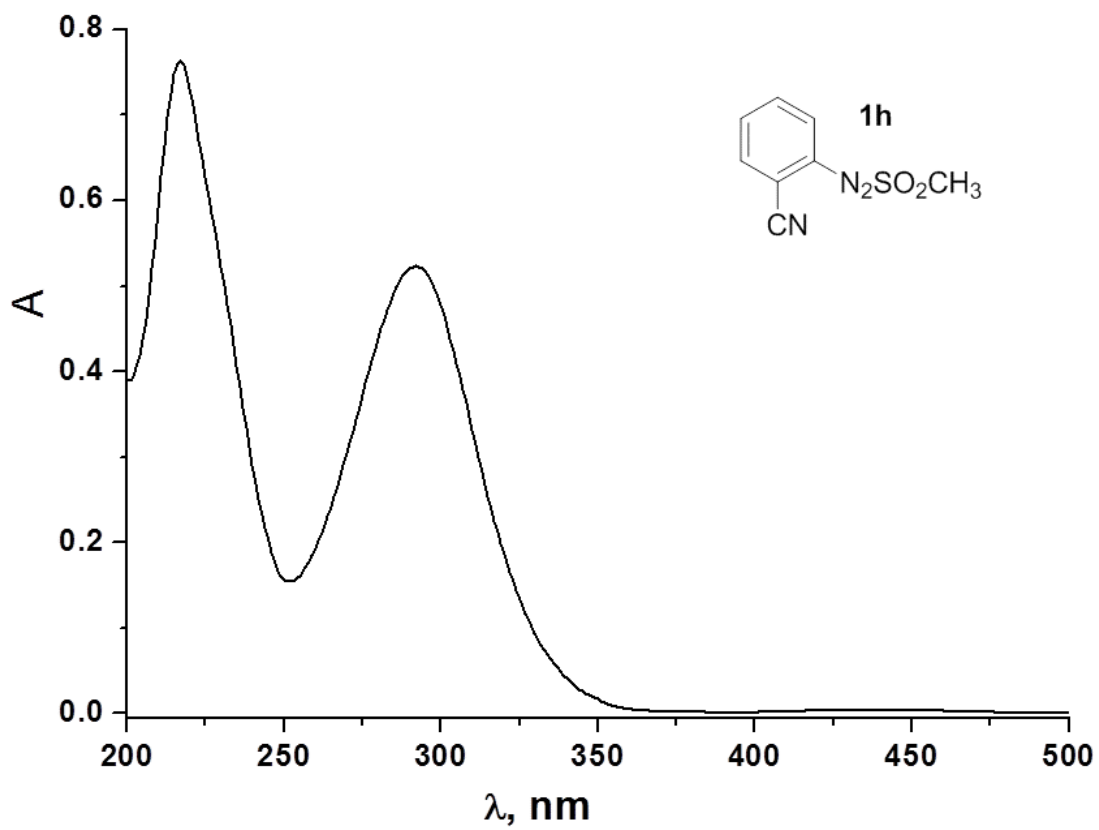
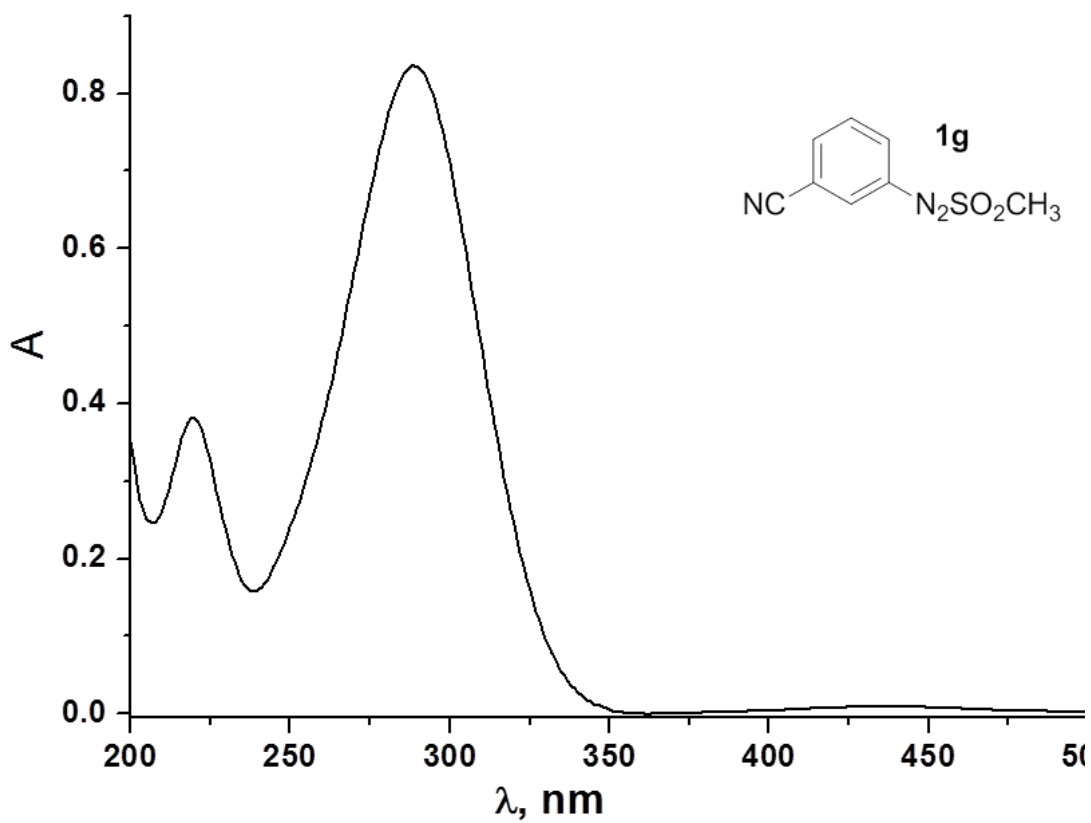
7.3.3 UV absorption spectra of compounds **1a–h** in MeCN ( $5 \times 10^{-5}$  M)







New Intermediates from Photogenerated Phenyl Cations



### 7.3.4 Optimization of the reaction conditions for the synthesis of 2a.

Preliminary experiments were carried out by using arylazosulfone 1a as the model compound. Thus, degassed solutions of the substrate (0.05 M) were irradiated in the presence of furan (2 M). Since the UV-Vis absorption spectra of arylazo sulfones significantly overlaps the short wavelength of the sunlight spectrum at the earth's surface, reactions were performed by using nitrogen-purged solutions in a Pyrex glass vessel (5 mL) sealed with a rubber septum reported in Figure S2 using a solar light simulator apparatus (Solarbox 1500e COFOMEGRA Xe lamp, conditions: 500 W/m<sup>2</sup> of irradiance, filter: IR + outdoor) as the light source. In some instances irradiations were carried out by means of a phosphor coated Hg lamp (15 W,  $\lambda = 366$  nm) or a LED (1 W,  $\lambda = 450$  nm).



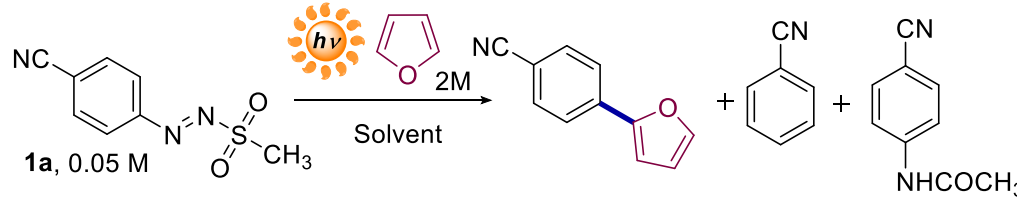
**Figure 7.24** Pyrex vessel containing a 0.05 M solution of **1a**.

The obtained results are summarized in Table 7.5. Two competing processes have been observed, namely arylation of furan to afford heterobiaryl 2a and reductive elimination of the azosulfone moiety to give benzonitrile 3a. Reduction to 3a was predominant in media such as dichloromethane and 1,4-dioxane (entries 1,2). The use of a 1,4-dioxane–water 9:1 mixture (entry 3) led to a slight improvement of the 2a/3a ratio. Higher amount of water (entry 4), however, made the arylation less clean. 2a was obtained in good yields in ethyl acetate, diethyl carbonate and acetone (entries 5-7), along with a significant amount of 3a. The use of an acetone–water 9:1 mixture did not show any substantial changes in the process. Protic media such as methanol, methanol/water mixture and 2,2,2-trifluoroethanol (TFE) (entries 9:12) led to unsatisfying results (in TFE, GC analyses also pointed out the formation of 4-fluorobenzonitrile in 12% yield). Irradiation of 1a in acetonitrile afforded discrete amount of 2a (46% yield, entry 13) along with 5% of 3a. However, when moving to acetonitrile/water 9:1 mixture (entry 14), arylation to 2a took place selectively (61% yield). A similar yield of 2a (56%, entry 15) was likewise observed

### New Intermediates from Photogenerated Phenyl Cations

when exposing the solution to natural sunlight (3 days, 8 hours a day insulation). As observed in the case of acetone, higher amounts of water (entry 16) led to a strong decrease in the 2a yield. These results encouraged us to consider an acetonitrile/water 9:1 mixture as the preferred reaction medium in the following experiments. Gratifyingly, when doubling the concentration of 1a (0.1 M), 2-arylfuran 2a was obtained in 78% yield (entry 17), along with a small amount of 4-cyanophenyl acetanilide 9a (6% yield). A decrease in the concentration of furan (1 M) still gave 2a in a satisfying amount (70% yield, entry 18).

**Table 7.5 Irradiation of 1a in the presence of furan.**



Entry	Solvent	2a (% yield)	3a (% yield)	9a (% Yield)
1	CH <sub>2</sub> Cl <sub>2</sub>	11	54	-
2	1,4-dioxane	38	43	-
3	1,4-dioxane-H <sub>2</sub> O 9:1	40	10	-
4	1,4-dioxane-H <sub>2</sub> O 5-1	44	32	-
5	CH <sub>3</sub> COOEt	63	11	-
6	Diethylcarbonate	68	9	-
7	Acetone	53	7	-
8	Acetone-H <sub>2</sub> O 9-1	39	7	-
9	MeOH	40	9	-
10	MeOH-H <sub>2</sub> O 9-1	29	9	-
11	MeOH-H <sub>2</sub> O 5-1	33	10	-
12	CF <sub>3</sub> CH <sub>2</sub> OH	18	15	- [a]
13	MeCN	46	9	-
14	MeCN-H <sub>2</sub> O 9-1	61	-	-
15	MeCN-H <sub>2</sub> O 5-1	28	7	-
16	MeCN-H <sub>2</sub> O 9-1 <sup>b</sup>	56	-	-
17	MeCN-H <sub>2</sub> O 9-1 <sup>c</sup>	78	-	9a, 6
18	MeCN-H <sub>2</sub> O 9-1 <sup>d</sup>	70	-	9a, 7

<sup>a</sup> 4-Fluorobenzonitrile formed in 12% yield. <sup>b</sup> Reaction carried out by exposing the reaction vessel under natural sunlight (3 days, 8 hours a day). <sup>c</sup> A 0.1 M solution of 1a in the presence of furan (2 M). <sup>d</sup> A 0.1 M solution of 1a in the presence of furan (1 M).

### 7.3.5 General Procedure for Solar Light Metal-free Arylations via Aryl Azosulfones.

A solution (5 mL) of the aryl azosulfone (**1**, 0.05-0.1 M), and the (hetero)aromatic (1-2 M) in MeCN-H<sub>2</sub>O 9:1 mixture was poured into a glass Pyrex vessel and purged for 10 min with nitrogen, capped and exposed to solar simulated light (in a Solarbox) or natural sunlight on a window ledge. In some cases, it was found convenient to use LEDs (450 nm, 1 W) or phosphor coated Hg lamps (366 nm ± 20 nm, 15 W) as light sources. After the completion of the reaction (as detected by HPLC analysis), the solvent was removed in vacuo from the photolyzed solution and the end products were isolated by column chromatography (stationary phase: silica gel chromatography; eluant: cyclohexane/ethyl acetate mixture).

Copy of the NMR spectra is reported in <sup>[4]</sup>.

**4-(Furan-2-yl)benzotrile (2a).** From 105 mg (0.50 mmol) of **1a** and 365 μL (5 mmol, 1 M) of furan in MeCN-H<sub>2</sub>O 9:1 (5 mL). Purification by column chromatography (eluant: cyclohexane/ethyl acetate from 95:5 to 9:1) afforded 59 mg of **2a** (colourless solid, 70% yield, mp 52.5-53.7 °C, lit.<sup>[308]</sup> 54-56 °C). A 56% yield of **2a** was obtained when exposing a 0.05 M solution of **1a** in the presence of furan (2 M) to natural sunlight for three days (8 hours a day). The spectroscopic data of **2a** were in accordance with literature.<sup>[165]</sup> Anal. Calcd. for C<sub>11</sub>H<sub>7</sub>NO: C, 78.09; H, 4.17; N, 8.28. Found: C, 78.1; H, 4.2; N, 8.0.

**2-(4-(Acetyl)phenyl)furan (2b).** From 113 mg of **1b** and 365 μL (0.50 mmol, 1 M) of furan in MeCN-H<sub>2</sub>O 9:1 (5 mL). Purification by column chromatography (eluant: cyclohexane/ethyl acetate from 99:1 to 9:1) afforded 58 mg of **2b** (colourless solid, 62% yield. mp 98.8-100.7 °C, lit.<sup>[309]</sup> 96-98 °C). Compound **2b** was obtained in 87% yield when irradiating a 0.05 M solution of **1a** in the presence of furan (2 M) in MeCN-H<sub>2</sub>O 9:1 (5 mL). The spectroscopic data of **2b** were in accordance with literature.<sup>[166]</sup> Anal. Calcd. for C<sub>12</sub>H<sub>10</sub>O<sub>2</sub>: C, 77.40; H, 5.41. Found: C, 77.1; H, 5.2

**2-(4-Chlorophenyl)furan (2c).** From 109 mg (0.50 mmol) of **1c** and 365 μL (5 mmol, 1 M) of furan in MeCN-H<sub>2</sub>O 9:1 (5 mL). Purification by column chromatography (eluant: cyclohexane/ethyl acetate from 99:1 to 9:1) afforded 84 mg of **2c** (94% yield colourless solid, mp 64.8-66.1 °C, lit.<sup>[308]</sup> 65-66 °C). The spectroscopic data of **2c** were in accordance with literature.<sup>[310]</sup> Anal. Calcd. for C<sub>10</sub>H<sub>7</sub>ClO: C, 67.24; H, 3.95. Found: C, 67.1; H, 4.1.

**2-Phenylfuran (2d).** From 92 mg (0.5 mmol, 0.1 M) of **1d** and 365 μL (5 mmol, 1 M) of furan in MeCN-H<sub>2</sub>O 9:1 (5 mL). Purification by column chromatography (eluant: cyclohexane/ethyl acetate 99:1) afforded 50.5 mg of **2d** (oil, 70% yield). The

spectroscopic data of **2d** were in accordance with literature.<sup>[311]</sup> Anal. Calcd. for C<sub>10</sub>H<sub>8</sub>O: C, 83.31; H, 5.59. Found: C, 83.1; H, 5.3.

**2-(4-(tert-Butyl)phenyl)furan (2e)**. From 60 mg (0.25 mmol, 0.05 M) of **1e** and 730 μL (10 mmol, 2 M) of furan in MeCN-H<sub>2</sub>O 9:1 (5 mL). Purification by column chromatography (eluant: cyclohexane/ethyl acetate from 99:1 to 9:1) afforded 35.5 mg of **2e** (oil, 71% yield). The spectroscopic data of **2e** were in accordance with literature.<sup>[312]</sup> Anal. Calcd. for C<sub>14</sub>H<sub>16</sub>O: C, 83.96; H, 8.05. Found: C, 84.0; H, 7.9.

**2-(4-methoxyphenyl)furan (2f)**. From 54 mg (0.25 mmol., 0.05 M) of **1f** and 730 μL (10 mmol, 2 M) of furan in MeCN-H<sub>2</sub>O 9:1 (5 mL). Purification by column chromatography (eluant: cyclohexane/ethyl acetate from 99:1 to 9:1) gave 42.8 mg of **2f** (pale grey solid, 96% yield, mp 48.6-49.0 °C, lit.<sup>[313]</sup> 49.7-51.2 °C). The spectroscopic data of **2f** were in accordance with literature.<sup>[314]</sup> Anal. Calcd. for C<sub>11</sub>H<sub>10</sub>O<sub>2</sub>: C, 75.84; H, 5.79. Found: C, 75.8; H, 5.4.

**3-(Furan-2-yl)benzotrile (2g)**. From 104 mg (0.5 mmol, 0.1M) of **1g** and 365 μL (5 mmol, 1 M) of furan in MeCN-H<sub>2</sub>O 9:1 (5 mL). Purification by column chromatography (eluant: cyclohexane/ethyl acetate 95:5) afforded 57.5 mg of **2g** (oil, 68% yield) The spectroscopic data of **2g** were in accordance with literature.<sup>[315]</sup> Anal. Calcd. for C<sub>11</sub>H<sub>7</sub>NO: C, 78.09; H, 4.17; N, 8.28. Found: C, 77.8; H, 4.3; N, 8.1.

**2-(Furan-2-yl)benzotrile (2h)**. From 104 mg of **1h**, and 365 μL (5 mmol, 1 M) of furan in MeCN-H<sub>2</sub>O 9:1 (5 mL). Purification by column chromatography (eluant: cyclohexane/acetate 95:5) gave 60 mg of **2i** (oil, 71% yield). The spectroscopic data of **2h** were in accordance with literature.<sup>[316]</sup> Anal. Calcd. for C<sub>11</sub>H<sub>7</sub>NO: C, 78.09; H, 4.17; N, 8.28. Found: C, 78.4; H, 4.5; N, 8.0.

**4-(Thiophen-2-yl)benzotrile (4a)**. From 52 mg (0.25 mmol, 0.05 M) of **1a** and 800 μL (10 mmol, 2 M) of thiophene in MeCN-H<sub>2</sub>O 9:1 (5 mL). Purification by column chromatography (eluant: cyclohexane/acetate from 99:1 to 9:1) afforded 34 mg of **4a** (pale yellow solid 74% yield, mp 88.9-89.3 °C, lit.<sup>[317]</sup> 88 °C). Compound **4a** was obtained in 68% yield when exposing the reaction vessel to natural sunlight for three days (8 hours a day). The spectroscopic data of **4a** were in accordance with literature.<sup>[318]</sup> Anal. Calcd. for C<sub>11</sub>H<sub>7</sub>NS: C, 71.32; H, 3.81; N, 7.56. Found: C, 71.4; H, 3.7; N, 7.3.

**2-(4-(Acetyl)phenyl)thiophene (4b)**. From 57 mg of **1b** (0.25 mmol, 0.05 M) and 800 μL (10 mmol, 2 M) of thiophene in MeCN-H<sub>2</sub>O 9:1 (5 mL). Purification by column chromatography (eluant: cyclohexane/acetate from 99:1 to 9:1) gave 38 mg of **4b** (colourless solid, 75% yield. mp 120.5-120.8 °C, lit.<sup>[319]</sup> 120-122 °C). The spectroscopic

data of **4b** were in accordance with literature.<sup>[320]</sup> Anal. Calcd. for C<sub>12</sub>H<sub>10</sub>OS: C, 71.25; H, 4.98. Found: C, 71.4; H, 5.1.

**2-(4-(tert-Butyl)phenyl)thiophene (4e)**. From 60 mg of **1e** (0.25 mmol, 0.05 M) and 800  $\mu$ L (10 mmol, 2 M) of thiophene in MeCN-H<sub>2</sub>O 9:1 (5 mL). Purification by column chromatography (eluant: cyclohexane/acetate from 99:1 to 9:1) afforded 37 mg of **4e** (oil, 69% yield). Compound **3e** was likewise formed in 27% yield as evaluated on the basis of GC calibration curves. The spectroscopic data of **4e** were in accordance with literature.<sup>[321]</sup> Anal. Calcd. for C<sub>14</sub>H<sub>16</sub>S: C, 77.72; H, 7.45. Found: C, 77.7; H, 7.3.

**2-(4-Methoxyphenyl)thiophene (4f)**. From 54 mg (0.25 mmol, 0.05 M) of **1f** and 800  $\mu$ L (10 mmol, 2 M) of thiophene in MeCN-H<sub>2</sub>O 9:1 (5 mL). Purification by column chromatography (eluant: cyclohexane/acetate from 99:1 to 9:1) afforded 27 mg of **4f** (pale yellow solid, 57% yield, mp 99.9-101.1 °C, lit.<sup>[322]</sup> 102-103 °C). Compound **3f** was likewise formed in 27% yield as evaluated on the basis of GC calibration curves. The spectroscopic data of **4f** were in accordance with literature.<sup>[323]</sup> Anal. Calcd. for C<sub>11</sub>H<sub>10</sub>OS: C, 69.44; H, 5.30. Found: C, 69.7; H, 5.2.

**4-(5-Methylthiophen-2-yl)benzotrile (5a)** and **4-(2-methylthiophen-3-yl)benzotrile (5'a)**. From 52 mg (0.25 mmol, 0.05 M) of **1a** and 995  $\mu$ L (10 mmol, 2 M) of 2-methylthiophene. Purification by column chromatography (eluant: cyclohexane/acetate 95:5) gave 36 mg of a mixture containing **5a**<sup>[324]</sup> and **5'a**<sup>[325]</sup> in a 3:1 ratio (72% overall yield). **5a (major isomer)**: <sup>1</sup>H NMR (from the mixture, 300 MHz, CDCl<sub>3</sub>)  $\delta$ : 7.64 (s, 4H), 7.19-7.16 (d, *J* = 5.3 Hz, 1H), 6.80-6.78 (m, 1H), 2.58 (s, 3H); <sup>13</sup>C NMR (from the mixture, 75 MHz, CDCl<sub>3</sub>)  $\delta$ : 142.1, 139.5, 138.8, 132.6 (CH), 126.7 (CH), 125.4 (CH), 125.0 (CH), 118.9, 109.8, 15.4 (CH<sub>3</sub>). **5'a (minor isomer)**: <sup>1</sup>H NMR (from the mixture, 300 MHz, CDCl<sub>3</sub>)  $\delta$ : 7.74–7.50 (AA'BB', 4H), 7.20–7.15 (d, *J* = 3 Hz, 1H), 7.10-7.05 (d, *J* = 3 Hz, 1H), 2.51 (s, 3H). <sup>13</sup>C NMR (from the mixture, 75 MHz, CDCl<sub>3</sub>)  $\delta$ : 147.9, 144.2, 136.6, 135.9, 132.1 (CH), 129.0 (CH), 128.4 (CH), 122.3 (CH), 109.9, 14.1 (CH<sub>3</sub>).

**2-(4-Cyano-phenyl)-pyrrole-1-carboxylic acid tert-butyl ester (6a)**. From 21 mg (0.1 mmol) of **1a** and 84  $\mu$ L (0.5 mmol, 0.5 M) of *N*-Boc-Pyrrole in MeCN-H<sub>2</sub>O 9:1 (1 mL). Purification by column chromatography (eluant: cyclohexane/acetate 9:1) gave 11.5 mg of **6a** (pale yellow solid, 43% yield, mp 98.2-98.5 °C, lit.<sup>[326]</sup> 110-112 °C). Compound **6a** was obtained in 59% yield exposing the reaction vessel to a 450 nm LED (1W) for 15 hours. The spectroscopic data of **6a** were in accordance with literature.<sup>[165]</sup> Anal. Calcd. for C<sub>16</sub>H<sub>16</sub>N<sub>2</sub>O<sub>2</sub>: C, 71.62; H, 6.01; N, 10.44. Found: C, 71.6; H, 6.1; N, 10.2.

**1,1'-Biphenyl-4-carbonitrile (7a).** From 52 mg of **1a** (0.25 mmol, 0.05 M), and 890  $\mu\text{L}$  (10 mmol, 2 M) of benzene in MeCN-H<sub>2</sub>O 9:1 (5 mL). Purification by column chromatography (eluant: cyclohexane/acetate from 99:1 to 9:1) gave 33 mg of **7a** (colourless solid, 74 % yield. mp 84.1-85.7 °C, lit.<sup>[327]</sup> 83-84 °C). Compound **3a** was likewise formed in 14% yield as evaluated on the basis of GC calibration curves. Compound **7a** was obtained in 70% yield when exposing the reaction vessel to natural sunlight for three days (8 hours a day). Compound **7a**, was isolated in 72% yield when carrying out the reaction in neat benzene. The spectroscopic data of **7a** were in accordance with literature.<sup>[328]</sup> Anal. Calcd. for C<sub>13</sub>H<sub>9</sub>N: C, 87.12; H, 5.06; N, 7.82. Found: C, 87.1; H, 5.1; N, 7.9.

**4-(Acetyl)-1,1'-biphenyl (7b).** From 57 mg of **1b** (0.25 mmol, 0.05 M) and 890  $\mu\text{L}$  (10 mmol, 2 M) of benzene in MeCN-H<sub>2</sub>O 9:1 (5 mL). Purification by column chromatography (eluant: cyclohexane/acetate 99:1) afforded 22.5 mg of **7b** (colourless solid, 46% yield. mp 117.7-118.2 °C, lit. 117-118 °C<sup>[329]</sup>). Compound **3b** was likewise formed in 43% yield as evaluated on the basis of GC calibration curves. Compound **7b** was found in 52% yield when carrying out the reaction in neat benzene. The spectroscopic data of **7b** were in accordance with literature.<sup>[330]</sup> Anal. Calcd. for C<sub>14</sub>H<sub>12</sub>O: C, 85.68; H, 6.16. Found: C, 85.7; H, 6.3

**4-(tert-Butyl)-1,1'-biphenyl (7e).** From 60 mg of **1e** (0.25 mmol, 0.05 M) and 890  $\mu\text{L}$  (10 mmol, 2 M) of benzene in MeCN-H<sub>2</sub>O 9:1 (5 mL). Purification by column chromatography (eluant: cyclohexane/acetate 99:1) gave 30.5 mg of **7e** (colourless solid, 58% yield, mp 45.1-46.7 °C, lit.<sup>[331]</sup> 48-49 °C). Compounds **3e** (21% yield) and **9e** (13% yield) were also determined on the basis of GC calibration curves. Compound **7e** was isolated in 53% yield when carrying out the reaction in neat benzene. The spectroscopic data of **7e** were in accordance with literature.<sup>[332]</sup> Anal. Calcd. for C<sub>16</sub>H<sub>18</sub>: C, 91.37; H, 8.63. Found: C, 91.5; H, 8.4

**4-methoxy-1,1'-biphenyl (7f).** From 54 mg of **1f** (0.25 mmol, 0.05 M) and 890  $\mu\text{L}$  (10 mmol, 2 M) of benzene in MeCN (5 mL). Purification by column chromatography (eluant: cyclohexane/acetate 99:1) afforded 32 mg of **7f** (colourless solid, 70% yield. mp 83.6-85.9 °C, lit.<sup>[333]</sup> 84-85 °C). Compound **3f** was likewise formed in 12% yield as evaluated on the basis of GC calibration curves. Compound **7f** was found in 51% yield when carrying out the reaction in neat benzene. The spectroscopic data of **7f** were in accordance with literature.<sup>[334]</sup> Anal. Calcd. for C<sub>13</sub>H<sub>12</sub>O: C, 84.75; H, 6.57. Found: C, 84.8; H, 6.4



**2',4',6'-Trimethyl-[1,1'-biphenyl]-4-carbonitrile (8a).** From 52 mg of **1a** (0.25 mmol, 0.05 M) and 1390  $\mu\text{L}$  (10 mmol, 2 M) of mesitylene in MeCN-H<sub>2</sub>O 9:1 (5 mL). Purification by column chromatography (eluant: cyclohexane/acetate 99:1) gave 31 mg of **8a** (colourless solid, 56% yield. mp 58.4–59.6 °C). Compound **8a** was likewise formed in 71% yield (as evaluated on the basis of GC calibration curves) by irradiating at 366 nm. The spectroscopic data of **8a** were in accordance with literature.<sup>[335]</sup> Anal. Calcd. for C<sub>16</sub>H<sub>15</sub>N: C, 86.84; H, 6.83; N, 6.33. Found: C, 86.9; H, 6.5; N, 6.6.

**1-(2',4',6'-Trimethyl-[1,1'-biphenyl]-4-yl)ethan-1-one (8b).** From 57 mg of **1b** (0.25 mmol, 0.05 M) and 1390  $\mu\text{L}$  (10 mmol, 2 M) of mesitylene in MeCN-H<sub>2</sub>O 9:1 (5 mL). Purification by column chromatography (eluant: cyclohexane/acetate 99:1) gave 19 mg of **8b** (colourless solid, 32 % yield. mp 96.3-96.8 °C, lit.<sup>[336]</sup> 95-96 °C). Compound **8b** was likewise formed in 73% yield (as evaluated on the basis of GC calibration curves) by irradiating at 366 nm. The spectroscopic data of **8b** were in accordance with literature.<sup>[337]</sup> Anal. Calcd. for C<sub>17</sub>H<sub>18</sub>O: C, 85.67; H, 7.61. Found: C, 85.7; H, 7.9.

## 7.4 Experimental details relative to Chapter 5

All the calculations herein performed were carried out using the Gaussian 09 Revision D01<sup>[284]</sup> and MOLCAS version v8.0.15-06-18<sup>[205]</sup> program packages. The procedure used for the calculations is CASSCF, a multiconfigurational *ab initio* method (MCSCF) which make use of all the configurations involving a set of molecular orbitals (MOs, the so-called active space) and a given number of electrons. Hence, this set of configurations is dubbed CASSCF( $n,m$ ) where  $n$  is the number of electrons and  $m$  the number of orbitals involved (both occupied and virtual).<sup>[338]</sup> In particular, the State-Averaged SA $x$  CASSCF calculation is applied, in which a single set of molecular orbitals is defined to compute all the  $x$  states that are averaged. The method has the advantage that all orbitals in SA-CASSCF are orthogonal to each other, allowing faster calculations, even though every state possesses its own set of optimized CI (Configuration Interaction) indices.<sup>[300]</sup>

Gaussian suite state average SA2-CASSCF(6,6)/6-31G(d) level of theory based on the 2 lower singlet roots was applied for stationary points and conical intersection optimization. No symmetry constraints were imposed to the structures investigated. Analytical frequency calculations to evaluate the transition states nature and Intrinsic Reaction Coordinate (IRC) optimizations were carried out at the SA2-CASSCF(6,6)/6-31G\* level of theory as implemented in the MOLCAS program. IRC analysis was performed from the transition state geometries following a 0.10 a.u. radius hypersphere. The energies of the two lower triplet states were calculated starting from the IRC geometries as single-point calculations at the SA2-CASSCF(6,6)/6-31G\* level.

A multistate second-order perturbation CASPT2 treatment (MS-CASPT2) was followed to account for dynamical correlation,<sup>[339,340]</sup> hence employing a MS-CASPT2//SA2-CASSCF(6,6)/6-31G\* approach.<sup>[341]</sup> The aforementioned method applies a perturbation on the energies of the CASSCF eigenvectors and afterward mixes the perturbed states, preventing artifacts near conical intersections (CoIn) or avoided crossing to arise, as observed by Serrano-Andres *et al.*<sup>[212]</sup> To avoid the intruder states (mostly Rydberg ones<sup>[342]</sup>) to cause singularities in the CASPT2 computed energies, an Imaginary Level Shift of 0.2 Hartree was introduced.<sup>[343]</sup>

The feasibility of an intersystem crossing was assessed using the RASSI program as coded in MOLCAS, using an equal number of singlet and triplet roots. The Atomic Natural Orbital<sup>[344]</sup> basis set was preferred to the segmented one,<sup>[345]</sup> due to the RASSI program is built for spherical type basis only. An esteem of the Spin Orbit Coupling between the states is furnished by plotting the absolute value of the Complex Spin Orbit-

Hamiltonian matrix elements over spin components of spin-free eigenstates (SFS), applying a print threshold of  $0.01 \text{ cm}^{-1}$ .

Constrained optimization calculations (thus imposing to zero the energy difference between the states of interest) were used to determine the Minimum Energy Crossing Point (MECP), using the SA2-CASSCF(6,6)/6-31G\* methodology implemented in MOLCAS.

DFT calculations were performed using GAUSSIAN. All the energies reported for the isodesmic equation were obtained by summing the electronic energy of the molecule with the ZVPE energy calculated after running a frequency analysis of the optimized molecule. The frequencies of all the optimized structures were inspected and none of them were found to possess imaginary values.

## 7.4.1 Cartesian coordinates of stationary points and conical intersections of compounds 1-10

1-S1				1-TS				1-CoIn			
C	-1.03350	-0.00001	-0.33595	C	1.02027	-0.00001	-0.30557	C	1.12632	-1.24545	-0.00739
C	-0.27785	0.95876	0.44793	C	0.29685	-1.08380	0.34032	C	1.12632	1.24545	-0.00739
C	1.14593	1.16291	0.16829	C	-1.14311	-1.17976	0.15207	C	-0.30582	-1.25110	-0.00341
C	1.88746	0.00000	-0.05515	C	-1.87284	-0.00001	-0.04350	C	-0.30582	1.25110	-0.00342
C	1.14592	-1.16293	0.16824	C	-1.14314	1.17972	0.15217	C	-0.99375	0.00000	0.00098
C	-0.27784	-0.95878	0.44793	C	0.29683	1.08378	0.34031	C	1.83386	0.00000	-0.00082
N	3.22766	-0.00002	-0.47801	N	-3.23390	-0.00007	-0.41410	H	1.66865	-2.17134	-0.03236
H	1.57518	2.14718	0.19194	H	-1.62013	-2.14192	0.20454	H	1.66865	2.17135	-0.03225
H	1.57517	-2.14720	0.19180	H	-1.62017	2.14186	0.20486	H	-0.85874	-2.16822	-0.00620
H	-0.79014	-1.58384	1.15729	H	0.80110	1.73881	1.02746	H	-0.85874	2.16822	-0.00619
H	-0.79016	1.58382	1.15727	H	0.80110	-1.73879	1.02752	Cl	-2.72831	0.00000	0.00707
H	3.72728	0.81542	-0.18950	H	-3.71957	-0.81312	-0.09503	N	3.22213	-0.00002	-0.06997

2-S1				2-TS				2-CoIn			
C	-0.87778	0.03089	0.00124	C	0.90286	0.05572	-0.32013	C	0.90772	0.05881	-0.33163
C	0.17855	-0.93311	0.00916	C	-0.13905	-0.71715	0.32600	C	-0.13602	-0.65911	0.37300
C	0.74642	1.89131	-0.00361	C	-0.85970	1.80480	0.01583	C	-0.87511	1.79887	0.00341
C	-0.60813	1.43364	-0.00768	C	0.44854	1.27090	0.34156	C	0.41514	1.22910	0.37728
H	0.95238	2.94361	-0.00391	H	-1.03653	2.86240	0.07417	H	-1.03148	2.86015	0.03555
H	-1.42340	2.12955	-0.01257	H	1.08015	1.75174	1.06677	H	1.03709	1.70117	1.11667
H	-0.04057	-1.98156	0.04394	H	0.10359	-1.47203	1.05382	H	0.11426	-1.39934	1.11342
Cl	-2.52329	-0.51838	-0.00258	Cl	2.56140	-0.44089	-0.11368	Cl	2.56686	-0.42984	-0.12688
C	1.81991	0.94347	0.00356	C	-1.86200	0.89049	-0.29216	C	-1.87576	0.88355	-0.30536
H	2.84001	1.27737	0.02531	H	-2.84038	1.18143	-0.62720	H	-2.84808	1.16609	-0.66452
C	1.53274	-0.45976	0.00070	C	-1.52753	-0.44583	-0.03054	C	-1.52925	-0.44228	-0.02545
N	2.57305	-1.37998	0.07662	N	-2.44507	-1.48504	-0.06329	N	-2.41497	-1.51243	-0.07761

3-S1				3-TS				3-CoIn			
C	2.39491	-0.20705	0.00316	C	2.39665	-0.25461	-0.31124	C	2.40485	-0.25901	-0.32115
C	1.62965	1.00179	-0.05786	C	1.62832	0.91454	-0.43305	C	1.63205	0.90448	-0.44971
C	1.72927	-1.46925	0.05778	C	1.73313	-1.31232	0.29229	C	1.72862	-1.30032	0.29116
C	0.19531	0.95119	-0.05529	C	0.22167	0.83418	-0.07054	C	0.23274	0.79480	-0.03662
C	-0.45517	-0.33077	-0.00627	C	-0.49721	-0.41262	-0.37108	C	-0.50858	-0.42138	-0.39934
C	0.30095	-1.54413	0.05283	C	0.30811	-1.10774	0.60058	C	0.31409	-1.01961	0.62461
H	2.30198	-2.37605	0.09976	H	2.20906	-2.24319	0.53881	H	2.16857	-2.25352	0.51655
H	-0.20615	-2.48654	0.09353	H	-0.13366	-1.52563	1.48724	H	-0.12702	-1.39516	1.53081
Cl	-2.19012	-0.43078	0.01180	Cl	-2.23998	-0.46315	-0.21112	Cl	-2.24674	-0.46730	-0.22112
H	3.46660	-0.16373	0.00282	H	3.42124	-0.30837	-0.62641	H	3.42298	-0.32637	-0.65421
H	2.11795	1.95444	-0.13558	H	2.03699	1.86949	-0.70444	H	2.01652	1.86010	-0.75022
N	-0.52887	2.12492	-0.18987	N	-0.40445	1.97471	0.41222	N	-0.39520	1.95204	0.43476

## Chapter 7: Experimental Section

4-S1				4-TS				4-CoIn			
C	-0.52955	-0.00278	0.06900	C	-0.57555	-0.00001	-0.32327	C	-0.58901	-0.00022	-0.33707
C	0.16644	1.24830	0.03206	C	0.19812	1.05091	0.31867	C	0.21759	0.97042	0.37978
C	1.59888	1.24051	-0.03794	C	1.61451	1.17644	-0.00315	C	1.61575	1.16595	-0.01489
C	2.31227	-0.00164	-0.06882	C	2.32319	0.00000	-0.26363	C	2.32787	-0.00006	-0.29711
C	1.60027	-1.24440	-0.03110	C	1.61449	-1.17646	-0.00319	C	1.61567	-1.16592	-0.01513
C	0.16779	-1.25331	0.03827	C	0.19812	-1.05089	0.31873	C	0.21780	-0.97006	0.38058
H	2.13270	2.17051	-0.06606	H	2.08330	2.14230	0.02364	H	2.05199	2.14654	-0.01210
H	2.13505	-2.17397	-0.05424	H	2.08330	-2.14232	0.02348	H	2.05151	-2.14670	-0.01341
H	-0.38106	-2.17285	0.06718	H	-0.26378	-1.70346	1.03683	H	-0.23912	-1.59993	1.12252
H	-0.38332	2.16733	0.05557	H	-0.26383	1.70364	1.03657	H	-0.24000	1.60063	1.12104
Cl	-2.26083	-0.00350	0.15329	Cl	-2.30764	-0.00001	-0.10714	Cl	-2.31783	-0.00005	-0.12668
H	3.38400	-0.00117	-0.11948	H	3.35359	-0.00002	-0.56414	H	3.34460	-0.00041	-0.64147
C	-0.52955	-0.00278	0.06900	C	-0.57555	-0.00001	-0.32327	C	-0.58901	-0.00022	-0.33707

**New Intermediates from Photogenerated Phenyl Cations**

5-S1				5-TS				5-CoIn			
C	1.13636	1.26026	0.00017	C	1.00364	-0.00011	-0.30354	C	1.01662	0.00012	-0.33002
C	1.14844	-1.23633	-0.00005	C	0.27215	-1.06356	0.36976	C	0.25447	-0.95712	0.45303
C	-0.29722	1.25824	-0.00014	C	-1.16677	-1.16982	0.16028	C	-1.16913	-1.15560	0.17031
C	-0.28264	-1.24971	0.00026	C	-1.87406	0.01340	-0.04700	C	-1.88789	0.01490	-0.05616
C	-0.98006	0.00095	0.00013	C	-1.15391	1.19534	0.14795	C	-1.15464	1.18144	0.15653
C	1.83497	0.01762	0.00023	C	0.28481	1.07298	0.36362	C	0.26700	0.96630	0.44838
H	1.69373	2.17514	0.00096	H	-1.64939	-2.12858	0.22715	H	-1.61250	-2.13326	0.21634
H	1.69815	-2.15905	-0.00211	H	-1.64038	2.15076	0.18784	H	-1.59710	2.15783	0.17005
H	-0.85509	2.17201	-0.00062	H	0.78814	1.71364	1.06415	H	0.77745	1.58623	1.16330
H	-0.82976	-2.17004	-0.00063	H	0.76897	-1.70476	1.07434	H	0.76041	-1.57899	1.16918
Cl	-2.71216	-0.01230	0.00000	Cl	2.74557	-0.01177	-0.20145	Cl	2.75530	-0.01200	-0.23668
O	3.18440	0.08351	-0.00092	O	-3.19732	0.08297	-0.35104	O	-3.19586	0.08228	-0.40600
H	3.56538	-0.78330	0.00614	H	-3.55859	-0.78408	-0.46705	H	-3.56014	-0.78633	-0.49970

6-S1				6-TS				6-CoIn			
C	0.87129	0.03303	0.00043	C	0.90041	0.05733	-0.32304	C	0.90535	0.05985	-0.33040
C	-0.16601	-0.95377	0.00023	C	-0.12973	-0.73103	0.33154	C	-0.12862	-0.68238	0.36876
C	-0.79788	1.86189	-0.00005	C	-0.90265	1.77073	0.00581	C	-0.91298	1.76497	-0.00462
C	0.57008	1.43233	0.00010	C	0.41215	1.24863	0.35378	C	0.38494	1.21142	0.38444
H	-1.02715	2.90910	0.00015	H	-1.09016	2.82693	0.04318	H	-1.08057	2.82459	0.00688
H	1.36860	2.14693	0.00009	H	1.02536	1.74312	1.08514	H	0.99001	1.69706	1.12898
H	0.05128	-2.00149	0.00069	H	0.10942	-1.49439	1.04822	H	0.11657	-1.43293	1.09740
Cl	2.52618	-0.47809	-0.00019	Cl	2.56718	-0.40250	-0.11613	Cl	2.57196	-0.39432	-0.12722
C	-1.85015	0.89219	-0.00013	C	-1.89238	0.83727	-0.29611	C	-1.90299	0.83241	-0.30652
H	-2.87872	1.20241	-0.00027	H	-2.87764	1.10812	-0.62950	H	-2.88282	1.09778	-0.65992
C	-1.51922	-0.49838	0.00002	C	-1.51492	-0.48106	-0.03204	C	-1.51661	-0.47739	-0.02944
O	-2.47136	-1.45743	-0.00002	O	-2.34930	-1.53741	0.02673	O	-2.32585	-1.55541	0.01793
H	-3.33701	-1.07377	-0.00091	H	-3.25197	-1.25327	-0.02627	H	-3.23426	-1.29320	-0.04754

7-S1				7-TS				7-CoIn			
C	2.39239	-0.06149	0.00009	C	2.39194	-0.23183	-0.30121	C	2.38644	-0.27467	-0.33945
C	1.56036	1.10170	0.00028	C	1.62150	0.93758	-0.36895	C	1.62745	0.89926	-0.44264
C	1.79735	-1.36341	0.00008	C	1.72186	-1.32779	0.23144	C	1.70195	-1.31517	0.26971
C	0.13625	0.95383	-0.00021	C	0.21245	0.82546	-0.03332	C	0.23723	0.78047	-0.01173
C	-0.45616	-0.35014	-0.00019	C	-0.52145	-0.38981	-0.38903	C	-0.53949	-0.39960	-0.39108
C	0.37316	-1.51949	-0.00021	C	0.29379	-1.15090	0.53522	C	0.29497	-1.02114	0.61633
H	2.42199	-2.23582	0.00036	H	2.20607	-2.26191	0.44675	H	2.13888	-2.26798	0.50075
H	-0.07856	-2.49031	-0.00048	H	-0.14921	-1.62283	1.39330	H	-0.14418	-1.40445	1.52041
Cl	-2.17311	-0.52679	0.00011	Cl	-2.24805	-0.42513	-0.19572	Cl	-2.26304	-0.41512	-0.22054
H	3.45965	0.04312	0.00043	H	3.42134	-0.26380	-0.60217	H	3.40162	-0.34989	-0.67917
H	1.99186	2.08546	-0.00166	H	2.03003	1.90429	-0.60024	H	2.01862	1.85466	-0.73812
O	-0.68568	2.02026	-0.00008	O	-0.46156	1.88885	0.44952	O	-0.41536	1.86205	0.47854
H	-0.18665	2.82485	0.00110	H	0.08051	2.38442	1.04850	H	0.12819	2.31334	1.11014

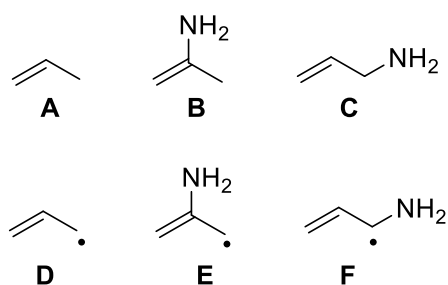
Chapter 7: Experimental Section

8-S1				8-TS				8-CoIn			
C	1.10884	-1.23188	-0.00022	C	1.03800	0.00001	-0.31226	C	-1.04645	-0.00004	-0.32760
C	1.10040	1.24294	-0.00022	C	0.31554	-1.05526	0.37925	C	-0.30269	0.96605	0.45866
C	-0.32601	-1.24649	-0.00006	C	-1.12231	-1.17118	0.18028	C	1.12441	1.15960	0.19272
C	-0.33166	1.24935	-0.00010	C	-1.86522	-0.00003	-0.02426	C	1.87419	0.00000	-0.02835
C	-1.02642	-0.00035	-0.00001	C	-1.12233	1.17114	0.18031	C	1.12441	-1.15962	0.19265
C	1.83538	0.00784	-0.00036	C	0.31554	1.05524	0.37927	C	-0.30267	-0.96600	0.45878
H	1.64336	-2.16310	-0.00040	H	-1.58818	-2.13718	0.25354	H	1.55673	2.14179	0.24054
H	1.62905	2.17706	-0.00008	H	-1.58821	2.13713	0.25354	H	1.55669	-2.14183	0.24043
H	-0.87168	-2.16836	0.00010	H	0.83114	1.71211	1.05577	H	-0.82284	-1.59572	1.15819
H	-0.88209	2.16840	-0.00005	H	0.83116	-1.71211	1.05578	H	-0.82294	1.59581	1.15797
Cl	-2.76027	-0.00438	0.00013	Cl	2.78241	0.00001	-0.21982	Cl	-2.78773	0.00000	-0.25891
C	3.33978	-0.00484	0.00037	C	-3.33264	0.00003	-0.36764	C	3.32905	0.00000	-0.41893
H	3.72884	-0.51544	0.87784	H	-3.82823	0.87657	0.03643	H	3.83679	-0.87733	-0.03254
H	3.72955	-0.52364	-0.87192	H	-3.49020	0.00117	-1.44230	H	3.44875	-0.00001	-1.49825
H	3.74566	1.00012	-0.00415	H	-3.82798	-0.87753	0.03452	H	3.83677	0.87736	-0.03256

9-S1				9-TS				9-CoIn			
C	0.89597	0.02221	0.00010	C	0.92029	0.04758	-0.32294	C	0.92656	0.05251	-0.33607
C	-0.19977	-0.90109	0.00005	C	-0.15060	-0.70822	0.30925	C	-0.14332	-0.62397	0.37658
C	-0.65755	1.93138	-0.00014	C	-0.78167	1.85088	0.00239	C	-0.80540	1.83879	-0.01513
C	0.68638	1.43650	-0.00002	C	0.52293	1.28778	0.32080	C	0.46675	1.22656	0.37762
H	-0.83261	2.98971	-0.00018	H	-0.92461	2.91486	0.03457	H	-0.91821	2.90616	-0.02018
H	1.52503	2.10324	0.00001	H	1.17140	1.76348	1.03371	H	1.09870	1.68747	1.11555
H	-0.00514	-1.95549	0.00020	H	0.08069	-1.47726	1.02450	H	0.09985	-1.36750	1.11536
Cl	2.51692	-0.59318	0.00015	Cl	2.56167	-0.50774	-0.10527	Cl	2.56962	-0.48879	-0.12577
C	-1.76100	1.02001	-0.00017	C	-1.82047	0.96034	-0.26917	C	-1.83937	0.94954	-0.29520
H	-2.76396	1.40299	-0.00028	H	-2.79590	1.29195	-0.57313	H	-2.80577	1.26698	-0.64098
C	-1.54885	-0.40167	-0.00007	C	-1.53952	-0.38977	-0.01418	C	-1.53989	-0.38708	-0.01100
C	-2.70032	-1.36991	-0.00010	C	-2.57646	-1.47712	0.00920	C	-2.53144	-1.51463	-0.00346
H	-2.67381	-2.01462	-0.87503	H	-2.40565	-2.20336	-0.78067	H	-2.29611	-2.25610	-0.76218
H	-2.67400	-2.01445	0.87497	H	-2.54770	-2.01574	0.95286	H	-2.52863	-2.02521	0.95639
H	-3.65233	-0.85181	-0.00025	H	-3.57364	-1.07126	-0.11433	H	-3.53668	-1.15274	-0.18596

10-S1				10-TS				10-CoIn			
C	2.39239	-0.06149	0.00009	C	2.40084	-0.21523	-0.32490	C	2.39425	-0.27735	-0.35565
C	1.56036	1.10170	0.00028	C	1.60595	0.93168	-0.44456	C	1.61824	0.87656	-0.51348
C	1.79735	-1.36341	0.00008	C	1.77367	-1.28980	0.30122	C	1.74283	-1.28737	0.33965
C	0.13625	0.95383	-0.00021	C	0.19887	0.83978	-0.06260	C	0.23027	0.79176	-0.04450
C	-0.45616	-0.35014	-0.00019	C	-0.47361	-0.42444	-0.36918	C	-0.49847	-0.43394	-0.37294
C	0.37316	-1.51949	-0.00021	C	0.34537	-1.15158	0.58143	C	0.33185	-1.01750	0.65775
H	2.42199	-2.23582	0.00036	H	2.29727	-2.17591	0.60793	H	2.21390	-2.19609	0.66300
H	-0.07856	-2.49031	-0.00048	H	-0.09204	-1.59265	1.45860	H	-0.10619	-1.36768	1.57566
Cl	-2.17311	-0.52679	0.00011	Cl	-2.21107	-0.54502	-0.22943	Cl	-2.23405	-0.52305	-0.24630
H	3.45965	0.04312	0.00043	H	3.43108	-0.23771	-0.62542	H	3.41058	-0.35265	-0.69331
H	1.99186	2.08546	-0.00166	H	2.01347	1.88575	-0.72556	H	2.01576	1.81440	-0.85474
C	-0.80386	2.17359	-0.00007	C	-0.51210	2.03505	0.51831	C	-0.43927	2.01445	0.53433
H	-1.41979	2.14927	-0.87467	H	-1.07024	2.55930	-0.25419	H	-0.85929	2.62599	-0.26102
H	-1.42240	2.14706	0.87263	H	-1.21976	1.74369	1.28360	H	-1.24751	1.74989	1.20243
H	-0.22257	3.07192	0.00194	H	0.19438	2.72992	0.95700	H	0.27333	2.61838	1.08411

## 7.4.2 Cartesian coordinates of the optimized geometries for the isodesmic reaction (A–F)



A			
C	-1.25374	-0.17041	0.00009
H	-1.32225	-1.25715	-0.00021
H	-2.19512	0.37258	0.00017
C	-0.08020	0.46293	0.00020
H	-0.07766	1.55298	0.00041
C	1.27163	-0.21460	0.00004
H	1.40139	-0.85354	-0.88226
H	2.08693	0.51532	-0.00038
H	1.40186	-0.85299	0.88267
C	-1.25374	-0.17041	0.00009
H	-1.32225	-1.25715	-0.00021

B			
C	0.04696	0.08135	0.00804
N	-1.35421	-0.01752	-0.01935
H	-1.72767	-0.77743	0.54000
H	-1.83196	0.85056	0.19780
C	0.70720	1.24962	-0.02867
H	0.18726	2.20444	-0.01921
H	1.78780	1.27684	-0.10587
C	0.74630	-1.25366	-0.00492
H	0.49627	-1.83955	0.89137
H	0.43558	-1.84644	-0.87429
H	1.83132	-1.13080	-0.03432
C	0.04696	0.08135	0.00804
N	-1.35421	-0.01752	-0.01935
H	-1.72767	-0.77743	0.54000

C			
C	0.54589	-0.35235	0.13619
H	0.42862	-1.38519	0.46349
C	-0.53498	0.39481	-0.12559
H	-0.39727	1.42671	-0.45436
N	1.88604	0.01766	-0.05283
H	2.01831	1.01789	-0.16576
H	2.51261	-0.33725	0.66168
C	-1.94867	-0.10424	-0.02613
H	-1.98046	-1.14053	0.33021
H	-2.54904	0.50335	0.66574
H	-2.46458	-0.07461	-0.99667
C	0.54589	-0.35235	0.13619
H	0.42862	-1.38519	0.46349
C	-0.53498	0.39481	-0.12559

D			
C	1.13940	1.21604	0.11820
H	0.07078	1.27215	0.30841
H	1.67149	2.15366	-0.00371
C	1.78980	-0.00525	0.03669
H	2.86307	0.00840	-0.15582
C	1.18224	-1.24277	0.18140
H	1.74702	-2.16608	0.10661
H	0.11605	-1.32607	0.37532
C	1.13940	1.21604	0.11820
H	0.07078	1.27215	0.30841
H	1.67149	2.15366	-0.00371

E			
C	1.83655	-0.01051	-0.01276
N	3.19338	-0.00127	-0.39964
H	3.68564	0.84373	-0.13408
H	3.70934	-0.81680	-0.09055
C	1.15424	1.19772	0.11872
H	0.09784	1.20705	0.35731
C	1.18899	-1.22915	0.18276
H	1.70656	-2.17710	0.07263
H	1.64460	2.15295	-0.04164
H	0.13307	-1.25615	0.42228
C	1.83655	-0.01051	-0.01276
N	3.19338	-0.00127	-0.39964
H	3.68564	0.84373	-0.13408

F			
C	1.12833	1.24886	0.02064
H	0.04475	1.32954	0.02432
C	1.13122	-1.18698	0.41796
H	1.69322	2.16228	-0.12663
H	0.04702	-1.25152	0.44971
C	1.76293	0.03348	0.20170
H	2.85531	0.02185	0.17671
N	1.79185	-2.41023	0.49054
H	2.78558	-2.35234	0.68481
H	1.34338	-3.11451	1.06452
C	1.12833	1.24886	0.02064
H	0.04475	1.32954	0.02432
C	1.13122	-1.18698	0.41796



To obtain a qualitative picture of the energies of the orbitals a simple Hartree Fock HF/6-31G\* calculation was performed for **1-5,8TS** and for **1-5,8** (Figure 7.25). The orbital energies show some interesting features. Notably, the different nature and position of the substituent on the aromatic ring doesn't affect greatly the energies of the orbitals in the **S1** minimum (in Figure 7.25 **1** only is shown for the sake of comparison). On the other hand, if we compare **1** and **1TS** it is shown there's a switch between the respective HOMO-HOMO-1 and LUMO-LUMO+1 pairs, if we proceed towards the TS along the reaction path. This aspect explains the presence of a barrier between the **S1** and the CoIn, that arises from the change in electronic configuration of the wavefunction on the excited state.<sup>[173]</sup>

A more interesting facet is derived from the analysis of the orbital energies in the transition state structures. The complete aromaticity loss and the formation of the allyl-tricyclic diradical structure of the prefulvenic conical intersection allows the substituents to impart a difference in the orbital distribution. In particular, if the unsubstituted **4TS** is taken as a reference, the interaction with the heteroatom raises the HOMO in the meta and ortho isomer of the parachloroaniline, due to full-full orbital interactions, while the HOMO of **1TS** remains almost unaffected due to the lone pair contribution is nullified by the presence of the nodal plane. Moreover, in the para derivative the HOMO-1 is greatly destabilized by the interaction with the heteroatom, while for meta and parachloroaniline this phenomenon is less dramatic, due to the minor orbital coefficients on the carbon bearing the nitrogen. Also, the unoccupied orbitals are slowly shifted due to orbital interactions with the heteroatom, however they're influenced by a lower extent than the occupied ones, due to the higher differences in energy between the N lone pair and the empty orbitals, compared to the filled ones.<sup>[6]</sup> In particular in the transition structure of para chloroaniline the LUMO is slightly higher in energy than in chlorobenzene TS.

The same reasoning could be extended to the case of phenol, while toluene, due to the minor perturbative effects furnished by the methyl group the orbital energies are not greatly influenced by substitution.

New Intermediates from Photogenerated Phenyl Cations

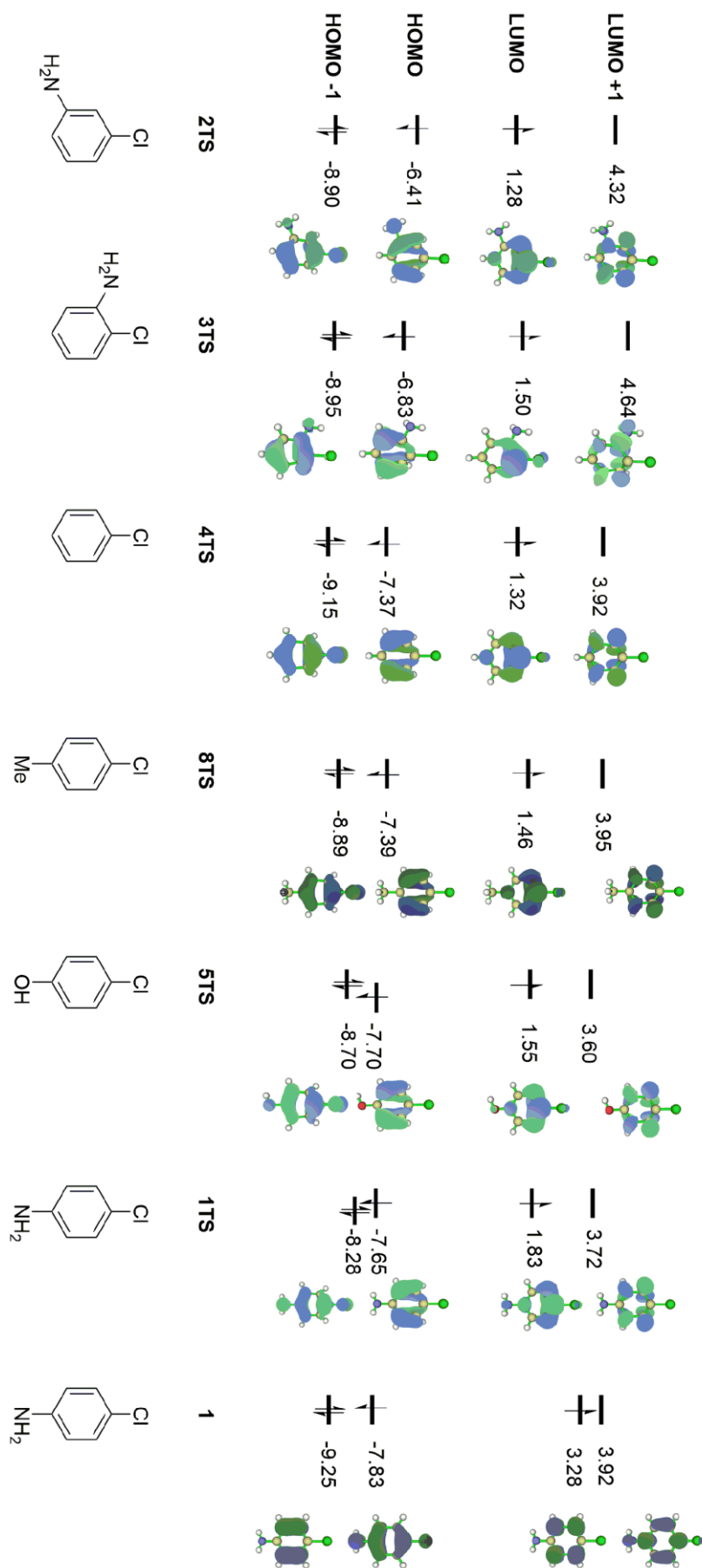


Figure 7.25 Frontier orbitals for 1-5,8TS and 1

## 7.5 Experimental details relative to Chapter 6

All NMR spectra were measured at room temperature using a Bruker Avance 300 (300 MHz for  $^1\text{H}$ , 75 MHz for  $^{13}\text{C}$ ) NMR spectrometer. All chemical shifts are reported in  $\delta$ -scale as parts per million [ppm] (multiplicity, coupling constant  $J$ , number of protons) relative to the solvent residual peaks as the internal standard. The spectra were analyzed by first order and coupling constants  $J$  are given in Hertz [Hz]. Abbreviations used for signal multiplicity:  $^1\text{H}$ -NMR: s = singlet, d = doublet, t = triplet, q = quartet, dd = doublet of doublets, ddd = doublet of doublet of doublets, dt = doublet of triplets, and tt = triplet of triplets. The mass spectrometrical measurements were performed at the CentralAnalytical Laboratory of the University of Regensburg. All mass spectra were recorded on a Finnigan MAT 95, ThermoQuest Finnigan TSQ 7000, Finnigan MAT SSQ 710 A or an Agilent Q-TOF 6540 UHD instrument. GC measurements were performed on a GC 7890 from Agilent Technologies. Data acquisition and evaluation was done with Agilent ChemStation Rev.C.01.04. GC/MS measurements were performed on a 7890A GC system from Agilent Technologies with an Agilent 5975 MSD Detector. Data acquisition and evaluation was done with MSD ChemStation E.02.02.1431.A capillary column HP-5MS/30 m x 0.25 mm/0.25  $\mu\text{M}$  film and helium as carrier gas (flow rate of 1 mL/min) were used. The injector temperature (split injection: 40:1 split) was 280  $^\circ\text{C}$ , detection temperature 300  $^\circ\text{C}$  (FID). GC measurements were made and investigated via integration of the signal obtained. The GC oven temperature program was adjusted as follows: initial temperature 40  $^\circ\text{C}$  was kept for 3 minutes, the temperature was increased at a rate of 15  $^\circ\text{C}/\text{min}$  over a period of 16 minutes until 280  $^\circ\text{C}$  was reached and kept for 5 minutes, the temperature was again increased at a rate of 25  $^\circ\text{C}/\text{min}$  over a period of 48 seconds until the final temperature (300  $^\circ\text{C}$ ) was reached and kept for 5 minutes. Purification by column chromatography was performed with silica gel 60 M (40-63  $\mu\text{m}$ , 230-440 mesh, Merck) on a Biotage<sup>®</sup> Isolera<sup>TM</sup> Spektra One device. For irradiation with blue light OSRAM Oslon SSL 80 LDCQ7P-1U3U (blue,  $\lambda_{\text{max}} = 455$ ,  $I_{\text{max}} = 1000$  mA, 1.12 W) was used.

### 7.5.1 Preparation of aryldiazonium tetrafluoroborates **1a–1d**

Compounds were prepared according a modification of a literature procedure.<sup>[346]</sup> In a mixture of 2 mL of EtOH and 5 mL of 50% hydrofluoroboric acid, 15 mmol of the appropriate aniline were dissolved, assisting at the precipitation of a thick salt. The reaction mixture was then cooled to 0 °C using an ice bath, consequently a solution of 20 mmol of sodium nitrite in distilled water (1.35 g in 2 mL, 1.5 eqv) was added dropwise in 5 minutes. The suspension was stirred for an additional 20 min at 0 °C and then the temperature was allowed to raise to RT, while the reaction was stirred for 30 minutes. The mixture was filtered and the recovered solid was washed with cold methanol, rinsed several times with diethyl ether and dried under vacuum.

### 7.5.2 Reaction time optimization

Reaction between **1a** (1equiv.) and **2** (3 equiv.) was screened at different reaction times, using [Ru(bpy)<sub>3</sub>]<sup>2+</sup> (2 mol%) as catalyst and dry MeCN as solvent. Best conversion was found after 2 hours of irradiation (Entry 5, Table 7.6)

Entry	Time [min]	<b>3</b> [%]
1	10	54
2	30	60
3	60	66
4	90	84
5	120	90
6	1440	89

### 7.5.3 Photocatalytic synthesis of isochromanones and isochromenones

In a 5 mL snap vial 0.25 mmol of the appropriate aryl diazonium tetrafluoroborate, 0.75 mmol (3 equiv.) of the olefin or aromatic, and 3.7 mg (0.02 equiv.) [Ru(bpy)<sub>3</sub>]Cl<sub>2</sub> were dissolved in 1 mL of dry MeCN with a stirring bar. The vial was sealed with a septum and degassed via the “freeze-pump-method” (3×). The reaction mixture was stirred at 23 °C and irradiated from the bottom side of the vial for 2 h using blue LEDs (455 nm). After the irradiation time the mixture was diluted with water and washed three times with diethyl ether. The combined organic layers were dried over Na<sub>2</sub>SO<sub>4</sub>, filtered, and concentrated in vacuum. The resulting crude product was further purified by column

chromatography using a petrol ether/ethyl acetate as an eluent. For GC analysis, the samples were taken directly after irradiation, 20  $\mu\text{L}$  of isochroman were added as internal standard, and the mixture submitted to GC without further purification.

**3-Phenylisochroman-1-one (3).** Colourless solid (48.2 mg, yield 86%), mp 89–90°C (lit. 90–91°C<sup>[347]</sup>). <sup>1</sup>H NMR (300 MHz, CDCl<sub>3</sub>)  $\delta$  8.16 (dd,  $J = 7.5, 1.5$  Hz, 1H), 7.57 (td,  $J = 7.5, 1.5$  Hz, 1H), 7.52 – 7.36 (m, 6H), 7.29 (d,  $J = 7.5$  Hz, 1H), 5.56 (dd,  $J = 12.0, 3.3$  Hz, 1H), 3.34 (dd,  $J = 16.5, 12.0$  Hz, 1H), 3.13 (dd,  $J = 16.5, 3.3$  Hz, 1H). <sup>13</sup>C NMR (75 MHz, CDCl<sub>3</sub>)  $\delta$  165.4, 139.0, 138.6, 134.0, 130.4, 128.7, 128.7, 127.9, 127.4, 126.1, 125.1, 80.0, 35.6. IR (neat, cm<sup>-1</sup>) 3071, 2922, 2855, 1715, 1603, 1457, 1267, 1222, 991, 909, 764, 693. HRMS (EI) calcd.  $m/z$  for C<sub>15</sub>H<sub>12</sub>O<sub>2</sub> [M<sup>+</sup>] 224.08318; found 224.08275. The spectroscopic data of **3** are in accordance with previous data reported in the literature.<sup>[347]</sup>

**8-Methyl-3-phenylisochroman-1-one (4).** Colourless solid (51.8 mg, yield 87%), mp 147–148 °C. <sup>1</sup>H NMR (300 MHz, CDCl<sub>3</sub>)  $\delta$  7.53 – 7.33 (m, 6H), 7.26 – 7.21 (m, 1H), 7.11 (d,  $J = 7.4$  Hz, 1H), 5.46 (dd,  $J = 12.0, 2.9$  Hz, 1H), 3.32 (dd,  $J = 16.2, 12.0$  Hz, 1H), 3.08 (dd,  $J = 16.2, 2.9$  Hz, 1H), 2.72 (s, 3H). <sup>13</sup>C NMR (75 MHz, CDCl<sub>3</sub>)  $\delta$  164.7, 143.1, 140.0, 138.6, 132.8, 131.3, 128.7, 128.6, 126.2, 125.2, 123.7, 79.3, 36.8, 22.3. IR (neat, cm<sup>-1</sup>) 3075, 3019, 2952, 2922, 2855, 1707, 1595, 1461, 1282, 1126, 1066, 753, 704. HRMS (EI) calcd.  $m/z$  for C<sub>16</sub>H<sub>14</sub>O<sub>2</sub> [M<sup>+</sup>] 238.09883; found 238.09805.

**5-Methyl-3-phenylisochroman-1-one (5).** Colourless solid (15.0 mg, yield 25%), mp 90–91°C. <sup>1</sup>H NMR (300 MHz, CDCl<sub>3</sub>)  $\delta$  8.08 – 7.96 (m, 1H), 7.56 – 7.30 (m, 8H), 5.52 (dd,  $J = 10.0, 5.4$  Hz, 1H), 3.25 – 3.04 (m, 2H), 2.33 (s, 3H). <sup>13</sup>C NMR (75 MHz, CDCl<sub>3</sub>)  $\delta$  165.8, 138.8, 137.6, 135.3, 135.2, 128.7, 128.7, 128.3, 127.3, 126.2, 125.1, 79.4, 32.9, 18.9. IR (neat, cm<sup>-1</sup>) 3067, 2963, 2922, 1707, 1595, 1469, 1245, 1107, 999, 741, 697. HRMS (EI) calcd.  $m/z$  for C<sub>16</sub>H<sub>14</sub>O<sub>2</sub> [M<sup>+</sup>] 238.09883; found 238.09821.

**7-Nitro-3-phenylisochroman-1-one (6).** Pale yellow solid (47.1 mg, yield 70%), mp 172–173 °C. <sup>1</sup>H NMR (300 MHz, CDCl<sub>3</sub>)  $\delta$  8.14 (dd,  $J = 7.7, 1.5$  Hz, 1H), 7.62 – 7.51 (m, 3H), 7.44 (tt,  $J = 7.7, 1.1$  Hz, 1H), 7.39 – 7.33 (m, 2H), 7.28 (d,  $J = 7.7$  Hz, 1H), 5.52 (dd,  $J = 11.9, 3.3$  Hz, 1H), 3.29 (dd,  $J = 16.4, 11.9$  Hz, 1H), 3.12 (dd,  $J = 16.4, 3.3$  Hz, 1H). <sup>13</sup>C NMR (75 MHz, CDCl<sub>3</sub>)  $\delta$  165.1, 138.6, 137.6, 134.1, 131.9, 130.5, 128.0, 127.8, 127.4, 125.0, 122.6, 79.2, 35.5. IR (neat, cm<sup>-1</sup>) 3082, 3037, 2926, 2855, 1726, 1614, 152, 1424, 1346, 1260, 1137, 1066, 998, 760, 693. HRMS (EI) calcd.  $m/z$  for C<sub>15</sub>H<sub>11</sub>NO<sub>4</sub> [M<sup>+</sup>] 269.06826; found 269.06724.

**3-(4-Methoxyphenyl)isochroman-1-one (7).** White solid (29.9 mg, yield 47%), mp 109–110°C. (lit. 108-109°C<sup>[348]</sup>). <sup>1</sup>H NMR (300 MHz, CDCl<sub>3</sub>) δ 8.14 (dd, *J* = 7.8, 1.3 Hz, 1H), 7.56 (td, *J* = 7.5, 1.5 Hz, 1H), 7.43 (d, *J* = 7.8 Hz, 1H), 7.40 (d, *J* = 8.6 Hz, 2H), 7.28 (d, *J* = 7.8 Hz, 1H), 6.93 (d, *J* = 8.8 Hz, 2H), 5.50 (dd, *J* = 12.0, 3.1 Hz, 1H), 3.82 (s, 3H), 3.34 (dd, *J* = 16.5, 12.1 Hz, 1H), 3.09 (dd, *J* = 16.5, 3.2 Hz, 1H). <sup>13</sup>C NMR (75 MHz, CDCl<sub>3</sub>) δ 165.5, 159.8, 139.1, 133.9, 130.6, 130.4, 127.8, 127.7, 127.4, 125.1, 114.0, 79.9, 55.4, 35.5. IR (neat, cm<sup>-1</sup>) 3071, 2959, 2926, 2855, 1707, 1606, 1513, 1457, 1245, 1025, 831, 734. HRMS (EI) calcd. *m/z* for C<sub>16</sub>H<sub>14</sub>O<sub>3</sub> [M<sup>+</sup>] 254.09375; found 254.09331.

The spectroscopic data of **7** are in accordance with previous data reported in the literature.<sup>[227]</sup>

**3-(4-Fluorophenyl)isochroman-1-one (8).** Pale yellow solid (47.8 mg, yield 79%), mp 84–85°C. <sup>1</sup>H NMR (300 MHz, CDCl<sub>3</sub>) δ 8.15 (dd, *J* = 7.8, 1.4 Hz, 1H), 7.58 (td, *J* = 7.5, 1.4 Hz, 1H), 7.52 – 7.39 (m, 3H), 7.29 (d, *J* = 7.6 Hz, 1H), 7.18 – 7.05 (m, 2H), 5.54 (dd, *J* = 12.1, 3.2 Hz, 1H), 3.32 (dd, *J* = 16.5, 12.1 Hz, 1H), 3.11 (dd, *J* = 16.4, 3.2 Hz, 1H). <sup>13</sup>C NMR (75 MHz, CDCl<sub>3</sub>) δ 165.2, 162.8 (d, *J* = 247.4 Hz), 138.7, 134.4, 134.0, 130.5, 128.1, 128.0, 127.4, 125.0, 115.7 (d, *J* = 21.6 Hz), 79.3, 35.6. IR (neat, cm<sup>-1</sup>) 3067, 3019, 2922, 2855, 1718, 1603, 1510, 1271, 1222, 1061, 831, 738. HRMS (EI) calcd. *m/z* for C<sub>15</sub>H<sub>11</sub>FO<sub>2</sub> [M<sup>+</sup>] 242.07376; found 242.07305. The spectroscopic data of **7** are in accordance with previous data reported in the literature.<sup>[349]</sup>

**3-(4-Chlorophenyl)isochroman-1-one (9).** White solid (14.9 mg, yield 23%), mp 82–83°C (lit. 81–83°C<sup>[227]</sup>). <sup>1</sup>H NMR (300 MHz, CDCl<sub>3</sub>) δ 8.14 (dd, *J* = 7.8, 1.5 Hz, 1H), 7.58 (td, *J* = 7.5, 1.5 Hz, 1H), 7.49 – 7.36 (m, 5H), 7.28 (d, *J* = 7.6 Hz, 1H), 5.54 (dd, *J* = 11.9, 3.3 Hz, 1H), 3.30 (dd, *J* = 16.4, 11.9 Hz, 1H), 3.12 (dd, *J* = 16.4, 3.3 Hz, 1H). <sup>13</sup>C NMR (75 MHz, CDCl<sub>3</sub>) δ 165.1, 138.6, 137.1, 134.5, 134.1, 130.5, 128.9, 128.0, 127.5, 127.4, 125.0, 79.2, 35.6. IR (neat, cm<sup>-1</sup>) 3067, 2918, 1722, 1603, 1413, 1271, 1114, 831, 746, 705. HRMS (EI) calcd. *m/z* for C<sub>15</sub>H<sub>11</sub>FO<sub>2</sub> [M<sup>+</sup>] 258.04421; found 258.04377. The spectroscopic data of **9** are in accordance with previous data reported in the literature.<sup>[227]</sup>

**3-(4-Bromophenyl)isochroman-1-one (10).** White solid (37.9 mg, yield 50%), mp 106–107 °C. <sup>1</sup>H NMR (300 MHz, CDCl<sub>3</sub>) δ 8.14 (dd, *J* = 7.8, 1.3 Hz, 1H), 7.62 – 7.51 (m, 3H), 7.49 – 7.40 (m, 1H), 7.39 – 7.33 (m, 2H), 7.28 (d, *J* = 7.5 Hz, 1H), 5.52 (dd, *J* = 11.8, 3.3 Hz, 1H), 3.28 (dd, *J* = 16.4, 11.9 Hz, 1H), 3.11 (dd, *J* = 16.5, 3.3 Hz, 1H). <sup>13</sup>C NMR (75 MHz, CDCl<sub>3</sub>) δ 165.1, 138.6, 137.6, 134.1, 131.9, 130.5, 128.0, 127.8, 127.4, 125.0, 122.6, 79.2, 35.5. IR (neat, cm<sup>-1</sup>) 3067, 2915, 1722, 1599, 1487, 1271, 1066, 1006, 839, 738, 693. HRMS (EI) calcd. *m/z* for C<sub>15</sub>H<sub>11</sub>BrO<sub>2</sub> [M<sup>+</sup>] 301.99220; found 301.99270.

**3-(4-Cyanophenyl)isochroman-1-one (11).** White solid (59.2 mg, yield 95%), mp 152–153 °C. <sup>1</sup>H NMR (300 MHz, CDCl<sub>3</sub>) δ 8.12 (dd, *J* = 7.8, 1.3 Hz, 1H), 7.74 – 7.58 (AA'BB', 4H), 7.57 (dd, *J* = 7.5, 1.4 Hz, 1H), 7.43 (tt, *J* = 7.6, 1.0 Hz, 1H), 7.29 (d, *J* = 7.6 Hz, 1H), 5.61 (dd, *J* = 11.4, 3.8 Hz, 1H), 3.27 (dd, *J* = 16.4, 11.5 Hz, 1H), 3.16 (dd, *J* = 16.4, 3.8 Hz, 1H). <sup>13</sup>C NMR (75 MHz, CDCl<sub>3</sub>) δ 164.7, 143.7, 138.2, 134.3, 132.6, 130.5, 128.2, 127.4, 126.7, 124.7, 118.4, 112.5, 78.8, 35.4. IR (neat, cm<sup>-1</sup>) 3056, 2930, 2229, 1707, 1607, 1458, 1274, 1062, 839, 749, 690. HRMS (EI) calcd. *m/z* for C<sub>16</sub>H<sub>11</sub>NO<sub>2</sub> [M<sup>+</sup>] 249.07843; found 249.07729.

**3-(4-Methylphenyl)isochroman-1-one (12).** White solid (45.3 mg, yield 76%), mp 96–97 °C (92–94 °C<sup>[S4]</sup>). <sup>1</sup>H NMR (300 MHz, CDCl<sub>3</sub>) δ 8.15 (dd, *J* = 7.8, 1.4 Hz, 1H), 7.57 (td, *J* = 7.5, 1.5 Hz, 1H), 7.42 (tt, *J* = 7.6, 1.1 Hz, 1H), 7.39 – 7.19 (AA'BB', 4H), 7.28 (d, *J* = 7.8 Hz, 1H), 5.51 (dd, *J* = 12.0, 3.3 Hz, 1H), 3.33 (dd, *J* = 16.5, 12.0 Hz, 1H), 3.10 (dd, *J* = 16.5, 3.3 Hz, 1H), 2.37 (s, 3H). <sup>13</sup>C NMR (75 MHz, CDCl<sub>3</sub>) δ 165.5, 139.1, 138.5, 135.6, 133.9, 130.4, 129.3, 127.8, 127.4, 126.1, 125.2, 80.0, 35.6, 21.2. IR (neat, cm<sup>-1</sup>) 3034, 2918, 1718, 1606, 1461, 1267, 1118, 812, 738, 689. HRMS (EI) calcd. *m/z* for C<sub>16</sub>H<sub>14</sub>O<sub>2</sub> [M<sup>+</sup>] 238.09883; found 238.09868.

**3-Methyl-3-phenylisochroman-1-one (13).** White solid (45.9 mg, yield 77%), mp 50–52 °C <sup>1</sup>H NMR (300 MHz, CDCl<sub>3</sub>) δ 8.01 (dd, *J* = 7.6, 1.3 Hz, 1H), 7.50 – 7.39 (m, 3H), 7.32 – 7.15 (m, 5H), 3.52 (d, *J* = 16.4 Hz, 1H), 3.40 (d, *J* = 16.3 Hz, 1H), 1.75 (s, 3H). <sup>13</sup>C NMR (75 MHz, CDCl<sub>3</sub>) δ 165.3, 143.6, 137.9, 133.9, 130.0, 128.5, 127.7, 127.6, 127.5, 125.2, 124.7, 83.7, 39.1, 30.2. IR (neat, cm<sup>-1</sup>) 3064, 2982, 2930, 1707, 1603, 1286, 1114, 760, 697. HRMS (EI) calcd. *m/z* for C<sub>16</sub>H<sub>14</sub>O<sub>2</sub> [M<sup>+</sup>] 238.09883 found 238.09827. The spectroscopic data of **13** are in accordance with previous data reported in the literature.<sup>[306]</sup>

**3,3-Diphenylisochroman-1-one (14).** White solid (66.1 mg, yield 88%), mp 148–149 °C (lit. 148–149 °C<sup>[S7]</sup>). <sup>1</sup>H NMR (300 MHz, CDCl<sub>3</sub>) δ 7.98 (dd, *J* = 7.8, 1.3 Hz, 1H), 7.50 (td, *J* = 7.5, 1.4 Hz, 1H), 7.47 – 7.39 (m, 4H), 7.36 – 7.16 (m, 9H), 3.82 (s, 2H). <sup>13</sup>C NMR (75 MHz, CDCl<sub>3</sub>) δ 165.1, 143.0, 138.2, 134.1, 130.2, 128.5, 127.7, 127.6, 127.5, 126.2, 125.7, 86.6, 39.1. IR (neat, cm<sup>-1</sup>) 3030, 3067, 2922, 2855, 1718, 1603, 1446, 1282, 1237, 760, 701. HRMS (EI) calcd. *m/z* for C<sub>21</sub>H<sub>16</sub>O<sub>2</sub> [M<sup>+</sup>] 300.11448; found 300.11383

The <sup>1</sup>H NMR and IR data of **14** are in accordance with previous data reported in the literature.<sup>[350]</sup>

**Methyl 3-methyl-1-oxoisochromane-3-carboxylate (15).** White solid (35.2 mg, yield 64%), mp 105–107 °C (lit. 104–105 °C<sup>[351]</sup>). <sup>1</sup>H NMR (300 MHz, CDCl<sub>3</sub>) δ 8.06 (dd, *J* =

7.7, 1.3 Hz, 1H), 7.51 (td,  $J = 7.5, 1.5$  Hz, 1H), 7.42 – 7.33 (m, 1H), 7.20 (dt,  $J = 7.6, 0.6$  Hz, 1H), 3.59 (s, 3H), 3.39 (d,  $J = 16.3$  Hz, 1H), 3.29 – 3.14 (m, 1H), 1.75 (s, 3H).  $^{13}\text{C}$  NMR (75 MHz,  $\text{CDCl}_3$ )  $\delta$  172.2, 164.3, 136.3, 134.0, 130.1, 128.1, 127.5, 124.5, 82.0, 53.1, 37.0, 25.0. IR (neat,  $\text{cm}^{-1}$ ) 3030, 2967, 2922, 2855, 1750, 1722, 1606, 1454, 1208, 1081, 738, 685. HRMS (ESI) calcd.  $m/z$  for  $\text{C}_{21}\text{H}_{16}\text{O}_2\text{H}^+$   $[(\text{M} + \text{H})]^+$  221.0814; found 221.0818

**2-Methoxy-6H-benzo[c]chromen-6-one (16).** White solid (33.4 mg, yield 59%), mp 123–124 °C (lit. 122–124<sup>[352]</sup>).  $^1\text{H}$  NMR (300 MHz,  $\text{CDCl}_3$ )  $\delta$  8.45 – 8.32 (m, 1H), 8.11 – 7.98 (m, 1H), 7.81 (dddd,  $J = 8.0, 7.3, 1.5, 0.6$  Hz, 1H), 7.57 (ddt,  $J = 8.0, 7.3, 0.8$  Hz, 1H), 7.48 – 7.43 (m, 1H), 7.33 – 7.23 (m, 1H), 7.03 (ddd,  $J = 9.0, 2.9, 0.6$  Hz, 1H), 3.89 (s, 3H).  $^{13}\text{C}$  NMR (75 MHz,  $\text{CDCl}_3$ )  $\delta$  161.3, 156.3, 145.6, 134.7, 134.6, 130.6, 128.9, 121.7, 121.3, 118.7, 118.5, 117.1, 106.3, 55.8. IR (neat,  $\text{cm}^{-1}$ ) 3071, 2963, 2922, 2833, 1707, 1599, 1573, 1494, 1412, 1204, 1036, 801, 764, 682. HRMS (EI) calcd.  $m/z$  for  $\text{C}_{14}\text{H}_{10}\text{O}_3$   $[\text{M}^+]$  226.06245; found 226.06179.

**6H-Isochromeno[4,3-b]pyridin-6-one (17).** White solid (22.2 mg, yield 45%), mp 134–136 °C (lit. 134–136 °C).<sup>[353]</sup>  $^1\text{H}$  NMR (300 MHz,  $\text{CDCl}_3$ )  $\delta$  8.72 – 8.65 (m, 1H), 8.61 (dd,  $J = 4.5, 1.5$  Hz, 1H), 8.38 (ddd,  $J = 7.9, 1.4, 0.6$  Hz, 1H), 7.91 (ddd,  $J = 8.1, 7.3, 1.4$  Hz, 1H), 7.74 – 7.61 (m, 2H), 7.43 (dd,  $J = 8.3, 4.5$  Hz, 1H).  $^{13}\text{C}$  NMR (75 MHz,  $\text{CDCl}_3$ )  $\delta$  160.2, 147.7, 146.0, 136.8, 135.6, 135.2, 130.6, 130.1, 124.9, 124.8, 123.4, 122.4. IR (neat,  $\text{cm}^{-1}$ ) 3056, 2922, 285, 1737, 1588, 1070, 723, 682. HRMS (ESI) calcd.  $m/z$  for  $\text{C}_{13}\text{H}_9\text{NO}_2\text{H}^+$   $[(\text{M} + \text{H})]^+$  198.0550; found 198.0558. The spectroscopic data of **17** are in accordance with previous data reported in the literature.<sup>[248]</sup>

**2-Methyl-6H-isochromeno[4,3-b]pyridin-6-one (18).** White solid (29.0 mg, yield 55%), mp 139–140 °C (lit. 138–139<sup>[353]</sup>).  $^1\text{H}$  NMR (300 MHz,  $\text{CDCl}_3$ )  $\delta$  8.71 – 8.67 (m, 1H), 8.36 (dt,  $J = 7.8, 0.9$  Hz, 1H), 7.93 – 7.84 (m, 1H), 7.67 (ddd,  $J = 8.0, 7.3, 1.3$  Hz, 1H), 7.53 (d,  $J = 8.4$  Hz, 1H), 7.26 (d,  $J = 8.5$  Hz, 1H), 2.66 (s, 3H).  $^{13}\text{C}$  NMR (75 MHz,  $\text{CDCl}_3$ )  $\delta$  160.5, 155.0, 145.9, 135.7, 135.5, 135.0, 135.0, 130.3, 130.0, 125.1, 124.8, 123.4, 122.4, 24.2. IR (neat,  $\text{cm}^{-1}$ ) 3078, 2952, 2855, 1730, 1573, 1435, 1267, 824, 743. HRMS (ESI) calcd.  $m/z$  for  $\text{C}_{13}\text{H}_9\text{NO}_2\text{H}^+$   $[(\text{M} + \text{H})]^+$  212.0712; found 212.0719.

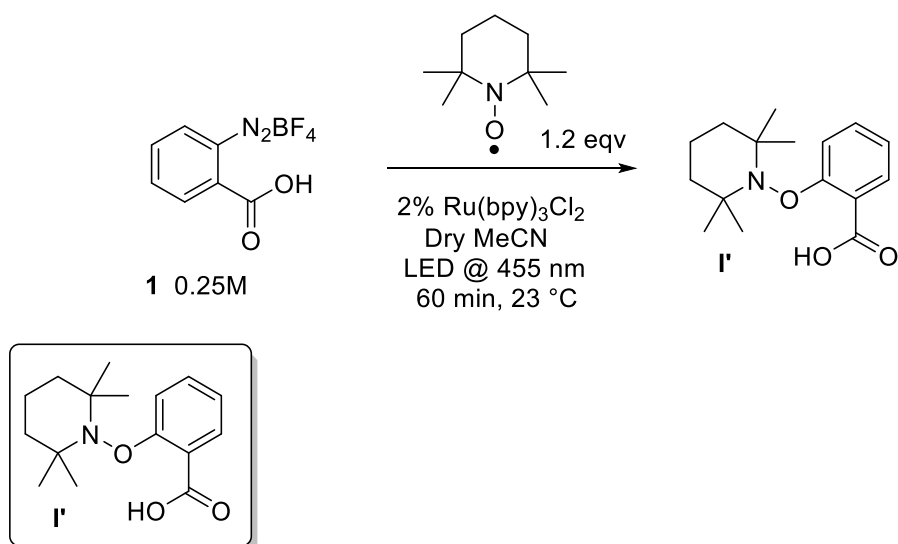
**2,7-Dimethyl-6H-isochromeno[4,3-b]pyridin-6-one (19).** White solid (24.8 mg, yield 44%) mp 150–152 °C  $^1\text{H}$  NMR (300 MHz,  $\text{CDCl}_3$ )  $\delta$  8.68 – 8.56 (m, 1H), 7.71 (t,  $J = 7.7$  Hz, 1H), 7.54 – 7.40 (m, 2H), 7.22 (d,  $J = 8.4$  Hz, 1H), 2.85 (s, 3H), 2.64 (s, 3H).  $^{13}\text{C}$  NMR (75 MHz,  $\text{CDCl}_3$ )  $\delta$  159.77, 154.62, 145.72, 143.72, 136.97, 135.67, 134.23, 133.48, 124.61, 124.51, 121.50, 120.61, 24.24, 23.48. IR (neat,  $\text{cm}^{-1}$ ) 3086, 2922, 2851,



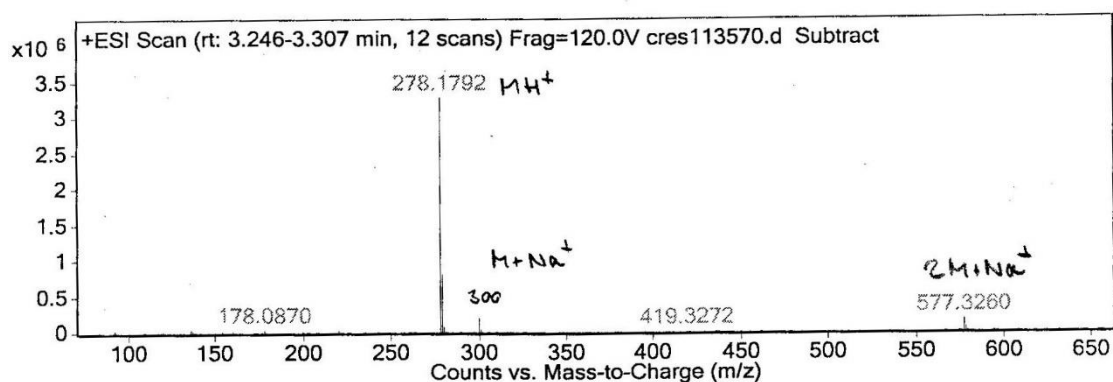
1730, 1584, 1469, 1245, 1211, 1036, 828, 753. HRMS (ESI) calcd.  $m/z$  for  $C_{14}H_{11}NO_2H^+$   $[(M+H)]^+$  226.0870; found 226.0885.

### 7.5.4 Experimental procedure for capturing intermediate radicals with TEMPO

In a 5 mL snap vial 59 mg (0.25 mmol) of the anthranilic acid diazonium tetrafluoroborate **1**, 47 mg of TEMPO (0.3 mmol, 1.2 eqv), and 3.7 mg (0.02 eqv)  $[Ru(bpy)_3]Cl_2$  were dissolved in 1 mL of dry MeCN with a stirring bar. The vial was sealed with a septum and degassed via the “freeze-pump-method” (3 $\times$ ). The reaction mixture was stirred at 23 °C and irradiated from the bottom side of the vial using blue LEDs (455 nm). After 30 min, TEMPO adduct **I'** was detected by ESI-MS.



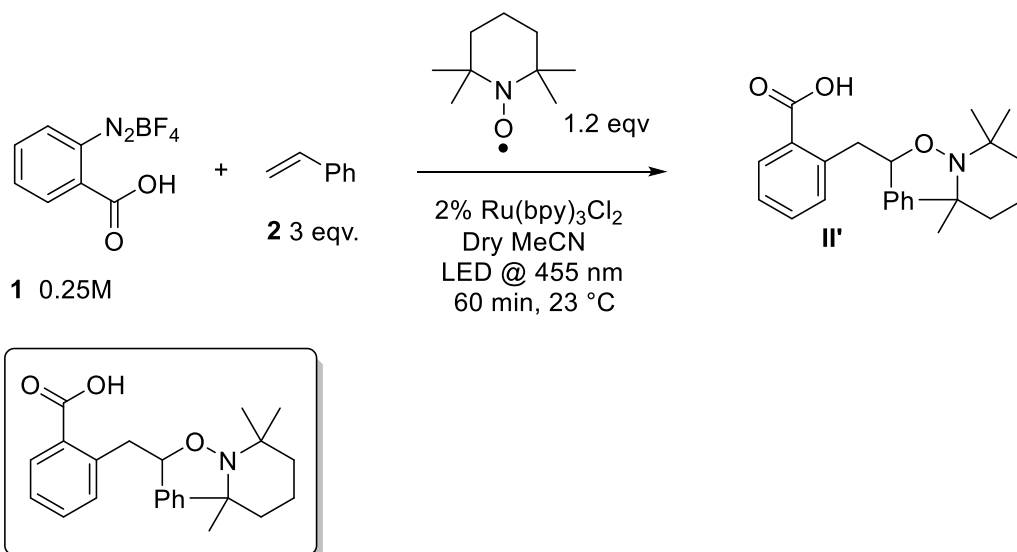
HRMS (ESI) calcd. for  $C_{16}H_{23}NO_3 (M+H)^+$  ( $m/z$ ) 277.1678 found 277.1792



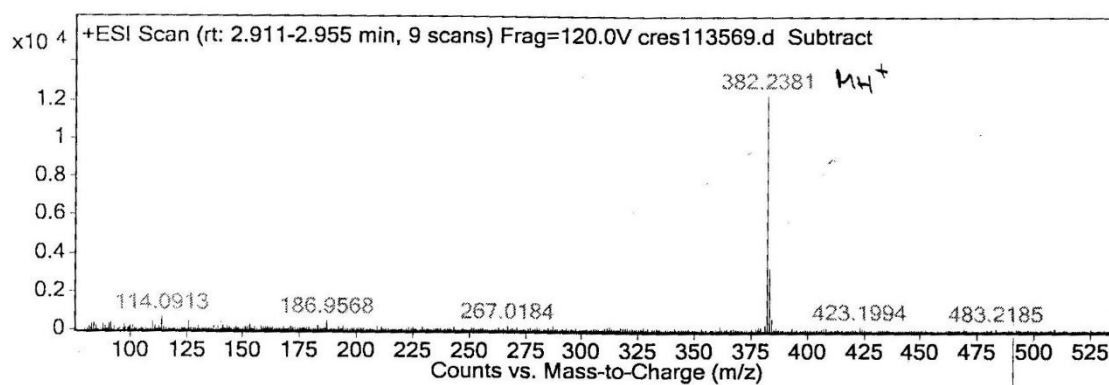
In a 5 mL snap vial 59 mg (0.25 mmol) of the anthranilic acid diazonium tetrafluoroborate **1**, 78  $\mu$ L of styrene (0.75 mmol 3 eqv), 47 mg of TEMPO (0.3 mmol, 1.2 eqv), and 0.02 eqv  $[Ru(bpy)_3]Cl_2$  were dissolved in 1 mL of dry MeCN with a stirring bar. The vial was sealed with a septum and degassed via the “freeze-pump-method” (3 $\times$ ). The reaction

### New Intermediates from Photogenerated Phenyl Cations

mixture was stirred at 23 °C and irradiated from the bottom side of the vial using blue LEDs (455 nm). After 1 h a TEMPO adduct was detected by ESI-MS.



HRMS (ESI) calcd. for C<sub>16</sub>H<sub>23</sub>NO<sub>3</sub> (M + H)<sup>+</sup> (m/z) 382.2378 found 382.2381



#### 7.5.5 Synthesis of 1,4-dihydro-1,4-epoxynaphthalene (**21**)<sup>[354]</sup>

Under nitrogen atmosphere a solution of dibromobenzene (14 mmol, 1.7 mL) and furan (0.4 mol, 30 mL) in anhydrous THF (100 mL) is treated dropwise with BuLi at -78 °C. The solution is stirred for 1.5 h. 20 mL of water are then added and the organic phase is separated, washed with water (3×20 mL), collected and dried on Na<sub>2</sub>SO<sub>4</sub>. The crude is purified with MPLC. White solid (1.03 g, yield 51%) <sup>1</sup>H NMR (300 MHz, CDCl<sub>3</sub>) δ 7.33–7.20 (m, 1H), 7.04 (t, *J* = 1.0 Hz, 2H), 6.98 (dd, *J* = 5.1, 3.0 Hz, 2H), 5.73 (s, 2H). <sup>13</sup>C NMR (75 MHz, CDCl<sub>3</sub>) δ 148.98, 143.03, 125.02, 120.29, 82.3



## New Intermediates from Photogenerated Phenyl Cations

# BIBLIOGRAPHY

- [1] S. Protti, D. Ravelli, B. Mannucci, A. Albini, M. Fagnoni, *Angew. Chem. Int. Ed.* **2012**, *51*, 8577–8580.
- [2] S. Crespi, D. Ravelli, S. Protti, A. Albini, M. Fagnoni, *Chem. - Eur. J.* **2014**, *20*, 17572–17578.
- [3] D. Ravelli, S. Protti, M. Fagnoni, *J. Org. Chem.* **2015**, *80*, 852–858.
- [4] S. Crespi, S. Protti, M. Fagnoni, *J. Org. Chem.* **2016**, *81*, 9612–9619.
- [5] M. S. Singh, *Reactive Intermediates in Organic Chemistry: Structure, Mechanism, and Reactions*, Wiley-VCH, Weinheim, **2014**.
- [6] I. Fleming, *Molecular Orbitals and Organic Chemical Reactions*, Wiley, Hoboken, N.J., **2010**.
- [7] E. V. Anslyn, D. A. Dougherty, *Modern Physical Organic Chemistry*, University Science, Sausalito, CA, **2006**.
- [8] A. Rauk, *Orbital Interaction Theory of Organic Chemistry*, Wiley-Interscience, New York, **2001**.
- [9] T. A. Albright, J. K. Burdett, M.-H. Whangbo, *Orbital Interactions in Chemistry*, Wiley, Hoboken, New Jersey, **2013**.
- [10] P. Muller, *Pure Appl. Chem.* **1994**, *66*, 1077–1184.
- [11] A. Albini, M. Fagnoni, Eds., *Photochemically-Generated Intermediates In Synthesis*, John Wiley & Sons, Inc., Hoboken, New Jersey, **2013**.
- [12] N. J. Turro, V. Ramamurthy, J. C. Scaiano, *Modern Molecular Photochemistry of Organic Molecules*, University Science Books, Sausalito, Calif, **2010**.
- [13] A. Albini, M. Fagnoni, *Green Chem.* **2004**, *6*, 1–6.
- [14] R. Noyori, *Tetrahedron* **2010**, *66*, 1028.
- [15] M. Fagnoni, A. Albini, *Acc. Chem. Res.* **2005**, *38*, 713–721.
- [16] M. Aschi, J. N. Harvey, *J. Chem. Soc. Perkin Trans. 2* **1999**, 1059–1062.
- [17] M. Freccero, M. Fagnoni, A. Albini, *J. Am. Chem. Soc.* **2003**, *125*, 13182–13190.
- [18] S. Lazzaroni, D. Dondi, M. Fagnoni, A. Albini, *J. Org. Chem.* **2008**, *73*, 206–211.
- [19] D. Ravelli, S. Protti, M. Fagnoni, A. Albini, *J. Org. Chem.* **2013**, *78*, 3814–3820.
- [20] V. Dichiarante, D. Dondi, S. Protti, M. Fagnoni, A. Albini, *J. Am. Chem. Soc.* **2007**, *129*, 5605–5611.
- [21] V. Dichiarante, M. Fagnoni, A. Albini, in *Mod. Arylation Methods* (Ed.: L. Ackermann), Wiley-VCH Verlag GmbH & Co. KGaA, Weinheim, Germany, **2009**, pp. 513–535.
- [22] S. Lazzaroni, D. Dondi, M. Fagnoni, A. Albini, *J. Org. Chem.* **2010**, *75*, 315–323.
- [23] W. Bleckmann, M. Hanack, *Chem. Ber.* **1984**, *117*, 3021–3033.
- [24] W. Holweger, M. Hanack, *Chem. Ber.* **1984**, *117*, 3004–3020.
- [25] M. Hanack, R. Rieth, *Chem. Ber.* **1987**, *120*, 1659–1666.
- [26] Y. Himeshima, H. Kobayashi, T. Sonoda, *J. Am. Chem. Soc.* **1985**, *107*, 5286–5288.
- [27] Y. Apeloig, D. Arad, *J. Am. Chem. Soc.* **1985**, *107*, 5285–5286.
- [28] V. Dichiarante, A. Salvaneschi, S. Protti, D. Dondi, M. Fagnoni, A. Albini, *J. Am. Chem. Soc.* **2007**, *129*, 15919–15926.
- [29] L. S. Romsted, J. Zhang, L. Zhuang, *J. Am. Chem. Soc.* **1998**, *120*, 10046–10054.
- [30] C. Galli, *Chem. Rev.* **1988**, *88*, 765–792.

- [31] C. Raviola, D. Ravelli, S. Protti, A. Albini, M. Fagnoni, *Synlett* **2015**, 26, 471–478.
- [32] M. Fagnoni, *Lett. Org. Chem.* **2006**, 3, 253–259.
- [33] C. Raviola, V. Canevari, S. Protti, A. Albini, M. Fagnoni, *Green Chem.* **2013**, 15, 2704–2708.
- [34] C. Raviola, S. Protti, D. Ravelli, M. Mella, A. Albini, M. Fagnoni, *J. Org. Chem.* **2012**, 77, 9094–9101.
- [35] A. Albini, M. Fagnoni, Eds., *Handbook of Synthetic Photochemistry*, Wiley-VCH, Weinheim, **2010**.
- [36] S. Protti, D. Dondi, M. Mella, M. Fagnoni, A. Albini, *Eur. J. Org. Chem.* **2011**, 2011, 3229–3237.
- [37] V. Dichiarante, M. Fagnoni, M. Mella, A. Albini, *Chem. - Eur. J.* **2006**, 12, 3905–3915.
- [38] M. Mella, P. Coppo, B. Guizzardi, M. Fagnoni, M. Freccero, A. Albini, *J. Org. Chem.* **2001**, 66, 6344–6352.
- [39] S. Protti, M. Fagnoni, A. Albini, *Angew. Chem. Int. Ed.* **2005**, 44, 5675–5678.
- [40] S. Protti, M. Fagnoni, A. Albini, *J. Org. Chem.* **2012**, 77, 6473–6479.
- [41] V. Dichiarante, M. Fagnoni, A. Albini, *Angew. Chem. Int. Ed.* **2007**, 46, 6495–6498.
- [42] B. Guizzardi, M. Mella, M. Fagnoni, A. Albini, *Tetrahedron* **2000**, 56, 9383–9389.
- [43] M. Slegt, H. S. Overkleeft, G. Lodder, *Eur. J. Org. Chem.* **2007**, 2007, 5364–5375.
- [44] S. Protti, M. Fagnoni, A. Albini, *Org. Biomol. Chem.* **2005**, 3, 2868–2871.
- [45] M. Fagnoni, M. Mella, A. Albini, *Org. Lett.* **1999**, 1, 1299–1301.
- [46] B. Guizzardi, M. Mella, M. Fagnoni, M. Freccero, A. Albini, *J. Org. Chem.* **2001**, 66, 6353–6363.
- [47] S. Protti, V. Dichiarante, D. Dondi, M. Fagnoni, A. Albini, *Chem. Sci.* **2012**, 3, 1330–1337.
- [48] M. J. Lo Fiego, M. T. Lockhart, A. B. Chopa, *J. Organomet. Chem.* **2009**, 694, 3674–3678.
- [49] H. Heaney, *Chem. Rev.* **1962**, 62, 81–97.
- [50] P. M. Tadross, B. M. Stoltz, *Chem. Rev.* **2012**, 112, 3550–3577.
- [51] H. H. Wenk, M. Winkler, W. Sander, *Angew. Chem. Int. Ed.* **2003**, 42, 502–528.
- [52] A. W. Gann, J. W. Amoroso, V. J. Einck, W. P. Rice, J. J. Chambers, N. A. Schnarr, *Org. Lett.* **2014**, 16, 2003–2005.
- [53] J. Torres-Alacan, *J. Org. Chem.* **2016**, 81, 1151–1156.
- [54] B. Engels, M. Hanrath, *J. Am. Chem. Soc.* **1998**, 120, 6356–6361.
- [55] L. Salem, C. Rowland, *Angew. Chem. Int. Ed. Engl.* **1972**, 11, 92–111.
- [56] T. S. Hughes, B. K. Carpenter, *J. Chem. Soc. Perkin Trans. 2* **1999**, 2291–2298.
- [57] A. G. Myers, C. A. Parrish, *Bioconjug. Chem.* **1996**, 7, 322–331.
- [58] A. V. Kuzmin, V. V. Popik, *Chem. Commun.* **2009**, 5707–5709.
- [59] C.-F. Lin, M.-J. Wu, *J. Org. Chem.* **1997**, 62, 4546–4548.
- [60] I. Suzuki, Y. Tsuchiya, A. Shigenaga, H. Nemoto, M. Shibuya, *Tetrahedron Lett.* **2002**, 43, 6779–6781.
- [61] I. Suzuki, S. Uno, Y. Tsuchiya, A. Shigenaga, H. Nemoto, M. Shibuya, *Bioorg. Med. Chem. Lett.* **2004**, 14, 2959–2962.
- [62] U. Galm, M. H. Hager, S. G. Van Lanen, J. Ju, J. S. Thorson, B. Shen, *Chem. Rev.* **2005**, 105, 739–758.
- [63] B. Breiner, K. Kaya, S. Roy, W.-Y. Yang, I. V. Alabugin, *Org. Biomol. Chem.* **2012**, 10, 3974–3987.
- [64] Y.-S. Zhen, X.-Y. Ming, B. Yu, T. Otani, H. Saito, Y. Yamada, *J. Antibiot. (Tokyo)* **1989**, 42, 1294–1298.
- [65] A. G. Myers, P. S. Dragovich, *J. Am. Chem. Soc.* **1989**, 111, 9130–9132.

- [66] A. G. Myers, E. Y. Kuo, N. S. Finney, *J. Am. Chem. Soc.* **1989**, *111*, 8057–8059.
- [67] A. G. Myers, P. S. Dragovich, E. Y. Kuo, *J. Am. Chem. Soc.* **1992**, *114*, 9369–9386.
- [68] J. E. Baldwin, R. C. Thomas, L. I. Kruse, L. Silberman, *J. Org. Chem.* **1977**, *42*, 3846–3852.
- [69] M. Schmittel, S. Kiau, *Liebigs Ann.* **1997**, *1997*, 1391–1399.
- [70] S. M. Bachrach, *Computational Organic Chemistry*, Wiley, Hoboken, New Jersey, **2014**.
- [71] Chen, J.-W. Zou, C.-H. Yu, *J. Org. Chem.* **2003**, *68*, 3663–3672.
- [72] P. G. Wenthold, M. A. Lipton, *J. Am. Chem. Soc.* **2000**, *122*, 9265–9270.
- [73] A. B. Padias, H. K. Hall, *J. Org. Chem.* **1987**, *52*, 4536–4539.
- [74] M. E. Cremeens, T. S. Hughes, B. K. Carpenter, *J. Am. Chem. Soc.* **2005**, *127*, 6652–6661.
- [75] P. G. Wenthold, S. G. Wierschke, J. J. Nash, R. R. Squires, *J. Am. Chem. Soc.* **1993**, *115*, 12611–12612.
- [76] P. G. Wenthold, S. G. Wierschke, J. J. Nash, R. R. Squires, *J. Am. Chem. Soc.* **1994**, *116*, 7378–7392.
- [77] P. Neuhaus, S. Henkel, W. Sander, *Aust. J. Chem.* **2010**, *63*, 1634–1637.
- [78] U. E. Wiersum, T. Nieuwenhuis, *Tetrahedron Lett.* **1973**, *14*, 2581–2584.
- [79] S. Protti, D. Ravelli, M. Fagnoni, A. Albini, *Pure Appl. Chem.* **2013**, *85*, 1479–1486.
- [80] A. Griesbeck, M. Oelgemöller, F. Ghetti, *CRC Handbook of Organic Photochemistry and Photobiology, Third Edition - Two Volume Set*, CRC Press, **2012**.
- [81] M. De Carolis, S. Protti, M. Fagnoni, A. Albini, *Angew. Chem. Int. Ed.* **2005**, *44*, 1232–1236.
- [82] E. Abitelli, S. Protti, M. Fagnoni, A. Albini, *J. Org. Chem.* **2012**, *77*, 3501–3507.
- [83] J. L. Stratenus, E. Havinga, *Recl. Trav. Chim. Pays-Bas* **1966**, *85*, 434–436.
- [84] Y. Ogata, K. Takagi, S. Yamada, *J. Chem. Soc. Perkin Trans. 2* **1977**, 1629–1632.
- [85] J. Andraos, G. G. Barclay, D. R. Medeiros, M. V. Baldovi, J. C. Scaiano, R. Sinta, *Chem. Mater.* **1998**, *10*, 1694–1699.
- [86] L. K. Crevatín, S. M. Bonesi, R. Erra-Balsells, *Helv. Chim. Acta* **2006**, *89*, 1147–1157.
- [87] Y. Kageyama, R. Ohshima, K. Sakurama, Y. Fujiwara, Y. Tanimoto, Y. Yamada, S. Aoki, *Chem. Pharm. Bull. (Tokyo)* **2009**, *57*, 1257–1266.
- [88] M. Terpolilli, D. Merli, S. Protti, V. Dichiarante, M. Fagnoni, A. Albini, *Photochem Photobiol Sci* **2011**, *10*, 123–127.
- [89] W. M. Horspool, F. Lenci, *CRC Handbook of Organic Photochemistry and Photobiology*, CRC Press, Boca Raton, **2004**.
- [90] S. V. Bondarchuk, B. F. Minaev, *Chem. Phys.* **2011**, *389*, 68–74.
- [91] S. V. Bondarchuk, B. F. Minaev, *J. Phys. Chem. A* **2014**, *118*, 3201–3210.
- [92] J. P. Dinnocenzo, S. Farid, J. L. Goodman, I. R. Gould, S. L. Mattes, W. P. Todd, *J. Am. Chem. Soc.* **1989**, *111*, 8973–8975.
- [93] K. Taylor, K. Miura, F. Akinfaderin, A. J. Fry, *J. Electrochem. Soc.* **2003**, *150*, D85–D86.
- [94] E. Havinga, R. O. de Jongh, W. Dorst, *Recl. Trav. Chim. Pays-Bas* **1956**, *75*, 378–383.
- [95] H. E. Zimmerman, V. R. Sandel, *J. Am. Chem. Soc.* **1963**, *85*, 915–922.
- [96] H. E. Zimmerman, S. Somasekhara, *J. Am. Chem. Soc.* **1963**, *85*, 922–927.
- [97] H. E. Zimmerman, *J. Am. Chem. Soc.* **1995**, *117*, 8988–8991.
- [98] M. Kira, H. Yoshida, H. Sakurai, *J. Am. Chem. Soc.* **1985**, *107*, 7767–7768.

- [99] H. Hiratsuka, Y. Kadokura, H. Chida, M. Tanaka, S. Kobayashi, T. Okutsu, M. Oba, K. Nishiyama, *J. Chem. Soc. Faraday Trans.* **1996**, *92*, 3035–3041.
- [100] S. Lazzaroni, D. Ravelli, S. Protti, M. Fagnoni, A. Albini, *Comptes Rendus Chim.* **2016**, DOI 10.1016/j.crci.2015.11.024.
- [101] S. Protti, V. Dichiarante, D. Dondi, M. Fagnoni, A. Albini, *Chem. Sci.* **2012**, *3*, 1330–1337.
- [102] C. Raviola, D. Ravelli, S. Protti, M. Fagnoni, *J. Am. Chem. Soc.* **2014**, *136*, 13874–13881.
- [103] Q. N. N. Nguyen, D. J. Tantillo, *J. Org. Chem.* **2016**, *81*, 5295–5302.
- [104] M. W. Bowler, M. J. Cliff, J. P. Waltho, G. M. Blackburn, *New J. Chem.* **2010**, *34*, 784–794.
- [105] F. Westheimer, *Science* **1987**, *235*, 1173–1178.
- [106] T. S. Elliott, A. Slowey, Y. Ye, S. J. Conway, *MedChemComm* **2012**, *3*, 735–751.
- [107] Y. Okamoto, N. Iwamoto, S. Takamuku, *J Chem Soc Chem Commun* **1986**, 1516–1517.
- [108] Y. Okamoto, N. Iwamoto, S. Toki, S. Takamuku, *Bull. Chem. Soc. Jpn.* **1987**, *60*, 277–282.
- [109] A. R. Katritzky, B. Pilarski, J. W. Johnson, *Org. Prep. Proced. Int.* **1990**, *22*, 209–213.
- [110] R. G. Franz, *AAPS PharmSci* **2001**, *3*, 1–13.
- [111] P. Boule, C. Guyon, J. Lemaire, *Toxicol. Environ. Chem.* **1984**, *7*, 97–110.
- [112] I. B. Berlman, *Handbook of Fluorescence Spectra of Aromatic Molecules*, Academic Press, New York, **1971**.
- [113] P. Krtil, *J. Electrochem. Soc.* **1993**, *140*, 3390–3395.
- [114] H. Okamoto, T. Gojuki, N. Okano, T. Kuge, M. Morita, A. Maruyama, Y. Mukouyama, *Electrochimica Acta* **2014**, *136*, 385–395.
- [115] J. H. Vleeming, B. F. . Kuster, G. B. Marin, *Carbohydr. Res.* **1997**, *303*, 175–183.
- [116] I. Manet, S. Monti, P. Bortolus, M. Fagnoni, A. Albini, *Chem. - Eur. J.* **2005**, *11*, 4274–4282.
- [117] M. Abe, *Chem. Rev.* **2013**, *113*, 7011–7088.
- [118] J. M. R. Narayanam, C. R. J. Stephenson, *Chem Soc Rev* **2011**, *40*, 102–113.
- [119] C. K. Prier, D. A. Rankic, D. W. C. MacMillan, *Chem. Rev.* **2013**, *113*, 5322–5363.
- [120] T. P. Yoon, *ACS Catal.* **2013**, *3*, 895–902.
- [121] J. Xuan, W.-J. Xiao, *Angew. Chem. Int. Ed.* **2012**, *51*, 6828–6838.
- [122] D. A. Nicewicz, T. M. Nguyen, *ACS Catal.* **2014**, *4*, 355–360.
- [123] D. Ravelli, M. Fagnoni, A. Albini, *Chem Soc Rev* **2013**, *42*, 97–113.
- [124] S. Protti, M. Fagnoni, D. Ravelli, *ChemCatChem* **2015**, *7*, 1516–1523.
- [125] J. Yoshida, K. Kataoka, R. Horcajada, A. Nagaki, *Chem. Rev.* **2008**, *108*, 2265–2299.
- [126] M. F. Saraiva, M. R. C. Couri, M. Le Hyaric, M. V. de Almeida, *Tetrahedron* **2009**, *65*, 3563–3572.
- [127] S. Ni, J. Cao, H. Mei, J. Han, S. Li, Y. Pan, *Green Chem* **2016**, *18*, 3935–3939.
- [128] H. Tan, H. Li, W. Ji, L. Wang, *Angew. Chem. Int. Ed.* **2015**, *54*, 8374–8377.
- [129] S. Protti, G. A. Artioli, F. Capitani, C. Marini, P. Dore, P. Postorino, L. Malavasi, M. Fagnoni, *RSC Adv* **2015**, *5*, 27470–27475.
- [130] C. G. S. Lima, T. de M. Lima, M. Duarte, I. D. Jurberg, M. W. Paixão, *ACS Catal.* **2016**, *6*, 1389–1407.
- [131] E. Arceo, I. D. Jurberg, A. Álvarez-Fernández, P. Melchiorre, *Nat. Chem.* **2013**, *5*, 750–756.
- [132] N. Kamigata, M. Kobayashi, *Sulfur Rep.* **1982**, *2*, 87–128.
- [133] J. L. Kice, R. S. Gabrielsen, *J. Org. Chem.* **1970**, *35*, 1004–1009.



- [134] M. Kobayashi, M. Gotoh, H. Minato, *J. Org. Chem.* **1975**, *40*, 140–142.
- [135] J. L. Kice, R. S. Gabrielsen, *J. Org. Chem.* **1970**, *35*, 1010–1015.
- [136] G. Rosini, R. Ranza, *J. Org. Chem.* **1971**, *36*, 1915–1918.
- [137] M. Yoshida, N. Furuta, M. Kobayashi, *Bull. Chem. Soc. Jpn.* **1981**, *54*, 2356–2359.
- [138] M. J. Evers, L. E. Christiaens, M. R. Guillaume, M. J. Renson, *J. Org. Chem.* **1985**, *50*, 1779–1780.
- [139] M. J. Evers, L. E. Christiaens, M. J. Renson, *J. Org. Chem.* **1986**, *51*, 5196–5198.
- [140] I. Sapountzis, P. Knochel, *Angew. Chem. Int. Ed.* **2004**, *43*, 897–900.
- [141] Z. Zhang, Y. Gao, Y. Liu, J. Li, H. Xie, H. Li, W. Wang, *Org. Lett.* **2015**, *17*, 5492–5495.
- [142] M. Kobayashi, S. Fujii, H. Minato, *Bull. Chem. Soc. Jpn.* **1972**, *45*, 2039–2042.
- [143] I. R. Dunkin, A. Gittinger, D. C. Sherrington, P. Whittaker, *J. Chem. Soc. Perkin Trans. 2* **1996**, 1837–1842.
- [144] J. Eastoe, M. Sanchez-Dominguez, H. Cumber, G. Burnett, P. Wyatt, R. K. Heenan, *Langmuir* **2003**, *19*, 6579–6581.
- [145] P. Schroll, D. P. Hari, B. König, *ChemistryOpen* **2012**, *1*, 130–133.
- [146] M. N. Hopkinson, B. Sahoo, F. Glorius, *Adv. Synth. Catal.* **2014**, *356*, 2794–2800.
- [147] W. Guo, L.-Q. Lu, Y. Wang, Y.-N. Wang, J.-R. Chen, W.-J. Xiao, *Angew. Chem. Int. Ed.* **2015**, *54*, 2265–2269.
- [148] M. Majek, A. Jacobi von Wangelin, *Angew. Chem. Int. Ed.* **2015**, *54*, 2270–2274.
- [149] J. Zoller, D. C. Fabry, M. Rueping, *ACS Catal.* **2015**, *5*, 3900–3904.
- [150] J. Zhang, J. Chen, X. Zhang, X. Lei, *J. Org. Chem.* **2014**, *79*, 10682–10688.
- [151] F. Gomes, V. Narbonne, F. Blanchard, G. Maestri, M. Malacria, *Org Chem Front* **2015**, *2*, 464–469.
- [152] S. Milanesi, M. Fagnoni, A. Albini, *J. Org. Chem.* **2005**, *70*, 603–610.
- [153] E. F. Ullman, P. Singh, *J. Am. Chem. Soc.* **1972**, *94*, 5077–5078.
- [154] S. J. Garden, D. V. Avila, A. L. J. Beckwith, V. W. Bowry, K. U. Ingold, J. Luszyk, *J. Org. Chem.* **1996**, *61*, 805–809.
- [155] D. P. Hari, B. König, *Angew. Chem. Int. Ed.* **2013**, *52*, 4734–4743.
- [156] S. Donck, A. Baroudi, L. Fensterbank, J.-P. Goddard, C. Ollivier, *Adv. Synth. Catal.* **2013**, *355*, 1477–1482.
- [157] S. V. Bondarchuk, B. F. Minaev, *J. Mol. Struct. THEOCHEM* **2010**, *952*, 1–7.
- [158] V. Dichiarante, M. Fagnoni, *Synlett* **2008**, *2008*, 787–800.
- [159] L. Ackermann, M. Dell’Acqua, S. Fenner, R. Vicente, R. Sandmann, *Org. Lett.* **2011**, *13*, 2358–2360.
- [160] Y. Wu, S. M. Wong, F. Mao, T. L. Chan, F. Y. Kwong, *Org. Lett.* **2012**, *14*, 5306–5309.
- [161] D. P. Curran, A. I. Keller, *J. Am. Chem. Soc.* **2006**, *128*, 13706–13707.
- [162] Y. Qiu, Y. Liu, K. Yang, W. Hong, Z. Li, Z. Wang, Z. Yao, S. Jiang, *Org. Lett.* **2011**, *13*, 3556–3559.
- [163] A. Dewanji, S. Murarka, D. P. Curran, A. Studer, *Org. Lett.* **2013**, *15*, 6102–6105.
- [164] H. Zhao, J. Shen, J. Guo, R. Ye, H. Zeng, *Chem. Commun.* **2013**, *49*, 2323–2325.
- [165] D. P. Hari, P. Schroll, B. König, *J. Am. Chem. Soc.* **2012**, *134*, 2958–2961.
- [166] P. Maity, D. Kundu, B. C. Ranu, *Eur. J. Org. Chem.* **2015**, *2015*, 1727–1734.
- [167] I. Ghosh, T. Ghosh, J. I. Bardagi, B. Konig, *Science* **2014**, *346*, 725–728.
- [168] D. Cantillo, C. Mateos, J. A. Rincon, O. de Frutos, C. O. Kappe, *Chem. - Eur. J.* **2015**, *21*, 12894–12898.
- [169] A. M. Mfuh, J. D. Doyle, B. Chhetri, H. D. Arman, O. V. Larionov, *J. Am. Chem. Soc.* **2016**, *138*, 2985–2988.
- [170] F. P. Crisóstomo, T. Martín, R. Carrillo, *Angew. Chem. Int. Ed.* **2014**, *53*, 2181–2185.

- [171] N. Sadlej-Sosnowska, M. Kijak, *Struct. Chem.* **2012**, *23*, 359–365.
- [172] I. Haller, *J. Chem. Phys.* **1967**, *47*, 1117.
- [173] W. G. Dauben, L. Salem, N. J. Turro, *Acc. Chem. Res.* **1975**, *8*, 41–54.
- [174] N. Hoffmann, *Photochem. Photobiol. Sci.* **2012**, *11*, 1613–1641.
- [175] J. Cornelisse, E. Havinga, *Chem. Rev.* **1975**, *75*, 353–388.
- [176] J. Malkin, *Photophysical and Photochemical Properties of Aromatic Compounds*, CRC, Boca Raton, **1992**.
- [177] H. E. Zimmerman, *J. Phys. Chem. A* **1998**, *102*, 5616–5621.
- [178] J. Clayden, N. Greeves, S. G. Warren, *Organic Chemistry*, Oxford University Press, Oxford ; New York, **2012**.
- [179] J.-S. Yang, in *Chem. Anilines* (Ed.: Z. Rappoport), John Wiley & Sons, Ltd, Chichester, UK, **2007**, pp. 783–833.
- [180] E. K. Winarno, N. Getoff, *Z. Für Naturforschung C* **2002**, *57*, 512–515.
- [181] V. Dichiarante, M. Fagnoni, A. Albinì, *Chem. Commun.* **2006**, 3001–3003.
- [182] S. Ishikawa, K. Baba, Y. Hanada, Y. Uchimura, K. Kido, *Bull. Environ. Contam. Toxicol.* **1989**, *42*, 65–70.
- [183] K. Othmen, P. Boule, *J. Photochem. Photobiol. Chem.* **2000**, *136*, 79–86.
- [184] K. Othmen, P. Boule, C. Richard, *New J. Chem.* **1999**, *23*, 857–861.
- [185] B. Koutek, L. Musil, J. Velek, M. Souček, *Collect. Czechoslov. Chem. Commun.* **1985**, *50*, 1753–1763.
- [186] T. K. Pal, G. K. Mallik, S. Laha, K. Chatterjee, T. Ganguly, S. B. Banerjee, *Spectrochim. Acta Part Mol. Spectrosc.* **1987**, *43*, 853–859.
- [187] P. J. Krueger, *Can. J. Chem.* **1962**, *40*, 2300–2316.
- [188] C. M. Previtali, T. W. Ebbesen, *J. Photochem.* **1984**, *27*, 9–15.
- [189] K. Othmen, P. Boule, B. Szczepanik, K. Rotkiewicz, G. Grabner, *J. Phys. Chem. A* **2000**, *104*, 9525–9534.
- [190] D. M. Shold, *Chem. Phys. Lett.* **1977**, *49*, 243–246.
- [191] M. Olivucci, *Computational Photochemistry*, Elsevier, Amsterdam; Boston, **2005**.
- [192] Y.-J. Liu, P. Persson, S. Lunell, *J. Phys. Chem. A* **2004**, *108*, 2339–2345.
- [193] Y.-J. Liu, P. Persson, H. O. Karlsson, S. Lunell, M. Kadi, D. Karlsson, J. Davidsson, *J. Chem. Phys.* **2004**, *120*, 6502.
- [194] D. Polli, P. Altoè, O. Weingart, K. M. Spillane, C. Manzoni, D. Brida, G. Tomasello, G. Orlandi, P. Kukura, R. A. Mathies, et al., *Nature* **2010**, *467*, 440–443.
- [195] I. J. Palmer, I. N. Ragazos, F. Bernardi, M. Olivucci, M. A. Robb, *J. Am. Chem. Soc.* **1993**, *115*, 673–682.
- [196] L. Kaplan, K. E. Wilzbach, *J. Am. Chem. Soc.* **1968**, *90*, 3291–3292.
- [197] E. Riedle, T. Weber, U. Schubert, H. J. Neusser, E. W. Schlag, *J. Chem. Phys.* **1990**, *93*, 967–978.
- [198] M. A. Robb, M. Garavelli, M. Olivucci, F. Bernardi, in *Rev. Comput. Chem.* (Eds.: K.B. Lipkowitz, D.B. Boyd), John Wiley & Sons, Inc., Hoboken, NJ, USA, **2000**, pp. 87–146.
- [199] X. Xu, K. R. Yang, D. G. Truhlar, *J. Chem. Theory Comput.* **2013**, *9*, 3612–3625.
- [200] O. P. J. Vieuxmaire, Z. Lan, A. L. Sobolewski, W. Domcke, *J. Chem. Phys.* **2008**, *129*, 224307.
- [201] R. Omidyan, H. Rezaei, *Phys. Chem. Chem. Phys.* **2014**, *16*, 11679.
- [202] A. L. Sobolewski, W. Domcke, *Chem. Phys. Lett.* **1991**, *180*, 381–386.
- [203] A. L. Sobolewski, C. Woywod, W. Domcke, *J. Chem. Phys.* **1993**, *98*, 5627.
- [204] S. Cogan, Y. Haas, S. Zilberg, *J. Photochem. Photobiol. Chem.* **2007**, *190*, 200–206.

- [205] F. Aquilante, J. Autschbach, R. K. Carlson, L. F. Chibotaru, M. G. Delcey, L. De Vico, I. Fdez. Galván, N. Ferré, L. M. Frutos, L. Gagliardi, et al., *J. Comput. Chem.* **2016**, *37*, 506–541.
- [206] C. M. Marian, in *Rev. Comput. Chem.* (Eds.: K.B. Lipkowitz, D.B. Boyd), John Wiley & Sons, Inc., New York, USA, **2001**, pp. 99–204.
- [207] A. Rodriguez-Serrano, V. Rai-Constapel, M. C. Daza, M. Doerr, C. M. Marian, *Photochem. Photobiol. Sci.* **2012**, *11*, 1860–1867.
- [208] V. Veryazov, P. Å. Malmqvist, B. O. Roos, *Int. J. Quantum Chem.* **2011**, *111*, 3329–3338.
- [209] P. R. Taylor, in *Lect. Notes Quantum Chem.* (Ed.: B.O. Roos), Springer Berlin Heidelberg, Berlin, Heidelberg, **1992**, pp. 325–412.
- [210] I. Conti, P. Altoè, M. Stenta, M. Garavelli, G. Orlandi, *Phys. Chem. Chem. Phys.* **2010**, *12*, 5016–5023.
- [211] S. F. Altavilla, J. Segarra-Martá, A. Nenov, I. Conti, I. Rivalta, M. Garavelli, *Front. Chem.* **2015**, *3*, 1–12.
- [212] L. Serrano-Andrés, M. Merchán, R. Lindh, *J. Chem. Phys.* **2005**, *122*, 104107.
- [213] C. Hansch, A. Leo, R. W. Taft, *Chem. Rev.* **1991**, *91*, 165–195.
- [214] B. V. Mc Inerney, W. C. Taylor, in *Stud. Nat. Prod. Chem.*, Elsevier, **1995**, pp. 381–422.
- [215] S. Pal, V. Chatare, M. Pal, *Curr. Org. Chem.* **2011**, *15*, 782–800.
- [216] M. Yoshikawa, H. Matsuda, H. Shimoda, H. Shimada, E. Harada, Y. Naitoh, A. Miki, J. Yamahara, N. Murakami, *Chem. Pharm. Bull. (Tokyo)* **1996**, *44*, 1440–1447.
- [217] P. Jiao, J. B. Gloer, J. Campbell, C. A. Shearer, *J. Nat. Prod.* **2006**, *69*, 612–615.
- [218] J. Barbier, R. Jansen, H. Irschik, S. Benson, K. Gerth, B. Böhlendorf, G. Höfle, H. Reichenbach, J. Wegner, C. Zeilinger, et al., *Angew. Chem. Int. Ed.* **2012**, *51*, 1256–1260.
- [219] K. Nozawa, M. Yamada, Y. Tsuda, K. Kawai, S. Nakajima, *Chem. Pharm. Bull. (Tokyo)* **1981**, *29*, 2689–2691.
- [220] N. Fusetani, T. Sugawara, S. Matsunaga, H. Hirota, *J. Org. Chem.* **1991**, *56*, 4971–4974.
- [221] P. Kongsaree, S. Prabpai, N. Sriubolmas, C. Vongvein, S. Wiyakrutta, *J. Nat. Prod.* **2003**, *66*, 709–711.
- [222] M. Yoshikawa, E. Uchida, N. Chatani, N. Murakami, J. Yamahara, *Chem. Pharm. Bull. (Tokyo)* **1992**, *40*, 3121–3123.
- [223] M. Toshikawa, E. Uchida, N. Chatani, H. Kobayashi, Y. Naitoh, Y. Okuno, H. Matsuda, J. Yamahara, N. Murakami, *Chem. Pharm. Bull. (Tokyo)* **1992**, *40*, 3352–3354.
- [224] G.-H. Ma, B. Jiang, X.-J. Tu, Y. Ning, S.-J. Tu, G. Li, *Org. Lett.* **2014**, *16*, 4504–4507.
- [225] I. V. Prokhorova, K. A. Akulich, D. S. Makeeva, I. A. Osterman, D. A. Skvortsov, P. V. Sergiev, O. A. Dontsova, G. Yusupova, M. M. Yusupov, S. E. Dmitriev, *Sci. Rep.* **2016**, *6*, 27720.
- [226] I. V. Pinchuk, P. Bressollier, I. B. Sorokulova, B. Verneuil, M. C. Urdaci, *Res. Microbiol.* **2002**, *153*, 269–276.
- [227] S. K. Mandal, S. C. Roy, *Tetrahedron* **2008**, *64*, 11050–11057.
- [228] H. Matsuda, H. Shimoda, M. Yoshikawa, *Bioorg. Med. Chem.* **1999**, *7*, 1445–1450.
- [229] P. Tomasik, Ed. , *Chemical and Functional Properties of Food Saccharides*, CRC Press, Boca Raton, **2004**.
- [230] Z. Mao, W. Sun, L. Fu, H. Luo, D. Lai, L. Zhou, *Molecules* **2014**, *19*, 5088–5108.
- [231] S. P. Fletcher, F. Dumur, M. M. Pollard, B. L. Feringa, *Science* **2005**, *310*, 80–82.

- [232] C.-W. Yang, T.-H. Hsia, C.-C. Chen, C.-K. Lai, R.-S. Liu, *Org. Lett.* **2008**, *10*, 4069–4072.
- [233] X. Ren, M. E. Kondakova, D. J. Giesen, M. Rajeswaran, M. Madaras, W. C. Lenhart, *Inorg. Chem.* **2010**, *49*, 1301–1303.
- [234] S. Essig, D. Menche, *J. Org. Chem.* **2016**, *81*, 1943–1966.
- [235] M. Shimogaki, M. Fujita, T. Sugimura, *Eur. J. Org. Chem.* **2013**, *2013*, 7128–7138.
- [236] Y. Xiao, J. Wang, W. Xia, S. Shu, S. Jiao, Y. Zhou, H. Liu, *Org. Lett.* **2015**, *17*, 3850–3853.
- [237] T.-S. Zhu, J.-P. Chen, M.-H. Xu, *Chem. - Eur. J.* **2013**, *19*, 865–869.
- [238] F. Wang, Z. Qi, J. Sun, X. Zhang, X. Li, *Org. Lett.* **2013**, *15*, 6290–6293.
- [239] K. Padala, M. Jeganmohan, *Org. Lett.* **2012**, *14*, 1134–1137.
- [240] E. T. da Penha, J. A. Forni, A. F. P. Biajoli, C. R. D. Correia, *Tetrahedron Lett.* **2011**, *52*, 6342–6345.
- [241] B. A. Egan, M. Paradowski, L. H. Thomas, R. Marquez, *Org. Lett.* **2011**, *13*, 2086–2089.
- [242] N. P. Ramirez, I. Bosque, J. C. Gonzalez-Gomez, *Org. Lett.* **2015**, *17*, 4550–4553.
- [243] Y. Li, Y.-J. Ding, J.-Y. Wang, Y.-M. Su, X.-S. Wang, *Org. Lett.* **2013**, *15*, 2574–2577.
- [244] K. Koch, J. Podlech, E. Pfeiffer, M. Metzler, *J. Org. Chem.* **2005**, *70*, 3275–3276.
- [245] B. I. Alo, A. Kandil, P. A. Patil, M. J. Sharp, M. A. Siddiqui, V. Snieckus, P. D. Josephy, *J. Org. Chem.* **1991**, *56*, 3763–3768.
- [246] W. Zhang, G. Pugh, *Tetrahedron* **2003**, *59*, 3009–3018.
- [247] M. Othman, P. Pigeon, B. Decroix, *Tetrahedron* **1998**, *54*, 8737–8744.
- [248] M. C. D. Fürst, L. R. Bock, M. R. Heinrich, *J. Org. Chem.* **2016**, *81*, 5752–5758.
- [249] I. Ghosh, L. Marzo, A. Das, R. Shaikh, B. König, *Acc. Chem. Res.* **2016**, *49*, 1566–1577.
- [250] H. Meerwein, E. Büchner, K. van Emster, *J. Für Prakt. Chem.* **1939**, *152*, 237–266.
- [251] L. Friedman, F. M. Logullo, *J. Org. Chem.* **1969**, *34*, 3089–3092.
- [252] P. Christopher Buxton, M. Fensome, H. Heaney, K. G. Mason, *Tetrahedron* **1995**, *51*, 2959–2968.
- [253] A. Wetzel, G. Pratsch, R. Kolb, M. R. Heinrich, *Chem. - Eur. J.* **2010**, *16*, 2547–2556.
- [254] M. Majek, F. Filace, A. J. von Wangelin, *Beilstein J. Org. Chem.* **2014**, *10*, 981–989.
- [255] B. Giese, *Angew. Chem. Int. Ed. Engl.* **1983**, *22*, 753–764.
- [256] W. E. Bachmann, H. T. Clarke, *J. Am. Chem. Soc.* **1927**, *49*, 2089–2098.
- [257] G. Wittig, *Naturwissenschaften* **1942**, *30*, 696–703.
- [258] L. Friedman, F. M. Logullo, *Angew. Chem. Int. Ed. Engl.* **1965**, *4*, 239–240.
- [259] Y. Himeshima, T. Sonoda, H. Kobayashi, *Chem. Lett.* **1983**, *12*, 1211–1214.
- [260] F. Shi, J. P. Waldo, Y. Chen, R. C. Larock, *Org. Lett.* **2008**, *10*, 2409–2412.
- [261] S. Yoshida, K. Uchida, T. Hosoya, *Chem. Lett.* **2015**, *44*, 691–693.
- [262] G. Wittig, L. Pohmer, *Chem. Ber.* **1956**, *89*, 1334–1351.
- [263] R. V. Stevens, G. S. Bisacchi, *J. Org. Chem.* **1982**, *47*, 2393–2396.
- [264] D. Peña, S. Escudero, D. Pérez, E. Guitián, L. Castedo, *Angew. Chem. Int. Ed.* **1998**, *37*, 2659–2661.
- [265] D. Peña, D. Pérez, E. Guitián, *Angew. Chem. Int. Ed.* **2006**, *45*, 3579–3581.
- [266] K. M. Allan, C. D. Gilmore, B. M. Stoltz, *Angew. Chem. Int. Ed.* **2011**, *50*, 4488–4491.
- [267] Z. Liu, R. C. Larock, *Org. Lett.* **2003**, *5*, 4673–4675.

- [268] R. J. Perkins, H.-C. Xu, J. M. Campbell, K. D. Moeller, *Beilstein J. Org. Chem.* **2013**, *9*, 1630–1636.
- [269] L. Ebersson, M. P. Hartshorn, J. J. McCullough, O. Persson, F. Radner, K. Ranta, T. Rojo, *Acta Chem. Scand.* **1998**, *52*, 1024–1028.
- [270] E. W.-G. Diao, J. Casanova, J. D. Roberts, A. H. Zewail, *Proc. Natl. Acad. Sci.* **2000**, *97*, 1376–1379.
- [271] W. Ried, M. Schön, *Justus Liebigs Ann. Chem.* **1965**, *689*, 141–144.
- [272] R. J. Crutchley, A. B. P. Lever, *J. Am. Chem. Soc.* **1980**, *102*, 7128–7129.
- [273] D. M. Schultz, J. W. Sawicki, T. P. Yoon, *Beilstein J. Org. Chem.* **2015**, *11*, 61–65.
- [274] D. J. Coughlin, R. G. Salomon, *J. Org. Chem.* **1979**, *44*, 3784–3790.
- [275] T. Hirao, C. Morimoto, T. Takada, H. Sakurai, *Tetrahedron* **2001**, *57*, 5073–5079.
- [276] R. B. Bates, T. J. Siahann, *J. Org. Chem.* **1986**, *51*, 1432–1434.
- [277] M. Ranchella, C. Rol, G. V. Sebastiani, *J. Chem. Soc. Perkin Trans. 2* **2000**, 311–315.
- [278] P. Fleming, D. F. O’Shea, *J. Am. Chem. Soc.* **2011**, *133*, 1698–1701.
- [279] R. K. Crossland, K. L. Servis, *J. Org. Chem.* **1970**, *35*, 3195–3196.
- [280] B. Song, T. Knauber, L. J. Gooßen, *Angew. Chem. Int. Ed.* **2013**, *52*, 2954–2958.
- [281] D. E. Frantz, D. G. Weaver, J. P. Carey, M. H. Kress, U. H. Dolling, *Org. Lett.* **2002**, *4*, 4717–4718.
- [282] G. K. Genkina, A. E. Shipov, T. A. Mastryukova, M. I. Kabachnik, *Russ J Org Chem* **1996**, *66*, 1742–1744.
- [283] W. H. Jeon, T. S. Lee, E. J. Kim, B. Moon, J. Kang, *Tetrahedron* **2013**, *69*, 5152–5159.
- [284] M. Frisch, G. Trucks, H. Schlegel, G. Scuseria, M. Robb, J. Cheeseman, G. Scalmani, V. Barone, B. Mennucci, G. Petersson, et al., *Gaussian 09 Revis. D01 Gaussian Inc Wallingford CT* **2009**.
- [285] A. D. Becke, *J. Chem. Phys.* **1993**, *98*, 5648.
- [286] S. H. Vosko, L. Wilk, M. Nusair, *Can. J. Phys.* **1980**, *58*, 1200–1211.
- [287] P. J. Stephens, F. J. Devlin, C. F. Chabalowski, M. J. Frisch, *J. Phys. Chem.* **1994**, *98*, 11623–11627.
- [288] V. Barone, M. Cossi, *J. Phys. Chem. A* **1998**, *102*, 1995–2001.
- [289] B. H. Besler, K. M. Merz, P. A. Kollman, *J. Comput. Chem.* **1990**, *11*, 431–439.
- [290] U. C. Singh, P. A. Kollman, *J. Comput. Chem.* **1984**, *5*, 129–145.
- [291] S. D. Larsen, C. H. Spilman, Y. Yagi, D. M. Dinh, K. L. Hart, G. F. Hess, *J. Med. Chem.* **1994**, *37*, 2343–2351.
- [292] N. Doubina, S. A. Paniagua, A. V. Soldatova, A. K. Y. Jen, S. R. Marder, C. K. Luscombe, *Macromolecules* **2011**, *44*, 512–520.
- [293] Z.-S. Chen, Z.-Z. Zhou, H.-L. Hua, X.-H. Duan, J.-Y. Luo, J. Wang, P.-X. Zhou, Y.-M. Liang, *Tetrahedron* **2013**, *69*, 1065–1068.
- [294] W. Miao, Y. Gao, X. Li, Y. Gao, G. Tang, Y. Zhao, *Adv. Synth. Catal.* **2012**, *354*, 2659–2664.
- [295] K. Takaki, Y. Itono, A. Nagafuji, Y. Naito, T. Shishido, K. Takehira, Y. Makioka, Y. Taniguchi, Y. Fujiwara, *J. Org. Chem.* **2000**, *65*, 475–481.
- [296] C. W. Thomas, L. L. Leveson, *J. Chem. Soc. Perkin Trans. 2* **1973**, 20.
- [297] N. Kreutzkamp, G. Cordes, *Arch. Pharm. (Weinheim)* **1962**, *295*, 276–283.
- [298] H. Gross, C. Böck, B. Costisella, J. Gloede, *J. Für Prakt. Chem.* **1978**, *320*, 344–350.
- [299] C. C. Kotoris, W. Wen, A. Lough, S. D. Taylor, *J. Chem. Soc. [Perkin 1]* **2000**, 1271–1281.
- [300] J. StåLring, A. Bernhardsson, R. Lindh, *Mol. Phys.* **2001**, *99*, 103–114.

- [301] Y. Li, W. Xie, X. Jiang, *Chem. - Eur. J.* **2015**, *21*, 16059–16065.
- [302] S. Kim, J. Rojas-Martin, F. D. Toste, *Chem Sci* **2016**, *7*, 85–88.
- [303] K. Shin, S.-W. Park, S. Chang, *J. Am. Chem. Soc.* **2015**, *137*, 8584–8592.
- [304] J.-B. Liu, F.-J. Chen, E. Liu, J.-H. Li, G. Qiu, *New J Chem* **2015**, *39*, 7773–7776.
- [305] M. E. Lorris, R. A. Abramovitch, J. Marquet, M. Moreno-Mañas, *Tetrahedron* **1992**, *48*, 6909–6916.
- [306] S. Kindt, K. Wicht, M. R. Heinrich, *Angew. Chem. Int. Ed.* **2016**, *55*, 8744–8747.
- [307] A. P. Colleville, R. A. J. Horan, N. C. O. Tomkinson, *Org. Process Res. Dev.* **2014**, *18*, 1128–1136.
- [308] K. Snégaroff, S. Komagawa, F. Chevallier, P. C. Gros, S. Golhen, T. Roisnel, M. Uchiyama, F. Mongin, *Chem. - Eur. J.* **2010**, *16*, 8191–8201.
- [309] N. Friebe, K. Schreiter, J. Kübel, B. Dietzek, N. Moszner, P. Burtscher, A. Oehlke, S. Spange, *New J Chem* **2015**, *39*, 5171–5179.
- [310] R. Cella, R. L. O. R. Cunha, A. E. S. Reis, D. C. Pimenta, C. F. Klitzke, H. A. Stefani, *J. Org. Chem.* **2006**, *71*, 244–250.
- [311] D. Alickmann, R. Fröhlich, A. H. Maulitz, E.-U. Würthwein, *Eur. J. Org. Chem.* **2002**, *2002*, 1523–1537.
- [312] W. Su, S. Urgaonkar, P. A. McLaughlin, J. G. Verkade, *J. Am. Chem. Soc.* **2004**, *126*, 16433–16439.
- [313] Y. Y. Qian, K. L. Wong, M. W. Zhang, T. Y. Kwok, C. T. To, K. S. Chan, *Tetrahedron Lett.* **2012**, *53*, 1571–1575.
- [314] L. Pauli, R. Tannert, R. Scheil, A. Pfaltz, *Chem. - Eur. J.* **2015**, *21*, 1482–1487.
- [315] Y. Yabe, T. Maegawa, Y. Monguchi, H. Sajiki, *Tetrahedron* **2010**, *66*, 8654–8660.
- [316] D. Wu, Z.-X. Wang, *Org. Biomol. Chem.* **2014**, *12*, 6414.
- [317] A. Seggio, A. Jutand, G. Priem, F. Mongin, *Synlett* **2008**, *2008*, 2955–2960.
- [318] G. Manolikakes, P. Knochel, *Angew. Chem. Int. Ed.* **2009**, *48*, 205–209.
- [319] A. P. Kourounakis, C. Charitos, E. A. Rekka, P. N. Kourounakis, *J. Med. Chem.* **2008**, *51*, 5861–5865.
- [320] S. Sase, M. Jaric, A. Metzger, V. Malakhov, P. Knochel, *J. Org. Chem.* **2008**, *73*, 7380–7382.
- [321] C. C. C. Johansson Seechurn, S. L. Parisel, T. J. Colacot, *J. Org. Chem.* **2011**, *76*, 7918–7932.
- [322] S. E. Denmark, J. D. Baird, C. S. Regens, *J. Org. Chem.* **2008**, *73*, 1440–1455.
- [323] H. A. Stefani, J. M. Pena, F. Manarin, R. A. Ando, D. M. Leal, N. Petragani, *Tetrahedron Lett.* **2011**, *52*, 4398–4401.
- [324] B.-T. Luo, H. Liu, Z.-J. Lin, J. Jiang, D.-S. Shen, R.-Z. Liu, Z. Ke, F.-S. Liu, *Organometallics* **2015**, *34*, 4881–4894.
- [325] M.-H. Lin, Y.-C. Huang, C.-K. Kuo, C.-H. Tsai, Y.-S. Li, T.-C. Hu, T.-H. Chuang, *J. Org. Chem.* **2014**, *79*, 2751–2757.
- [326] G. A. Molander, B. Canturk, L. E. Kennedy, *J. Org. Chem.* **2009**, *74*, 973–980.
- [327] G. Ishii, R. Harigae, K. Moriyama, H. Togo, *Tetrahedron* **2013**, *69*, 1462–1469.
- [328] V. Domingo, C. Prieto, A. Castillo, L. Silva, J. F. Quílez del Moral, A. F. Barrero, *Adv. Synth. Catal.* **2015**, *357*, 3359–3364.
- [329] B. Mu, T. Li, W. Xu, G. Zeng, P. Liu, Y. Wu, *Tetrahedron* **2007**, *63*, 11475–11488.
- [330] I. J. S. Fairlamb, A. R. Kapdi, A. F. Lee, *Org. Lett.* **2004**, *6*, 4435–4438.
- [331] X.-H. Fan, L.-M. Yang, *Eur. J. Org. Chem.* **2010**, *2010*, 2457–2460.
- [332] H. Li, C.-L. Sun, M. Yu, D.-G. Yu, B.-J. Li, Z.-J. Shi, *Chem. - Eur. J.* **2011**, *17*, 3593–3597.
- [333] S. Riggelman, P. DeShong, *J. Org. Chem.* **2003**, *68*, 8106–8109.
- [334] E. Alacid, C. Nájera, *Org. Lett.* **2008**, *10*, 5011–5014.
- [335] Z. Liu, N. Dong, M. Xu, Z. Sun, T. Tu, *J. Org. Chem.* **2013**, *78*, 7436–7444.

- [336] L. Zhu, J. Duquette, M. Zhang, *J. Org. Chem.* **2003**, *68*, 3729–3732.
- [337] J. L. Bolliger, C. M. Frech, *Adv. Synth. Catal.* **2010**, *352*, 1075–1080.
- [338] B. O. Roos, P. R. Taylor, P. E. M. Si $\equiv$ gbahn, *Chem. Phys.* **1980**, *48*, 157–173.
- [339] K. Andersson, P. A. Malmqvist, B. O. Roos, A. J. Sadlej, K. Wolinski, *J. Phys. Chem.* **1990**, *94*, 5483–5488.
- [340] J. Finley, P.-Å. Malmqvist, B. O. Roos, L. Serrano-Andrés, *Chem. Phys. Lett.* **1998**, *288*, 299–306.
- [341] C. E. Crespo-Hernández, L. Martínez-Fernández, C. Rauer, C. Reichardt, S. Mai, M. Pollum, P. Marquetand, L. González, I. Corral, *J. Am. Chem. Soc.* **2015**, *137*, 4368–4381.
- [342] X.-J. Hou, P. Quan, T. Höltzl, T. Veszprémi, M. T. Nguyen, *J. Phys. Chem. A* **2005**, *109*, 10396–10402.
- [343] N. Forsberg, P.-Å. Malmqvist, *Chem. Phys. Lett.* **1997**, *274*, 196–204.
- [344] K. Pierloot, B. Dumez, P.-O. Widmark, B. O. Roos, *Theor. Chim. Acta* **1995**, *90*, 87–114.
- [345] R. Ditchfield, *J. Chem. Phys.* **1971**, *54*, 724.
- [346] G. Danoun, B. Bayarmagnai, M. F. Grünberg, L. J. Gooßen, *Angew. Chem. Int. Ed.* **2013**, *52*, 7972–7975.
- [347] T. Dohi, N. Takenaga, A. Goto, A. Maruyama, Y. Kita, *Org. Lett.* **2007**, *9*, 3129–3132.
- [348] P. P. Fu, L. E. Unruh, D. W. Miller, L. W. Huang, D. T. C. Yang, *J. Org. Chem.* **1985**, *50*, 1259–1261.
- [349] P. Bovicelli, P. Lupattelli, B. Crescenzi, A. Sanetti, R. Bernini, *Tetrahedron* **1999**, *55*, 14719–14728.
- [350] K. C. Hildebran, T. L. Cordray, K. W. Chan, C. F. Beam, *Synth. Commun.* **1994**, *24*, 779–788.
- [351] P. Schiess, M. Eberle, M. Huys-Francotte, J. Wirz, *Tetrahedron Lett.* **1984**, *25*, 2201–2204.
- [352] J. V. Suárez-Meneses, A. Oukhrib, M. Gouygou, M. Urrutigoity, J.-C. Daran, A. Cordero-Vargas, M. C. Ortega-Alfaro, J. G. López-Cortés, *Dalton Trans* **2016**, *45*, 9621–9630.
- [353] N. Dennis, A. R. Katritzky, S. K. Parton, *J. Chem. Soc. Chem. Commun.* **1972**, 1237–1238.
- [354] R. Luo, J. Liao, L. Xie, W. Tang, A. S. C. Chan, *Chem. Commun.* **2013**, *49*, 9959–9961.

## New Intermediates from Photogenerated Phenyl Cations